Max Planck Institut für Kolloid- und Grenzflächenforschung
Abteilung für Grenzflachen

Thermodynamics, kinetics and rheology of surfactant adsorption layers at water/oil interfaces

Dissertation
zur Erlangung des akademischen Grades
"doctor rerum naturalium"
(Dr. rer. nat.)
in der Wissenschaftsdisziplin "Kolloidchemie"

eingereicht an der
Mathematisch-Naturwissenschaftlichen Fakultät
der Universität Potsdam

von
Nenad Mucic

Potsdam, den 24. September 2012

ABSTRACT

This thesis presents a quantitative analysis of surfactant's or macromolecule's adsorption layers at the water/oil interface in respect to their equilibrium and dynamic states. The molecules in water/oil adsorption layer interact with each other and with the oil molecules via electrostatic and van der Waals interactions, respectively. Therewith, the thermodynamic and dynamic properties of the adsorption layer directly depend on the physical characteristics of the molecules, i.e. the length of the surfactants' tails and the oil chain length. The longer the surfactant tail is, the stronger is the mutual interaction between the surfactant molecules in the adsorption layer and the more are the oil molecules will be squeezed out from the adsorption layer. On the other side, if the oil molecules possess longer chains, they will bind stronger to the surfactant's tail and resist against the squeezing out from the adsorption layer.

When some other molecules or impurities are dissolved in a surfactant aqueous solution, they might transfer to the oil phase depending on their hydrophobicity. Due to this process the impurities do not leave any additional effects on the equilibrium and dynamic interfacial tension properties of the adsorbed prime surfactant. On the contrary, at the water/air interface the impurities leave significant effects on the solution's surface tension, form a mixed adsorption layer, and can even dominate it.

The interaction between surfactant and oil molecules can be investigated at the water/oil vapor interface too. The surfactant molecules, once adsorb, attract the oil molecules from the vapor phase through hydrophobic interaction. In addition, the surfactant molecules at the interface change their orientation at different surface concentrations which influences the amount of adsorbed oil molecules.

Investigating the dilational rheology of surfactants at the water/oil interface it was found that additional processes follow the adsorption/desorption of the surfactant molecules. During interfacial perturbation, the adsorbed surfactants are effected by the attractive forces of the hydrophobic oil molecules. On the other hand, desorption of surfactant molecules from the water/oil interface can be decelerated by the same attractive hydrophobic interaction with the oil molecules.

This work also considers the interfacial properties of pure macromolecules and their mixtures with surfactants at the water/hexane interface. It is dedicated to the investion of the equilibrium and dynamic behavior of non-ionic triblock copolymers, Pluronics, when varying the number of poly(ethylene oxide) and poly(propylene oxide) groups. By comparing the experimental results with the respective theoretical model for protein solutions, it was found that the best fit is achieved when a multilayer adsorption is considered.

A part of this work is also devoted to mixtures of the cationic polyelectrolyte PAH and the anionic surfactant SDS and describes their interfacial tension and dilational rheology. The formation of PAH/SDS complexes governs the dilational elasticity values, depending on the concentrations of surfactant and polyelectrolyte and their mixing ratio. It was found that with increasing the surfactant concentration the SDS dominates in the adsorption layer whereas the polyelectrolyte-surfactant complexes remain in the bulk phase.

The experiments were generally performed on the Profile Analysis Tensiometer, PAT-1, or the Capillary Pressure Tensiometer, ODBA, or the combination of the two instruments when required. A systematic analysis was performed to show the optimum experimental conditions for studies of the adsorption dynamics and dilational visco-elasticity of surfactant interfacial layer. The received experimental results were analyzed by fitting with the respective theoretical models. In this way the interfacial properties of the adsorptions layers have been quantified.

LIST OF PAPERS AND MY CONTRIBUTIONS

I. Effects of dodecanol on the adsorption kinetics of SDS at the water/hexane interface
A. Javadi, N. Mucic (40%), D. Vollhardt, V.B. Fainerman and R. Miller
Journal of Colloid and Interface Science 351 (2010) 537-541.

II. Adsorption of alkyl trimethylammonium bromides at the water/air and water/hexane interface
V. Pradines, V.B. Fainerman, E.V. Aksenenko, J. Krägel, N. Mucic (30%) and R. Miller
Colloids and Surfaces A 371 (2010) 22-28

III. Adsorption layer properties of alkyl trimethylammonium bromides at interfaces between water and different alkanes
N. Mucic (70%), N.M. Kovalchuk, V.B. Fainerman, E.V. Aksenenko and R. Miller
to be submitted

IV. Mixed adsorption layers at the aqueous C_nTAB solution / hexane vapor interface
N. Mucic (70%), N. Moradi, A. Javadi, E.V. Aksenenko, V.B. Fainerman and R. Miller
to be submitted

V. Dynamics of interfacial layers – Experimental feasibilities of adsorption kinetics and dilational rheology
N. Mucic (70%), A. Javadi, N.M. Kovalchuk, E.V. Aksenenko and R. Miller
Advances in Colloid and Interface Science 168 (2010) 167-178.

VI. Fast dynamic interfacial tension measurements and dilational rheology of interfacial layers by using the capillary pressure technique
A. Javadi, J. Krägel, A.V. Makievski, N.M. Kovalchuk, V.I. Kovalchuk, N. Mucic (10%), G. Loglio, P. Pandolfini, M. Karbaschi and R. Miller
Colloids and Surfaces A, 407 (2012) 159-168

VII. Dynamic properties of CnTAB adsorption layers at the water/oil interface
N. Mucic (70%), N.M. Kovalchuk, V. Pradines, A. Javadi, E.V. Aksenenko, J. Krägel and R. Miller
Colloids and Surfaces A, submitted 2012

VIII. Dynamic interfacial tension of triblock copolymers solutions at the water/hexane interface
P. Ramirez, J. Munoz, V.B. Fainerman, E.V. Aksenenko, N. Mucic (10%) and R. Miller
Colloids and Surfaces A 391 (2011) 119-124

IX. Dilational rheology of polymer/surfactant mixtures at water/hexane interface
A. Sharipova, S. Aidarova, N. Mucic (20%) and R. Miller
Colloids and Surfaces A 391 (2011) 130-134

X. Competitive adsorption at water/oil interface as a tool for controlling the emulsion stability and breaking (Beiersdorf project report, 2012)
N. Mucic (70%), B. Reetz and R. Miller

LIST OF PUBLICATIONS NOT INCLUDED IN THIS THESIS

I. Interrelation between surfactant adsorption kinetics, interfacial rheology and emulsion stability
T. Sobisch, N. Mucic, J. Krägel, A.V. Makievski, R. Miller and D. Lerche
Proceedings of the 5th World's Emulsion Congress, 2010, Lyon, No. 0065, 1-7

II. Capillary pressure studies of adsorption layers at water/hydrocarbon Interfaces
R. Miller, A. Javadi, N. Mucic, N. Moradi, M. Born, J. Krägel, G. Loglio, P. Pandolfini, A.V. Makievski, M.E. Leser, L. Liggieri, F. Ravera, Ch. Eigenbrod, S. Mawn and V.I. Kovalchuk
Proceedings of the 5th World's Emulsion Congress, 2010, Lyon, No. 0232, 1-6

III. Adsorption characteristics of ionic surfactants at water/hexane Interface
N. Mucic, V. Pradines, A. Javadi, A. Sharipova, J. Krägel, M.E. Leser, E.V. Aksenenko, V.B. Fainerman and R. Miller
Proceedings of the 5th World's Emulsion Congress, 2010, Lyon, No. 0233, 1-4

IV. Rheology of interfacial layers
R. Miller, J.K. Ferri, A. Javadi, J. Krägel, N. Mucic and R. Wüstneck
Colloid and Polymer Science 288 (2010) 937-950

V. Adsorption kinetics of surfactants, in "Encyclopedia of Colloid and Interface Science" Th. Tadros (Ed.)
N. Mucic, A. Javadi, M. Karbaschi, A. Sharipova, V.B. Fainerman, E.V. Aksenenko, N.M. Kovalchuk and R. Miller
Springer, Germany (submitted 2012)

VI. Experimental methods for interfacial dynamics, in "Encyclopedia of Colloid and Interface Science" Th. Tadros (Ed.)
A. Javadi, N. Mucic, M. Karbaschi, J.Y. Won, V.B. Fainerman, A. Sharipova, E.V. Aksenenko, V.I. Kovalchuk, N.M. Kovalchuk, J. Krägel and R. Miller
Springer, Germany (submitted 2012)

VII. Surfactant adsorption layers at liquid interfaces, in "Surfactant Science and Technology: Retrospects and Prospects"
R. Miller, V.B. Fainerman, V. Pradines, V.I. Kovalchuk, N.M. Kovalchuk, E.V. Aksenenko, L. Liggieri, F. Ravera, G. Loglio, A. Sharipova, Y. Vysotsky, D. Vollhardt, N. Mucic, R. Wüstneck, J. Krägel and A. Javadi
CRC Press/Taylor &Francis (submitted 2012)

VIII. Adsorption characteristics of ionic surfactants at water/hexane interface obtained by PAT and ODBA
N. Mucic, V. Pradines, A. Javadi, A. Sharipova, J. Krägel, M.E. Leser, E.V. Aksenenko, V.B. Fainerman and R. Miller
Proceedings of the 5th World's Emulsion Congress, Lyon, 2010.

Table of Contents

CHAPTER 1

Introduction

This thesis is dedicated to discover the physicochemical properties of surfactant adsorption layers at water/oil interfaces. Surfactants are omnipresent in our modern world and are applied in almost any field of our daily life. They are used to modify the properties of interfaces in a defined way such that products are easier or better produced or more stable over the products' lifetime. Most investigations on the interfacial properties of surfactant adsorption layers have been performed at the water/air interface. The reason for this is mainly the easier approach of this interface by experimental methods or theoretical models. The much more important interface is that between two liquids, mainly the interface between water and oil. A large number of application fields require a tailored system of surfactants with adequate characteristics in order to produce respective products with well defined properties and required stability. Examples are the emulsification of oils in water or vice versa of two immiscible liquids. Although emulsions exist for a long time, many new challenges appear, as products in food or pharmacy for instance have to be reformulated due to a required replacement of compounds by other more healthy ones. Therefore quantitative knowledge of surfactant adsorption layers at the water/oil interface appears to be much more important.

Many experimental methods, however, are easily applied to water/gas interfaces but cannot be used for investigations of water/oil interfaces. The reason can be quite manifold. For example, optical methods, such as Brewster Angle Microscopy (BAM), interfacial ellipsometry or Second Harmonic Generation (SHG), often fail due to the small difference in the refractive index of the two fluids, and the probing beam has to travel at least through one fluid. Obstacles for other methods can be the smaller difference in the density. In particular for dynamic methods, the hydrodynamics of the involved fluid can have strong influences on the quality of experiments and set much stronger limitations for the applicability of certain experimental tools. The much higher complexity of the water/oil system as compared to water/air systems is also given by the fact that non-ionic surfactants are soluble in both liquid phases. Moreover, the interaction of the hydrophobic parts of an adsorbed surfactant with the oil molecules can be quite significant while it is more or less negligible for the interaction with air.

In summary we have to state that studies on a quantitative characterization of surfactants at water/oil interfaces are much more demanding than equivalent investigations at the water/air interface. Therefore, systematic studies are scarce. Due to the above mentioned facts, clear conclusions about the quantitative behavior of surfactants at water/oil interfaces require investigations with quite a number of complementary methods. In addition the analysis of the resulting data is possible only with much more sophisticated theoretical models taking into account the peculiarities of the studied interface.

The presented results in the thesis were obtained from pure fundamental investigations. Therefore, any parts in the following text on practical applications are just examples of a possible utilization of the fundamental results in industry.

Molecular interactions are more complex at water/oil than at water/air interfaces. In such systems there are not only interactions between the adsorbed surfactant molecules but also with the oil molecules. These surfactant-oil interactions are the subject of this thesis. For the sake of simplicity we have investigated just single surfactant adsorption layers. The interactions between oil molecules and surfactants have impact on the area per surfactant molecule in an adsorption layer. Practically, the area per surfactant molecule is obtained after analyzing the experimental results with respective theoretical models. Therewith a thorough analysis of most recent theoretical models is also part of the investigations presented in this thesis. Each of the thermodynamic, kinetic and rheological results can be described by particular theoretical models which in the end help to create a physical picture of surfactant adsorption layers on a molecular level. To achieve relationships between all three theoretical models – thermodynamics, adsorption kinetics and dilational visco-elasticity - is

much more complex at the water/oil interface by involving more physical effects and program parameters as compared to the water/air interface.
Beside at the water/oil interface, the interactions between surfactants and oil molecules can be investigated at the water/oil vapor interface too. Measuring the CnTAB adsorption kinetics before and after injection of the oil vapor into the gas phase leads us to additional information about the influence of the different surfactants' alkyl chain lengths on the decrease of interfacial tension during the oil co-adsorption from the vapor phase.
We have tackled the problems of natural impurities in aqueous surfactant solutions and investigated their influence on the surfactant adsorption layers at water/oil interfaces. It was found that in our system impurities have strong effects at the water/air interface, while at water/oil interfaces, due to the oil solubility, the impurities transfer from the aqueous into the oil phase without affecting the surfactant adsorption layer properties remarkably.
In addition to the adsorption thermodynamics, the thesis is particularly devoted to investigation of the dynamic properties in the adsorption layer. The subjects of this study are surfactants, polymers and their mixtures. The dynamics in the adsorption layers was studied by measuring the dynamic interfacial tension and dilational rheology. Here it will be shown that the adsorption dynamics of triblock copolymers (Pluronic) can be theoretically well described by a model based on the analysis of the chemical potentials of the solvent and the dissolved substances, for physically reasonable values of the adsorption layer thickness and diffusion coefficient.
When mixing a polyelectrolyte with a surfactant, two-dimensional rigid structures can be observed at the water/oil interface and they can be destroyed when the surfactant concentration is raised above a certain concentration. By analyzing the dilational rheology results it was found that polyelectrolyte-surfactant mixed adsorption layers have a higher dilational elasticity and viscosity than layers formed by surfactants alone.
We have reported also new aspects of the optimization of experimental tools for investigations of the fast interfacial dynamics. Following this, it will be shown how the adsorption kinetics and dilational rheology depend closely on the correct choice of the instrument and theoretical model for analyzing the data afterwards.
When speaking about adsorption layers at water/air interfaces, the most important effect on the layer characteristics in general arises from the interaction between the adsorbed molecules. The lateral interactions between molecules in an adsorption layer are manifested through the hydrophobic attraction of surfactants' alkyl chains and electrostatic repulsion of surfactants' polar heads. Oppositely charged ions (counterions) in the surfactant aqueous solution reduce the electrostatic repulsions between adsorbed surfactants by screening the surfactants' charge. This effect reduces the surfactant area per molecule, and consequently, leads to a significant decrease in surface tension. On the other hand, the effect of surfactant chain-length compatibility in surfactant adsorption layers is particularly important for interfacial properties too. For mixed adsorption layers comprised of surfactants of different chain lengths, the shorter hydrocarbon tails have more freedom to disrupt the molecular packing through conformational disorder and thermal motion. This causes a slight increase in the intermolecular distance and, hence, the average area per molecule. For the sake of simplicity, our investigation was focused just on single surfactant adsorption layers.

1.1 Background

For many years the behavior of surfactants in solution or at liquid/fluid interfaces has been widely studied and found as very important for understanding of many processes and technologies, such as detergency, food processing, pharmaceutical industry, or cosmetics [1,2,3,4]. The general characteristics of disperse systems, such as foams, emulsions and suspensions, are practically defined by the interfacial properties of liquid films stabilized by single surfactants or mixtures of surface active compounds. Due to the availabilities of suitable instruments, most adsorption studies have been performed at the water/air interface [5,6,7,8,9,10] for which surface tension measurements [11], sum frequency spectroscopy [12], or neutron reflection experiments [13,14], followed by a modeling of the experimental data are very powerful methods to give an accurate idea

of the interfacial layer properties (adsorbed amount, thickness of the layer, molar area and orientation of adsorbed molecules). Contrary to this, so far only few systematic experimental studies involving also a theoretical treatment of the data have been dedicated to the adsorption of surfactants at water/oil interfaces [15,16,17]. One of the reasons for this is technical difficulties to measure for example with optical methods due to the presence of the upper oil phase. The purification of the oil phases which often contain traces of surface active molecules, and their volatility which limits the experimental time, are additional critical points. Moreover, the difficulty of such studies increases when the surfactants are soluble in both water and oil phases. This fact entails, in addition to all mentioned parameters, the need of determination of the partition coefficient [18,19] in experiments.

The questions regarding the role of the oil molecules at the water interfaces are still unclear and so the interactions between the oil molecules and surfactants and the mutual surfactant interactions at the water/oil interface. Some of the answers can be found when comparing the results obtained at water/air and the water/oil interfaces. In the past, Hutchinson suggested the presence of a competitive adsorption between surfactant and oil molecules at the water/non-polar solvent interface [20]. Gillap et al. [21] have observed a strong increase of the adsorbed amount of sodium dodecyl and decyl sulfate at the water/oil interface as compared to the water/air interface, certainly due to the presence of hydrophobic interactions between adsorbed surfactants and oil molecules.

Systematic study of the water/oil interfaces started also with investigations of the surfactant's natural impurities and their behavior at water/oil interfaces. It was shown that depending on the volume ratio of water and oil, the initial concentrations of the surfactant in the two phases and the partition coefficient, a minimum in $\gamma(t)$ can be observed and explained by the transfer of surfactant from the phase of smaller volume to the other phase [22]. This behavior is typical for oil and water soluble substances such as dodecanol ($C_{12}OH$), the natural impurity of aqueous SDS solution. Compared to SDS, $C_{12}OH$ is only slightly soluble in water and about 400 times higher surface active at the water/air interface [23].

In comparison with spreading oil on the water/air interface there is much less published work on the adsorption of alkane from the vapor phase on aqueous surfactant solution surfaces [24, 25]. Aveyard et al. reported that for nonionic surfactants, dodecane adsorption decreases with increasing temperature at low surface concentration of the oil whereas it increases at high surface concentrations. With the ionic surfactant DoTAB, the temperature effect showed a similar crossover in the behavior but the changes in adsorption were opposite in direction to those seen for the non-ionic surfactant. Javadi et al. have found that the surface tension value reached in presence of a saturated hexane atmosphere due to hexane co-adsorption depends on the surfactant concentration.

Understanding the surfactant dynamic behavior in an adsorption layer has significant importance not just for fundamental science but also for different technological applications, such as foaming or emulsification, broadly used in the pharmaceutical, food and mining industry and in oil recovery. By studying the dynamic interfacial behavior, it is possible to obtain important information about the interaction between molecules, change of conformation and aggregation of molecules, kinetics of chemical reactions, kinetics of formation and disintegration of micelles, and other processes which take place on a molecular level [26,27]. Interfacial rheology gives insight into many relaxation processes within the adsorption layer, which is of fundamental interest and also of great applied value [28].

Surfactants of low surface activity generally adsorb fairly quickly due to the required high bulk concentration. This in turn requires experimental techniques able to measure changes in surface tension already after a few milliseconds or even less. On the other side, highly surface active substances are used at rather low bulk concentrations and, therefore, their adsorption kinetic is slow, i.e. the equilibrium state is established only after long adsorption times. In this case one should choose instruments which provide data for adsorption times of many hours or even days rather than recording the surface tension in less than a few milliseconds. In both cases, the most important point is to select and properly apply the right experimental techniques for getting the required information.

Similar problems arise in investigations of the frequency dependence of the interfacial tension response to small harmonic perturbations of the interfacial area, i.e. when we want to measure the dilational visco-elasticity of a surfactant adsorption layer. For a weak surfactant a method is obviously needed that works at very high frequencies as the required compression/expansion perturbations should be fast enough to create a deviation of the surface layer from equilibrium before this equilibrium is reestablished by desorption/adsorption. Again, on the contrary, for the very highly surface active substances a method is required to allow slow compression and expansion (measurements at low frequencies of interfacial perturbations).
As a part of this thesis is devoted to investigations of macromolecular block copolymers (Pluronics) and mixtures of polyelectrolytes (polyallyl amine hydrochloride) and surfactants at the water/oil interface, in the following paragraphs work will be presented done so far only at the water/air interface.
Surface properties of adsorbed and spread Pluronics block copolymer (PEO-PPO-PEO) films at the water/air interface have been studied by equilibrium and dynamic surface tension measurements [29,30], ellipsometry [29,30,31,32], neutron reflectivity [33,34,35], and surface rheology measurements [36,37,38,39,40,41]. It was found that by increasing the surface concentration of these copolymers, they are passing through different conformational changes at the water/air interface. The layer structure changes from a two-dimensional flat structure with both PEO and PPO segments lying flat at the surface to a brush-like structure where the PEO segments are protruding into the solution bulk.
The interfacial behavior of polyelectrolyte-surfactant mixtures at water/oil interfaces has only very recently been studied systematically, since suitable experimental tools are available, and only few papers are so far devoted to this subject [42].
The dilational surface rheology is used to obtain additional information on the polyelectrolyte-surfactant complex formation in the surface layer. Measurements of the dynamic surface visco-elasticity can be used to study every single chemical and physical process in the system and provide more information on the dynamics of polymer chains and their interactions with surfactant molecules at the surface, supposed the measurements are done in a suitable frequency range.

1.2 Emulsions

Emulsions are systems where the water/oil interfacial properties play a key role. As the water/oil interface is the subject of the thesis, the following part summarizes some general knowledge about emulsions.
Emulsions are dispersions (often colloidal) of one fluid phase in another stabilized by the presence of surfactants adsorbed at fluid interfaces. The dependencies of the interfacial tension on the adsorption, and its dependence on bulk composition, temperature, etc., play a key role in the hydrodynamics of coalescence phenomena which determines the stability of emulsions.
Dispersed phase droplets in emulsions have usually a diameter less than 100 µm. Corresponding to the size of the droplets, the type can be macro–, mini-, nano- and micro–emulsions. The macro–emulsions, simply called emulsions, are thermodynamically unstable, showing characteristic properties such as segregation (sedimentation or creaming due to gravity), flocculation (clustering of emulsion droplets) and coalescence (the merging of droplets into larger droplets), and drop size disproportionation. Coalescence is preceded by flocculation, in which the drops are drawn together by net long–range attraction, although they are mechanically transported, by gravity, filtration, etc., into sufficient proximity to coalesce. The liquid interface between adjacent droplets is flattened and separated by a thinning film of the external liquid phase. The liquid films, when stable, drain to some "critical thickness" h_c, are found to be of the order of 50–100 nm and remain metastable for a finite period of time ("resting" time), before they suddenly rupture.
In order to prolong the "resting" time, emulsions must contain a third constituent (in addition to oil and water) known as an emulsifier or emulsifying agent. The first class of emulsifiers is low molecular weight surfactants, which adsorb and orient at the interface. They play both mechanical and physico-chemical roles in emulsion stabilization. Other emulsifiers are macromolecular

substances. These might include proteins, gums, starches and derivatives from such substances (such as dextrin, methyl cellulose, lignosulfonates, etc.) as well as certain synthetic polymers or polyelectrolytes. These materials are also strongly adsorbed at the interface and confer stability primarily through "steric" and mechanical effects. Finally, finely dispersed solids may act as emulsifiers too, as it is the case for "Pickering emulsions". In addition there is also a fourth type of emulsifier, i.e. certain inorganic anions which adsorb to the interface in sufficient quantity to confer some electrostatic stabilization. Common among these are the thiocyanate ions (CNS).

1.3 Adsorption layers

In the previous section emulsions were presented as complex systems of thin films between dispersed droplets. A thin film can be considered as adsorption bilayer of some surfactants. Therefore, by analyzing the behavior of single adsorption layers, one is able to understand the behavior of the total emulsion.

The characteristics that surfactants provide to an interface are not just a matter of their chemical structure. The polarity of the two liquids has to be taken in consideration too. Namely, the polarity of liquids directly influences the interactions with surfactants adsorbed at the interface. In practice, water or an aqueous electrolyte solution are most frequently considered as a polar phase, and hydrocarbons or their mixtures, e.g. oil fractions, as an apolar phase. In this connection, substances practically completely soluble in water are ascribed to the so called water–soluble surfactants.

Nonionics like alcohol ethoxylates, alkylphenols and alkyloamides having an average hydrocarbon radical length of C_{12} – C_{16}, products containing up to 4 EO moles are ascribed to oil–soluble, those containing over 10 moles as water–soluble and those with 4 to 10 EO moles to water–oil–soluble. In this case, the surfactant is distributed between the aqueous and oil phases. The affinity of surfactants to the aqueous or the oil phase is quantified by the distribution coefficient $K = c_w/c_o$ where c_w is the surfactant concentration in the aqueous phase and c_o is the surfactant concentration in the oil phase. The value K is considerably influenced by temperature, oil phase polarity and electrolyte content in water [43,44]. It is observed that some rules of the water/air interface (Szyszkowski equation, Traube rule etc.) can be utilized for the water/oil interface too. Note that the adsorption of oil – soluble surfactants at the oil-air interface is weak and changes only slightly with the chain length in a homologous series.

One of the principal distinctions between the liquid-liquid and liquid-gas interface is the possibility to achieve very low interfacial tensions (close to zero). This possibility is provided by using surfactants soluble in both, the aqueous and oil phases, as well as using binary mixtures of water–soluble and oil–soluble surfactants.

Numerous systematic experimental studies of surfactants, macromolecules or their mixtures have been performed using various complementary methods: dynamic and equilibrium interfacial tension measurements [45,46,47], ellipsometry [48,49,50,51], surface light scattering [52,53], dilational and shear rheology [54,55,56]. New or recently developed experimental technique broaden the sources of information, such as FRAP (Fluorescence Recovery After Photobleaching) [57,58], which enables one to measure the molecular mobility in adsorption layers, Brewster Angle Microscopy [59,60,61] and Atomic Force Microscopy [62,63,64], which allow the visualization of macroscopic structures in the adsorption layers. IRRAS (Infrared Reflection Adsorption Spectroscopy) [65], SHG (Second Harmonic Generation) and other new non-linear optical principles have been proven to be applicable to study the arrangement of individual molecular moieties in monolayers at different liquid interfaces.

Theoretical adsorption models

The thermodynamics and dynamics of interfacial layers have gained large interest in interfacial research. An accurate description of the thermodynamics of adsorption layers at liquid interfaces is the vital prerequisite for a quantitative understanding of the equilibrium or any non–equilibrium processes going on at the surface of liquids or at the interface between two liquids. The

thermodynamic analysis of adsorption layers at liquid-fluid interfaces is provided by the equation of state which expresses the surface pressure as a function of surface layer composition, and the adsorption isotherm, which determines the dependence of adsorption of each dissolved component on their bulk concentrations. From these equations, the surface tension (pressure) isotherm can also be calculated and compared with experimental data. The description of experimental data by the Langmuir adsorption isotherm or the corresponding von Szyszkowski surface tension equation often shows significant deviations. These equations can be derived for a surface layer model where the molecules of the surfactant and the solvent from which the molecules adsorb obey two conditions:
(i) no interaction between adsorbed molecules
(ii) equal molar areas at the interface.
In a number of cases, deviations from the Langmuir behavior can be explained by an invalidity of the former condition, for example by the presence of interactions between adsorbed molecules or differences in the molecular areas.
The adsorption isotherm and equation of state for adsorption layers proposed by Frumkin [66] describe the adsorption of low molecular weight surfactants rather well, provided the systems under investigation deviate only slightly from an ideal (Langmuir) behavior. Reasonable agreement between theory and experiment was found when interactions between all components in the system were taken into consideration [67,68,69]. However, the intermolecular interaction parameters which can be estimated from a comparison of experimental data and model isotherms do not always correlate with the properties of the surfactants or solvents. Often they have to be regarded simply as matching parameters. A better understanding of the physical reasons for deviations between experimental data and theoretical models should result from new models for the adsorption isotherm and the corresponding equation of state. Such new models should account for the effects of, e.g., the size of the surfactant or protein molecules, molecular reorientation within the surface, dimerisation, cluster formation, etc.

CHAPTER 2

Theory

2.1 Chemistry of surfactants and polymers

Surfactants are amphiphilic substances which adsorb and by that decrease the surface (interfacial) tension. In some literature, the word "surfactant" is used for all kind of molecules that are surface active, including low and high molecular-weight substances. Here we will use the terminology "surfactant" just for low molecular-weight surface active substances that, in a more specific sense, possess an asymmetric molecular structure. On the other hand, polymers, polyelectrolytes and proteins belong to the high molecular-weight group of substances characterized by some other more specific properties.

Generally, surfactants consist of two parts, which possess properties opposite to each other by their nature. One part of the molecule is the hydrophilic polar head group, for example, $-NH_2$, -OH, -COOH, $-SO_3H$, $-OSO_3H$, -COOMe, $-OSO_3Me$, $-N(CH_3)_3Cl$, $-CH_2CH_2O$. The other part is formed by a rather long hydrocarbon or hydrofluorine hydrophobic (oleophilic) chain. In contrast, high molecular-weight surfactants can contain alternating hydrophilic and hydrophobic molecular groups distributed along the whole molecule chain.

According to the chemical nature, surfactants can be divided into two major groups – non-ionic and ionic surfactants which consist of a long-chain (surface active) ion and an ordinary inorganic counter ion. The non-ionic surfactants contain polar groups consisting of atoms of oxygen, nitrogen, phosphorus or sulphur (alcohols, amines, ethers etc.). These polar groups are unable to dissociate and possess a significant affinity to water and other polar substances. Contrary to this, ionic surfactants can be represented by anionic and cationic surfactants depending on the sign of the charge of the polar head group. A more detailed categorization of ionic surfactants will be presented further below.

Among the anionic surfactants, the most significant are salts of fatty acids (RCOOMe), alkyl sulphates (sulphoether salts) $ROSO_3Me$, alkyl sulphonates RSO_3Me, alkyl aryl sulphonates $RC_6H_5SO_3Me$, alkyl phosphates $ROPO(OMe)_2$, salts of sulphosuccinic acids. The typical surfactants which belong to this class are sodium dodecyl sulphate (SDS), sodium oleate and sodium dodecyl benzene sulphonate.

Among the cationic surfactants, the most common are the salts of (primary, secondary and tertiary) amines, and quaternary salts of ammonium, for example, cetyl trimethyl ammonium bromide (C_{16}TAB) and octadecyl pyridinium chloride.

2.1.1 Surface properties of surfactants and polymers

The tendency of molecules to adsorb at interfaces in an oriented direction is one of the most interesting and important properties of surfactants. The adsorption has been studied largely [70,71,72] to determine the surfactant excess concentration at the interface, the orientation of the molecules at the interface, the efficiency of adsorption and energy changes in the system resulting from the adsorption. The most useful method to study surface phenomena in an aqueous system is the measurement of changes in the values of the surface tension of aqueous surfactant solutions.

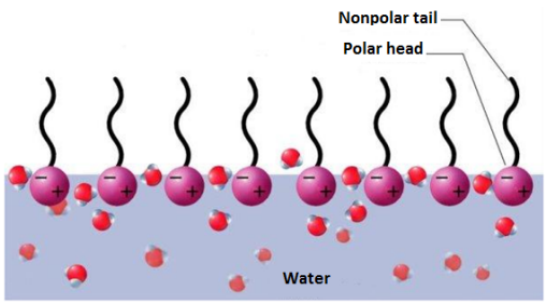

Figure 1. Surfactant molecules at water surface. Picture was taken from Wikipedia.com [73].

In this thesis we have used theoretical models, explained in the following part, to describe the results of surface and interfacial tension measurements of aqueous surfactant and polymer solutions at the water/air and water/oil interfaces, respectively. In this way it is possible to accurately determine the physical properties of the surfactants in the adsorption layer. Using the most simple theoretical model, the Langmuir adsorption model, it is possible to determine the adsorption constant b and the maximum adsorption Γ_∞. The adsorption constant b is a measure of the surfactant's surface activity or tendency to adsorb at an interface. The maximum adsorption Γ_∞ represents the surface concentration of the surfactant at the interface. It is also possible to define the surface coverage by surfactants, θ, and the molar area of the adsorbed molecules, ω. If the compressibility of the adsorbed layer ε is taken into account the molar area depends on the surface pressure and it changes with the surface coverage.
Another, more complex model is the Frumkin adsorption model, which considers the interaction between molecules at the interface expressed via the intermolecular interaction constant *a*. The newer version of the Frumkin adsorption model gives the option to take into account added electrolyte ions together with the surfactant ions and counterions, if the experiment is performed in salt solution.
For some surfactants the molecules in the adsorption layer can change their orientation with increasing surface coverage leading to a transition from a state of larger to one with a smaller molar interfacial area. The behavior of such surfactants is described most precisely by the so-called Reorientation model, where two different molar areas ω_1 and ω_2 are taken into account, presenting the two states of molecules at the interface with different molecular orientations.
Surface properties of the high molecular-weight substances depend on the structure of the molecules, i.e. on the order of the active groups in the molecule. Therewith, pluronic as a non-ionic triblock copolymer consisting of poly(ethylene oxide) and poly(propylene oxide) blocks, adopts different conformations as adsorption increases. The layer structure changes from a two-dimensional flat structure to a brush-like structure.

2.1.2 Bulk properties of surfactants and polymers

Surface active agents, as mentioned above, are compounds that reduce the surface tension of aqueous solutions. Note that a surface activity also exists in non-aqueous media, but the extent of surface tension reduction is generally much less. The discussion given here is dedicated just to aqueous systems.
Surfactants are broadly classified into five categories, based on the charged structure of their hydrophilic "head" groups: anionic, cationic, nonionic, amphoteric and zwitterionic surfactants. Other, more exotic, types of surfactants have also been identified, such as gemini surfactants, consisting of two single-tail surfactants whose heads are connected by a hydrophilic or hydrophobic spacer chain. Another example is the telechelic surfactant, in which two hydrophobic groups are connected by a hydrophilic chain. Bolaform surfactants, on the other hand, are hydrophobic chains with hydrophilic groups on each end.
With increasing bulk concentration of a surfactant the surface tension of the solution decreases until it reaches the point where it shows essentially no further decrease but a constant value, as one can see in Fig. 2. The concentration, at which the flat part of the curve starts, is called "critical micelle concentration" (CMC). Here the surfactant molecules in the bulk are organized in aggregates, called micelles (see Fig. 3). This process is driven by the tendency of any system to reach a state of less free energy. At about the same concentration, many other properties of the solution also show sharp breaks in slope, as shown schematically in Fig. 4.
The precise size and shape of micellar aggregates differ from case to case, but quite often they are spherical and contain a few tens to hundreds of monomer units each. The CMC is a characteristic concentration of each surfactant at a given solution state, i.e. at well defined T, p, and $C_{\text{additional solutes}}$.
If the concentration of the surfactant molecules is much larger than the CMC, more complex surfactant's self-assembled structures might appear, depending on the critical packing parameter

CPP, such as cylindrical micelles, curved bilayers, unilamellar vesicles and tubules, bicontinuous structures of zero mean curvature, normal hexagonal and lamellar phases.

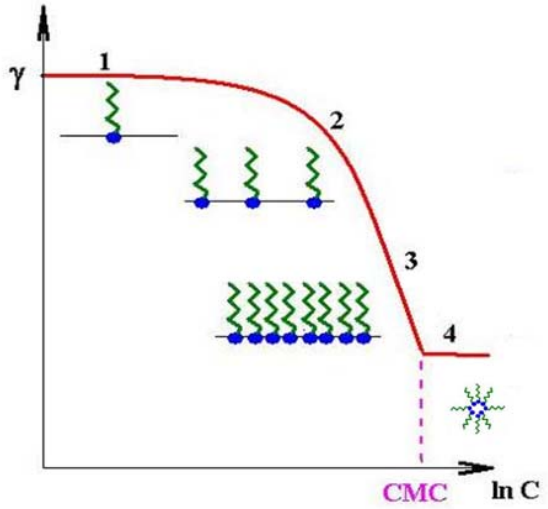

Figure 2. Adsorption isotherm of low-molecular weight surfactants.

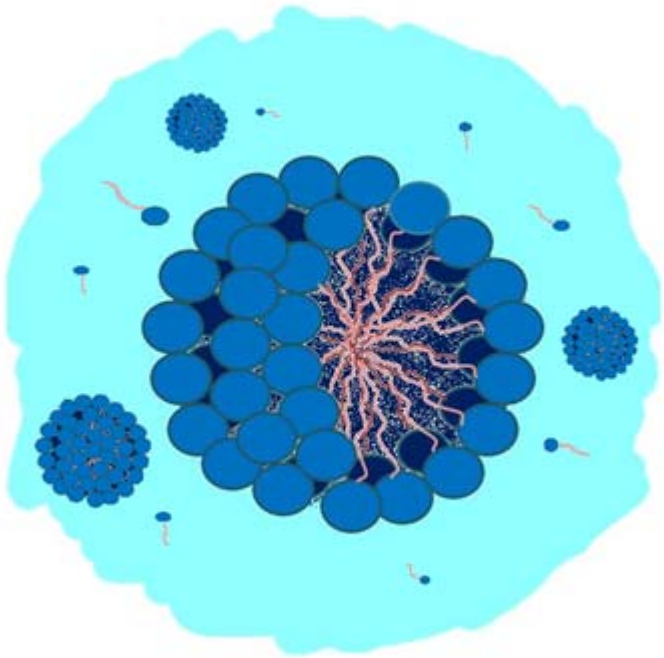

Figure 3. Spherical micelle in water.

Depending on the composition of the polar and non-polar parts in a polymer, different polymer structures can be obtained in the aqueous bulk phase. Generally, the polar groups are exposed to the aqueous phase, while non-polar parts are “hidden” in the coil of a globular macro-molecule. On the other hand, polyelectrolytes do not include non-polar parts in the structure and therefore they are not surface active. Their structure is linear in the bulk. However, by adding surfactant in the electrolyte aqueous solution, different bulk and surface conformations of the electrolyte-surfactant complex can be obtained depending on the surfactant concentration.

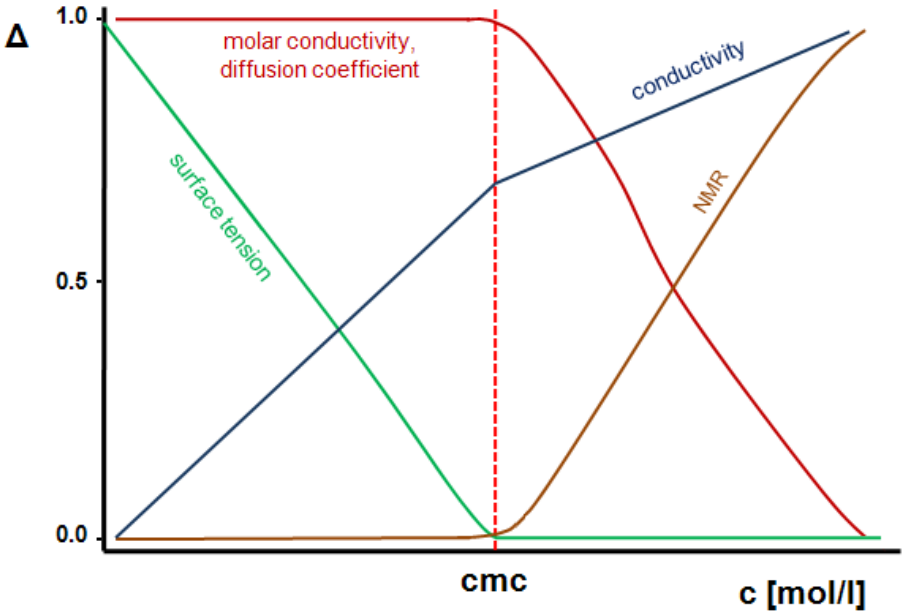

Figure 4. Different methods for CMC determination.

2.2 The Gibbs dividing surface and adsorption

In a multi-component two-phase system, the various components do not distribute themselves uniformly at equilibrium among the two phases of the system. It is evident that the concentration of each surface active component in one of the two bulk phases is higher than in the other bulk phase, and that it is particularly high in the interfacial region (Fig. 5). The figure also shows a representation of the solute concentration profile through the interfacial region.

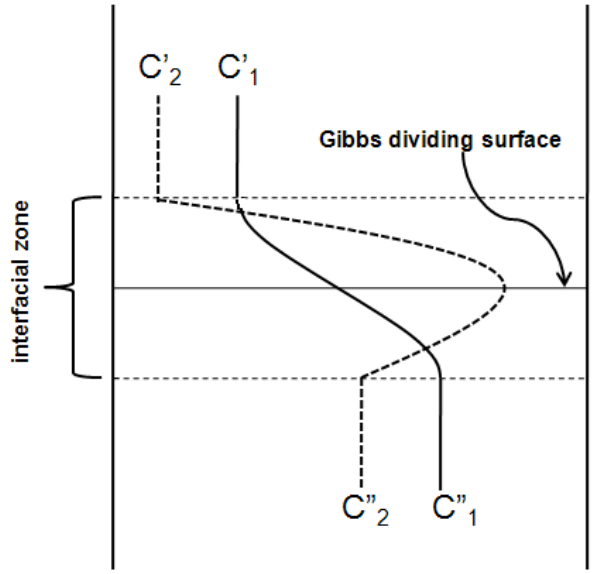

Figure 5. Gibbs dividing surface drawn in a binary liquid-gas capillary system. The bulk phase concentrations of the species are C'_1, C''_1, C'_2 and C''_2.

Gibbs replaced the interfacial layer by a (zero-thickness) “dividing surface”, oriented normal to the density gradient in the interfacial zone. Note that the Gibbs dividing surface is not applicable for describing the mass distribution in systems comprised of two pure components.

For a binary system, writing the material balance for the solvent and solute components, it is possible to determine the components' surface excesses per unit interfacial area, Γ_1 and Γ_2, respectively:

$$\frac{\Gamma_{2,1}}{\Gamma_1} = \frac{\Gamma_2}{\Gamma_1} - \left(\frac{C_2^{''}}{C_1^{''}}\right) \tag{1}$$

for $C_1^{'} << C_1^{''}$

$C_2^{'} << C_2^{''}$

where $\Gamma_{2,1}$ is the relative adsorption of component 2 with respect to component 1.

At equilibrium, the interfacial tension, the surface concentration and the composition of the adjacent bulk phases are related through the Gibbs adsorption equation. Its derivation is purely thermodynamic and can be regarded as the two-dimensional analogue to the Gibbs-Duhem equation (2).

$$A d\gamma + S^{\sigma} dT + \sum_i n_i^{\sigma} d\mu_i = 0 \tag{2}$$

$$d\gamma = -S_a^{\sigma} dT - \sum_i \Gamma_i d\mu_i \tag{3}$$

where γ is the surface tension, S the entropy, T the absolute temperature, A the interfacial area, Γ the surface concentration, μ_i the chemical potential of the i[th] component, and n_i the number of moles. The summation in (2) and (3) includes all components, except the solvent, for which the surface concentration is set to zero according to the Gibbs convention for positioning the dividing surface as the location of the interface. At constant temperature we obtain

$$\mathrm{d}\gamma = -\sum_i \Gamma_i \mathrm{d}\mu_i \tag{4}$$

If the relation between two of the variables is known, the third one can be calculated using the Gibbs equation. For example the adsorption isotherm gives the relation between the surface concentration and bulk composition, $\Gamma_i(X_i)$ from which the interfacial tension can be derived. For fluid interfaces the Gibbs adsorption equation is often used to establish adsorbed amounts from the experimentally determined dependency of γ on Xi, where $X_i \equiv n_i \Big/ \sum_i n_i$.

Another, more common way to write the Gibbs adsorption equation is obtained when the adsorbed amount of solvent molecules is taken equal to zero and only the adsorbed amount of the solute Γ is considered.

$$\Gamma = -\frac{1}{\mathrm{RT}} \frac{\mathrm{d}\gamma}{\mathrm{d}\ln \mathrm{c}} \tag{5}$$

2.3 Surface and interfacial tension

Everyday experience reveals that a fluid interface wants to contract in order to assume a minimum area, subject to whatever constraints are put upon it. This is the result of the surface tension acting at the surface. The first definition of the surface tension γ was proposed by Thomas Young as "Young's membrane model" in 1805. This was a mechanical definition of γ as a scalar quantity with units of force/length. In the bulk of a liquid each molecule is surrounded by identical neighbors and the sum of all short and long range forces acting at any point in the bulk is the same, i.e. the net force is zero. At the surface of the liquid, molecules have different neighbors. These molecules are being pulled inwards by the molecules from the denser bulk phase, but they are less attracted by the molecules from the neighboring less dense phase (air or another liquid). Therefore all molecules at the surface are subject to an inward force of molecular attraction which can be balanced only by the resistance of the liquid to compressions. For any homogeneous composition of a fluid interface the

surface tension is uniform. The macroscopic mechanical model of a fluid interface is thus a zero-thickness membrane. The units of surface tension, force/length, are the same as those of an energy (or work) per unit area. Hence, surface tension can also be interpreted in terms of a mechanical energy required to create new area of a liquid surface.
As stated above, the terminology “surface tension” is usually reserved for the tension observed at a liquid/gas interface, whereas “interfacial tension” is used in reference to all kinds of interface, but in the present context to liquid/liquid interfaces. The same molecular picture developed above explains the existence of the interfacial tension between two liquids too. If two liquids are immiscible and form an interface, the molecules of each bulk phase prefer to stay together rather than to mix. On the molecules at the interface the interactions with the molecules of the two phases are asymmetric, resulting in interfacial tension. The values of the interfacial tension for each water/oil system differ from each other, depending on the nature, but mainly on the polarity of the oil.

2.4 Thermodynamic adsorption models

The first real adsorption model for surfactants at liquid interfaces as proposed by Langmuir was originally developed for the gas adsorption at solid surfaces [74]. Later Frumkin showed that the additional assumption of an interaction between molecules in the adsorption layer can improve the agreement between the theory and experimental data. Although refinements have been recently published reflecting some specific features of adsorbed surfactant molecules, as described in detail elsewhere [75], in many cases the Langmuir model is still used by many authors. This rather simple model is at least acceptable when semi-quantitative evaluations are needed. An accurate analysis of experimental data should of course be done on the basis of an optimum model for the respective studied surfactant.

2.4.1 Langmuir adsorption model

The adsorption isotherm for the Langmuir model [76] reads:

$$\Gamma = \Gamma_\infty \frac{bc}{1+bc} \tag{6}$$

and the corresponding Szyszkowski-Langmuir equation of state has the form

$$\gamma_o - \gamma = \Pi = -RT\Gamma_\infty \ln(1-\frac{\Gamma}{\Gamma_\infty}) = RT\Gamma_\infty \ln(1+bc) \tag{7}$$

Here γ_0 is the interfacial tension in the absence of surfactant, c is the surfactant bulk concentration, Π is the surface pressure γ_0-γ, R and T are the gas law constant and absolute temperature, respectively, Γ_∞ is the maximum adsorption, and b is the adsorption constant with the dimension of a reciprocal concentration. The physical idea behind this model is a localized adsorption layer where each molecule requires a certain area at the interface.

2.4.2 Frumkin adsorption model

The Frumkin adsorption isotherm and the corresponding equation of state are given in the following form [77]:

$$bc = \frac{\theta}{1-\theta}\exp(-2a\theta) \tag{8}$$

$$-\frac{\Pi\omega_0}{RT} = \ln(1-\theta) + a\theta^2 \tag{9}$$

where *a* is the intermolecular interaction constant, θ is the surface coverage by surfactant molecules, θ = Γω, and ω is the molar area of the adsorbed molecule. If the compressibility of the

adsorbed layer is additionally taken into account then the molar area is considered to depend on the surface pressure $\omega = \omega_0(1 - \varepsilon\Pi\theta)$, where ω_0 is the molar area of a solvent molecule, and ε is the two dimensional compressibility coefficient [78].

2.4.3 Reorientation model

For some surfactants the molecules in the adsorption layer can change their orientation upon increasing the surface coverage to that with smaller molar area. The behaviour of such surfactants is described most precisely by the so-called Reorientation model [79]:

$$b_1 c = \frac{\Gamma_1 \omega_{10}}{(1-\theta)^{\omega_1 / \omega_{10}}} \exp\left(-\frac{\omega_1}{\omega_{10}}(2a\theta)\right) \tag{10}$$

$$-\frac{\Pi \omega_{10}}{RT} = \ln(1-\theta) + \Gamma(\omega - \omega_{10}) + a\theta^2 \tag{11}$$

$$\omega\Gamma = \theta = \omega_1\Gamma_1 + \omega_2\Gamma_2 \tag{12}$$

$$\Gamma = \Gamma_1 + \Gamma_2 \tag{13}$$

$$\frac{\Gamma_2}{\Gamma_1} = \left(\frac{\omega_2}{\omega_1}\right)^{\alpha} (1-\theta)^{\frac{\omega_2 - \omega_1}{\omega_{10}}} \exp\left[\frac{\omega_2 - \omega_1}{\omega_{10}}(2a\theta)\right] \tag{14}$$

$$\omega_1 = \omega_{10}(1 - \varepsilon\Pi\theta) \tag{15}$$

where indices 1 and 2 correspond to the two states with different molecular orientations and therefore with different molar areas. Eq. (15) accounts for the surface compressibility of the state with smaller molar area.

2.5 Dynamic adsorption models

2.5.1 Ward and Tordai equation

Assumed the adsorption process is diffusion controlled, the kinetics is given by the equation derived by Ward and Tordai for a flat interface [80]:

$$\Gamma(t) = \sqrt{\frac{4D}{\pi}}\left[c_0\sqrt{t} - \int_0^{\sqrt{t}} c_s(t-\tau)\,d\sqrt{\tau}\right] \tag{16}$$

where c_0 is the bulk concentration of surfactant and c_s is the so-called subsurface concentration related to the adsorption Γ through the adsorption isotherm, for example, Eq. (6). The equation (16) was later extended to the case of adsorption at a spherical interface of radius r as [2]

$$\Gamma(t) = \sqrt{\frac{4D}{\pi}}\left[c_0\sqrt{t} - \int_0^{\sqrt{t}} c_s(t-\tau)\,d\sqrt{\tau}\right] \pm \frac{D}{r}\left[c_0 t - \int_0^{t} c_s(t-\tau)\,d\tau\right] \tag{17}$$

The plus sign in Eq. (17) corresponds to adsorption from outside the droplet. The short time approximation useful to describe the very beginning of the adsorption process is

$$\Gamma(t) = 2c\sqrt{\frac{Dt}{\pi}} + \frac{cDt}{r} \tag{18}$$

The quantitative solution of the Ward-Tordai equation has been discussed for example in [81].

As is obvious from Eq. (16), the adsorption of the surfactant molecules depends on the bulk concentration c_0. Once $\Gamma(t)$ has been obtained, the corresponding dynamic interfacial tension is calculated via the corresponding equation of state, for example, Eq. (7).

2.5.2 Lucassen and van den Temple model

Another important concept for characterising the adsorption dynamics is the surface dilational visco-elasticity modulus, which displays the response of the interfacial tension upon compression or expansion of the interfacial area [82]:

$$E = \frac{d\gamma}{d\ln\Gamma}\frac{d\ln\Gamma}{d\ln A} \tag{19}$$

The modulus can be presented as a complex quantity where the real part represents the surface elasticity and the imaginary part the surface viscosity. The first factor in the r.h.s. of Eq. (19) is called the limiting Gibbs elasticity corresponding to the high frequency limit when the surfactant layer behaves like an insoluble monolayer. Using the same Langmuir adsorption model, the high frequency limit of the elasticity is given by

$$E_0 = \frac{d\gamma}{d\ln\Gamma} = RT\Gamma_\infty bc \tag{20}$$

The dilational visco-elasticity, measured at a certain frequency $f = \omega/2\pi$, was presented for a diffusional exchange of matter by Lucassen and van den Temple [83, 84] in a complex form via

$$E(i\omega) = E' + iE'' = E_0\frac{\sqrt{i\omega}}{\sqrt{i\omega}+\sqrt{2\omega_0}} \tag{21}$$

Here E′ and E″ are the real and imaginary parts of E, corresponding to the elastic and viscous parts of the dilational visco-elasticity, respectively:

$$E'(\omega) = E_0\frac{1+\sqrt{\omega_0/\omega}}{1+2\sqrt{\omega_0/\omega}+2\omega_0/\omega} \tag{22}$$

$$E''(\omega) = E_0\frac{\sqrt{\omega_0/\omega}}{1+2\sqrt{\omega_0/\omega}+2\omega_0/\omega} \tag{23}$$

These equations contain the key parameter ω_0 which is the characteristic frequency of the diffusional matter exchange

$$\omega_0 = \frac{D}{2}(dc/d\Gamma)^2 \tag{24}$$

It includes in turn the adsorption activity of the surfactant $dc/d\Gamma$ and corresponds to the slope of the adsorption isotherm.

CHAPTER 3

Experimental section

3.1 Materials

3.1.1 Surfactants

The main substances investigated in this thesis are members of the homologous series of alkyl trimethylammonium bromides, i.e. decyl trimethylammonium bromide C_{10}TAB (MW = 280.29 g/mol, purity ≥ 98%), dodecyl trimethylammonium bromide C_{12}TAB (MW = 308.35 g/mol, purity ≥ 99%), hexadecyl trimethylammonium bromide C_{16}TAB (MW = 364.46 g/mol, purity ≥ 99%) purchased from Fluka (Switzerland), and tetradecyl trimethylammonium bromide C_{14}TAB (MW = 336.40 g/mol, purity 99%) purchased from Aldrich. The surfactants were purified by triple re-crystallization in ethanol and acetone. All surfactant solutions were prepared in phosphate buffer NaH_2PO_4/Na_2HPO_4 (10mM, pH7) purchased from Fluka with a purity ≥ 99%, using ultrapure Milli-Q water (resistivity = 18.2 MΩcm).
Sodium dodecyl sulphate, SDS, was used in experiments purified or not depending on where this was required due to the specificity of the experiments. SDS was purchased from Fluka with purity ≥ 99%. The solutions were prepared in 10mM aqueous phosphate buffer solution, pH 7, using Milli-Q water. Dodecanol (Fluka, ≥ 99%) was used in the experiments to mimic the natural impurities in aqueous SDS solution, where SDS hydrolyses to dodecanol and sulfuric acid salt.

3.1.2 Macromolecules

Pluronics are symmetric non-ionic triblock copolymers of the form $(PEO)_x$-$(PPO)_y$-$(PEO)_x$, where PEO and PPO are the oxyethylene and oxypropylene units, respectively. The Pluronic L64 and F68 were purchased from Sigma-Aldrich, whereas Pluronic P9400 was provided by BASF. All Pluronics were used without further purification. The block copolymers have been chosen to form two pairs, one of them (L64 and P9400) with the same percentages of PEO and PPO, 40% (w/w) and 60% (w/w), respectively, and increasing average molecular weight, and the other pair with the same number of PPO units and increasing number of PEO ones (L64 and F68), which results in a larger average HLB (15 to > 24). The solutions studied were prepared with ultrapure Milli-Q water.
Polyallylamine hydrochloride (PAH) is a cationic polyelectrolyte prepared by polymerization of allylamine. In our experiments we used PAH with a molecular weight of MW = 56000 g/mol, purchased from Aldrich. The properties of polyelectrolyte/surfactant complexes depend on their preparation and can drastically change with the mixing protocol [85]. To prepare polymer/surfactant complexes in these experiments polymer and surfactant stock solutions of respective concentrations were diluted and mixed with each other and kept in an ultrasonic bath for 30 min. Freshly prepared solutions were kept for 24h and then used for the measurements.

3.1.3 Oil phase

The experiments were performed at water/oil and water/oil vapor interfaces, where different alkanes were chosen as the oil phase. Hexane was purchased from Fluka (Switzerland), heptane, octane, nonane, decane from ACROS Organics, and dodecane and tetradecane from Alfa Aesar. The oils were distilled and purified with Florisil. According to [86] the interfacial tensions at 25°C for the water/hexane interface is 51.1 mN/m, water/heptane interface 51 mN/m, water/octane interface 51.2 mN/m, water/nonane interface 51.5 mN/m, water/decane interface 52 mN/m, water/dodecane interface 51.9 mN/m and water/tetradecane interface 52.2 mN/m. Dimeticone used in the application example is a free trade name for a silicon oil (Polydimethylsiloxane) which is

common used in cosmetics e.g. in skin-moisturizing lotions and has been provided by Beiersdorf, Germany.

3.2 Methods

3.2.1 Capillary Pressure Tensiometry

The method of capillary pressure tensiometry was developed with the availability of fast computers and liquid proofed electronic pressure sensors, which practically allow measurements of dynamic interfacial tensions between two immiscible liquids. It is a modern technique built up on the basic principle of the bubble pressure technique, which however, is dedicated only to liquid/gas interfaces.

The main part of the instrument is the pressure sensor which measures the pressure in a drop. From this pressure, the interfacial tension can be calculated when the radius of curvature of the measured liquid drop is known. For spherical drops the radius of curvature is identical to the drop radius and can be determined from the video image of the drop. The method is established very well now [87] and allows to record changes of the interface tension with time in a time window down to few milliseconds [88,89]. There are several protocols for investigating the adsorption dynamics from capillary pressure experiments. The two most frequently used protocols are the continuously growing drop/bubble [90,91,92,93] and the fast expanding drop [94,95,96] methods. In addition, this methodology is obviously the only one that works at small Bond numbers, e.g. for interfaces between two liquids having a similar density, or under microgravity conditions [97]. This method also allows looking into spherical foam or emulsion films as it was proposed for example by Soos et al. [98] and others [99, 100, 101] to study directly the film tension or the film visco-elasticity. An important additional feature of the capillary pressure tensiometer is the option of generating high frequency oscillations of small spherical drops/bubbles (ODBA) for determining the dilational visco-elasticity of interfacial layers over a broad frequency range. The device ODBA contains a piezo drive for exact size control of a small droplet (0.01 to 1 mm^3, depending on the capillary tip size and solution properties) with an accuracy of 0.0001 mm^3 (100 pl) and low amplitude oscillations in the frequency range of 0.1 to 300 Hz. During the generation of precise oscillations the pressure variations are recorded via an accurate relative pressure sensor as a function of time. This signal contains the capillary pressure contribution along with hydrostatic pressure and hydrodynamic effects. The hydrodynamic effects are negligible for low frequencies, however, they can be very significant for high frequencies depending on the applied piezo amplitude, fluid viscosities, capillary tip size and capillary/cell geometry.

The schema of the set-up is shown in Fig. 6 and a photo in Fig. 7. The used capillary pressure tensiometer (ODBA) has been developed as an additional module for the profile analysis tensiometer (PAT-1) (both from Sinterface Technologies, Germany). In Fig. 6 it is seen that beside the pressure sensor (PDCR-4000, GE-DRUCK, Germany) and the piezoelectric translator (P-843.40 Physik Instrumente, Germany) the instrument contains a syringe dosing system (ILS, Stützerbach, Germany) for a rough manual drop/bubble formation and manipulation.

The surface/interfacial tension is determined from the classical Gauss-Laplace equation for capillary pressure (25) that describes the mechanical equilibrium conditions for two homogeneous fluids separated by an interface.

$$\frac{2\gamma}{R} = \Delta P \qquad (25)$$

It relates the pressure difference ΔP across a curved interface to the surface tension γ and the radius of curvature R of the interface.

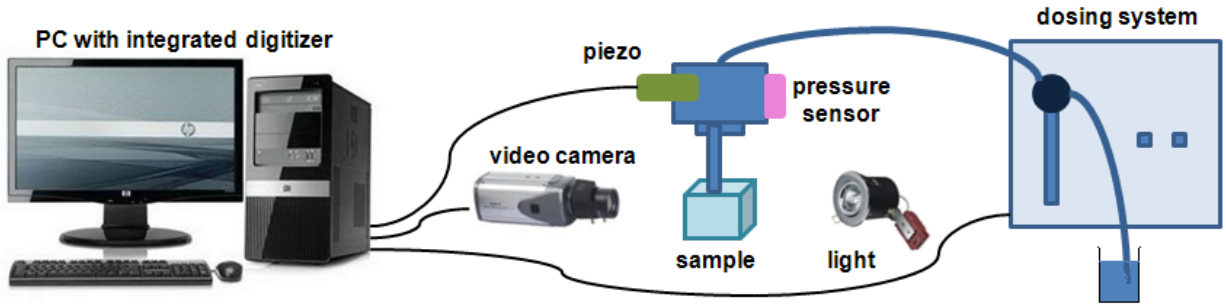

Figure 6. Set-up of the Capillary Pressure Analyzer (SINTERFACE Technologies, Germany).

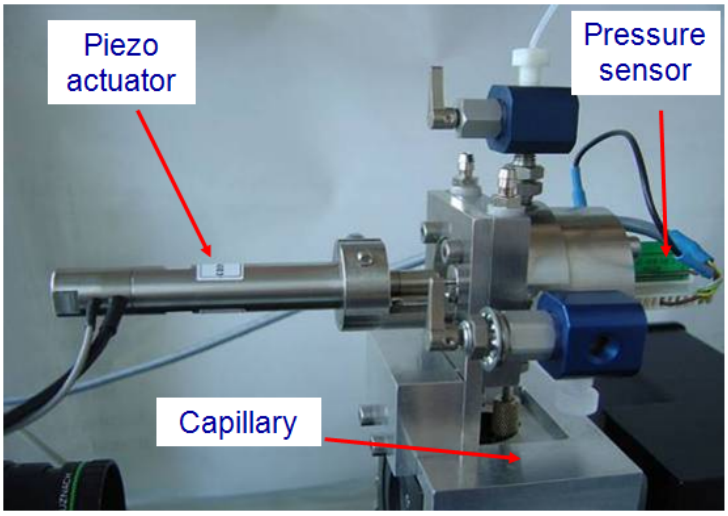

Figure 7. Photo of the Capillary Pressure Analyzer module (SINTERFACE Technologies, Germany).

3.2.2 Profile Analysis Tensiometry (PAT)

The drop and bubble profile analysis tensiometer requires only very small amounts of liquid, just enough to form one drop. It is suitable for liquid-gas, liquid-vapor and liquid-liquid interfaces, and applicable to systems ranging from molten metals to pure organic solvents and diluted and concentrated solutions. There is also no limitation on the magnitude of surface or interfacial tension [102]. For measurements at constant interfacial area the time window ranges from about one second up to hours and days so that even extremely slow processes can be easily followed. There is an option to generate a periodic perturbation of the drop surface area, in order to measure surface (or interfacial) dilational rheology. The frequency window spans over some decades in the low frequency range, i.e. frequencies below 0.2 Hz. At faster oscillations, a frequency threshold appears when the drop/bubble profile is no more in mechanical equilibrium.

The principle of this method is based on analyzing the shape of the drop or bubble, whereas this shape is determined by the influence of two oppositely acting forces. One is the surface tension that tends to make drops spherical, and the other is gravity, which works in opposite direction tending to elongate the drop/bubble. The scheme of the profile analysis tensiometer is shown in Fig. 8.

The set-up integrates a dosing system and a thin capillary at the tip of which the drop or bubble is formed. Then, via a video camera equipped with an objective an image of the drop is taken. The system is completed by a light source and a frame grabber to digitize and transfer the image to a PC.

During the experiment performed on PAT, the camera is taking images of the drop of the investigated solution, the shape of which is fitted with the respective Laplace equations, as schematically shown in Fig. 9. The same procedure works also for an air bubble immersed into liquid. This technique is called ADSA (Axisymmetric Drop Shape Analysis) which provides an algorithm for minimizing a target function representing the deviation of the experimental profile from the

theoretical one. This target function is actually the sum of the squares of the normal distances between the experimental points and the calculated curve. As input parameters the coordinate points along the drop profile are needed, the value of the density difference across the interface, the gravitational constant and the distance between the base of the drop and the horizontal coordinate axis. The output parameters received from ADSA are: the interfacial tension, the contact angle, the drop surface area, the drop volume and radius of curvature.

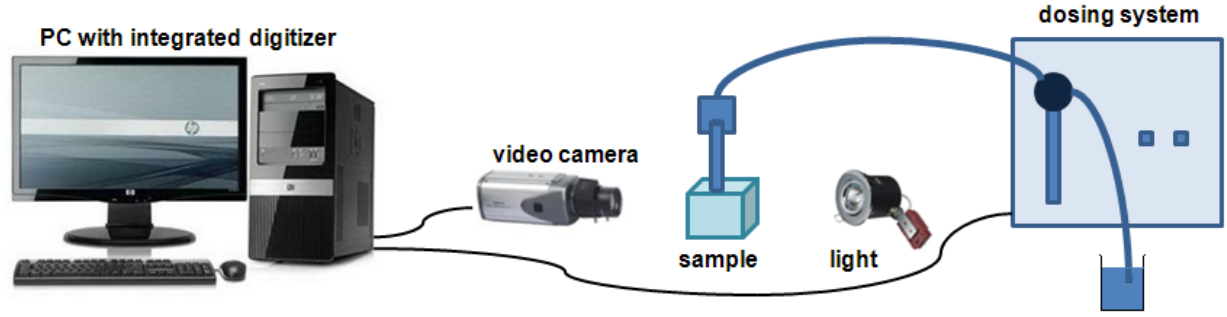

Figure 8. Set-up of the Profile Analysis Tensiometer, PAT-1 (SINTERFACE Technologies, Germany).

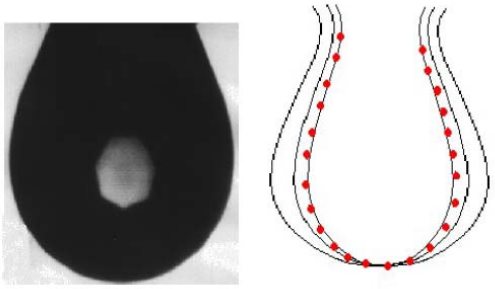

Figure 9. Picture of a pendant drop and a representation of a family of theoretical curves fitting the experimental points.

For an axisymmetric drop the Laplace equation of capillarity can be written in a parametric form:

$$\frac{dx}{ds} = \cos\Theta$$

$$\frac{dz}{ds} = \sin\Theta$$

$$\frac{d\Theta}{ds} = \frac{1}{R_1} = \frac{2}{b} \pm cz - \frac{\sin(\Theta)}{x}$$

$$\frac{dV}{ds} = \pi x^2 \sin\Theta$$

$$\frac{dA}{ds} = 2\pi x$$

$$x(0) = z(0) = \Theta(0) = V(0) = A(0) = 0$$

where *s* is the arc length (Fig. 10), *x* and *z* are the coordinates of the drop profile, R_1 is the radius of curvature at (x, z), *b* is the radius of curvature at the apex (0, 0) and c=($\Delta\rho$)g/γ is the capillary constant of the system. θ is the tangential angle, which for sessile drops becomes the contact angle at the three phase contact line.

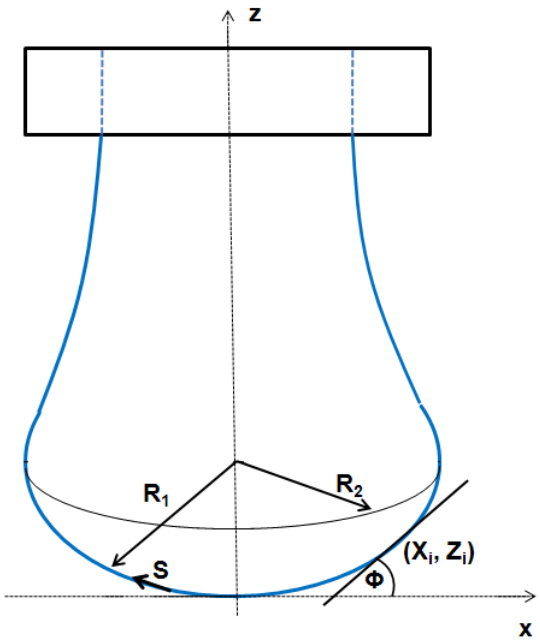

Figure 10. Definition of drop coordinates in three dimensions.

To solve the above set of equations a numerical integration scheme is required. One of the most efficient and flexible numerical methods is the fifth and sixth order Runge-Kutta-Verner integration algorithm [103].

In the following the new principle of water/vapor experiments performed on PAT will be briefly explained. A drop is formed in a closed cuvette (3cm × 3cm × 3cm) and after a certain time (typically 300 s) a defined amount of alkane is injected to the bottom of the cuvette. The cell is closed such that after a few minutes a saturated hexane vapor atmosphere is established. No extra pressure in the cell after drop formation or alkane injection is expected. Further, the interfacial tension is measured as explained in the text above.

CHAPTER 4

Results and discussion

The results briefly discussed in this section have been the subject of publications in peer reviewed journals. The details of each publication are not repeated here but only the respective main subjects and some selected results. All details are given in the copies of the manuscripts or reprints attached further below.
The results enclosed in the PhD thesis can be divided into two parts, the thermodynamics of surfactant adsorption layers, as one part, and kinetics and rheology of surfactants adsorption layers, as second part. Generally in these experiments we used common surfactants, such as alkyl trimethylammonium bromides and sodium dodecyl sulphate. Another part of the investigations were dedicated to macromolecules, such as Pluronics and polyallylamine hydrochloride (polyelectrolyte).

4.1 Thermodynamics of surfactant adsorption layers

It is essential to know the influence of impurities on surfactant adsorption properties (Paper 1). Because of its chemical structure, dodecanol is surface active and tends to adsorb at water surfaces, which in general disturbs the adsorption of SDS particularly at the water/air interface. On the contrary, at the water/hexane interface dodecanol transfers to the hexane phase and does not leave any remarkable effect on the interfacial pressure.
It was found in Paper 2 that at the water/oil interface, the adsorption of the studied surfactant starts at lower concentrations than at the water/air interface. Due to the affinity of the hydrophobic chain for the oil phase, the surfactants interact with the alkane molecules located at the interface which favors their adsorption.
At high surface coverage, it is seen that for C_{12}TAB, C_{14}TAB and C_{16}TAB the surfactants´ adsorbed amounts Γ and molar areas ω at the water/hexane interface are similar to those at the water/air interface. Thus, for these surfactants at high surface coverage there are no oil molecules intercalating into the adsorption layers at the water/hexane interface. For C_{10}TAB at high surface coverage Γ becomes higher at the water/air interface than at the water/hexane interface, meaning that a kind of competitive adsorption between this short chain surfactant C_{10}TAB and the hexane molecules takes a place.
The interfacial tension measurements have been performed for C_{10}TAB and C_{12}TAB surfactants also at the interfaces between water and different alkanes (Paper 3), including heptane, octane, nonane, decane, dodecane and tetradecane interfaces, respectively. For the sake of simplicity and easy understanding, the physics behind these results is schematically presented in Table 1. Note, the scheme corresponds to the state of closest packing, i.e. close to the CMC of each surfactant.
At high surface coverage, the behavior becomes a function of not just the surfactant's chain length, but of the length of the alkane molecules too. It was found that for surfactants with a short alkyl chain (C_{10}TAB), the interactions between surfactant and oil molecules dominate the mutual surfactant interaction so that finally oil molecules are embedded in the C_{10}TAB adsorption layer. This is the case for all oils measured in this thesis. On the other hand, the next surfactant in the homologous series (C_{12}TAB) shows different behavior at the various water/oil interfaces. Here it is found that at the interfaces of water against hexane, heptane, octane, nonane and decane, the mutual surfactant interactions are stronger than between surfactant and oil molecules, so that, in general the oil molecules are squeezed out from the surfactant adsorption layers with increasing surfactant concentration. The oil molecules with longer alkane chains, i.e. dodecane and tetradecane, interact with the surfactants at the interface and at high surface coverage stay embedded into the surfactant adsorption layer.

Table 1: Scheme of the molecular interactions between different chain lengths surfactant and oil molecules.

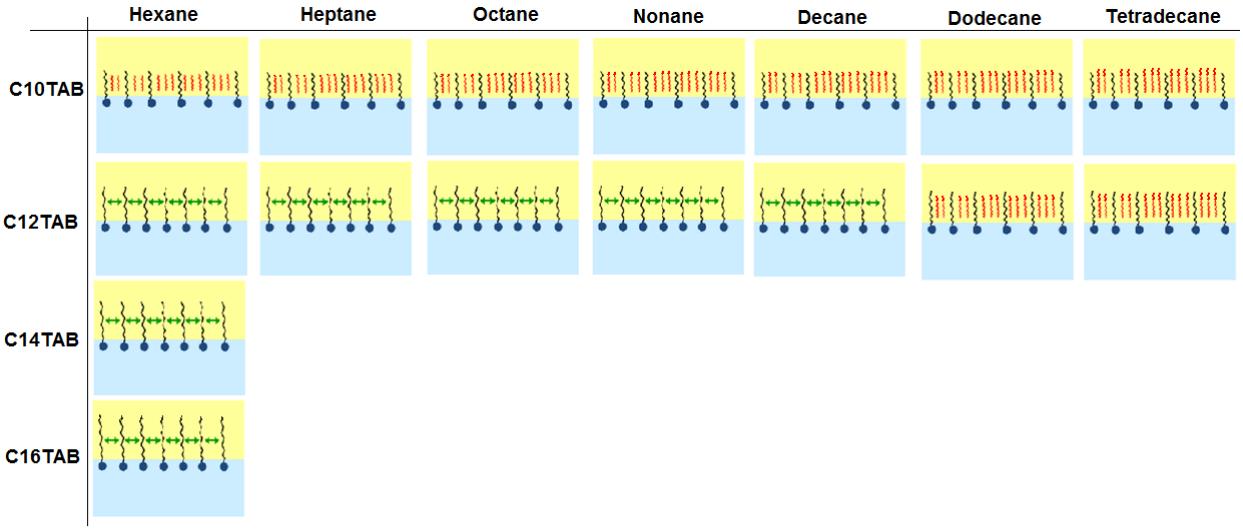

In contrast to the water/oil interface, a competitive adsorption is observed for all aqueous C_nTAB solutions at the water/hexane vapor interface (Paper 4). With increasing C_nTAB surface concentration, the hexane molecule co-adsorption is more efficient. Probably, the surfactant chains act like collectors for hexane molecules, to which they bind via hydrophobic (van der Waals) interactions.

Following the low-molecular surfactants´ adsorption characterization, their interaction with polyelectrolytes and the formation of mixed adsorption layers were investigated too (Paper 9). It was found that the interfacial characteristics of PAH/SDS complexes depend on the concentration of SDS. With increasing SDS concentration the system passes through three states. The first state happens when PAH/SDS complexes adsorb to the water/hexane interface, the second is indicated as a flat part of the adsorption isotherm revealing that the interface is more or less saturated with PAH/SDS complexes. In the final third state the PAH/SDS complexes become hydrophilic again due to the hydrophobic interaction between the complex and the additionally available SDS molecules. The complexes desorb back into the bulk phase, replaced by adsorbed free SDS molecules.

4.2 Kinetics and rheology of surfactant adsorption layers

For investigations of the adsorption kinetics and dilational rheology it is important to know that with increasing surfactant concentration the adsorption kinetics is accelerated, i.e. a shorter time is needed to establish the adsorption equilibrium. This influences the selection of suitable interfacial tension and rheology methods for characterizing a particular surfactant (Paper 5). It was found that usually the combination of two or more techniques is necessary to gain the whole adsorption kinetics curves for the complete range of concentrations. It is also seen (Paper 6) that the capillary pressure tensiometer is a powerful technique that covers a broad time range starting from 0.01 s (or 0.0002 s for an air bubble in water when it works on the principle of bubble pressure tensiometry). For studies of the dilational rheology the capillary pressure tensiometer is capable of producing relatively high frequencies, from 0.1 Hz to 100 Hz. With improving the geometry of the capillary, it is possible to perform also experiments at higher frequencies.

The influence of impurities on the adsorption kinetics is essential. Comparing the adsorption kinetics at the water/hexane with that at the water/air interface [104] it is evident that at the water/air interface the dodecanol adsorption additionally decreases the surface tension gradually over a long adsorption time. This is not the case at the water/hexane interface where the adsorption equilibrium depends just on the SDS concentration and it is reached much faster than at the water/air interface. This can be explained only by the transfer of dodecanol molecules to the hexane

phase without interfering remarkably with the SDS adsorption. Therefore, at the water/hexane interface it is possible to theoretically describe just SDS adsorption without taking into account the competitive adsorption of dodecanol (Fig. 11) as is the case at the water/air interface.

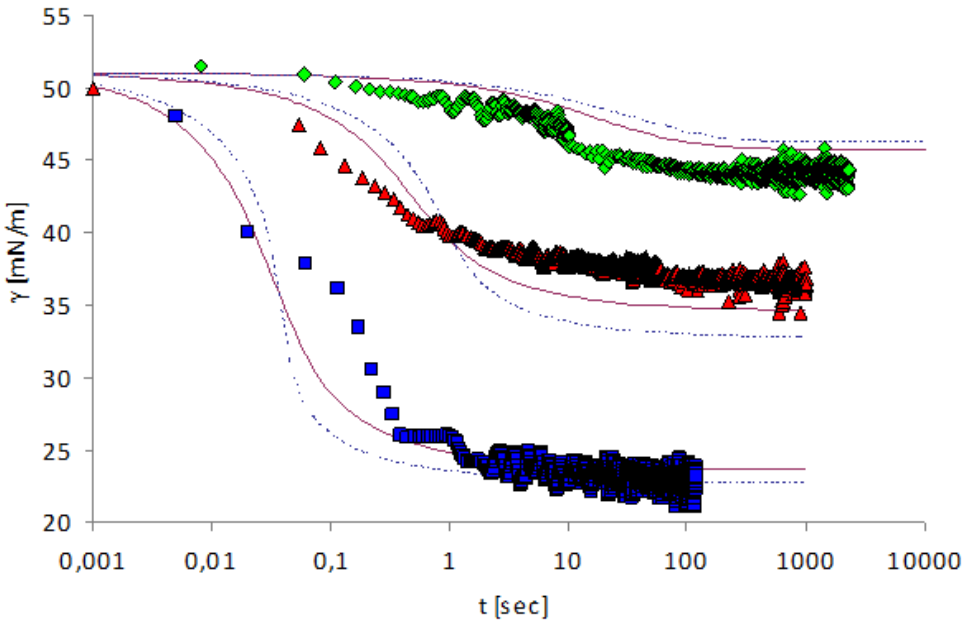

Figure 11. Dynamic surface tension of SDS solutions 10^{-5} (◆), 10^{-4} (▲), 5×10^{-4} (■) mol/l in aqueous buffer at pH 7 against hexane, compared with data calculated with the Frumkin (solid thin line) and Langmuir (dotted thin line) adsorption model.

Note, the theoretical curves in Fig. 11 are not best fits but just result from the equilibrium adsorption parameter and an average diffusion coefficient for the SDS molecules.
In Paper 7 it is shown that each surfactant has a characteristic adsorption time in which the adsorption can be followed if the instrument provides an adequate measuring time window. Combining the profile analysis and capillary pressure tensiometry it is possible to measure completely the adsorption kinetics of C_{16}TAB and C_{14}TAB surfactants at the water/hexane interface. For the shorter chains C_{12}TAB and C_{10}TAB mainly the equilibrium interfacial tension can be measured. However, it is not needed to have the whole adsorption kinetic curve in order to successfully fit the experimental data by a theoretical model. The most important is that a major part of the curve is available before reaching equilibrium. If not, the fitting of such a curve can lead to unrealistic values of the model parameters.
The same rules work for measurements of the dilational rheology too. The fitting of the experimental dilational visco-elasticity data with theoretical models (Frumkin Ionic Compressibility and Langmuir Compressibility), which are primarily made for water/air interfaces, can lead to slightly different values as compared to the kinetic and equilibrium values of the adsorption model parameters. This is possibly caused by additional processes at the water/hexane interface. It might be that oil molecules participate in the dynamics more than expected and those mechanisms cannot be described yet quantitatively by the existing theoretical models.
The adsorption of macromolecules such as Pluronics is followed by the formation of multilayers at the water/hexane interface (Paper 8). It was found that the Pluronics P9400 and L64 form three layers (m = 3) and F68 two layers (m = 2) at the water/hexane interface.
For mixtures of polyelectrolyte and surfactant (PAH/SDS) it was found that the values of dilational elasticity and viscosity depend on the concentration of both components (Paper 9). The high dilational elasticity for the mixtures at low surfactant concentration indicates that the PAH/SDS complexes are adsorbed at the interface and have adsorption and desorption relaxation times longer than the pure SDS molecules. The further increase of the surfactant concentration leads to an

increase of the dilational elasticity and then a sharp decrease at higher concentrations presumably due to the destruction of the two-dimensional rigid structure and the formation of micro-aggregates in the interfacial layer.

Application example

In paper 10 a practical implementation of the fundamental knowledge in interfacial science for controlling the emulsion stability and breaking was approached. Generally, the competitive adsorption of two different types of surfactants, i.e. one aqueous and one oil soluble surfactant, can lead to the break-down of an emulsion. The competitive adsorption is possible only when appropriate concentrations of both surfactants are reached. By changing the concentration of the oil soluble surfactant, the emulsion breaks after a longer or shorter time or can last for long or short times, respectively. From Fig. 12 it is seen that by adding 1.37×10^{-3} mol/l Span80 into the oil phase (Dimeticone) the break-down time is significantly shorter than for the emulsion formed with pure oil. The stability time, after which the emulsions start breaking down, is for both samples similar and amounts to around 25 s.

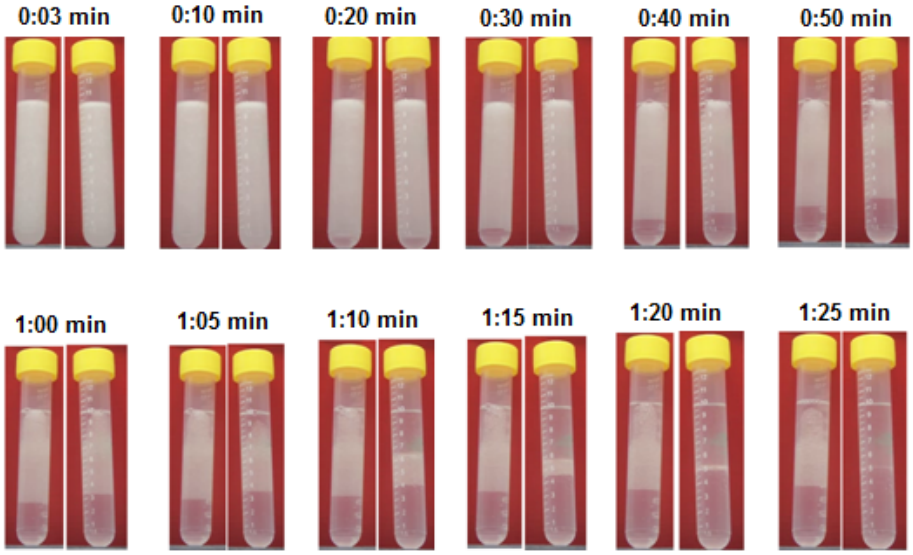

Figure 12. Comparison of the emulsion break-down in presence and absence of surfactant in the oil phase; 10× diluted water with emulsifier as water phase and dimeticone without surfactant (left) and with c = 1.37×10^{-3} mol/l Span80 (right).

CHAPTER 5

Conclusions

Thermodynamics of surfactant adsorption layer

The dynamic and equilibrium interfacial tensions of SDS solutions against hexane can be obtained without disturbing effects by the presence of the natural impurity dodecanol due to its good solubility in hexane. As a result of this thesis it was shown that the interfacial tension isotherm of SDS can be well described by the Frumkin adsorption model. In such a way the diffusion coefficient can be obtained from the dynamic interfacial tensions at the water/hexane interface without any influence of the presence of $C_{12}OH$, in contrast to data observed at the water/air interface.

$C_{12}OH$ dissolved in water shows a significant decrease of the surface tension against air even at very small concentrations. On the other hand, $C_{12}OH$ dissolved in hexane does not show any remarkable surface activity.

The results obtained from C_nTAB buffer solutions at the water/air interface have shown a strong increase of the adsorption due to the screening by the added electrolyte leading to a decrease of electrostatic repulsion. The experiments in the presented thesis show, that at the water/oil interface, the high adsorbed amounts are due to the presence of oil molecules which interact with the surfactants at low surface coverage. At high surface coverage, the behavior becomes a function of the surfactant chain length and the length of the oil molecule too. We concluded in this work that we deal here with a kind of competitive adsorption for the shortest chain surfactant ($C_{10}TAB$) and all measured oils (hexane, heptane, octane, nonane, decane, dodecane and tetradecane). For the longer chain surfactant ($C_{12}TAB$), the mutual interactions are strong enough to replace the molecules of the all measured oils at the interface except dodecane and tetradecane. With dodecane and tetradecane a competitive adsorption was observed. $C_{14}TAB$ and $C_{16}TAB$ show strong surfactant mutual interactions and single adsorption layers without embedded hexane molecules. In the presence of phosphate buffer, the use of a modified Frumkin Ionic Compressibility model (FIC), taking into account the average activity of the ions, has shown a remarkable accuracy in the determination of the fitting parameters and for the calculation of the adsorbed amount and molar area as compared with the classical Frumkin model.

The studies performed in this thesis on the co-adsorption of surfactants with oil molecules from the vapor phase clearly demonstrate that the interfacial layers incorporate or squeeze out the oil between the surfactant chains, depending on the alkyl chain lengths of both components. This phenomenon is observed at the water/bulk oil interface as well. Hence, the water/oil vapor interface can serve as an intermediate situation providing several advantages from an experimental point of view. However, basic theoretical models for a quantitative data analysis are yet pending.

A good complementary work would be to study these systems with neutron reflectivity, ellipsometry or sum frequency spectroscopy in order to reach as close as possible the values of the adsorbed amount in the presence of buffer.

Kinetics and rheology of surfactant adsorption layers

As part of this thesis we have analyzed the suitability of available experimental tools and found that for a given surfactant one can estimate whether the adsorption kinetics and dilational rheology can be studied appropriately, and which experimental methods are most suitable, using the Langmuir adsorption model and the Ward and Tordai equation for diffusion controlled adsorption processes.

Fast dynamic liquid interfaces require sophisticated techniques such as the Oscillating Drop and Bubble Analyzer (ODBA) and a suitable way of its use. Optimization of the experimental setup is very important. Smaller drops are favorable as the measured absolute capillary pressure is higher, however, it is increasingly difficult to handle defined changes of smaller amounts of liquids by the dosing systems, such as syringes or piezo translators. Note, smaller drops require more narrow capillaries, which can cause much higher hydrodynamic effects on the other hand. However, there is

an optimum capillary tip size and design according to the hydrodynamic effects which allows us presently to apply a reliable regular hydrodynamic analysis model for data gained at frequencies up to about 80 Hz.
The adsorption kinetics and dilational rheology depend closely on the correct choice of the right instrument and theoretical model for analyzing the data afterwards. Generally the Langmuir compressibility model gives a good description of dynamic and rheological types of data. In the perfect case a single diffusion coefficient is used for fitting all thermodynamic, kinetic and dilational rheology experimental results. However, as example, for the studied cationic surfactants C_{14}TAB and C_{16}TAB it was necessary to manipulate the model parameters and choose different values of the diffusion coefficient to reach a perfect fit. From these findings of the thesis we were able to conclude that the different diffusion coefficients are caused by possible additional processes at the water/hexane interface during oscillations of the interface.
The experimental data for the equilibrium and dynamic interfacial tensions of Pluronic triblock copolymers at their aqueous solution/hexane interface are compared with the theoretical values calculated from a thermodynamic model based on the analysis of the chemical potentials of the solvent and the dissolved substances. To reproduce the surface tension values at high bulk concentrations of the Pluronics, i.e. in the post-critical range, a simple model is proposed which assumes the proportionality between the surface pressure of the solution and the adsorption of the polymer (expressed in kinetic units). The theoretical predictions agree well with the experimental data for physically reasonable values of the adsorption layer thickness and realistic values of the diffusion coefficient.
For PAH/SDS mixtures the dilational elasticity values depend on the SDS concentrations. The increase of the SDS concentration in PAH/SDS mixtures, leads to a slight increase of the dilational elasticity up to a mixing ratio of $n = c_{SDS}/c_{PAH} = 1$, and then a sharp decrease is observed. This sharp decrease happens in a narrow range presumably due to the destruction of a two-dimensional rigid structure and the formation of micro-aggregates in the interfacial layer.
The dilational viscosity of PAH/SDS mixtures for harmonic expansions/compressions of the water/hexane interface at small frequencies is much higher than for SDS alone. This effect could be caused by a release/binding relaxation of SDS molecules with the polymer at the interface.

Application example

As a practical result in this thesis we proposed the competitive adsorption as a process suitable for controlling the break-down of an emulsion. Adapting the concentration of the aqueous surfactant, the O/W emulsion stability can be improved or not depending on the number of aqueous surfactants at the interface. On the other hand, by changing the concentration of a surfactant in the oil phase, the O/W emulsion can break after longer or shorter time and can also last for a longer or shorter time, respectively, controlled by the dynamics of surfactant adsorption from either bulk phase.

ACKNOWLEDGEMENT

I would like to express my sincerely gratitude to everyone from Interface department of Max Planck Institute:

My supervisor Helmuth Möhwald and my group leader Reinhard Miller for believing in me and my work, great support with literature, instruments and limitless source of new ideas as well as many brainstorming discussions, enthusiasm and guidance. Without You, I would never grow up as a scientist so rapidly and determined.

My excellent senior colleagues Jürgen Krägel, Dieter Vollhardt, Rainer Wüstneck, Nina M. Kovalchuk, Volodja I. Kovalchuk, Eugene V. Aksenenko and Valentin B. Fainerman for working patient with me, unselfishly sharing the knowledge, experience and ideas. I look up to all of You as Your careers are one of the goals I would like to achieve.

Aliyar Javadi, Vincent Pradines, Georgi Gochev, Pablo Ramirez, James K. Ferri, Abhijit Dan, Alexander V. Makievski and Jaroslav M. Katona, have a special part in my heart as people who are on the right way to become great scientists and I had luck to closely work with them.

My great young scientists and the age group where I belong, Altynay Sharipova, Narges Moradi, Vamseekrishna Ulaganathan, Jooyoung Y. Won and Mohsen Karbaschi. We have been sharing all problems that the young scientists have during the PhD study, supporting each other and trying to give answers on many for us difficult questions.

I would like to give a special part in the acknowledgement to our dear technician Sabine Siegmund. Without her the experimental work would be much harder and definitely not so amusing.

My family which I owe more than I would ever be possible to give back, I thank very much for support through all my education and life in general.

The sweetest part in the acknowledgment list I left to thank to my wonderful wife Jelena for choosing me to be her husband and so going to share the joined future on behalf of love.

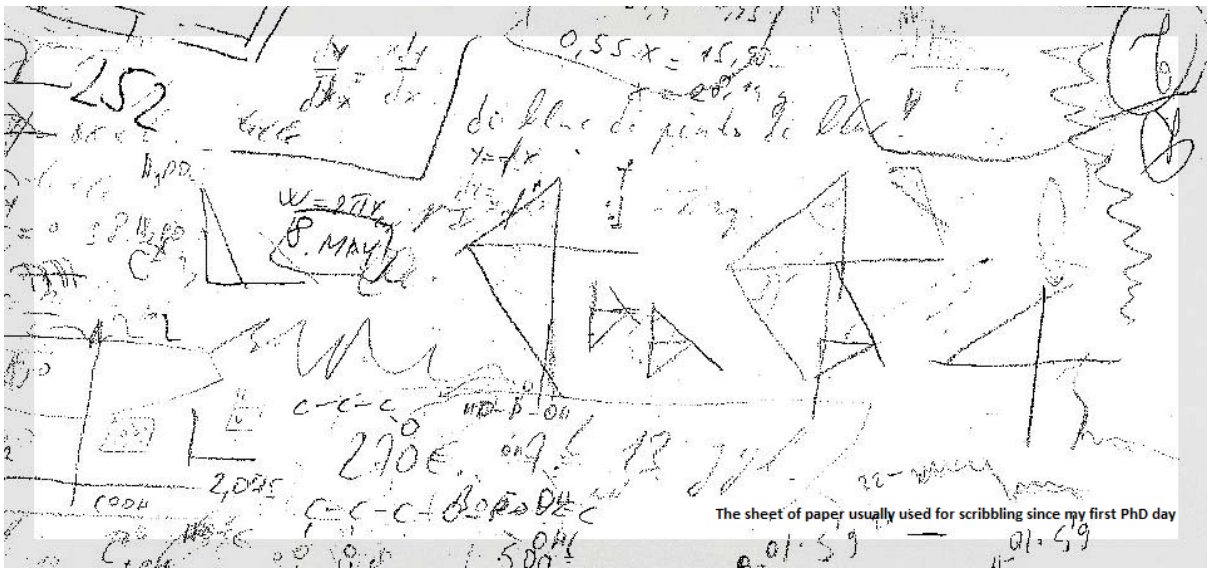

REFERENCES

[1] E. Dickinson, Soft Mater. 4 (2008) 932-942.
[2] M.E. Leser, L. Sagalowicz, M. Michel, H.J. Watzke, Adv. Colloid Interface Sci. 123-126 (2006) 125-136.
[3] R.H. Müller, C.M. Keck, J. Biotechnol. 133 (2004) 151-170.
[4] L.L. Schramm, E.N. Stasiuk, D.G. Marangoni, Annu. Rep. Prog. Chem. 99 (2003) 3-48.
[5] V.B. Fainerman, R. Miller, E.V. Aksenenko, A.V. Makievski, J. Krägel, G. Loglio, L. Liggieri, Adv. Colloid Interface Sci. 89 (2000) 83-101.
[6] C.-H. Chang, E.I. Franses, Colloids Surf. A 100 (1995) 1-45.
[7] P. Warszynski, W. Barzyk, K. Lunkenheimer, H. Fruhner, J. Phys. Chem. B 102 (1998) 10948-10957.
[8] V. Pradines, D. Lavabre, J.-C. Micheau, V. Pimienta, Langmuir 21 (2005) 11167-11172.
[9] V.B. Fainerman, R. Miller, E.V. Aksenenko, Adv. Colloid Interface Sci. 96 (2002) 339-259.
[10] K. Lunkenheimer, G. Czichocki, R. Hirte, W. Barzyk, Colloids Surf. A 101 (1995) 187-197.
[11] A.J. Prosser, E.I. Franses, Colloids Surf. A 178 (2001) 1-40.
[12] M.M. Knock, C.D. Bain, Langmuir 16 (2000) 2857–2865.
[13] J.R. Lu, R.K. Thomas, J. Penfold, Adv. Colloid Interface Sci. 84 (2000) 143-304.
[14] A. Zarbakhsh, A. Querol, J. Bowers, J.R.P. Webster, Faraday Discuss. 129 (2005) 155-167.
[15] R. Aveyard, D.A. Haydon, J. Colloid Sci. 20 (1965) 2255-2261.
[16] S.R. Deshiikan, D. Bush, E. Eschenazi, K.D. Papadopoulos, Colloids Surf. A 136 (1998) 133-150.
[17] M. Mulqueen, D. Blankschtein, Langmuir 18 (2001) 365-376.
[18] F. Ravera, M. Ferrari, L. Liggieri, Adv. Colloid Interface Sci. 88 (2000) 129-177.
[19] R. Tadmouri, C. Zedde, C. Routaboul, J.-C. Micheau, V. Pimienta, J. Phys. Chem. B 122 (2008) 12318-12325.
[20] E. Hutchinson, J. Colloid Sci. 3 (1948) 219-234.
[21] W.R. Gillap, N.D. Weiner, M. Gibaldi, J. Phys. Chem. 72 (1968) 2222-2227.
[22] L. Liggieri, F. Ravera, M. Ferrari, A. Passerone, R. Miller, J. Colloid Interface Sci. 186 (1997) 46.
[23] R. Miller, V.B. Fainerman, H. Möhwald, J. Colloid Interface Sci. 247 (2002) 193.
[24] A. Javadi, N. Moradi, V.B. Fainerman, H. Möhwald, R. Miller, Colloids Surf A 391 (2011) 19-24.
[25] R. Aveyard, B.P. Binks, P.D.I. Fletcher, J.R. Macnab, Ber. Bunser-Ges. Phys. Chem. 100 (1996) 224-231.
[26] S.S. Dukhin, G. Kretzschmar, R. Miller In: D. Möbius, R. Miller, editors. Dynamics of adsorption at liquid interfaces: theory, experiment, application. Studies in Interface Science, Vol. 1, Amsterdam, Elsevier; 1995.
[27] P. Joos, Dynamic surface phenomena. VSP: Dordrecht; 1999.
[28] R. Miller and L. Liggieri (Eds.), Interfacial Rheology, Vol. 1, Progress in Colloid and Interface Science, Brill Publ., Leiden, 2009.
[29] M.G. Munoz, F. Monroy, F. Ortega, R.G. Rubio, D. Langevin, Langmuir 16 (2000) 1083-1093.
[30] M.G. Munoz, F. Monroy, F. Ortega, R.G. Rubio, D. Langevin, Langmuir 16 (2000) 1094-1101.
[31] B.R. Blomqvist, J.W. Benjamins, T. Nylander, T. Arnebrant, Langmuir 21 (2005) 5061-5068.
[32] A. Hambardzumayan, V. Aguie-Beghin, M. Daoud, R. Douillard, Langmuir 20 (2004) 756-763.
[33] R. Sedev, R. Steitz, G.H. Findenegg, Physica B 315 (2002) 267-272.
[34] J.B. Vieira, Z.X. Li, R.K. Thomas, J. Phys. Chem. B 106 (2002) 5400-5407.
[35] J.B. Vieira, Z.X. Li, R.K. Thomas, J. Penfold, J. Phys. Chem. B 106 (2002) 10641-10648.
[36] A. Hambardzumyan, V. Aguir-Beghin, M. Daoud, R. Douillard. Langmuir 20 (2004) 756-763.
[37] B.R. Blomqvist, T. Warnheim, P.M. Claesson, Langmuir 21 (2005) 6373-6384.
[38] C. Kim, H. Yu, Langmuir 19 (2003) 4460-4464.
[39] F. Monroy, F. Ortega, R.G. Rubio, B.A. Noskov, Surface rheology studies of spread and adsorbed polymer layer, in: R. Miller, L. Liggieri (Eds.), Interfacial Rheology, Brill, Leiden, 2009.
[40] B.A. Noskov, Curr. Opin. Colloid Interface Sci. 15 (2010) 229-236.
[41] B.A. Noskov, A.V. Akentiev, G. Loglio, R. Miller, J. Phys. Chem. B 104 (2000) 7923-7931.
[42] Hong-Bo Fang, Colloid. Polym. Sci. 287 (2009) 1131-1137.
[43] W. Schönfeldt, Grenzflächenaktive Äthylenoxyd-Addukte – ihre Herstellung, Eigenschaften, Anwendung und Analyse, Wissenschafts Verlag mbH, Stuttgart, 1976.
[44] Nonionic Surfactant: Organic Chemistry, N.M. Van Os (Ed.), Surfactant Sci. Ser., Vol. 72, Marcel Dekker, New York, 1997.
[45] R. Miller, P. Joos, V.B. Fainerman, Adv. Colloid Interface Sci. 49 (1994) 249-302.
[46] N. Mucic, A. Javadi, N.M. Kovalchuk, E.V. Aksenenko, R. Miller, Adv. Colloid Interface Sci. 168 (2011) 167-178.
[47] V.B. Fainerman, S.V. Lylyk, E.V. Aksenenko, J.T. Petkov, J. Yorke, R. Miller, Colloid Surfaces A 354 (2010) 8-15.
[48] J.A. De Feijter, J. Benjamins, F.A. Veer, Biopolymers 17 (1978) 1759.
[49] H. Motschmann, R. Teppner, Ellipsometry in Interfacial Science in “Novel Methods to study interfacial layers” D. Möbius and R. Miller, Studies in Interface Science, Vol. 11, Amsterdam, Elsevier, (2001).
[50] J.P.R. Day, P.D.A. Pudney, C.D. Bain, Phys. Chem. Chem. Phys. 12 (2010) 4590-4599.
[51] S.C. Russev, T.Vl. Arguirov, T.D. Gurkov, Colloids Surfaces B 19 (2000) 89-100.
[52] D. Langevin, Light Scattering by Liquid Surfaces and Complimentary Techniques, Marcel Dekker (Eds.), New York, 1992.
[53] D. Vollhardt, G. Czichocki, R. Rudert, Colloids Surfaces A, 76 (1993) 217.
[54] A. Martin, M. Bos, M.C. Stuart, T. Vliet, Langmuir 18 (2002) 1238-1243.
[55] J. Benjamins, A. Cagna, E.H. Lucassen-Reynders, Colloids Surfaces A, 114 (1996) 245-254.
[56] G. Kretzschmar, K. Lunkenheimer, Ber. Bunsenges, Phys. Chem. 74 (1970) 1064.
[57] L.Y. Wang, M. Schonhoff, H. Möhwald, J. Physical Chemistry B. 106 (2002) 9135-9142.
[58] L.Y. Wang, M. Schonhoff, H. Möhwald, J. Physical Chemistry B 108 (2004) 4767-4774.
[59] A.R. Mackie, A.P. Gunning, M.J. Ridout, P.J. Wilde, J.R. Patino, Biomacromolecules 2 (2001) 1001-1006.
[60] Tzung-Han Chou, Yu-Shun Lin, Wei-Ta Li, Chien-Hsiang Chang, J. Colloid Interface Sci. 321 (2008) 384-392.
[61] S. Uredat, G.H. Findenegg, Langmuir 15 (1999) 1108.
[62] A.R. Mackie, A.P. Gunning, P.J. Wilde, V.J. Morris, Langmuir 16 (2000) 2242-2247.

[63] A.R. Mackie, A.P. Gunning, M.J. Ridout, P.J. Wilde, J.R. Patino, Biomacromolecules 2 (2001) 1001-1006.
[64] E. Bonaccurso, M. Kappl, H.J. Butt, Current Opinion Colloid Interface Sci. 13 (2008) 107-119.
[65] M.B.J. Meinders, G.G.M. van den Bosch, H.H.J. Jongh, Trends in Food Science & Technology, 11 (2000) 218.
[66] A.N. Frumkin, Z. Phys. Chem. (Leipzig), 166(1925)446.
[67] R. Wüstneck, R. Miller, J. Kriwanek, H.-R. Holzbauer, Langmuir, 10(1994)3738.
[68] R. Wüstneck, R. Miller, J. Kriwanek, J. Colloid Interface Sci., 1(1993)1.
[69] E.H. Lucassen-Reynders, J. Colloid Interface Sci., 42(1973)563.
[70] B.P. Binks, P.D.I. Fletcher, W.F.C. Sager, R.L. Thompson, Adsorption of semifluorinated alkanes at hydrocarbon-air surfaces, 1995.
[71] B.V. Derjaguin, S.S. Dukhin, A.E. Yaroshchuk, On the role of the electrostatic factor in stabilization of dispersions protected by adsorption layers of polymers, 1986.
[72] H. Diamant, G. Ariel, D. Andelman, Physicochemical and Engineering Aspects 183-185 (2001) 259-276.
[73] http://en.wikipedia.org/wiki/File:Surfactant.jpg
[74] I. Langmuir, J. Amer. Chem. Soc., 39 (1917) 1848.
[75] V.B. Fainerman and R. Miller, Adsorption isotherms at liquid interfaces, Encyclopedia of Surface and Colloid Science, P. Somasundaran and A. Hubbard (Eds.), 2nd. Edition, 1 (2009) pp. 1.
[76] B. Z. von Szyszkowski, Phys Chem (Leipzig) 1908;64:385.
[77] A.N. Frumkin, Z Phys Chem (Leipzig) 1925; 116:466-85.
[78] V.B. Fainerman, V.I. Kovalchuk, E.V. Aksenenko, M. Michel, M.E. Leser, R.Miller, J. Phys. Chem. B 108 (2004) 13700.
[79] V.B. Fainerman, S.V. Lylyk, E.V. Aksenenko, A.V. Makievski, J.T. Petkov, J. Yorke, R. Miller, Coll. Surf. A 334 (2009), 1.
[80] A. Ward F.H. and L. Tordai, J. Phys. Chem., 14 (1946) 453.
[81] M. Ziller and R. Miller, Colloid Polymer Sci., 264(1986)611
[82] M. van den Tempel, J. Lucassen and E.H. Lucassen-Reynders, J.Phys.Chem., 69 (1965) 1798-1804.
[83] J. Lucassen and M. van den Tempel, Chem. Eng. Sci., 27 (1972) 1283.
[84] J. Lucassen and M. van den Tempel, J. Colloid Interface Sci., 41 (1972) 491.
[85] K. Tonigold, I. Varga, T. Nylander, R.A. Campbell, Langmuir 25 (2009) 4036.
[86] A.H. Demond, A.S. Lindner, Environ.Sci.Technol. 27 (1993) 2318-2331
[87] L. Liggieri, F. Ravera, A. Passerone, J. Colloid Interface Sci. 169 (1995) 226
[88] V.I. Kovalchuk, F. Ravera, L. Liggieri, G. Loglio, A. Javadi, M.N. Kovalchuk, et al. Studies in capillary pressure tensiometry and interfacial dilational rheology. In: R. Miller, L. Liggieri, editors. Bubble and drop interfaces. Progress in Colloid and Interface Science Leiden: Brill Publ.; 2011. p. 175.
[89] G. Loglio, P. Pandolfini, L. Liggieri, A.V. Makievski, F. Ravera, Determination of interfacial properties by the pendant drop tensiometry: optimization of experimental and calculation procedures. In: R. Miller, L. Liggieri, editors. Bubble and drop interfaces. Progress in Colloid and Interface Science Leiden: Brill Publ. ; 2011.p. 8.
[90] R. Nagarajan, D.T. Wasan, J. Colloid Interface Sci. 159 (1993) 164.
[91] C.A. MacLeod, C.J. Radke, J. Colloid Interface Sci. 160 (1994) 435.
[92] X. Zhang, T. Harris, O.A. Basaran, J. Colloid Interface Sci. 168 (1994) 47.
[93] A. Javadi, J. Krägel, P. Pandolfini, G. Loglio, V.I. Kovalchuk, E.V. Aksenenko, et al. Colloids Surf. A 365 (2010) 62.
[94] L. Liggieri, F. Ravera, A. Passerone, J. Colloid Interface Sci. 169 (1995) 22.
[95] L. Liggieri, F. Ravera, A. Passerone, A. Sanfeld, A. Steinchen, Lect Notes Phys. 467 (1996) 175.
[96] P.J. Breen, Langmuir 11 (1995) 885.
[97] V.I. Kovalchuk, F. Ravera, L. Liggieri, G. Loglio, P. Pandolfini, A.V. Makievski, S. Vincent-Bonnieu, J. Krägel, A. Javadi, R. Miller, Adv. Colloid Interface Sci. 161 (2010) 102.
[98] J.M. Soos, K. Koczo, E. Erdos, D.T. Wasan, Rev. Sci. Instrum. 65 (1994) 3555.
[99] V.I. Kovalchuk, A.V Makievski, J. Krägel, P Pandolfini, G. Loglio, L. Liggieri, F. Ravera, R. Miller, Colloids Surfaces A 261 (2005) 115.
[100] D. Georgieva, A. Cagna, D. Langevin, Soft Matter 5 (2009) 2063.
[101] H. Bianco, A. Marmur, J. Colloid Interface Sci. 158 (1993) 295.
[102] R. Miller, V.B. Fainerman, A.V. Makievski, M. Ferrari, G. Loglio, Measuring dynamic surface tensions. In: Holmberg K., editor. Handbook of applied colloid and surface science. John Wiley & Sons; 2001. p. 775.
[103] C. Maze, G. Burnet, *Surface Sci.* 13 (1969) 451.
[104] V.B. Fainerman, S.V. Lylyk, E.V. Aksenenko, J.T. Petkov, J. Yorke, R. Miller, Colloids Surf. A 354 (2010) 8.

Paper I

Effects of dodecanol on the adsorption kinetics of SDS at the water/hexane interface

A. Javadi, N. Mucic, D. Vollhardt, V.B. Fainerman and R. Miller

Journal of Colloid and Interface Science 351 (2010) 537-541.

Journal of Colloid and Interface Science 351 (2010) 537–541

Contents lists available at ScienceDirect

Journal of Colloid and Interface Science

www.elsevier.com/locate/jcis

Effects of dodecanol on the adsorption kinetics of SDS at the water–hexane interface

A. Javadi [a,*], N. Mucic [a], D. Vollhardt [a], V.B. Fainerman [b], R. Miller [a]

[a] Max-Planck-Institut für Kolloid- und Grenzflächenforschung, Am Mühlenberg 1, 14424 Potsdam, Germany
[b] Donetsk Medical University, 16 Ilych Avenue, 83003 Donetsk, Ukraine

ARTICLE INFO

Article history:
Received 25 April 2010
Accepted 15 July 2010
Available online 18 July 2010

Keywords:
Adsorption kinetics
Sodium dodecyl sulphate (SDS)
Oil/water interface
Tensiometry
Dodecanol effects

ABSTRACT

Even though sodium dodecyl sulphate (SDS) is the most frequently studied surfactant, its properties at liquid interfaces are not easily accessible. This is mainly caused by the fact that in aqueous solution SDS is subject to hydrolysis, by which the homologous dodecanol (C12OH) is formed. Due to its enormously high surface activity it competes with SDS at the interface. We demonstrate here that this "natural" impurity C12OH does not remarkably affect the adsorption dynamics of SDS at the water/hexane interface, due to its high solubility in hexane. Therefore, the dynamic adsorption properties can be determined independent of disturbing dodecanol effects. The surfactant adsorbs diffusion controlled and the interfacial tension isotherm at the water/hexane interface is well described by a Frumkin model. However complementary experiments via direct admixture of dodecanol in hexane indicate a significant decrease in interfacial tension of the water–hexane interface at concentrations higher than 10^{-3} mol/l in hexane. This condition may happen when the oil phase is distributed as small droplets in a high concentrated solution of SDS. The distribution coefficient of C12OH between water and hexane is estimated from adsorption experiments to be $K_p = c_o/c_w = 6.7 \times 10^3$.

1. Introduction

A clear understanding of the adsorption mechanism of amphiphiles from aqueous solutions is of eminent importance in a majority of technical applications [1–3]. An important prerequisite for a correct analysis of this adsorption mechanism is the absence of any surface active impurities in the sample solution. For some even highly purified substance it can however happen that impurities are produced as soon as the sample is dissolved in water. For alkyl sulphates this was frequently described in literature [4–7]. Despite many attempts, it is still very difficult for example to determine quantitatively the dynamic adsorption properties of sodium dodecyl sulphate (SDS) at the solution/air interface. Although being the most frequently studied surfactant worldwide, there are all kinds of adsorption mechanisms discussed in literature, as it was summarised recently in [8]. In the same work it was demonstrated that assuming a certain (although unknown) amount of dodecanol, the adsorption kinetics of SDS follows a clear diffusion controlled mechanism.

For adsorption studies at liquid–liquid interfaces there is generally rather little work done, which is due to the higher complexity of interfaces between two immiscible liquids and significant difficulties with the adaptation of measuring tools to such systems [9]. Therefore, even for SDS there are very few investigations at water–oil interfaces as stressed in [10].

The first systematic adsorption study of non-ionic surfactants at the water/oil interface has shown that in particular the solubility of an amphiphile in water and oil leads to interesting time dependencies of surface tension $\gamma(t)$ [11]. Depending on the volume ratio of water and oil, the initial concentrations of the surfactant in the two phases and the partition coefficient, a minimum in $\gamma(t)$ can be observed and explained by the transfer of surfactant from the phase of smaller volume to the other phase [12].

In the present work we present investigations on SDS solutions using a surfactant sample without prior purification from possible surface active impurities. The major amount of potential impurities in SDS samples is the homologous alcohol dodecanol (C12OH) [13]. Compared to SDS, C12OH is only slightly soluble in water and about 400 times higher surface active at the water/air interface [14]. The effect of dodecanol on the co-adsorption with SDS from aqueous solutions at the air/water interface has been investigated by various methods, such as surface pressure measurements at equilibrium and dynamic conditions, Brewster angle microscopy (BAM) and Grazing incidence X-ray diffraction (GIXD) [15–17]. It was shown that already trace amounts of dodecanol in the solution bulk can lead to an adsorption layer mainly containing C12OH.

In water/oil systems we can expect an excellent solubility of C12OH in the oil phase [18], i.e. dodecanol will not be highly surface active at this interface. Therefore, we can expect that the adsorption of SDS from the aqueous phase at the water/hexane

* Corresponding author.
E-mail address: aliyar.javadi@mpikg.mpg.de (A. Javadi).

0021-9797/$ - see front matter © 2010 Elsevier Inc. All rights reserved.
doi:10.1016/j.jcis.2010.07.033

interface proceeds without significant disturbing impurity effect of C12OH because any alcohol molecule arriving from the aqueous phase at the interface should desorb quickly into the oil. However complementary experiments using dodecanol solution in hexane against water, demonstrate a limitation for this expectation which is discussed.

Then the investigations shown here are dedicated to the dynamics of adsorption of SDS from solutions contaminated by dodecanol, either due to hydrolysis or by addition of controlled amounts of C12OH to the aqueous or oil phase, respectively, at water/air and water/hexane interfaces.

2. Materials and methods

The experiments were performed with the bubble/drop profile analysis tensiometer PAT-1 and the oscillation drop and bubble analysis tensiometer ODBA (both from SINTERFACE Technologies, Germany), the principles of which were described in detail elsewhere [19–21]. The temperature of the measuring cell (having a volume of 20 ml) was kept constant at room temperature (22 °C). In this study we used pendant water drops formed at the tip of a PEEK capillary with a tip diameter of 1.60 mm, and buoyant air bubbles formed at the tip of an inverse steel capillary with a tip diameter of 2 mm immersed into the aqueous solution. The different capillary material was chosen to provide optimum wetting by the surfactant solutions. The PAT-1 allows measuring the surface or interfacial tensions from few seconds up to hours, while the ODBA provides experimental data in the short time range between some milliseconds and hours with a good overlap of the time windows of the two methods.

The studied sodium dodecyl sulphate, SDS, had a purity higher than 99% (Aldrich) and the dodecanol had a purity better than 99% (Fluka). Both substances were used without further purification.

All solutions were prepared in 10 mM phosphate buffer aqueous solution, pH 7, NaH2PO4/Na2HPO4 (Fluka, >99%) using Milli-Q water. Hexane was purchased from Aldrich and purified with aluminium oxide. The interfacial tension of the pure water/air and water/hexane interfaces were 72.5 mN/m and 51.1 mN/m, respectively.

3. Theory

The experimental data for the equilibrium and dynamic surface tensions of SDS solutions were analysed by using the Frumkin and Langmuir adsorption models [22,23]. For solutions of single surfactants adsorbed in a single state at the surface, the equation of state and adsorption isotherm for the Frumkin model are given by:

$$\Pi = -\frac{RT}{\omega_0}\left[\ln(1-\theta) + a\theta^2\right] \tag{1}$$

$$bc = \frac{\theta}{1-\theta}\exp[-2a\theta] \tag{2}$$

where Π is surface pressure, $\theta = \omega\Gamma$ is the surface coverage, Γ is the adsorption, ω is the molar area of the adsorbed molecules, ω_0 is the molar area of a solvent molecules, c is the surfactant concentration bulk, a is the intermolecular interactions constant, and b is the adsorption equilibrium constant.

In a more general Frumkin model it can be assumed that the molar area of an adsorbed surfactant molecule ω depends on the surface pressure $\Pi = \gamma_0 - \gamma$ and surface coverage θ according to the linear relationship [24],

$$\omega = \omega_0(1 - \varepsilon\Pi\theta) \tag{3}$$

where the factor ε is the so-called two-dimensional intrinsic compressibility coefficient of the surfactant surface layer. γ_0 and γ are the surface tension of solvent and solution, respectively.

When the coefficients a and ε are zero, the resulting equations are identical to the classical Langmuir model, which does not consider lateral interaction between adsorbed molecules.

For the description of the adsorption kinetics the equation of Ward and Tordai [25] developed for a diffusion-controlled adsorption mechanism and extended to an adsorption from inside a spherical drop, is used:

$$\Gamma(t) = 2\sqrt{\frac{D}{\pi}}\left(c_o\sqrt{t} - \int_0^{\sqrt{t}} c(0, t-\tau)d\sqrt{\tau}\right) - \frac{c_0 D}{r}t \tag{4}$$

Here D is the diffusion coefficient C_o is the surfactant bulk concentration, and r is the radius of the drop. The integral equation describes the change of surface concentration $\Gamma(t)$ with time t. For its mathematical solution an adsorption model has to be selected, such as given by Eqs. (1)–(3) [3]. A more details theoretical analysis of the adsorption kinetics, including adsorption at the surface of growing spherical drops and bubbles, was published recently [21].

4. Results and discussion

Fig. 1 illustrates the dynamic surface tension of aqueous SDS solutions against hexane at three different concentrations, as

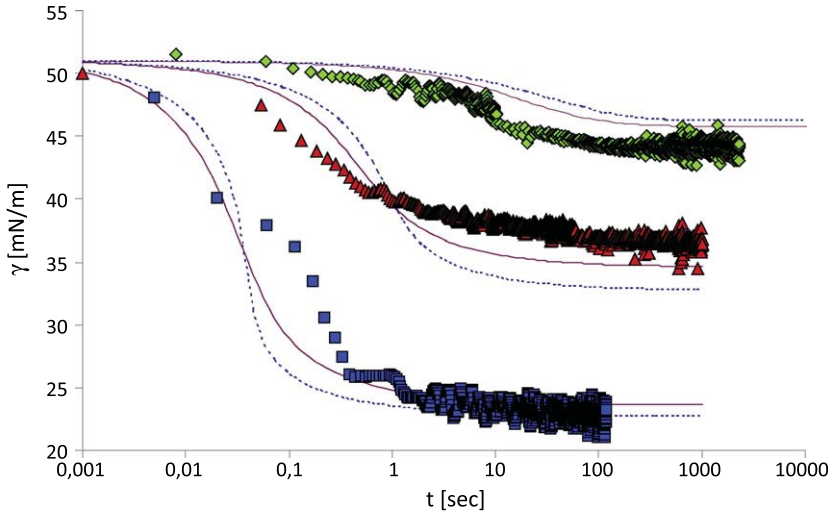

Fig. 1. Dynamic surface tension of SDS solutions at different concentrations: 10^{-5} (♦), 10^{-4} (▲), 5×10^{-4} (■) mol/l in aqueous buffer of pH 7 against hexane, compared with Frumkin (solid thin line) and Langmuir (dotted thin line) adsorption model.

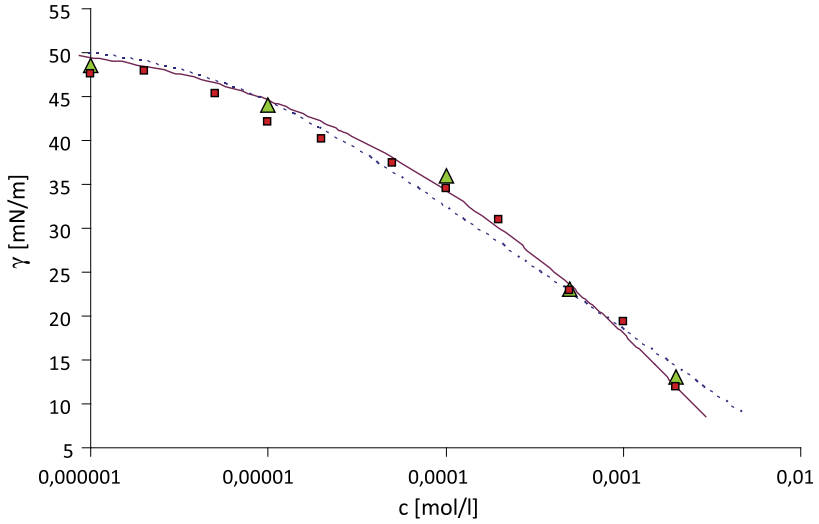

Fig. 2. Adsorption isotherm of SDS in aqueous buffer at the water–hexane interface, compared with Frumkin (solid thin line) and Langmuir (dotted thin line) adsorption model; ODBA (▲) and PAT-1 (■) techniques.

measured by capillary pressure tensiometry (ODBA). One can see that for these concentrations the adsorption equilibrium is attained quickly. The typical S-shape curves in a $\gamma(\log t)$ plot documents the adsorption process of one surfactant (SDS) and no visible effect of the obviously present C12OH. In contrast, the numerous investigations of SDS at the water–air interface have shown that even over hours the surface tension does not reach equilibrium values due to the slow adsorbing dodecanol present at low bulk concentrations. This was also discussed recently in [8].

The theoretical curves in Fig. 1 were calculated from Eqs. (1)–(4) using the following parameters obtained from fitting equilibrium data given in Fig. 2:

for the Frumkin model: $\omega_0 = 2.15 \times 10^5$ m^2/mol, $a = -3$, $b = 2.03 \times 10^2$ m^3/mol,
for the Langmuir model: $\omega_0 = 4 \times 10^5$ m^2/mol, $b = 1.91 \times 10^2$ m^3/mol.

The Frumkin isotherm describes the experimental points slightly better so that we used it in our further modelling. Note, for comparison with the ODBA results there are also data included in Fig. 2 which were obtained from drop profile tensiometry (PAT-1). A very good agreement can be observed.

Let us now compare the dynamic interfacial tensions in Fig. 1 with the theoretical model and with corresponding results in literature. For SDS we can neglect the solubility in hexane. While the solubility of C12OH in water is very small and amounts to a bulk fraction of about 6.6×10^{-6}, it is very large in hexane with a bulk fraction of 0.833 [26]. Therefore, instead of using a model for the adsorption of a mixture of two surfactants at the interface [27,28], we can neglect the adsorption of C12OH at the water/hexane interface. Hence, for our SDS sample with a certain admixture of dodecanol, we only need to assume the adsorption of SDS with a respective diffusion coefficient. A value of 5×10^{-10} m^2/s appeared optimum and physically reasonable, and led to the solid and dotted curves in Fig. 1. In contrast, a value of 10^{-11} m^2/s was needed in [8] for the same SDS to described properly the adsorption kinetics at the water/air interface in presence of C12OH. Note, these are not fitting results but correspond to the adsorption kinetics model using the known characteristic quantities (ω_0, b, a, D).

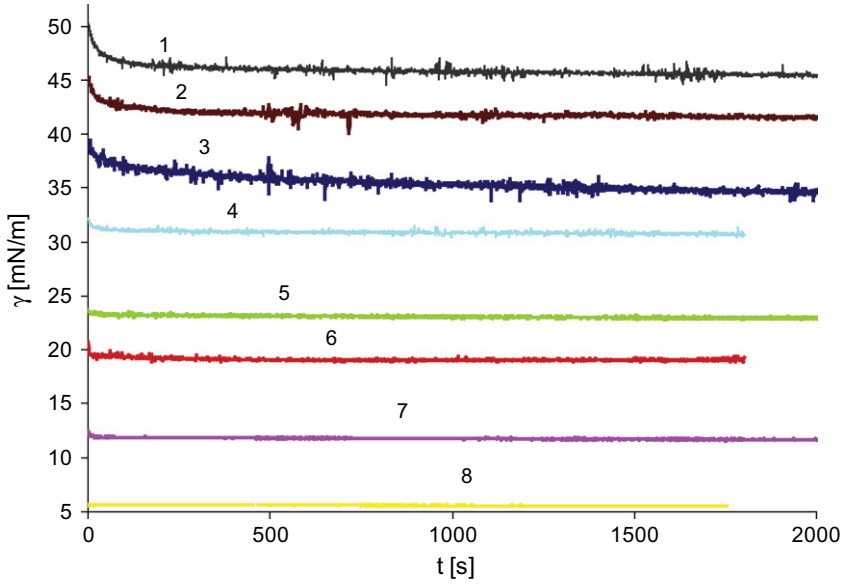

Fig. 3. Dynamic surface tension of SDS solution 5×10^{-6} (1), 10^{-5} (2), 10^{-4} (3), 2×10^{-4} (4), 5×10^{-4} (5), 10^{-3} (6), 2×10^{-3} (7), 5×10^{-3} (8) mol/l in aqueous buffer (pH 7) measured against pure hexane by PAT-1.

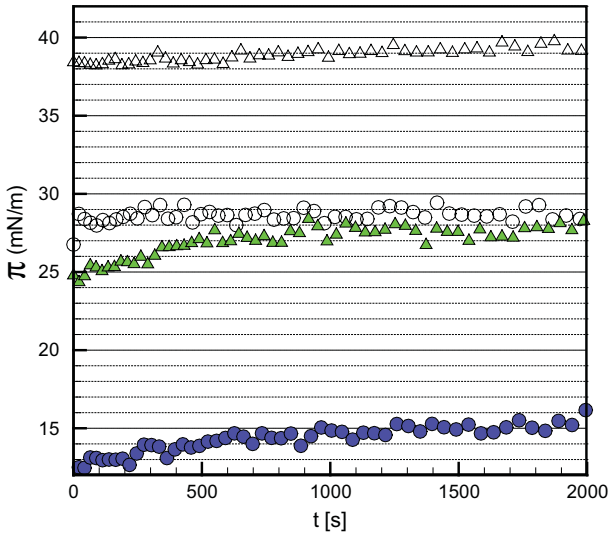

Fig. 4. Comparison of dynamic surface/interfacial pressure of SDS solution 5×10^{-4} (○, ●) and 2×10^{-3} (△, ▲) mol/l at water–air (filled symbols) and water–hexane (open symbols) interfaces, respectively; solution has been kept for 10 days aging.

The dynamic interfacial tensions measured for a series of aqueous SDS solutions against hexane in the concentration range between 5×10^{-6} mol/l and 5×10^{-3} mol/l are summarised in Fig. 3. As expected, with increasing concentration the tension values decrease and the observed rate of adsorption becomes larger, i.e. the equilibrium values are reached faster. At SDS concentrations above 5×10^{-4} mol/l we can actually not recognise any kinetics above few seconds of surface age. If we compare this with the long time data for SDS at the water–air interface published recently in [8] we easily see that at this interface changes are observed over a very large time interval (cf. Fig. 4 in Ref. [8]). This long time dynamics is definitely caused by the slow of adsorption of the C12OH, which cannot be observed at the water–hexane interface.

Comparing the surface pressure values measured for two selected SDS concentrations at water–hexane and water–air interfaces, respectively, two phenomena can be easily observed (Fig. 4). At first, the absolute values of surface pressure are much less at the water–air interface as compared to the water–hexane interface. And secondly, at the water–hexane interface the surface pressure changes happen within a few seconds, while at the water–air interface the equilibrium has not yet been reached even after half an hour.

The first phenomenon has been discussed in literature in terms of competing attraction forces between the surfactant's alkyl chains and the molecules of the oil phase [29–31]. This phenomenon is, however, not in the focus of this contribution. The second observation is caused by the presence of C12OH in the SDS solution, as already discussed above. Hence, the surface pressure data in Fig. 4 measured at the water–hexane interface show the expected fast adsorption of SDS molecules. Due to the slow diffusion of C12OH towards the interface and the very high solubility in the adjacent oil phase, its adsorption and hence competition at the water–hexane interface is negligible. In contrast, it causes the main adsorption effect after longer adsorption times at the solution–air interface.

To quantify the effects of dodecanol at the water–hexane interface and validate the given explanations, we performed additional experiments with pure dodecanol solutions at both interfaces (Fig. 5). A first set of experiments was performed at the water–hexane interface with C12OH being dissolved in hexane at concentrations of 2×10^{-5} (3), 10^{-3} (4), 10^{-2} (5) and 10^{-1} (6) mol/l. In addition we prepared aqueous C12OH solutions of 10^{-5} and 2×10^{-5} mol/l (solubility limit) and measured the dynamic surface tensions. Note, there is a phase transition visible in curve 2 at about 48 mN/m. Tsay et al. [32] found such phase transitions at about 54 mN/m, i.e. at higher γ-values, which can be explained by the slightly higher temperature of our experiments (22 °C). In addition, in our experiments with drops the phase transition happens at higher C12OH concentration which is surely due to the differences observed for drop and bubble experiments and explained by the depletion of surfactant from the drop at low concentrations and significant adsorption values [33].

An additional experiment was performed such that equal amounts of water and of a 10^{-1} mol/l C12OH solution in hexane were mixed, both phases saturated against each other, and finally separated. With the obtained aqueous phase, now containing a

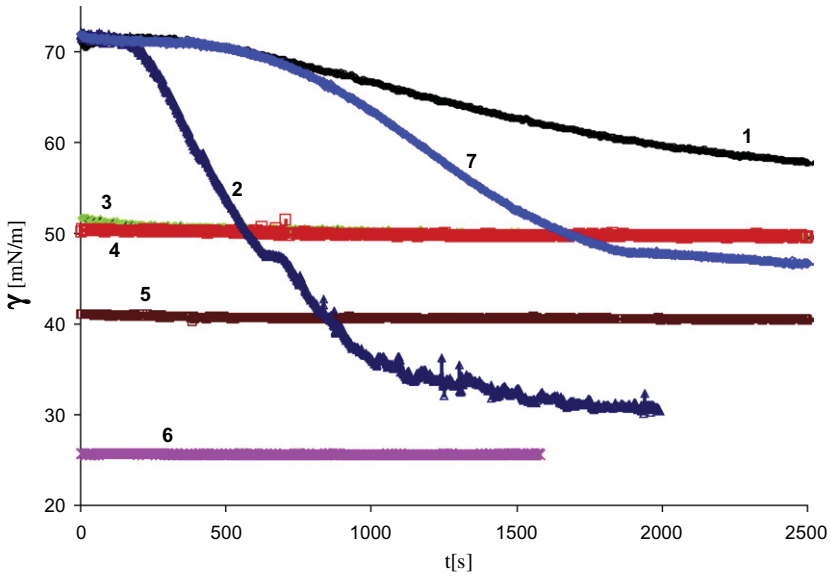

Fig. 5. Dynamic surface and interfacial tensions of C12OH solution of 10^{-5} (1) and 2×10^{-5} (2) mol/l in water against air, and of 2×10^{-5} (3), 10^{-3} (4), 10^{-2} (5) and 10^{-1} (6) mol/l in hexane against water, and the aqueous phase of C12OH obtained after saturation with a 10^{-1} mol/l C12OH in hexane, also measured against air (7).

respective amount of C12OH which refers to the partition equilibrium with hexane, also the dynamic surface tension was measured (curve 7 in Fig. 5).

The curves 3 and 4 in Fig. 5 demonstrate that at C12OH concentrations of 2×10^{-5} and 10^{-3} mol/l in hexane, no measurable adsorption effects can be observed. For the much higher C12OH concentrations of 10^{-2} and 10^{-1} mol/l in hexane, (curves 5 and 6) constant interfacial tensions of 41 mN/m and 26 mN/m, respectively, are obtained, without any kinetics due to the very high bulk concentrations. The curves 1 and 2, i.e. the surface tensions of the aqueous C12OH solutions at concentrations 10^{-5} and 2×10^{-5} mol/l (solubility limit in water), respectively, demonstrate the high surface activity of C12OH at the water–air interface. These results are in very good agreement with those published in [32]. As one can see, the curve 7 is in between curves 1 and 2 which allows us to conclude that the C12OH concentration in this aqueous solution is approximately 1.5×10^{-5} mol/l. As this aqueous solution was in equilibrium with a 10^{-1} mol/l solution of C12OH in hexane, we can estimate the partition coefficient of C12OH between hexane and water to be $K_p \approx 6.7 \times 10^3$. Unfortunately, due to our knowledge there are no values in literature to compare, however, the obtained value appears reasonable when compared to K_p values reported in [18] for shorter alcohols.

From these findings we can conclude that in typical situations of interfacial studies, i.e. extended bulk phases of water and oil, effects of an admixture like C12OH in SDS cannot play a measurable role due to its low surface activity and high partition coefficient. In particular experiments, however, when a small oil drop is formed in a larger volume of a SDS solution the transfer of C12OH could reach concentrations above 10^{-3} mol/l in the oil and then co-adsorption (impurity) effects will possibly be observed.

5. Conclusions

The dynamic and equilibrium interfacial tensions of SDS solutions against hexane, determined by using profile analysis (PAT-1) and capillary pressure (ODBA) tensiometry, can be obtained without disturbing effects by the present of natural impurity dodecanol. The isotherm interfacial tension of SDS can be described well by the Frumkin adsorption model. A diffusion coefficient of $D = 5 \times 10^{-10}$ m^2/s was obtained from the dynamic interfacial tensions at the aqueous solution–hexane interface, which is not affected by the presence of C12OH, in contrast to data observed at the water–air interface [8].

The experiments performed directly with C12OH allow validation of the adsorption behaviour of SDS at both water–air and water–hexane interfaces. C12OH dissolved in water shows a significantly surface tension decrease even at very small concentrations of 10^{-5} mol/l. From these experiment it was possible to estimate the partition coefficient $K_p = c_o/c_w$ of C12OH between water and hexane to be 6.7×10^3. On the other hand C12OH dissolved in hexane does not show any surface activity at concentrations lower than 10^{-3} mol/l. For concentrations higher than 10^{-3} mol/l which may happen when the oil phase is distributed as a small droplet in a high concentrated solution of SDS, the dodecanol effects can be significant also at the water/hexane interface.

Acknowledgments

The work was financially supported by a project of the German Space Agency (DLR 50WM0941) and the DFG (Mi418/18-1).

References

[1] H.J. De Boer, The Dynamical Character of Adsorption, Oxford University Press, 1945.
[2] A.W. Adamson, Physical Chemistry of Surfaces, fifth ed., Wiley, New York, 1990.
[3] S.S. Dukhin, G. Kretzschmar, R. Miller, Dynamics of adsorption at liquid interfaces, in: D. Möbius, R. Miller (Eds.), Studies in Interface Science, vol. 1, Elsevier, 1995.
[4] G. Czichocki, D. Vollhardt, H. Seibt, Tenside, Deterg. 18 (1981) 320.
[5] K. Lunkenheimer, G. Czichocki, J. Colloid Interface Sci. 160 (1993) 509.
[6] D. Vollhardt, G. Czichocki, Tenside, Deterg. 30 (1993) 349.
[7] B.A. Noskov, A.E. Alexandrov, E.V. Gumennik, V.V. Krotov, R. Miller, Colloid J. (Russ.) 60 (1998) 204.
[8] V.B. Fainerman, S.V. Lylyk, E.V. Aksenenko, J.T. Petkov, J. Yorke, R. Miller, Colloids Surf., A 354 (2010) 8.
[9] I.B. Ivanov, K.P. Ananthapadmanabhan, A. Lips, Adv. Colloid Interface Sci. 104 (2003) 245.
[10] P.A. Kralchevsky, K.D. Danov, V.L. Kolev, G. Broze, A. Mehreteab, Langmuir 19 (2003) 5004.
[11] M. Ferrari, L. Liggieri, F. Ravera, C. Amodio, R. Miller, J. Colloid Interface Sci. 186 (1997) 40.
[12] L. Liggieri, F. Ravera, M. Ferrari, A. Passerone, R. Miller, J. Colloid Interface Sci. 186 (1997) 46.
[13] D. Vollhardt, V.B. Fainerman, Adv. Colloid Interface Sci. 154 (2010) 1.
[14] R. Miller, V.B. Fainerman, H. Möhwald, J. Colloid Interface Sci. 247 (2002) 193.
[15] D. Vollhardt, G. Emrich, Colloids Surf., A 161 (2000) 173.
[16] D. Vollhardt, G. Brezesinski, S. Siegel, G. Emrich, J. Phys. Chem. B 105 (2001) 12061.
[17] V.B. Fainerman, D. Vollhardt, G. Emrich, J. Phys. Chem. B 105 (2001) 4324.
[18] F. Ravera, M. Ferrari, L. Liggieri, Adv. Colloid Interface Sci. 88 (2000) 129.
[19] D. Möbius, R. Miller (Eds.), Novel methods to study interfacial layers, in: Studies in Interface Science, vol. 11, Elsevier, 2001, pp. 439.
[20] S.A. Zholob, A.V. Makievski, R. Miller, V.B. Fainerman, Adv. Colloid Interface Sci. 322 (2007) 134.
[21] A. Javadi, J. Krägel, P. Pandolfini, G. Loglio, V.I. Kovalchuk, E.V. Aksenenko, F. Ravera, L. Liggieri, R. Miller, Colloids Surf., A 365 (2010) 62.
[22] A. Frumkin, Z. Phys. Chem. Leipzig 116 (1925) 466.
[23] V.B. Fainerman, S.A. Zholob, E.H. Lucassen-Reynders, R. Miller, J. Colloid Interface Sci. 261 (2003) 180.
[24] V.B. Fainerman, V.I. Kovalchuk, E.V. Aksenenko, M. Michel, M.E. Leser, R. Miller, J. Phys. Chem. 108 (2004) 13700.
[25] A.F.H. Ward, L. Tordai, J. Chem. Phys. 14 (1946) 453.
[26] P. Ruelle, U.W. Kesselring, Can. J. Chem. 76 (1998) 553.
[27] R. Miller, A.V. Makievski, C. Frese, J. Krägel, E.V. Aksenenko, V.B. Fainerman, Tenside, Surfactants, Deterg. 40 (2003) 256.
[28] R. Miller, V.B. Fainerman, E.V. Aksenenko, Colloids Surf., A 272 (2004) 123.
[29] R. Aveyard, D.A. Haydon, J. Colloid Sci. 20 (1965) 2255.
[30] K. Medrzycka, W. Zwierzykowski, J. Colloid Interface Sci. 230 (2000) 67.
[31] J. Bahtz, D. Knorr, C. Tedeschi, M.E. Leser, B. Valles-Pamies, R. Miller, Colloids Surf., B 74 (2009) 492.
[32] R.-Y. Tsay, T.-F. Wu, S.-Y. Lin, J. Phys. Chem. B 108 (2004) 18623.
[33] A.V. Makievski, G. Loglio, J. Krägel, R. Miller, V.B. Fainerman, A.W. Neumann, J. Phys. Chem. 103 (1999) 9557.

Paper II

Adsorption of alkyl trimethylammonium bromides at the water/air and water/hexane interface

V. Pradines, V.B. Fainerman, E.V. Aksenenko, J. Krägel, N. Mucic and R. Miller

Colloids and Surfaces A 371 (2010) 22-28

Colloids and Surfaces A: Physicochem. Eng. Aspects 371 (2010) 22–28

Contents lists available at ScienceDirect

Colloids and Surfaces A: Physicochemical and Engineering Aspects

journal homepage: www.elsevier.com/locate/colsurfa

Adsorption of alkyl trimethylammonium bromides at the water/air and water/hexane interfaces

Vincent Pradines[a,b,*], Valentin B. Fainerman[c], Eugene V. Aksenenko[d], Jürgen Krägel[a], Nenad Mucic[a], Reinhard Miller[a]

[a] Max Planck Institute für Kolloid-und Grenzflächenforschung, 14424 Potsdam, Germany
[b] Laboratoire de Chimie de Coordination, 31077 Toulouse Cedex 04, France
[c] Medical University Donetsk, 16 Ilych Avenue, 83003 Donetsk, Ukraine
[d] Institute of Colloid Chemistry of Water, 42 Vernadsky Avenue, 03680 Kiev, Ukraine

ARTICLE INFO

Article history:
Received 13 June 2010
Received in revised form 10 August 2010
Accepted 30 August 2010
Available online 9 September 2010

Keywords:
Adsorption
Cationic surfactant
Thermodynamic model
Alkyl trimethylammonium bromide
Water–air interface
Water–hexane interface
Effect of buffer

ABSTRACT

Surface and interfacial tension measurements have been performed at the water/air and water/hexane interface by drop profile analysis tensiometry for a series of alkyl trimethylammonium bromides with different chain lengths (C_{10}, C_{12}, C_{14} and C_{16}). The effect of neutral phosphate buffer (10 mM, pH 7) has been investigated and the results have been compared with literature data obtained for the same surfactants in the absence of salt. The use of a modified Frumkin isotherm (Ionic Compressibility) taking into account the mean activity of all ions in solution leads to a real improvement of the data interpretation, while the classical Frumkin Compressibility model yields similar results but overestimates the adsorption parameters. At the water/hexane interface, the hexane molecules are incorporated in the surfactant layer and it results a kind of competitive adsorption for the shortest chain surfactant (10 carbons). For the longest chains, the attractive interactions between the hydrophobic chains of the adsorbed surfactants are strong enough to replace the solvent molecules from the interface.

1. Introduction

The behaviour of surfactants in solution or at liquid/fluid interfaces has been widely studied for many years due to their enormous importance in many processes and technologies, such as detergency, food processing, pharmaceutical industry, or cosmetics [1–4]. The properties of disperse systems (foams, emulsions and suspensions) used in many applications are largely determined by the interfacial properties of liquid films stabilized by single surfactants or more generally by mixtures of surface active compounds. Most of adsorption studies have been performed at the water/air interface for which surface tension measurements [5], sum frequency spectroscopy [6], or neutron reflection experiments [7,8], followed by a modelling of the experimental data are very powerful methods to give an accurate idea of the interfacial layer properties (adsorbed amount, thickness of the layer, area and orientation of adsorbed molecules). In contrast to the huge number of works performed at the water/air interface [9–15], only few systematic experimental studies involving also a theoretical treatment of the data have been dedicated to the adsorption of surfactants at water/oil interfaces [16–20]. Technical difficulties encountered, for example the decrease of sensitivity of optical methods, are mainly due to the presence of the upper oil phase. The purification of these oil phases which often contain traces of surface active molecules, and their volatility which limits the experimental time, are additional critical points. Moreover, the difficulty of such studies increases when the surfactants are soluble in both water and oil phase. This fact entails that in addition to all mentioned parameters, also the partition coefficient [21,22] has to be determined, the value of which has a significant effect under dynamic conditions due to Marangoni effects [23,24].

So far, there is still an open question concerning the importance of both surfactant–surfactant and surfactant–solvent molecular interactions and on the role of oil molecules at the interface which are responsible for differences observed when compared with the water/air interface. In the past, Hutchinson suggested the presence of a competitive adsorption between surfactant and oil molecules at a water/non-polar solvent interface [25]. Due to solvent molecules interpenetrated between the surfactants, the attractive interactions and so the cohesion between surfactants observed very often at the water/air interface could be strongly decreased inducing a

* Corresponding author at: Laboratoire de Chimie de Coordination, 31077 Toulouse Cedex 04, France.
E-mail address: vincent.pradines@lcc-toulouse.fr (V. Pradines).

0927-7757/$ – see front matter © 2010 Elsevier B.V. All rights reserved.
doi:10.1016/j.colsurfa.2010.08.052

smaller adsorption at the water/oil interface [26]. On the contrary, Gillap et al. [27] have observed a strong increase of the adsorbed amount of sodium dodecyl and decyl sulfate at the water/oil interface as compared to the water/air interface, certainly due to the presence of hydrophobic interactions between adsorbed surfactants and oil molecules. Thus, the adsorption of ionic surfactants at the water/oil interface generally follows an ideal behaviour, and is well described by using the Langmuir adsorption isotherm although the Frumkin one is more suitable at the water/air interface [18,21,22].

The target of this work is to describe and compare the adsorption behaviour at the water/air and water/hexane interfaces of a series of alkyl trimethylammonium bromides with different alkyl chain lengths (10, 12, 14, 16 carbon atoms). For the sake of simplicity, the conventional nomenclature of these surfactants (DeTAB, DoTAB, TTAB and CTAB) was changed to C_nTAB where n corresponds to the number of carbon atoms in the hydrophobic chain. Systematic surface and interfacial tension measurements have been performed, followed by a theoretical interpretation of the experimental data with two different adsorption models giving access to thermodynamic adsorption parameters. The salt effects, due to the presence of phosphate buffer, have been taken into account using a modified Frumkin model, our motivations being to describe the adsorption behaviour of these surfactants in this medium in addition to the studies already done in the literature at the pure water/air interface. Such work is relevant when surfactants are combined with biological compounds such as proteins in which case it's necessary to control the number of charges (as a function of the pH). Surfactant layers or aggregates can also be used as the simplest model of biological membranes which justifies also the control of the pH. Thus, we have discussed the buffer effects at the water/air interface and compared our experiments with others performed without additional electrolyte [28–30]. Surface tension isotherms of the same series (n = 12, 14, 16) have been studied at the water/air interface by Stubenrauch et al. [28] using two different theoretical adsorption models which take into account lateral interactions (Frumkin model) and the possibility to change the interfacial molar area (reorientation model) of adsorbed surfactants as a function of the surface pressure (Frumkin Compressibility model). They showed that the second model described more accurately the rheological behaviour of the interfacial layer and the variation of the adsorbed amount at the interface by comparing the results obtained with neutron reflectivity experiments for C_{12}TAB and C_{14}TAB [31]. In this last study, single surfactants and also mixtures of C_{12}TAB and C_{14}TAB with dodecane were spread at the water/air interface. A schematic model of the interface has been proposed in which each surfactant molecule was separated by one alkane molecule showing a loss of the surfactant–surfactant interactions under these conditions. Medrzycka and Zwierzykowski [32] have also studied the adsorption of members of the series C_nTAB (n = 12, 14, 16) at the water/air and various water/alkane interfaces, each oil phase matching the chain length of the respective surfactant (dodecane, tetradecane, and hexadecane), in order to determine under which condition the interactions with the solvent molecules were the most favourable. Studying the variation of the adsorbed amount at the water/air and water/alkane interfaces, they have also suggested the presence of alkane molecules intercalated in the surfactant layer [33].

Regarding these works, we have discussed the different results obtained at both water/air and water/hexane interfaces (shapes of adsorption isotherms, thermodynamic adsorption parameters, variation of the adsorbed amount and molar area of surfactants) in order to understand the C_nTABs adsorption behaviour in neutral phosphate buffer conditions and to determine the role played by the hexane molecules at the interface.

2. Experimental

A stock solution of phosphate buffer 10 mM, pH 7, NaH_2PO_4/Na_2HPO_4 (Fluka, >99%) has been prepared with ultrapure MilliQ water (resistivity = 18.2 MΩ cm) and used to prepare all aqueous surfactant solutions. The surfactants decyl trimethylammonium bromide C_{10}TAB (MW = 280.29 g mol^{-1}, ≥98%), dodecyl trimethylammonium bromide C_{12}TAB (MW = 308.35 g mol^{-1}, ≥99%), cetyl trimethylammonium bromide C_{16}TAB (MW = 364.46 g mol^{-1}, >99.0%) were purchased from Fluka (Switzerland), and the tetradecyl trimethylammonium bromide C_{14}TAB (MW = 336.40 g mol^{-1}, 99%) was purchased from Aldrich. All experiments were performed at room temperature (22 °C). Hexane was purchased from Fluka (Switzerland). It was distilled and purified with aluminium oxide and subsequently saturated with ultrapure MilliQ water.

The experimental setup used to measure the dynamic surface tension of the different systems was the drop Profile Analysis Tensiometer PAT-1 (SINTERFACE Technologies, Berlin, Germany). Equilibrium surface tension values reported in the isotherms have been obtained after a sufficient adsorption time which depends on the concentration of surfactant (from 1 h for the highest concentrations close to the CMC up to 12 h for the lowest ones). The surface tension values of a pure buffer solution were checked at the water/air and water/hexane interfaces and were the same as for the ultrapure MilliQ water (72.5 and 49 mN m^{-1} at the water/air and water/hexane interface, respectively). For the investigations at the water/hexane interface a drop of aqueous solution was formed in a glass cuvette containing pure hexane.

Concerning the experimental data of C_{14}TAB and C_{16}TAB measured at the water/air and at the water/hexane interface, we have applied a correction of the concentration. Due to the strong adsorption of surfactants at the surface of the drop obtained by using very low bulk concentrations, we had surfactant depletion in the drop [34]. Using the first Frumkin model described below, we have obtained a new equilibrium bulk concentration with an iterative calculation protocol. We have taken into account the loss of surfactant from the bulk and checked the total mass balance between the amount of adsorbed surfactant and that present in the bulk phase.

3. Theoretical models

Most adsorption isotherms for non-ionic and ionic surfactants are very well described by the Frumkin model which takes into account the lateral interactions between adsorbed surfactants at the interface [35]. For electroneutral surface layers the following equation of state of the surface layer and the corresponding adsorption isotherm for the Frumkin adsorption model for ionic surfactants was recently proposed [28,36]:

$$\Pi = -\frac{2RT}{\omega_0}[\ln(1-\theta) + a\theta^2] \quad (1)$$

$$b[c(c+c_2)]^{1/2} f = \frac{\theta}{1-\theta}\exp(-2a\theta) \quad (2)$$

where Π is the surface pressure ($\Pi = \gamma_0 - \gamma$), γ and γ_0 are the surface tensions of the solution and the solvent, respectively, ω_0 is the partial molar area of the ionic surfactant at $\Pi = 0$ (two times larger than the molar area of the solvent or ions), a is the intermolecular interaction constant, b is the adsorption equilibrium constant, f is the average activity coefficient of ions in the bulk solution, c is the ionic surfactant concentration, c_2 is the inorganic salt concentration (we made an approximation and have considered the buffer as an electrolyte 1:1), $\theta = \Gamma\omega$ is the surface coverage, Γ is the surfactant adsorption, R is the gas law constant, and T is the temperature. For short-range interactions the Debye-Hückel equation accurately

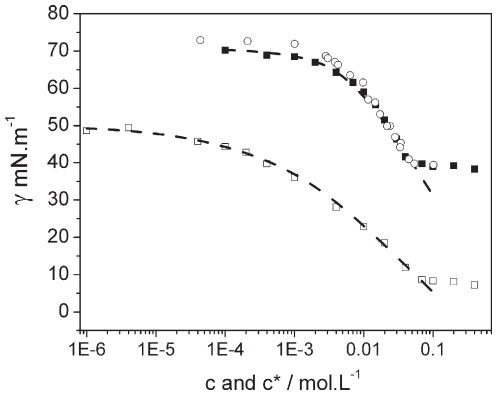

Fig. 1. Surface and interfacial tension isotherms of C_{10}TAB at the water/air (■) and water/hexane (□) interfaces in the presence of phosphate buffer (10 mM, pH 7) plotted versus c (mol L^{-1}). Dashed lines correspond to the theoretical curves obtained with the FIC model. (○) Data from literature [29] at the pure water/air interface plotted as a function of the average activity c^* (with $c_2 = 0$).

corrects the values of the average activity coefficient f:

$$\log f = -\frac{0.5115\sqrt{I}}{1 + 1.316\sqrt{I}} + 0.055I \quad (3)$$

where $I = c + c_2$ is the ionic strength expressed in mol L^{-1}. The numerical constants are reported for a temperature of 25 °C [36]. As previously proposed in Refs. [28,37], it can be assumed that the molar area of the surfactant ω depends on the surface pressure:

$$\omega = \omega_0(1 - \varepsilon\Pi\theta) \quad (4)$$

where ε is the two-dimensional relative surface layer compressibility coefficient, which characterizes the intrinsic compressibility of the molecules in the surface layer.

For several systems, it has been shown that this property was essential in order to describe properly the variation of the adsorbed amount and the dilational rheological behaviour of surfactant layers [17,28,37]. We name the model described by Eqs. (1)–(4), Frumkin Ionic Compressibility model – FIC.

The usual Frumkin model also used in this study is described below by Eqs. (5) and (6):

$$\Pi = -\frac{RT}{\omega_0}[\ln(1 - \theta) + a\theta^2] \quad (5)$$

$$bc = \frac{\theta}{1 - \theta}\exp(-2a\theta) \quad (6)$$

At sufficiently high concentrations of inorganic electrolyte, it is also possible to apply the usual Frumkin equation [38]. Instead of c in Eq. (6) the mean ion activity $c^* = fc$ can be used. When including Eq. (4) the resulting model can be called Frumkin Compressibility model – FC.

4. Results

Surface and interfacial tension measurements have been performed for the series of surfactants C_nTAB (n = 10, 12, 14, 16) at the water/air and water/hexane interfaces in the presence of phosphate buffer (10 mM, pH 7). As we have used ionic surfactants with a negligible solubility in hexane, we can neglect any transfer of surfactant into the oil phase and therefore a partitioning equilibrium totally in favour of the aqueous phase exists. Figs. 1–4 represent the equilibrium surface (filled square) and interfacial (open square) tensions of buffer solutions of C_{10}TAB, C_{12}TAB, C_{14}TAB, and C_{16}TAB, respectively, plotted versus the equilibrium bulk concentrations. The solid and dashed lines correspond to the theoretical curves obtained with the FC and FIC models, respectively. Note, for the FIC model we used

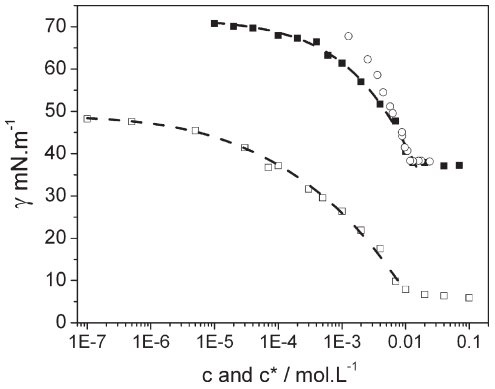

Fig. 2. Surface and interfacial tension isotherms of C_{12}TAB at the water/air (■) data from Ref. [17] and water/hexane (□) interfaces in the presence of phosphate buffer (10 mM, pH 7). Dashed lines correspond to the theoretical curves obtained with the FIC model. (○) Data from literature [28] at the pure water/air interface plotted as a function of the average activity c^* (with $c_2 = 0$).

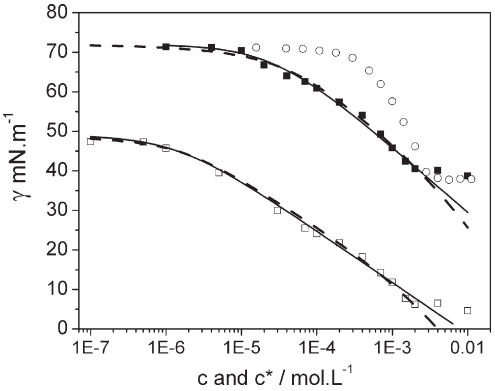

Fig. 3. Surface and interfacial tension isotherms of C_{14}TAB at the water/air (■) and water/hexane (□) interfaces in the presence of phosphate buffer (10 mM, pH 7). Solid and dashed lines correspond to the theoretical curves obtained with the FC and FIC models, respectively. (○) Data from literature [28] at the pure water/air interface plotted as a function of the average activity c^* (with $c_2 = 0$).

c_2 = 2 mM (see further below). Under these conditions the FC model appears applicable only for the highest interfacial active surfactants C_{14}TAB, and C_{16}TAB. In all fitting processes, we kept the intrinsic compressibility coefficient fixed at $\varepsilon = 0.01$ mN m^{-1} for all surfactants. This value will not be commented here in detail because its influence is mainly visible on the dilational rheological data, the

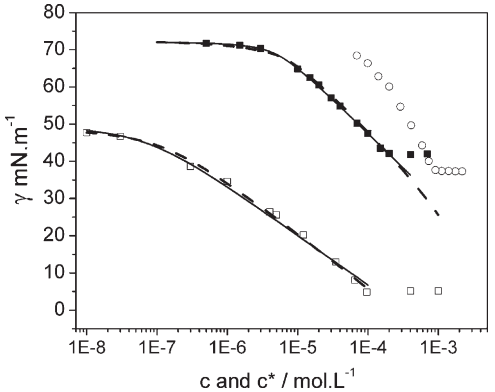

Fig. 4. Surface and interfacial tension isotherms of C_{16}TAB at the water/air (■) and water/hexane (□) interfaces in the presence of phosphate buffer (10 mM, pH 7). Solid and dashed lines correspond to the theoretical curves obtained with the FC and FIC models, respectively. (○) Data from literature [28] at the pure water/air interface plotted as a function of the average activity c^* (with $c_2 = 0$).

Table 1
Parameters of adsorption layer obtained with the FC and FIC models (salt concentration considered to be 2 mM) at the water/air interface. In the FC_{H_2O} column are reported the parameters obtained at the pure water/air interface from Ref. [28].

C_nTAB	ω_0, $m^2\ mol^{-1}$			a			b, $L\ mol^{-1}$		
	FC	FC_{H_2O}	FIC	FC	FC_{H_2O}	FIC	FC	FC_{H_2O}	FIC
$n=10$			3.4E+05			0.7			9.6E+01
$n=12$		2.20	3.2E+05		1.40	0.2		2.6E+02	5.3E+02
$n=14$	3.4E+05	2.12	3.6E+05	0	1.30	0.9	3.8E+04	9.4E+02	1.5E+03
$n=16$	3.0E+05	2.08	2.8E+05	1.2	1.58	1.6	6.1E+04	3.1E+03	1.8E+03

target of a forthcoming work. With both models, the experimental data are very well fitted for both water/air and water/hexane interfaces, which allowed the determination of the thermodynamic adsorption parameters. We have also compared our results with those measured at the pure water/air interface (Figs. 1–4, open circles). These results were plotted versus the average activity of the ions (surfactants) in solution c^* instead of the concentration c. However, in pure water solutions where there is no additional salt ($c_2 = 0$ in Eq. (3)), similar values for the activity c^* and the concentration c of the surfactants are obtained.

4.1. Water/air interface

First of all at the water/air interface we have noted a salt effect due to the presence of the phosphate buffer which is a 1:1 (Na^+, $H_2PO_4^-$) and 2:1 ($2Na^+$, HPO_4^{2-}) electrolyte. The comparison with the isotherms of C_nTAB (Figs. 1–4) measured at the pure water/air interface [28] without additional salt has shown a left shift of the curves and a decrease of the slope indicating a higher surface activity and a different value of the maximum molar area ω_0 of the surfactants. The CMC measured for $C_{10}TAB$ (5×10^{-2} mol L^{-1}), $C_{12}TAB$ (10^{-2} mol L^{-1}) and $C_{14}TAB$ (2×10^{-3} mol L^{-1}) are very close to those in pure water [29], however the shift increases with the chain length of surfactants and the CMC obtained for $C_{16}TAB$ (2×10^{-4} mol L^{-1}) is much lower as compared to the value found in the literature (8×10^{-4} mol L^{-1}). The adsorption parameters obtained with the FC model (Table 1) are different as compared to those of Ref. [28] which is evident by just looking at the shapes of the isotherms. Indeed for each surfactant at the pure water/air interface, about one decade is needed from the lowest concentration to reach the CMC while two to three decades are necessary in the presence of buffer.

It is difficult to directly compare the values of the parameters (b, ω_0 and a) with those described in the literature mainly due to the presence of salt which changes drastically the shape of the curves. As mentioned above, it was not reasonable to fit the surfactant isotherms for the short chain surfactants ($C_{10}TAB$ and $C_{12}TAB$) with the FC model. However, the tendency observed for $C_{14}TAB$ and $C_{16}TAB$ with the FC model (see Table 1) is similar to that obtained by Stubenrauch et al. [28] with an increase of the adsorption constant b and of the interaction parameters a with the surfactant chain length. The differences for the parameter b (one order of magnitude) as compared with the pure water systems, can be explained by the salt effect which decreases the electrostatic repulsion by a screening between the polar heads of ionic surfactants and favours their adsorption [6]. The variation of ω_0 obtained in the series (Table 1 FC) is a bit unexpected, nevertheless this difference is not significant and we can assume that at low surface coverage, all surfactants with the same head group have similar molar areas. Concerning the Frumkin interaction parameter, an evolution in the C_nTAB series (Table 1 FC) is observed from $a = 0$ ($C_{14}TAB$) to $a = 1.2$ ($C_{16}TAB$), in agreement with the results of the literature at the pure water/air interface [22,28].

In order to take into account the presence of salt, we used the so-called Frumkin Ionic Compressibility model (FIC) as second adsorption model, to which correction for the coefficient of the average activity of ions in solutions is based on the Debye-Hückel equation [36]. This model allows to average the salt effects taking into account the activity of all ions present in solution which can be very different at low and high surfactant concentrations. The concentration c_2 in the FIC model includes all added counterions available to play the role of counterion for the surfactant. In our case, we used the phosphate buffer (0.01 mol L^{-1}), which is a particular electrolyte composed of two salts (NaH_2PO_4 and Na_2HPO_4). Note, the buffer has only been used to control the pH and not to create salt effects. Thereby, it is considered as a weak acid and therefore its dissociation is not complete in aqueous solution. To estimate the real concentration of counterions c_2, we had to calculate manually (Eqs. (3) and (4)) the average activity of surfactant solutions and to compare the new isotherms obtained to those of the literature in pure aqueous solutions [28]. To do so, we used the isotherms of $C_{14}TAB$ and $C_{16}TAB$ for which the effect of the ionic strength is the largest. The surface tension isotherms measured in buffer and pure water, respectively, are quasi superimposed for $c_2 = 0.002$ mol L^{-1} (Fig. 5) which seems to be a reasonable approximation. According to the theoretical study of Lucassen-Reynders on the surface equation for ionized surfactant [39], the salting out effect produced by the buffer should only act on the adsorption constant b, which is described by the adsorption isotherm of the FIC model (Eq. (2)). Thus, taking into account the average activity instead of the concentration (FIC model), we should obtain the same parameters than those found at the pure water/air interface with the FC model which would be the case if the isotherm were exactly superimposed (Fig. 5). However the presence of non-ideal effects characteristic of ionic surfactants such as electrostatic (repulsions) or hydrophobic (attractions) interactions, as a function of the distance between adsorbed molecules in the interfacial layer, may explain the difference observed on ω and a, the values of the adsorption constant b being now similar to those obtained at the pure water/air interface (Table 1 FIC and FC_{H_2O}). In the series

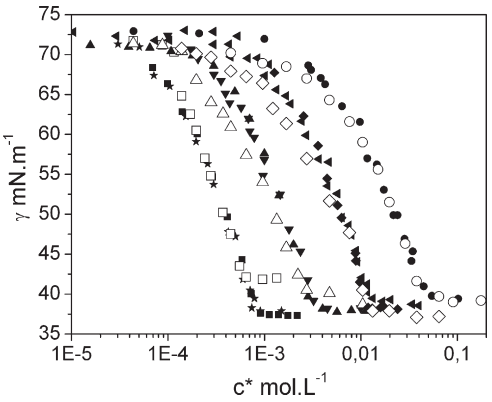

Fig. 5. Surface tension isotherms of C_nTABs plotted versus the activity c^*. $c^* = ((c + c_2)c)^{1/2} f$ where c is concentration of surfactant and c_2 those of counterions ($c_2 = 0.002$ mol L^{-1}): (○) $n = 10$; (◊) $n = 12$; (△) $n = 14$; (□) $n = 16$; data from literature with $c_2 = 0$: (●) $n = 10$; (♦, ◄) $n = 12$; (▲, ▼) $n = 14$; (ω, ■) $n = 16$ have been taken from Refs. [28,38].

Table 2
Parameters of adsorption layers obtained with the Frumkin Compressibility and Frumkin Ionic Compressibility models (salt concentration considered to be 2 mM) at the water/hexane interface.

C_nTAB	ω_0, $m^2\ mol^{-1}$		a		b, $L\ mol^{-1}$	
	FC	FIC	FC	FIC	FC	FIC
$n=10$		5.6E+05		0		2.2E+03
$n=12$		4.4E+05		0		4.3E+03
$n=14$	4.3E+05	4.4E+05	0	1.2	6.9E+06	5.5E+03
$n=16$	4.2E+05	3.8E+05	0	1.1	1.5E+07	2.2E+04

of the C_nTABs (Table 1 FIC), the values of ω_0 are similar to each other ($3.2 \times 10^5 \pm 0.4\ m^2\ mol^{-1}$). The Frumkin parameter is always positive indicating the presence of attractive lateral interactions between adsorbed surfactants, which is commonly observed. The value of the adsorption constant b increases with the chain length of the surfactant as expected.

For both models, we have taken into account the intrinsic compressibility parameter ε which allows the surfactants to get a smaller molar area with increasing surface coverage. At low surface coverage, the surfactant can use the maximum free space at the interface leading to a tilt of the alkyl chain [37]. Due to this possibility of orientation, the area of the surfactant will change as a function of the surface pressure and surface coverage. The values of ε obtained from the fitting of the dilational rheology data (not shown) were in agreement with the value in literature [28]. Indeed, it has been shown that a value different from zero was needed to describe more accurately the adsorption behaviour of the C_nTABs, in particular the evolution of the adsorbed amount.

4.2. Water/hexane interface

At the water/hexane interface, the CMC of surfactants are similar to those measured at the water/air interface indicating that the aggregation process is not influenced by the presence of hexane molecules to which solubility in water is very weak. However, large differences have been observed in the shape of the isotherm for each surfactant. The adsorption starts at concentrations much lower than at the water/air interface: for C_{14}TAB and C_{16}TAB (Figs. 3 and 4), four decades are now necessary to reach the CMC and this effect is even more pronounced for C_{10}TAB and C_{12}TAB (Figs. 1 and 2) with six decades. Hence, very small amounts of adsorbed C_nTAB molecules change the interfacial tension. Due to the affinity of the hydrophobic chains for the oil phase, the surfactants interact with the hexane molecules located at the interface which favours their adsorption. The parameters of the models reported in Table 2 are in agreement with these observations. The values of the adsorption constant b (both FC and FIC models) are much higher than at the water/air interface as well as those of the maximum molar area ω_0 which can also be explained by the presence of intercalated hexane molecules in the surfactant adsorption layers.

5. Discussion

Comparing the different parameters obtained for the series of C_nTAB ($n=10$, 12, 14 and 16), firstly between both models, and secondly between both interfaces; it is difficult to give a clear explanation due to the disparity of possible interpretations. Indeed, a clear trend, especially for ω_0, has not been observed and can be obscured by possible experimental errors due to the very long adsorption time necessary at low surfactant concentrations and also caused by the presence of the phosphate buffer. Actually, very different shapes of surface tension isotherms have also been observed as a function of the chain length for the series of n-alkyl sulfate ($n=7$–14) adsorbed at the water/air interface [14]. The cross-section area (molar area for a saturated layer) was not constant for all surfactants, decreasing with increasing chain length until $n=10$–12 due to the increase of the van der Waals interactions, and then increasing strongly for surfactants with $n \geq 12$. In our case, despite the variations observed, a realistic picture of the interfacial behaviour of the C_nTAB series has been obtained via the analysis of the adsorbed amount Γ and the molar area ω as a function of equilibrium bulk concentration. Moreover, we have observed that the surfactant's behaviour in the presence of phosphate buffer can be similarly described with both models. Nevertheless, the values of the parameters found with the FIC model are much more reasonable to describe the C_nTABs interfacial behaviour, which underlines the relevance of this model.

Additionally to the shape of the isotherms and to the parameters of the models, the visualisation of the evolution of the molar area ω and of the adsorbed amount Γ calculated from the modeling is essential in order to understand the interfacial behaviour of the surfactants. In Figs. 6–9, we have plotted the variation of Γ (solid line) and ω (dashed line) as a function of equilibrium bulk concentration of each surfactant. For C_{10}TAB and C_{12}TAB (Figs. 6 and 7), realistic values were obtained only with the FIC model, while the FC model is not applicable due to the constrains given above and would lead to a wrong idea of the interfacial behaviour. Actually, due to the shape of the isotherm (Figs. 1 and 2) with a decrease of the surface tension at very low bulk concentrations and during several decades to reach the CMC, a strong negative value of the Frumkin parameter would be needed to fit properly the experimental data. At the water/air interface, the behaviours of C_{10}TAB and C_{12}TAB obtained with the FIC model are similar (Figs. 6 and 7 black lines) showing an equivalent evolution of Γ and ω. On the other side, at the water/hexane interface (Figs. 6 and 7 grey lines), a similar behaviour for the two surfactants is observed only at low surface coverage where Γ is higher at the water/hexane interface than at the water/air interface due to the better affinity of the surfactant for the oil phase. The presence of intercalated solvent molecules in the surfactant layer

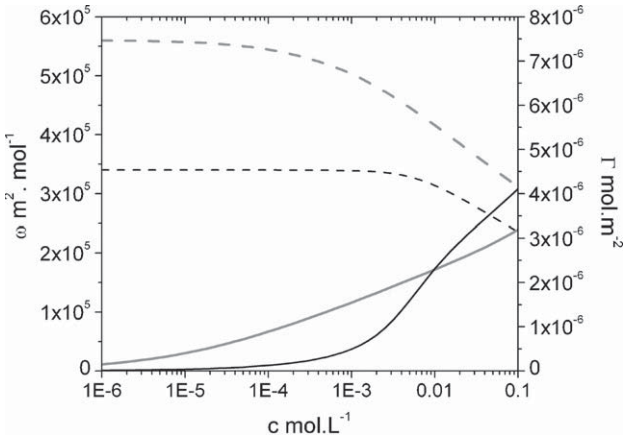

Fig. 6. Variation of the adsorbed amount Γ (solid line, right scale) and molar area ω (dashed line, left scale) of C_{10}TAB at the water/air (black) and water/oil (grey). Calculated with FIC model.

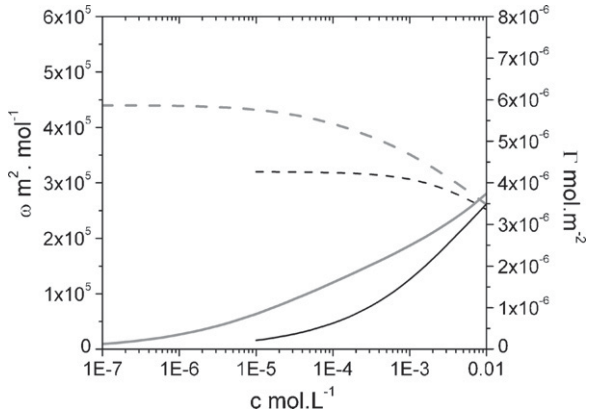

Fig. 7. Variation of the adsorbed amount Γ (solid line, right scale) and molar area ω (dashed line, left scale) of C_{12}TAB at the water/air (black) and water/oil (grey). Calculated with FIC model.

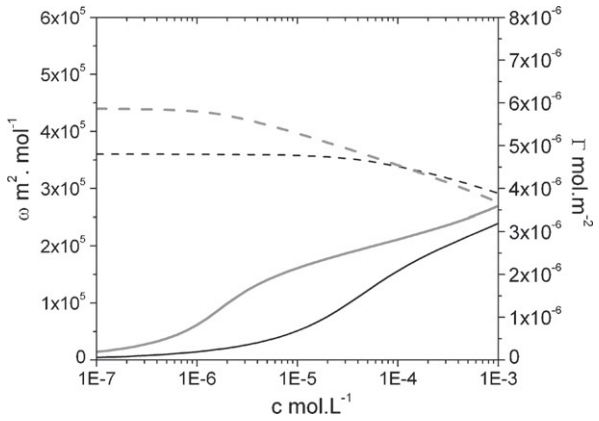

Fig. 8. Variation of the adsorbed amount Γ (solid line, right scale) and molar area ω (dashed line, left scale) of C_{14}TAB at the water/air (black) and water/oil (grey). Calculated with the FIC model.

explains also the higher molar area at the water/hexane interface than at the water/air interface. This explanation is not true anymore at high surface coverage for C_{10}TAB for which a cross-section between the curves of the adsorbed amount has been observed. Indeed at high surface coverage, $\Gamma_{C_{10}TAB}$ becomes higher at the water/air interface (Fig. 6 black solid line) than at the water/hexane interface (Fig. 6 grey solid line). The phenomenon observed in that case looks like a kind of competitive adsorption between the surfactant and the hexane molecules. A short chain surfactant such as C_{10}TAB is not able to completely replace the solvent molecules from the interface due to weak self-attractive interactions leading to a smaller adsorbed amount for a saturated layer. A higher value of ω at the water/hexane interface (Fig. 6 grey dashed line) has also confirmed this hypothesis. Indeed the presence of intercalated solvent molecules is interpreted by the model as an increase of the molar area of the surfactant at the interface. On the other hand for C_{12}TAB (Fig. 7), Γ and ω are similar at both water/air and water/hexane interfaces close to the CMC showing the same interfacial composition of the saturated layer. Even if the Frumkin parameter is also equal to 0, the lateral interactions between the C_{12} alkyl chains seem to be sufficient to change the interfacial behaviour as compared to C_{10}TAB.

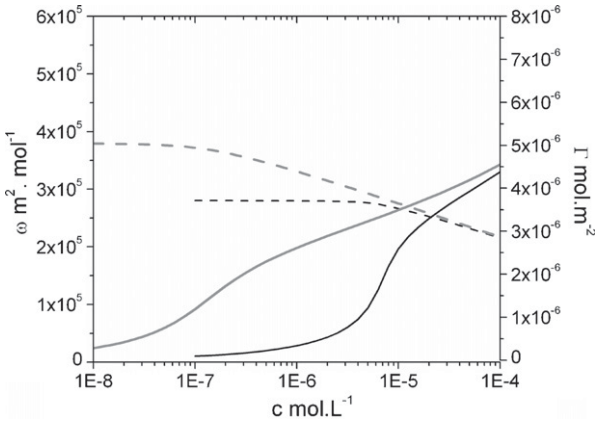

Fig. 9. Variation of the adsorbed amount Γ (solid line, right scale) and molar area ω (dashed line, left scale) of C_{16}TAB at the water/air (black) and water/oil (grey). Calculated with the FIC model.

Surprisingly, for the longest chain surfactants C_{14}TAB and C_{16}TAB a similar behaviour has been obtained with the FC (not shown) and the FIC models (Figs. 8 and 9) using very different parameters (Tables 1 and 2). The salt effect has resulted, identically to the short chain surfactants, in a decrease of surface tension (Figs. 3 and 4) at low bulk concentrations. This has been translated at both interfaces by the Frumkin Compressibility model by extremely high values of the adsorption constant b (cf. Tables 1 and 2 FC). This behaviour in buffer conditions has induced a different variation of the calculated adsorbed amounts of Γ for C_{14}TAB (Fig. 8) at the water/air interface as compared to the values measured by neutron reflectivity in pure water [31]. In our case, $\Gamma_{C_{14}TAB}$ is much more important at low bulk concentrations in the presence of buffer, which is explained by the screening effects of the added ions and so by the decrease of the electrostatic repulsions between adsorbed surfactant molecules.

Regarding both interfaces at low surface coverage, the interfacial behaviour for the long chain surfactants C_{14}TAB and C_{16}TAB (Figs. 8 and 9) showing a higher molar area ω and adsorbed amount Γ at the water/hexane interface than at the water/air interface, is similar to that of C_{10}TAB and C_{12}TAB (Figs. 6 and 7). This is due to the affinity of the surfactants for the oil phase which increases with the alkyl chain length. At high surface coverage (Figs. 8 and 9), the behaviours of C_{14}TAB and C_{16}TAB join the C_{12}TAB one (Fig. 7) which confirms a kind of transition between short ($n = 10$) and long ($n > 12$) chain surfactants. This difference is due to the presence of strong attractive surfactant–surfactant interactions which now dominate and allow the replacement of the solvent molecules at the water/hexane interface by the long chain surfactants. The values of the Frumkin parameters obtained from the best fitting at the water/oil interface are equal to zero or positive (Table 2 FC and FIC). Even if a positive value is not needed to obtain the best fitting (FC model), without any doubt we can expect the presence of self-interactions for the longest chain surfactants C_{14}TAB and C_{16}TAB. In contrast to Medrzycka and Zwierzykowski [32] who have observed the same behaviour for all surfactants of the series ($n = 12$, 14, and 16), we think, that the hexane molecules are not long enough (as compared to decane, dodecane and tetradecane) to interact sufficiently strong with the chain of the surfactants and to stay adsorbed at the interface together with the longest chain surfactants ($n = 14$ and 16) in the total range of surface coverage.

6. Conclusion

This experimental and theoretical study was dedicated to the adsorption behaviour of a series of C_nTAB ($n = 10$–16) at the water/air and water/hexane interface in the presence of neutral phosphate buffer. Some general trends were detected via the comparison of the results obtained at the water/air interface in the presence of buffer or in pure aqueous solution, and also by comparing the water/air and water/hexane interfaces. The results obtained

in buffer conditions at the water/air interface have shown a strong increase of the adsorption due to the screening effect of the added electrolyte leading to a decrease of electrostatic repulsions. At the water/hexane interface, the high adsorbed amounts are due to the presence of the hexane molecules which interact with the surfactants at low surface coverage. At high surface coverage, the behaviour becomes a function of the surfactant chain length: a kind of competitive adsorption has been observed for the shortest chain surfactant (C_{10}TAB) while for the longer chains (C_{12}TAB, C_{14}TAB and C_{16}TAB), the mutual interactions are strong enough to replace the solvent molecules at the interface. At high surface coverage and when the layer is saturated, identical values of the adsorbed amount Γ and of the molar area ω were found for the longest chain surfactants at the water/air and water/hexane interfaces meaning that intrinsic properties of the surfactants govern the adsorption. In the presence of phosphate buffer, the use of a modified Frumkin Ionic Compressibility model (FIC) taking into account the average activity of the ions has shown a remarkable accuracy in the determination of the fitting parameters and for the calculation of the adsorbed amount and molar area as compared with the classical Frumkin model. The FIC model avoids the effect of additional salts and takes finally into account only the effect of the surfactants which is translated into a relatively small variation of the parameters as compared to those obtained at the pure water/air interface (cf. Table 1). For C_{14}TAB and C_{16}TAB, the comparison of both FC and FIC models has shown very similar results on the tendencies and on the final values of Γ and ω. The main differences have been observed only on the value of the parameters (b, ω_0 and a) and especially on the adsorption constant b which has been overestimated by using the FC model.

A good complementary work would be to study these systems with neutron reflectivity, ellipsometry or sum frequency spectroscopy in order to reach as close as possible the value of the adsorbed amount in the presence of buffer. These results could then be compared with ours. Nevertheless, these techniques are not yet easily accessible which proves the importance of the development of new models able to better describe the surfactant adsorption at the water/air and water/oil interfaces.

Acknowledgements

This work was financially supported by a project of the DFG SPP 1273 (Mi418/16-2). V.P. thanks the Alexander von Humboldt foundation for the financial support and S. Siegmund for the technical support.

References

[1] E. Dickinson, Interfacial structure and stability of food emulsions as affected by protein-polysaccharide interactions, Soft Mater. 4 (2008) 932–942.
[2] M.E. Leser, L. Sagalowicz, M. Michel, H.J. Watzke, Self-assembly of polar food lipids, Adv. Colloid Interface Sci. 123–126 (2006) 125–136.
[3] R.H. Müller, C.M. Keck, Challenges and solutions for the delivery of biotech drugs—a review of drug nanocrystal technology and lipid nanoparticles, J. Biotechnol. 113 (2004) 151–170.
[4] L.L. Schramm, E.N. Stasiuk, D.G. Marangoni, Surfactants and their applications, Annu. Rep. Prog. Chem. 99 (2003) 3–48.
[5] A.J. Prosser, E.I. Franses, Adsorption and surface tension of ionic surfactants at the air–water interface: review and evaluation of equilibrium models, Colloids Surf. A 178 (2001) 1–40.
[6] M.M. Knock, C.D. Bain, Effect of counterion on monolayers of hexadecyltrimethylammonium halides at the air-water interface, Langmuir 16 (2000) 2857–2865.
[7] J.R. Lu, R.K. Thomas, J. Penfold, Surfactant layers at the air/water interface: structure and composition, Adv. Colloid Interface Sci. 84 (2000) 143–304.
[8] A. Zarbakhsh, A. Querol, J. Bowers, J.R.P. Webster, Structural studies of amphiphiles adsorbed at liquid–liquid interfaces using neutron reflectometry, Faraday Discuss. 129 (2005) 155–167.
[9] V.B. Fainerman, R. Miller, E.V. Aksenenko, A.V. Makievski, J. Krägel, G. Loglio, L. Liggieri, Effect of surfactant interfacial orientation/aggregation on adsorption dynamics, Adv. Colloid Interface Sci. 86 (2000) 83–101.
[10] C.-H. Chang, E.I. Franses, Adsorption dynamics of surfactants at the air/water interface: a critical review of mathematical models, data, and mechanisms, Colloids Surf. A 100 (1995) 1–45.
[11] P. Warszynski, W. Barzyk, K. Lunkenheimer, H. Fruhner, Surface tension and surface potential of nano-dodecyl sulfate at the air-solution interface: model and experiment, J. Phys. Chem. B 102 (1998) 10948–10957.
[12] V. Pradines, D. Lavabre, J.-C. Micheau, V. Pimienta, Determining the association constant and adsorption properties of ion pairs in water by fitting surface tension data, Langmuir 21 (2005) 11167–11172.
[13] V.B. Fainerman, R. Miller, E.V. Aksenenko, Simple model for prediction of surface tension of mixed surfactant solutions, Adv. Colloid Interface Sci. 96 (2002) 339–359.
[14] K. Lunkenheimer, G. Czichocki, R. Hirte, W. Barzyk, Novel results on the adsorption of ionic surfactants at the air/water interface—sodium-n-alkyl sulphates, Colloids Surf. A 101 (1995) 187–197.
[15] V.L. Kolev, K.D. Danov, P.A. Kralchevsky, G. Broze, A. Mehreteab, Comparison of the Van der Waals and Frumkin adsorption isotherms for sodium dodecyl sulfate at various salt concentrations, Langmuir 18 (2002) 9106–9109.
[16] S.R. Deshiikan, D. Bush, E. Eschenazi, K.D. Papadopoulos, SDS, Brij58 and CTAB at the dodecane-water interface, Colloids Surf. A 136 (1998) 133–150.
[17] C. Kotsmar, E.V. Aksenenko, V.B. Fainerman, V. Pradines, R. Miller, Equilibrium and dynamics of adsorption of mixed β-casein/surfactant solutions at the water/hexane interface, Colloids Surf. A 354 (2010) 210–217.
[18] V. Pradines, J. Krägel, V.B. Fainerman, R. Miller, Interfacial properties of mixed beta-lactoglobulin SDS layers at the water/air and water/oil interface, J. Phys. Chem. B 113 (2008) 745–751.
[19] A. Zarbakhsh, A. Querol, J. Bowers, M. Yaseen, J.R. Lu, J.R.P. Webster, Neutron reflection from the liquid-liquid interface: adsorption of hexadecylphosphorylcholine to the hexadecane-aqueous solution interface, Langmuir 21 (2005) 11704–11709.
[20] M. Mulqueen, D. Blankschtein, Theoretical and experimental investigation of the equilibrium oil-water interfacial tensions of solutions containing surfactant mixtures, Langmuir 18 (2001) 365–376.
[21] F. Ravera, M. Ferrari, L. Liggieri, Adsorption and partitioning of surfactants in liquid–liquid systems, Adv. Colloid Interface Sci. 88 (2000) 129–177.
[22] R. Tadmouri, C. Zedde, C. Routaboul, J.-C. Micheau, V. Pimienta, Partition and water/oil adsorption of some surfactants, J. Phys. Chem. B 112 (2008) 12318–12325.
[23] D. Lavabre, V. Pradines, J.-C. Micheau, V. Pimienta, Periodic Marangoni instability in surfactant (CTAB) liquid/liquid mass transfer, J. Phys. Chem. B 109 (2005) 7582–7586.
[24] V. Pradines, R. Tadmouri, D. Lavabre, J.-C. Micheau, V. Pimienta, Association, partition, and surface activity in biphasic systems displaying relaxation oscillations, Langmuir 23 (2007) 11664–11672.
[25] E. Hutchinson, Films at oil-water interfaces, J. Colloid Sci. 3 (1948) 219–234.
[26] E.A. Boucher, T.M. Grinchuck, A.C. Zettlemoyer, Surface activity of sodium salts of alpha-sulfo fatty esters: the air-water interface, J. Am. Oil Chem. Soc. 45 (1968) 49–52.
[27] W.R. Gillap, N.D. Weiner, M. Gibaldi, Ideal behavior of sodium alkyl sulfates at various interfaces. Thermodynamics of adsorption at the oil-water interface, J. Phys. Chem. 72 (1968) 2222–2227.
[28] C. Stubenrauch, V.B. Fainerman, E.V. Aksenenko, R. Miller, Adsorption behavior and dilational rheology of the cationic alkyl trimethylammonium bromides at the water/air interface, J. Phys. Chem. B 109 (2005) 1505–1509.
[29] V. Bergeron, Disjoining pressures and film stability of alkyltrimethylammonium bromide foam films, Langmuir 13 (1997) 3474–3482.
[30] F. Monroy, J.G. Kahn, D. Langevin, Dilational viscoelasticity of surfactant monolayers, Colloids Surf. A 143 (1998) 251–260.
[31] J.R. Lu, R.K. Thomas, R. Aveyard, B.P. Binks, P. Cooper, P.D.I. Fletcher, A. Sokolowski, J. Penfold, Structure and composition of dodecane layers spread on aqueous solutions of tetradecyltrimethylammonium bromide: neutron reflection and surface tension measurements, J. Phys. Chem. 96 (1992) 10971–10978.
[32] K. Medrzycka, W. Zwierzykowski, Adsorption of alkyltrimethylammonium bromides at the various interfaces, J. Colloid Interface Sci. 230 (2000) 67–72.
[33] M. Thoma, H. Möhwald, Phospholipid monolayers at hydrocarbon/water interfaces, J. Colloid Interface Sci. 162 (1994) 340–349.
[34] R. Miller, V.B. Fainerman, A.V. Makievski, M. Leser, M. Michel, E.V. Aksenenko, Determination of protein adsorption by comparative drop and bubble profile analysis tensiometry, Colloids Surf. B 36 (2004) 123–126.
[35] A. Frumkin, Electrocapillary curve of higher aliphatic acids and the state equation of the surface layer, Z. Phys. Chem. 116 (1925) 466–483.
[36] V.B. Fainerman, E.H. Lucassen-Reynders, Adsorption of single and mixed ionic surfactants at fluid interfaces, Adv. Colloid Interface Sci. 96 (2002) 295–323.
[37] V.B. Fainerman, R. Miller, V.I. Kovalchuk, Influence of the two-dimensional compressibility on the surface pressure isotherm and dilational elasticity of dodecyldimethylphosphine oxide, J. Phys. Chem. B 107 (2003) 6119–6121.
[38] V.B. Fainerman, D. Möbius, R. Miller, Surfactants: Chemistry, Interfacial Properties, Applications, Elsevier, Amsterdam, 2001.
[39] E.H. Lucassen-Reynders, Surface equation of state for ionized surfactants, J. Phys. Chem. 70 (1966) 1777.

Paper III

Adsorption layer properties of alkyl trimethylammonium bromides at interfaces between water and different alkanes

N. Mucic, N.M. Kovalchuk, V.B. Fainerman, E.V. Aksenenko and R. Miller

to be submitted

Adsorption layer properties of alkyl trimethylammonium bromides at interfaces between water and different alkanes

N. Mucic[1]*, N.M. Kovalchuk[2], E.V. Aksenenko[3], V.B. Fainerman[4] and R. Miller[1]

[1] *Max-Planck Institute of Colloids & Interfaces, Potsdam/Golm, Germany*

[2] *Institute of Biocolloid Chemistry, Vernadsky av. 42, 03142 Kiev, Ukraine*

[3] *Institute of Colloid Chemistry and Chemistry of Water, 03680 Kiev, Ukraine*

[4] *Donetsk Medical University, 16 Ilych Avenue, Donetsk 83003, Ukraine*

Abstract

The interfacial tensions of aqueous solutions against different oil phases were measured by Drop Profile Analysis Tensiometry (PAT-1, Sinterface Technologies, Germany) for decyl and dodecyl trimethylammonium bromide (C_{10}TAB and C_{12}TAB) in phosphate buffer (10mM, pH7). As oil phases the following alkanes were used: hexane, heptane, octane, nonane, decane, dodecane and tetradecane. The obtained equilibrium interfacial tension isotherms were fitted by the Frumkin Ionic Compressibility model (FIC). The surfactants adsorb at the water/oil interface in competition with the oil molecules. At high surfactant surface coverage this competitive adsorption is manifested in two ways; for short chain surfactants the oil molecules are embedded into the adsorption layer while for long chain surfactants the short alkane chains of the oil molecules are squeezed out from the adsorption layer due to strong mutual interaction between surfactants' chains.

Keywords: Cationic surfactants, adsorption isotherms, water-alkane interface, chain length dependence, interfacial tension, drop profile analysis tensiometry

* corresponding author

Introduction

Surfactants are applied in almost any modern technology, and they are needed for the modification of the properties of interfaces between water and different oils, such as in food technology [1], oil recovery [2], cosmetics [3]. In most cases their role as emulsifier or demulsifier has to be understood quantitatively in order to develop optimum formulations [4, 5, 6].

In the past most studies on the thermodynamics and kinetic properties of surfactants were investigated at the water/air interface, mainly caused by the accessibility of suitable experimental methods. Since recently, powerful methods are available which allow quantitative studies also at water/oil interfaces. Most of these methods are based on single drop studies, such as drop profile analysis or capillary pressure tensiometry [7]. However, also optical methods have been refined such that they allow measuring quantitatively the adsorption layer properties at liquid/liquid interfaces [8, 9, 10].

Not only experimentally, also the analysis of data gained on the adsorption of surfactants at water/oil interfaces seems to be more complex, although so far models developed for water/air interfaces were directly applied without taking any specificities into consideration. In order to better understand the effect of the oil phase on the adsorption layer structure and behavior of surfactants at liquid interfaces comparative studies were performed for the same surfactant solutions at the interfaces to air and different oils, respectively [10, 11]. The chain length of the oil and its polarity seem to have a remarkable effect on the adsorption layer properties of surfactants [12, 13]. Also the competition of surfactant and co-surfactant in emulsion systems is a matter of systematic investigations [14].

The incorporation of oil molecules into surfactant adsorption layers was also studied for the case of water/vapor interfaces where the oil molecules co-adsorb from the oil vapor phase [15, 16, 17]. This system represents an intermediate between the water/air and water/oil interfaces and conclusions for either situation are based on common argumentations. Depending on the alkyl chain length, the oil molecules of a fixed alkane, for example, are either incorporated into the surfactant interfacial layer or, for longer alkyl chains, the mutual interaction between these chains squeeze the oil molecules out, as it was shown by Pradines et al. recently [18].

In the present work we studied two cationic surfactants of the homologous series of alkyl trimethyl ammonium bromides at the water/oil interface. As oil phase we used alkanes of different chain length from hexane to tetradecane, i.e. alkanes with an aliphatic chain shorter or longer as the alkyl chain of the surfactant. It will be shown by interfacial tension studies performed with the drop profile analysis tensiometry that in the range of similar chain lengths of the surfactant and the oil, respectively, particular properties are observed. Especially the thermodynamic quantities of the corresponding adsorption model, such as the surfactant's surface activity and the molar interfacial area, are determined as a function of the alkane chain length.

Materials and methods

All surfactant solutions were prepared in the phosphate buffer NaH_2PO_4/Na_2HPO_4 (10mM, pH 7) purchased from Fluka (Switzerland) with purity higher than 99%. The surfactants decyl trimethyl ammonium bromide $C_{10}TAB$ (MW = 280.29 g/mol, $\geq$98%)

and dodecyl trimethyl ammonium bromide C_{12}TAB (MW = 308.35 g/mol, ≥99%) were also purchased from Fluka. Both surfactants have been purified by triple recrystallization in a mixture of absolute ethanol and acetone. We have performed the experiments at water interfaces against heptane, octane, nonane, decane, all purchased from ACROS Organics, and dodecane and tetradecane, purchased from Alfa Aesar. Oils were distilled and further purified with Florisil. All experiments were performed at room temperature (22°C - 25°C). The data for the water/hexane interface were taken from [18].

The experimental setup used for the investigation was the drop Profile Analysis Tensiometer PAT-1 (SINTERFACE Technologies, Berlin, Germany). The dynamic interfacial tension was measured for different concentrations of each surfactant at the respective water/oil interfaces. Then, the obtained equilibrium values of the interfacial tension were used to construct the respective adsorption isotherms. The time necessary to obtain adsorption equilibrium depends directly on the bulk concentration of the measured surfactant solution [19]. In these experiments sufficient equilibration times were from less than 1h for high concentrations close to CMC up to 3.5h for lower concentrations. The instrument was calibrated such that most accurate values were obtained for the pure water/oil interfacial tensions. The interfacial tensions at 25°C for water/hexane interface is 51.1 mN/m, water/heptane interface 50.8 mN/m, water/octane interface 51 mN/m, water/nonane interface 51 mN/m, water/decane interface 52.0 mN/m, water/dodecane interface 52.8 mN/m and water/tetradecane interface 52.2 mN/m, in agreement with data given in [20]. For the investigations a drop of the aqueous solution was formed in a glass cuvette containing the respective oil phase.

Results and discussion

Interfacial tension measurements have been performed for C_{10}TAB and C_{12}TAB surfactants at the water/hexane, water/heptane, water/octane, water/nonane, water/decane, water/dodecane and water/tetradecane interfaces. All aqueous solutions were prepared in a phosphate buffer (10mM, pH7). As we have used ionic surfactants with a negligible solubility in all alkanes, we can neglect any transfer of surfactant molecules into the oil phase and, therefore, the partitioning equilibrium is totally in favor of the aqueous phase.

Figs. 1-7 represent the equilibrium interfacial tensions of buffer solutions of C_{10}TAB and C_{12}TAB, respectively, at the interface to alkanes plotted versus the surfactant bulk concentrations. The solid lines correspond to the theoretical curves obtained with the so-called FIC model (Frumkin Ionic Compressibility model proposed in [1]). Note, for this model we used c_2 = 2 mM for the concentration of the added electrolyte in form of the buffer salts. Also in all fitting processes, we kept the intrinsic compressibility coefficient fixed at ε=0.01 mN/m for both studied surfactants. The coefficient ε just affects the kinetics and dilational rheology results. Here, we follow the procedure for fitting of C_nTABs dissolved in pH7 phosphate buffer, as explained in [18]. From Figs. 1-7 it is seen that the experimental data are very well fitted by this model, which allows us to determine the thermodynamic adsorption parameters.

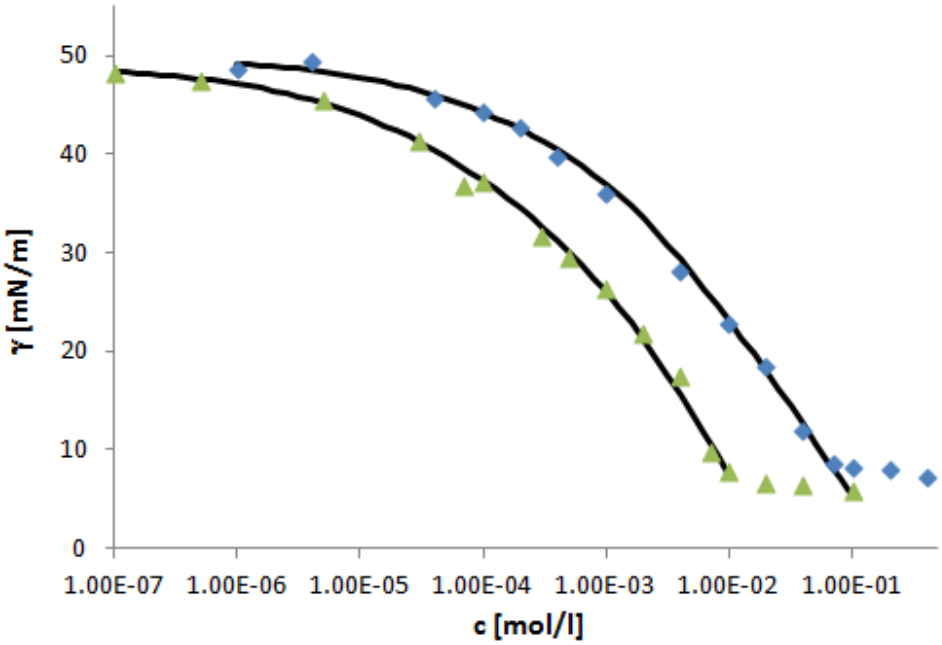

Fig. 1. Interfacial tension isotherms of C_{10}TAB (◆) and C_{12}TAB (▲) at the water/hexane interface in presence of phosphate buffer (10mM, pH7); solid lines corespond to the curves calculated with the FIC model; data from literature [18].

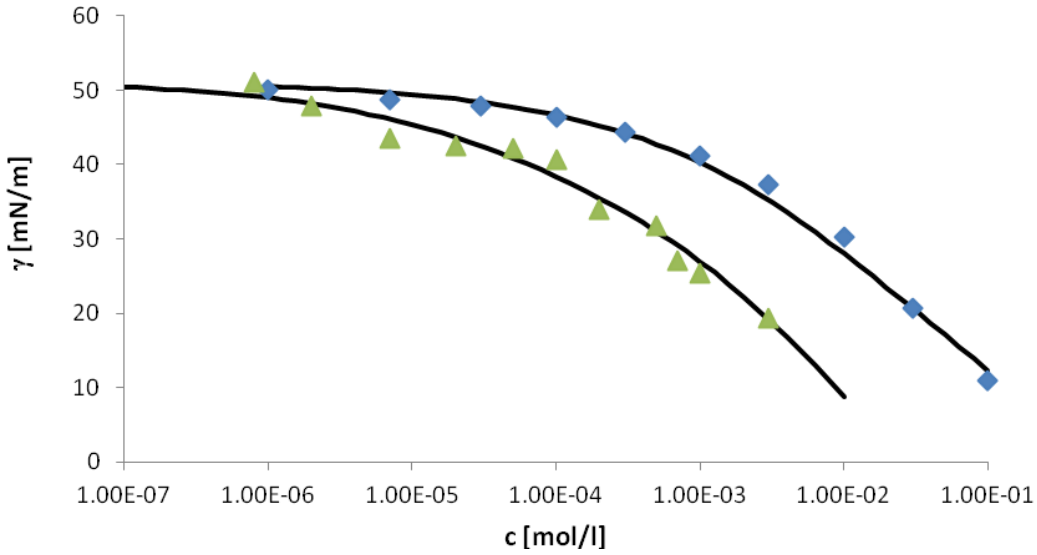

Fig. 2. Interfacial tension isotherms of C_{10}TAB (◆) and C_{12}TAB (▲) at the water/heptane interface in presence of phosphate buffer (10mM, pH7); solid lines corespond to the curves calculated with the FIC model.

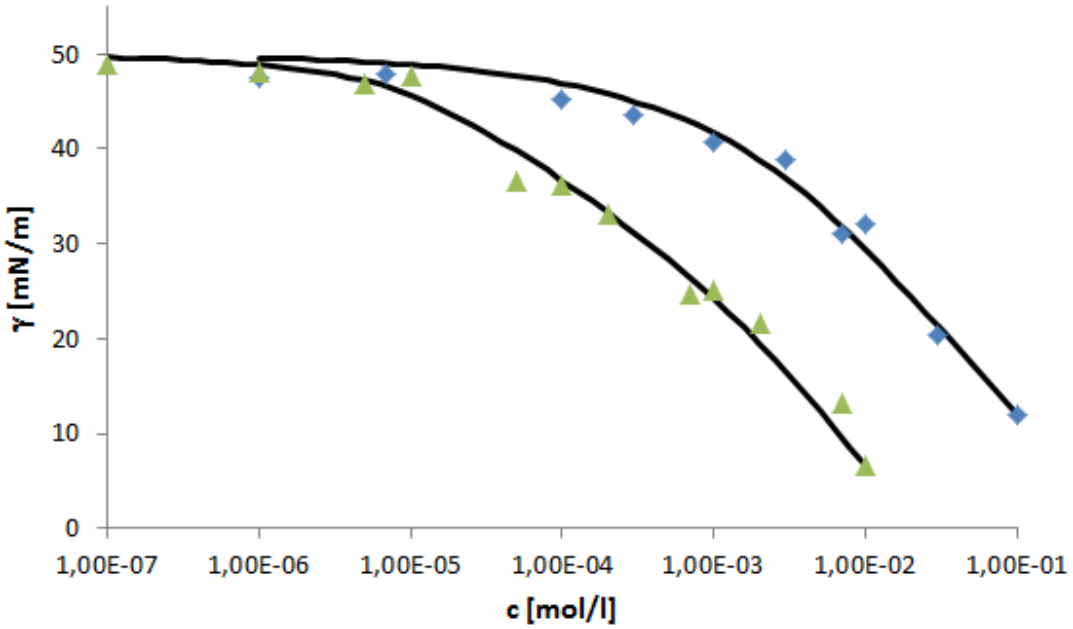

Fig. 3. Interfacial tension isotherms of C_{10}TAB (◆) and C_{12}TAB (▲) at the water/octane interface in presence of phosphate buffer (10mM, pH7); solid lines corespond to the curves calculated with the FIC model.

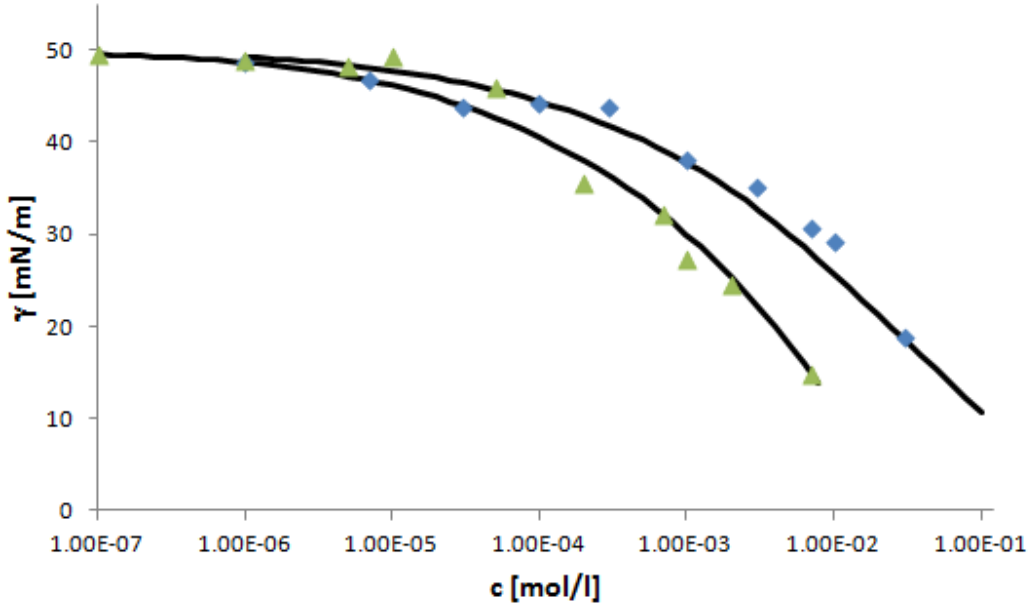

Fig. 4. Interfacial tension isotherms of C_{10}TAB (◆) and C_{12}TAB (▲) at the water/nonane interface in presence of phosphate buffer (10mM, pH7); solid lines corespond to the curves calculated with the FIC model.

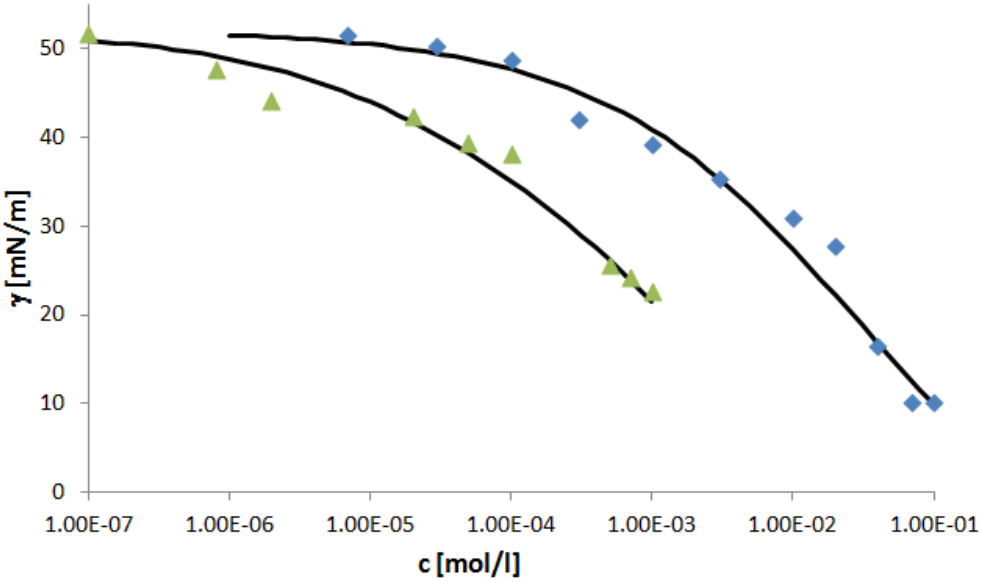

Fig. 5. Interfacial tension isotherms of C_{10}TAB (◆) and C_{12}TAB (▲) at the water/decane interface in presence of phosphate buffer (10mM, pH7); solid lines corespond to the curves calculated with the FIC model.

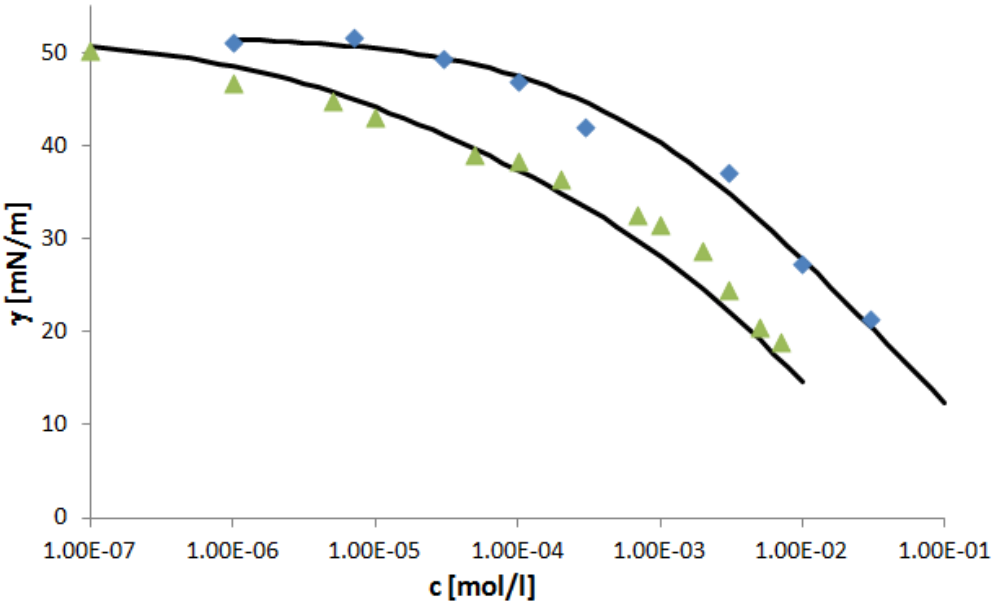

Fig. 6. Interfacial tension isotherms of C_{10}TAB (◆) and C_{12}TAB (▲) at the water/dodecane interface in presence of phosphate buffer (10mM, pH7); solid lines corespond to the curves calculated with the FIC model.

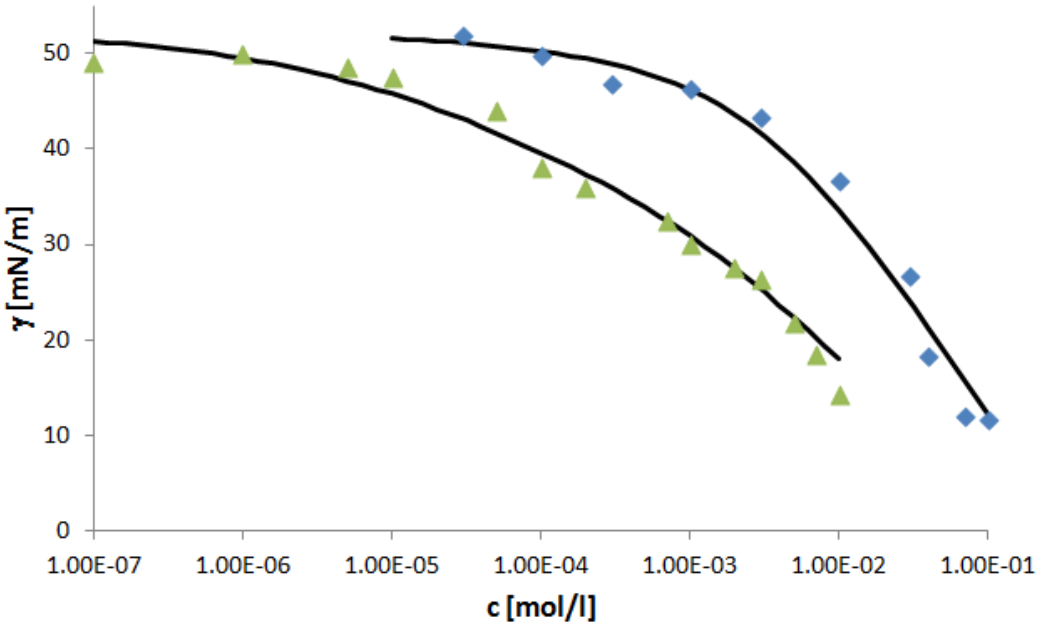

Fig. 7. Interfacial tension isotherms of C_{10}TAB (◆) and C_{12}TAB (▲) at the water/tetradecane interface in presence of phosphate buffer (10mM, pH7); solid lines corespond to the curves calculated with the FIC model.

From the Figs. 1-7 it is seen that the adsorption of C_{10}TAB and C_{12}TAB starts at concentrations much lower than at the water/air interface [19] and it spans over about five decades to reach the CMC. Hence, very small amounts of adsorbed C_nTAB molecules change already the interfacial tension. Due to the affinity of the hydrophobic chains for the oil phase, the surfactant molecules interact with the oil molecules located at the interface which favors their adsorption. The parameters of the models reported in Table 1 are in agreement with these observations. The values of the adsorption constant b are much higher than at the water/air interface. This is also true for the values of the maximum molar area ω_0 which can be explained by the presence of intercalated alkane molecules in the surfactant adsorption layers.

The model parameters obtained from the FIC model after fitting the adsorption isotherms are summarized in Table 1. Although some experimental points in the adsorption isotherms deviate a bit from the corresponding theoretical curve, the obtained model parameters provide a good agreement between theory and experiment. These deviations are possibly experimental errors due to the very long adsorption time necessary at low surfactant concentrations [19]. Comparing the model parameters in Table 1 for C_{10}TAB with those for C_{12}TAB for all measured oils, we can see a clear dependence for the adsorption coefficients b, i.e. for each of the oils the adsorption coefficient increases with increasing the surfactant's chain length. On the other hand, the values for the molar area at interfacial pressure Π=0, ω_0, scatter around a physically reasonable constant value. The interaction coefficient a has minor influence on the shape of the adsorption isotherm, therefore, we will not particularly comment on it here.

Table 1: Parameters of adsorption layers obtained after fitting of the adsorption isotherms in Figs. 1-7 with FIC model; total mean salt concentration considered to be 2mM and intrinsic compressibility parameter ε = 0.01 mN/m, according to [18].

	C_nTAB	ω_0 [m^2/mol]	a	b [m^3/mol]
water-hexane*	n=10	$5{,}60\times10^5$	0	2,2
	n=12	$4{,}40\times10^5$	0	4,3
water-heptane	n=10	$6{,}44\times10^5$	0,2	1,59
	n=12	$4{,}64\times10^5$	0	5,29
water-octane	n=10	$5{,}68\times10^5$	0	0,98
	n=12	$4{,}98\times10^5$	1,2	2,4
water-nonane	n=10	$6{,}68\times10^5$	0	2,58
	n=12	$4{,}44\times10^5$	0	3,06
water-decane	n=10	$5{,}75\times10^5$	0,2	1,38
	n=12	$4{,}08\times10^5$	0	6,96
water-dodecane	n=10	$6{,}64\times10^5$	0,6	1,39
	n=12	$6{,}44\times10^5$	0	12,8
water-tetradecane	n=10	$4{,}43\times10^5$	0	0,44
	n=12	$6{,}70\times10^5$	0	10,3

* taken from [18]

If we analyze the data in Table 1 looking at single surfactant and different oils, it is evident that there is not any particular dependence of the parameter *b* on the alkane chain length. The reason for this might be that each of the oils has its individual influence on the surfactant surface activity. Thus, some oils encourage surfactant adsorption more than others but still there is not a clear trend according to the change of the oil molecular size.

A realistic picture of the C_nTAB adsorption layers at water/oil interfaces has been obtained via the analysis of the adsorbed amount Γ and the molar area ω as a function of equilibrium surfactant bulk concentration.

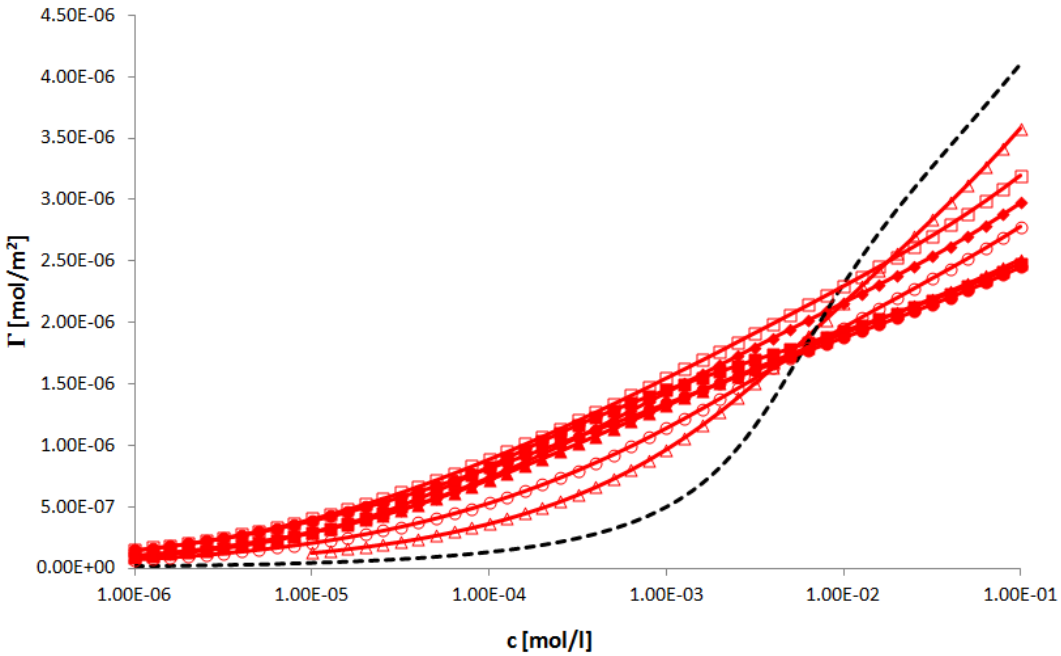

Fig. 8. Variations of the adsorbed amount Γ of C_{10}TAB at the water/air (dashed line), water/hexane (□), water/heptane (▲), water/octane (○), water/nonane (●), water/decane (◆), water/dodecane (■) and water/tetradecane (△); curves calculated with FIC model.

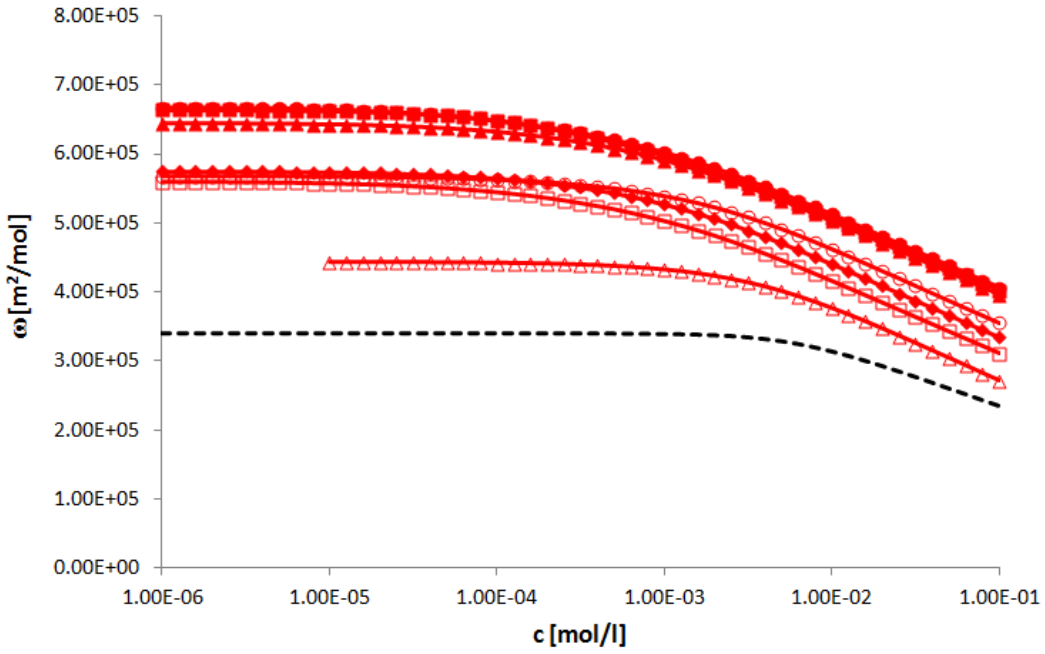

Fig. 9. Variations of the molar area ω of C_{10}TAB at the water/air (dashed line), water/hexane (□), water/heptane (▲), water/octane (○), water/nonane (●), water/decane (◆), water/dodecane (■) and water/tetradecane (△); curves calculated with FIC model.

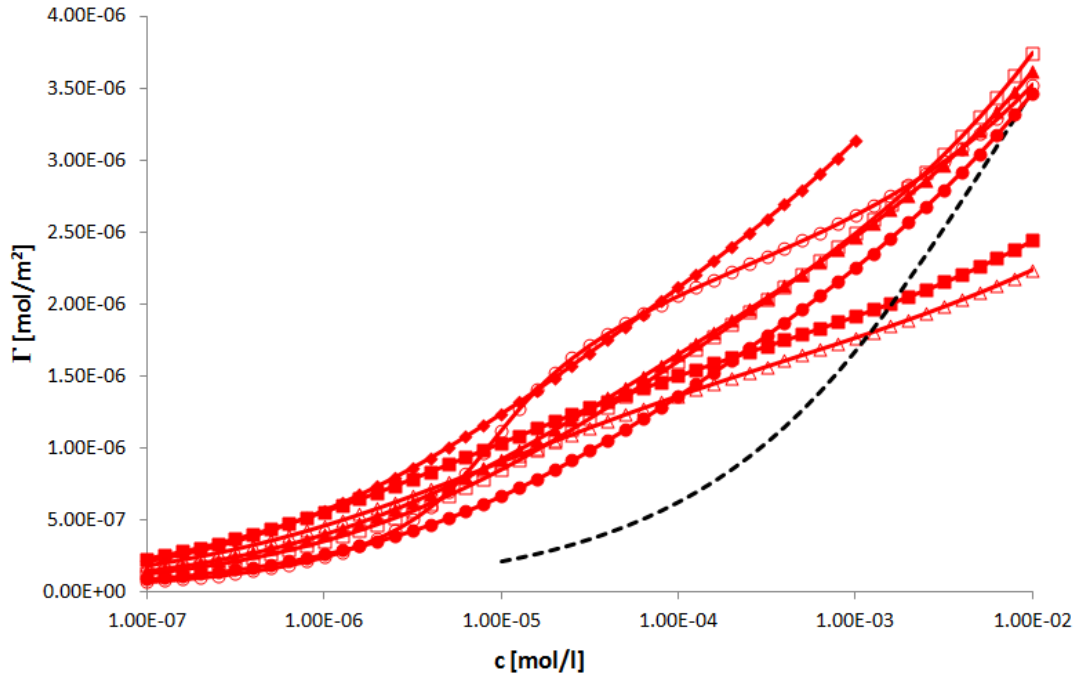

Fig. 10. Variations of the adsorbed amount Γ of C_{12}TAB at the water/air (dashed line), water/hexane (□), water/heptane (▲), water/octane (○), water/nonane (●), water/decane (◆), water/dodecane (■), water/tetradecane (△); curves calculated with FIC model.

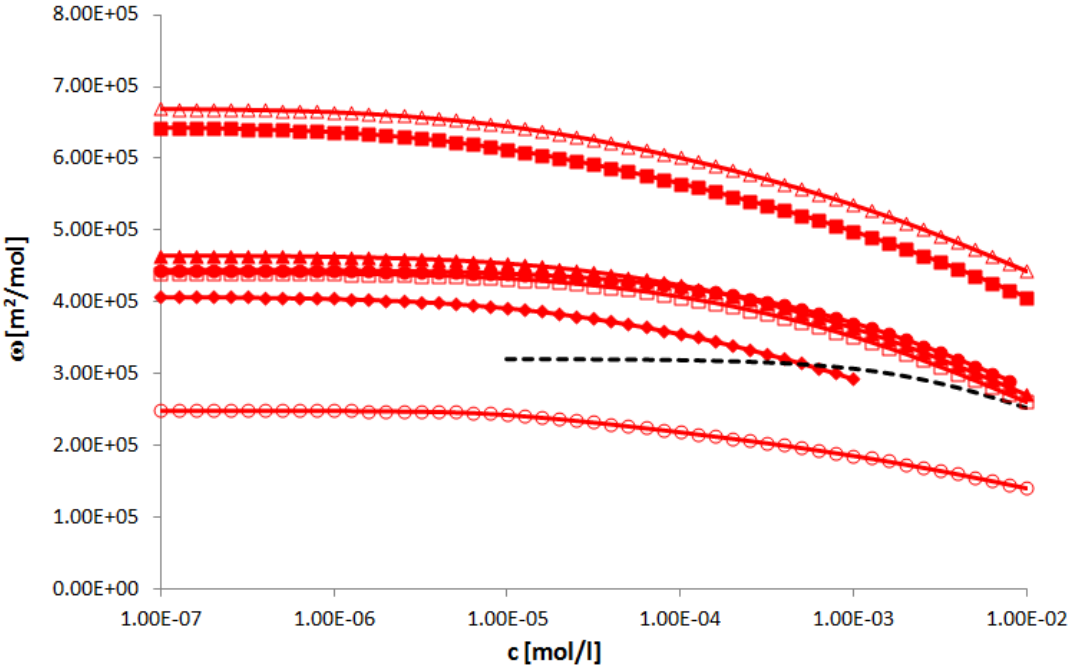

Fig. 11. Variations of the molar area ω of C_{12}TAB at the water/air (dashed line), water/hexane (□), water/heptane (▲), water/octane (○), water/nonane (●), water/decane (◆), water/dodecane, (■) water/tetradecane (△); curves calculated with FIC model.

In Figs. 8-11 the surface concentrations and molar areas, respectively, for C_{10}TAB and C_{12}TAB at different oil/water interfaces are compared with those obtained at water/air interface. It is seen that at high surface coverage by C_{10}TAB, the surface concentration at the water/air interface is higher than at all measured oil/water interfaces. For the same molecule, the molar area shows significantly lower values at water/air than at the different oil/water interfaces. Therefore for C_{10}TAB both the surface concentration and the molar area graphs confirm the same physics behind these results - at high surface coverage oil molecules are embedded in the C_{10}TAB adsorption layer, for the whole studied alkane homologous series.
On the other hand, at high surface coverage the C_{12}TAB adsorption layers show a higher surface concentration at the water/hexane, water/heptanes, water/octane, water/nonane and water/decane interfaces than at the water/air interface. At the water/dodecane and water/tetradecane interface, however, the respective surface concentrations are smaller than at the water/air interface. The molar areas of C_{12}TAB, at high surface coverage, are higher at water/dodecane and water/tetradecane than those at the water/air interface, but are smaller at the water/octane and water/decane interfaces. For other oils, hexane, heptane and nonane, it seems that molar area of the surfactant molecules at these water/oil interfaces are similar to the water/air interface. However, we can conclude that the mutual interaction between the surfactant's dodecyl chains is strong enough to squeeze the short alkane molecules (hexane, heptane, octane, nonane and decane) out of the adsorption layer. On the contrary, dodecane and tetradecane remain embedded within the C_{12}TAB adsorption layer.

Conclusion

All experiments presented in this paper are theoretically described in order to describe quantitatively the adsorption layers at water against different oils interfaces most precisely. Calculating the change of the surfactant surface concentration and molar area with increasing surfactant bulk concentration it is possible to clearly define the surfactant-surfactant and surfactant-oil molecular interactions at water/oil interfaces. These interactions can be separated into two types, either the mutual interactions between surfactant molecules dominate so that the oil molecules are squeezed out from the surfactant adsorption layer, or the interaction between surfactant and oil molecules are strong enough to keep oil molecules embedded into the surfactant adsorption layer. Note that the main conclusions are obtained by comparing the theoretical results of the water/air and water/oil interfaces for the surfaces highly covered by surfactant molecules. For lower surface coverages, there is no clear trend among the homologous oil molecules due to the individual influence on surface activity of the surfactants. This can be seen also from the more or less constant, however slightly scattering adsorption coefficient *b* for the single surfactant and different oil phases (Table 1). However, it is seen that for low surface coverage both surfactants, C_{10}TAB and C_{12}TAB, show higher surface activity at the water/oil interface than at the water/air interface, for all investigated alkane oils.
At high surface coverage, the behavior becomes a function of not just the surfactant's chain length [18], but also of the length of the oil alkane molecules too. We have found that for surfactants with the shorter alkyl chain (C_{10}TAB), the interactions between surfactant and oil molecules dominate the mutual surfactant interaction so that finally

the oil molecules are embedded in the C_{10}TAB adsorption layer. This is the case for all measured oils in this paper. On the other hand, the next surfactant in the homologous series (C_{12}TAB) shows different behavior at the water/oil interfaces. Here it is found that at the interfaces between water and hexane, heptane, octane, nonane and decane, the mutual surfactant interactions are stronger than surfactant-oil ones. Hence, in general the oil molecules are squeezed out from the surfactant adsorption layers with increasing surfactant concentration. The oil molecules with longer alkane chain, i.e. dodecane and tetradecane, interact with surfactants at the interface and even at high surface coverage stay embedded into the surfactant adsorption layer.
In summary it can be said that the competitive adsorption between surfactant and oil molecules at the water/oil interfaces are the result of both kinds of interactions at the interface (surfactant-surfactant and surfactant-oil molecule), and the behavior of the adsorption layer directly depends on which interaction dominates another.

Acknowledgements

The work was financially supported by projects of the DFG (Mi418/18-1), the DLR (50WM1129), the European Space Agency (PASTA) and the COST actions CM1101 and MP1106.

References

1 D.J. McClements, Food Emulsions: Principles, Practices, and Techniques, CRC Press; 2nd ed., (2004)
2 L.L. Schramm, Surfactants: Fundamentals and Applications in the Petroleum Industry, Cambridge University Press; (2010)
3 J. Lin, Manufacturing Cosmetic Emulsions Pragmatic Troubleshooting and Energy Conservation, Allured Pub Corp; (2009)
4 B. Binks, Modern Aspects of Emulsion, Royal Society of Chemistry, (1998)
5 F. Leal-Calderon (Author), V. Schmitt and J. Bibette; Emulsion Science: Basic Principles, Springer; 2nd ed., (2007)
6 Th.F. Tadros, Emulsion Science and Technology, Wiley-VCH, (2009)
7 V.I. Kovalchuk, F. Ravera, L. Liggieri, G. Loglio, P. Pandolfini, A.V. Makievski, S. Vincent-Bonnieu, J. Krägel, A. Javadi and R. Miller, Adv. Colloid Interface Sci., 161 (2010) 102–114
8 M.M. Knock, G.R. Bell, E.K. Hill, H.J. Turner, and C.D. Bain, J. Phys. Chem. B, 107 (2003) 10801-10814
9 M.L. Schlossmann and A.M. Tikhonov, Annu. Rev. Phys. Chem., 59 (2008) 153-177
10 H. Fang and D.O. Shah, J. Colloid Interface Sci. 205 (1998) 531-534
11 K. Medrzycka and W. Zwierzykowski, J.Colloid Interface Sci., 230 (2000) 67-72
12 W.K. Kegel, G.A. van Aken, M.N. Bouts, H.N.W. Lekkerkerker, J.T.G. Overbeek and P.L. de Bruyn, Langmuir, 9(1) (1993) 252-256
13 T.G. Gurkov, T.S. Horozov, I.B. Ivanov, and R.P. Borwankar, Colloids Surfaces A, 87 (1994) 81-92

14 L. Peltonen, J. Hirvonen and J. Yliruusi, J.Colloid Interface Sci., 240 (2001) 272-276
15 R. Aveyard, B.P. Binks, P.D.I. Fletcher and J.R. MacNab, Ber.Bunsenges. 100 (1996) 224-231
16 A. Javadi, N. Moradi, H. Möhwald and R. Miller, Soft Matter, 6 (2010) 4710-4714
17 A. Javadi, N. Moradi, M. Karbaschi, V.B. Fainerman, H. Möhwald and R. Miller, Colloids Surfaces A, 391 (2011) 19-24
18 V. Pradines, V.B. Fainerman, E.V. Aksenenko, J. Kraegel, N. Mucic and R. Miller, Colloids Surf. A, 371 (2010) 22-28
19 N. Mucic, A. Javadi, N.M. Kovalchuk, E.V. Aksenenko and R. Miller, Adv. Colloid Interface Sci., 168 (2011) 167-178.
20 A.H. Demond and A.S. Lindner, Environ.Sci.Technol., 27 (1993) 2318-2331.

Paper IV

Mixed adsorption layers at the aqueous CnTAB solution / hexane vapor interface

N. Mucic, N. Moradi, A. Javadi, E.V. Aksenenko, V.B. Fainerman and R. Miller

to be submitted

Mixed adsorption layers at the aqueous C_nTAB solution/hexane vapor interface

N. Mucic[1]*, N. Moradi[1], A. Javadi[1], E.V. Aksenenko[2], V.B. Fainerman[3] and R. Miller[1]

[1] *Max-Planck Institute of Colloids & Interfaces, Potsdam/Golm, Germany*

[2] *Institute of Colloid Chemistry and Chemistry of Water, 03680 Kiev, Ukraine*

[3] *Donetsk Medical University, 16 Ilych Avenue, Donetsk 83003, Ukraine*

Abstract

Interfacial tension experiments were performed at the water/oil vapor interface utilizing the drop profile analysis tensiometer PAT-1 for a series of alkyl trimethylammonium bromides with different chain lengths (C_{10}, C_{12}, C_{14} and C_{16}). At the water/hexane vapor interface the attractive interactions between the hydrophobic chains of the adsorbed surfactants and hexane molecules promote hexane adsorption at the interface. The length of the surfactant tail influences the surfactant's adsorbed amount, as expected from the Traube rule, however the hexane co-adsorption does not directly follow this rule.

Keywords: Cationic surfactants, adsorption isotherms, water-alkane vapor interface, chain length dependence, interfacial tension, drop profile analysis tensiometry

* corresponding author

Introduction

Recently, the competitive adsorption between aqueous surfactants and oil molecules has been more intensively investigated. New findings from experiments at water/oil and water/oil vapor interfaces via drop profile analysis have highly encouraged these investigations. The question about the interaction between surfactant molecules adsorped from the aqueous solution and oil molecule at the interface is of enormous importance for interfacial science. These interactions directly define the interfacial properties and so the properties of a whole system, such as emulsions.

The thermodynamic properties of surfactant – oil interactions were systematically investigated by the groups of Medrzycka et al. [1] and Pradines et al. [2] regarding the thermodynamic interfacial properties. They have found that the surfactant molar area and the surface concentration depend not only on the surface coverage by the surfactant molecules but also on the oil chain lengths. Thus, different chain lengths of surfactants and oils interact in different ways. Generally, surfactants with longer chain length are able to squeeze out the shorter oil molecules from the adsorption layer. In [3] the dynamic and rheological properties of such systems were investigated and it was found that the dynamics of the water/oil interface is more complex than expected for a pure diffusion process. This is obviously caused by the interaction between the surfactants' alkyl chains and the oil molecules. In a recent work the effect of different oils on the adsorption of the homologous C_nTABs was shown [4], and it was found that the behaviour of the adsorption layer directly depends on which type of interactions dominates, between surfactant-surfactant or surfactant-oil molecule.

In the present work we essentially discuss the attraction between surfactant chains and oil molecules via measurements of aqueous solutions of surfactants with different chain lengths (C_{10}TAB, C_{12}TAB, C_{14}TAB and C_{16}TAB) against hexane vapor. Therewith, we wanted to see differences in the adsorbed amount of hexane molecules at the aqueous solution surface of the different surfactants. The obtained results are compared with data measured at the interfaces between aqueous solutions against air and (bulk) oil, respectively.

Material and methods

The substances investigated in this paper, C_{10}TAB (decyl trimethylammonium bromide, Mw = 280.29 g/mol), C_{12}TAB (dodecyl trimethylammonium bromide, Mw = 308.35 g/mol), C_{14}TAB (tetradecyl trimethylammonium bromide, Mw = 336.40 g/mol) and C_{16}TAB (hexadecyl trimethylammonium bromide, Mw = 364.46 g/mol) were purchased from Fluka (Switzerland) with a purity of >99%. The substances were additionally purified by a triple recrystallization with a ethanol/acetone mixture. All solutions were prepared in 10mM NaH_2PO_4/$NaHPO_4$ phosphate buffer, pH 7, (Fluka, >99%) using ultrapure Milli-Q water (resistivity = 18.2 MΩcm). The experiments were performed at room temperature (23 – 24 °C). Hexane was purchased from Fluka, distillated, purified with aluminium oxide and subsequently saturated with ultrapure Milli-Q water.

The experiments were performed with the drop profile analysis tensiometer PAT-1 (SINTERFACE Technologies, Germany). In brief, the principle of the experiments consists in forming a drop in a closed cuvette (3cm × 3cm × 3cm), and after a certain time (typically 300s) a defined amount of alkane (1 ml) is injected to the bottom of the cuvette. The cell is closed such that after a few minutes the saturated hexane vapor atmosphere is established. The experimental details were explained elsewhere [5, 6].

Experimental results and discussion

The experiments were performed according to the protocol described in [6], where a drop of surfactant solution is primarily formed in air and then in addition the atmosphere around the drop is saturated with alkane vapor. Therefore, at the beginning of the measurement, the interfacial tension is decreasing

due to adsorption of the surfactant molecules from the drop bulk. The adsorption time depends on the surfactant bulk concentration [7]. However, it was estimated that within 300s the equilibrium interfacial tension must be reached for all measured concentrations. After 300s while the system approaches the equilibrium state, 1 ml hexane is injected into the cuvette. The formed hexane atmosphere leads quickly to a significant extra decrease in surface tension. From [6] it is know that the higher the surfactant concentration is, the faster and stronger the interfacial tension decreases due to the hexane co-adsorption from the vapor phase.

In the present work we focus on the finding that surfactants with different alkyl chain lengths effect the interfacial tension change during the hexane co-adsorption in a different way. In the following the adsorption kinetics of C_nTAB surfactants (n = 10, 12, 14 and 16) before and after injection of the hexane into the gas atmosphere will be compared. The data in Figs. 1 to 4 show the dynamic surface tensions for the four studied cationic surfactants, respectively.

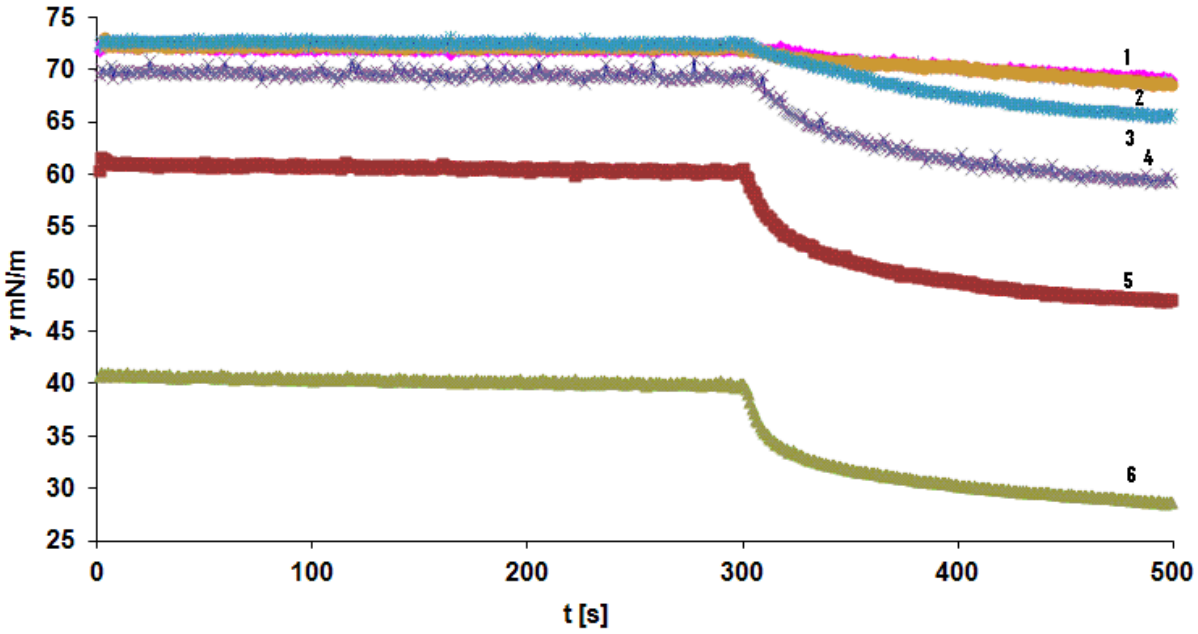

Fig. 1. Effect of hexane vapor on the dynamic surface tension of $C_{10}TAB$ solution drops at different concentrations of 10^{-7} mol/l (1); 10^{-5} mol/l (2); 10^{-4} mol/l (3); 10^{-3} mol/l (4); 10^{-2} mol/l (5); 10^{-1} mol/l (6); 1 ml of hexane was injected at t = 300 s at the bottom of the cuvette.

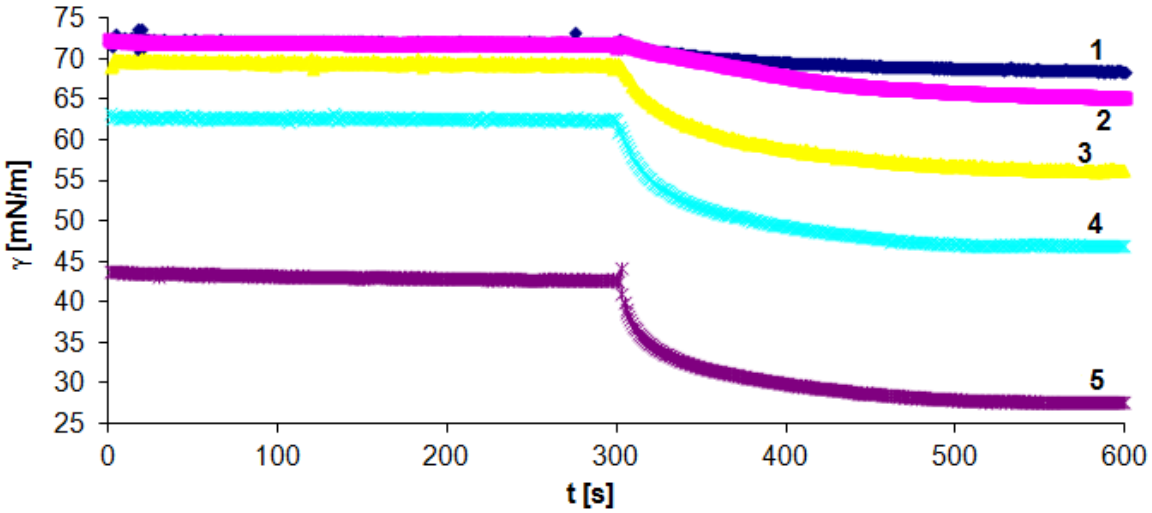

Fig. 2. Effect of hexane vapor on dynamic surface tension of C_{12}TAB solution drops at different concentrations of 10^{-6} mol/l (1); 10^{-5} mol/l (2); 10^{-4} mol/l (3); 10^{-3} mol/l (4); 10^{-2} mol/l; 1 ml of hexane was injected at t = 300 s at the bottom of the cuvette.

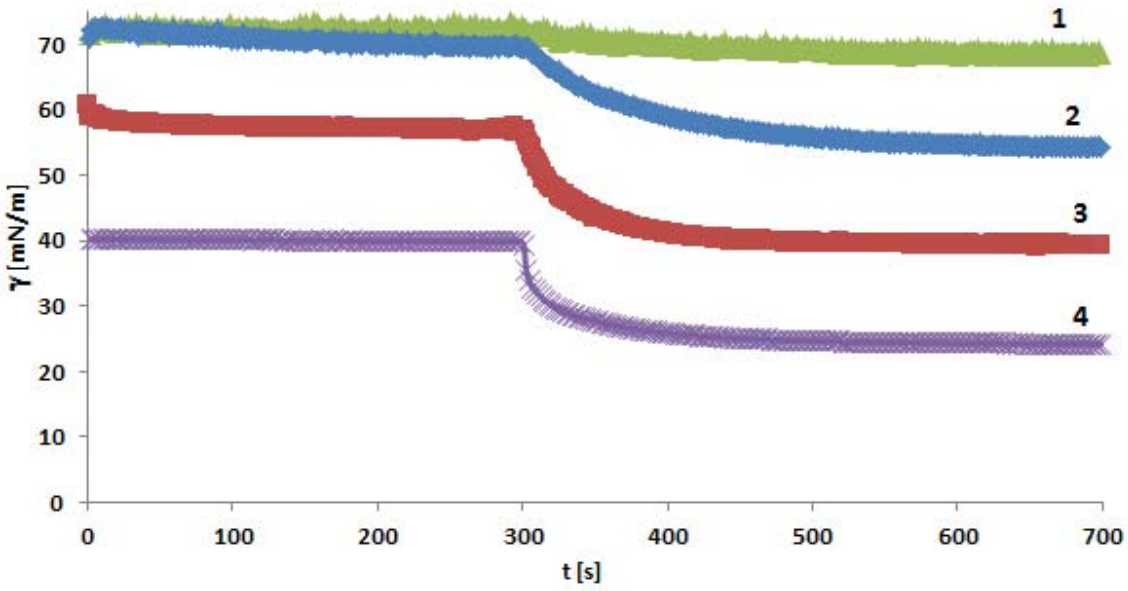

Fig. 3. Effect of hexane vapor on dynamic surface tension of C_{14}TAB solution drops at different concentrations of 10^{-6} mol/l (1); 10^{-5} mol/l (2); 10^{-4} mol/l (3); 2×10^{-3} mol/l (4); 1 ml of hexane was injected at t = 300 s at the bottom of the cuvette.

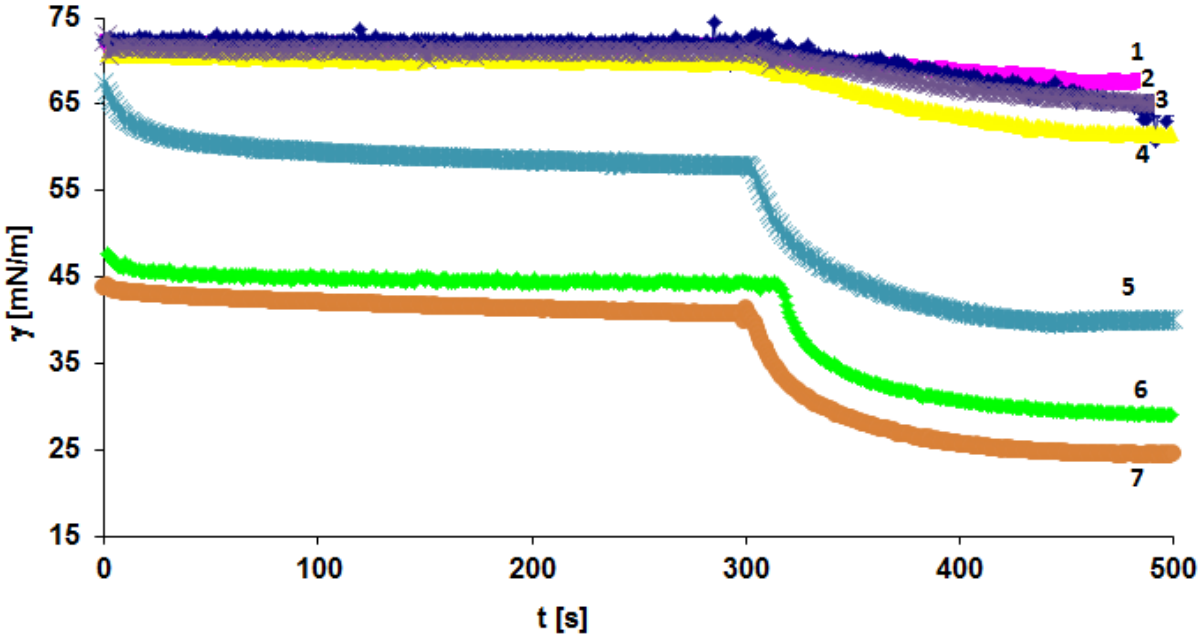

Fig. 4. Effect of hexane vapor on dynamic surface tension of C_{16}TAB solution drops at different concentrations of 10^{-7} mol/l (1); 10^{-6} mol/l (2); 3×10^{-6} mol/l (3); 10^{-5} mol/l (4); 3×10^{-5} mol/l (5); 10^{-4} mol/l (6); 3×10^{-4} mol/l (7): 1 ml of hexane was injected at t = 300 s at the bottom of the cuvette.

From the Figs. 1-4 we can also take the equilibrium surface tension values to draw the adsorption isotherms for the water/air and water/vapor interfaces. These values are complemented by the adsorption isotherms for the water/hexane interface as obtained in [2]. In this way, we are able to quantitatively discuss the relative adsorption of oil molecules from the vapor phase in respect to the bulk oil phase as obtained from the isotherm for the water/hexane interface.

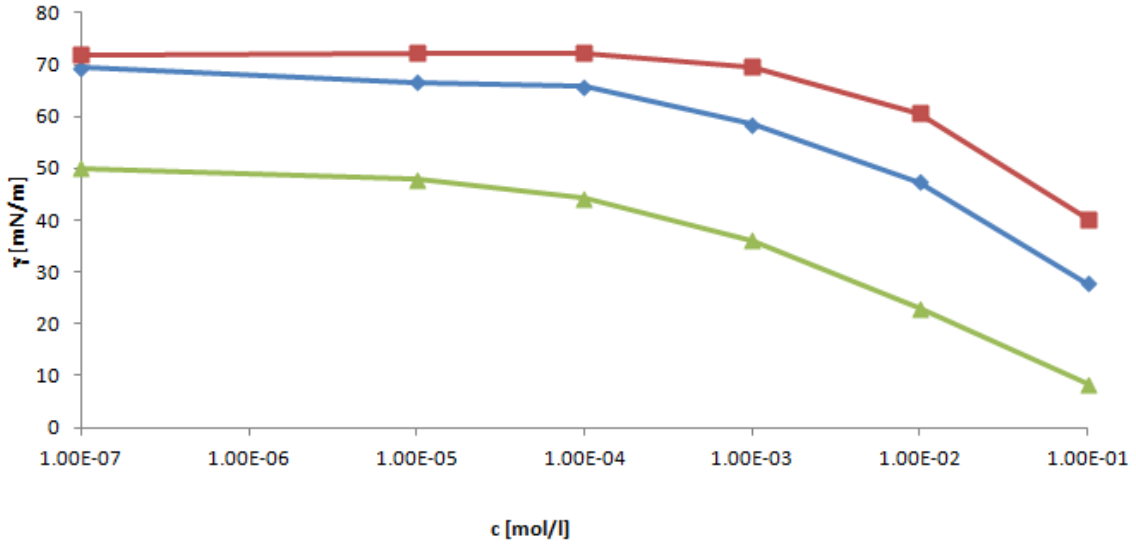

Fig. 5. Comparison of surface/interfacial tension of C_{10}TAB solution drops against air (■), hexane vapor (◆) and bulk liquid hexane (▲) as a function of surfactant concentration.

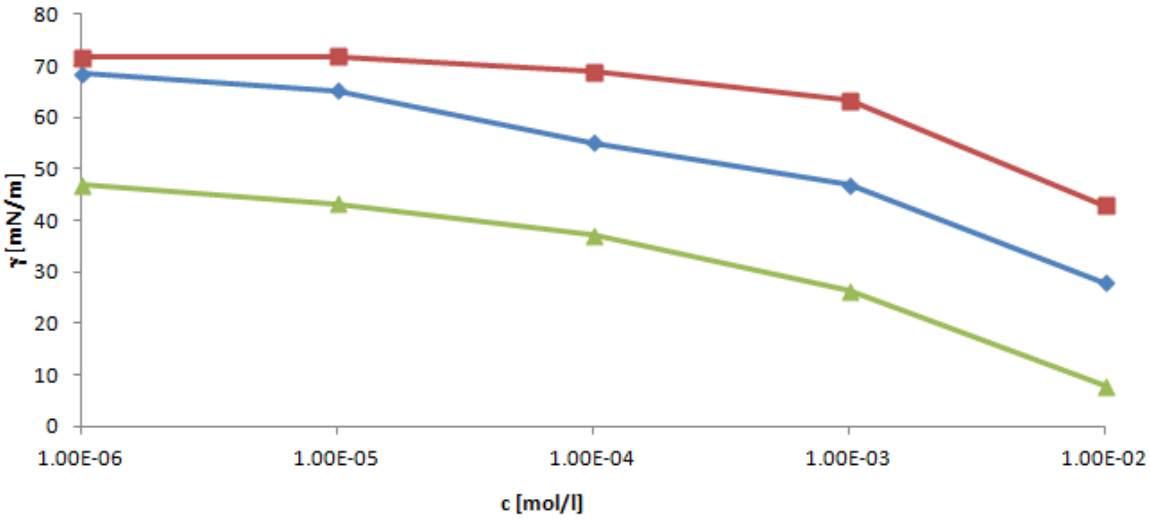

Fig. 6. Comparison of surface/interfacial tension of C_{12}TAB solution drops against air (■), hexane vapor (◆) and bulk liquid hexane (▲) as a function of surfactant concentration.

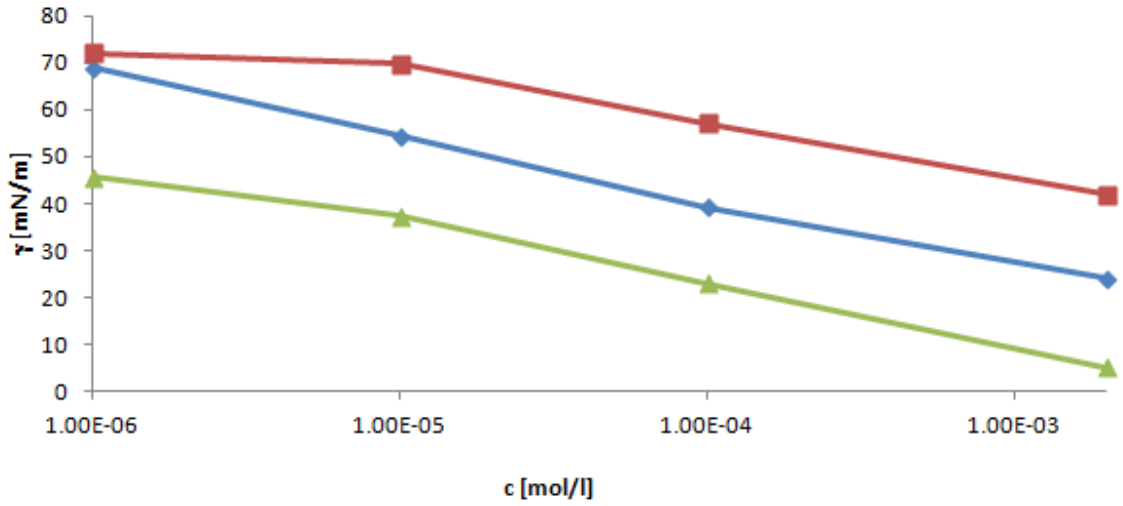

Fig. 7. Comparison of surface/interfacial tension of C_{14}TAB solution drops against air (■), hexane vapor (◆) and bulk liquid hexane (▲) as a function of surfactant concentration.

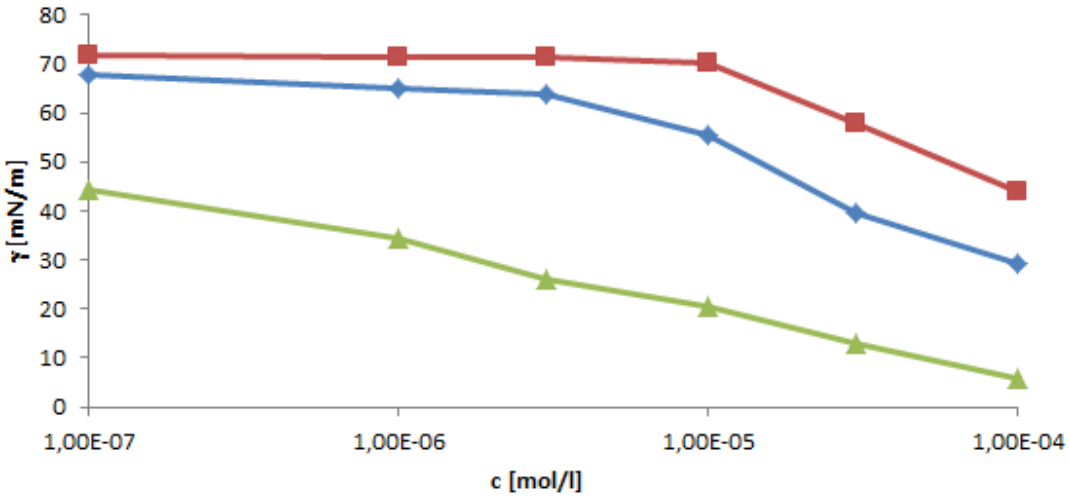

Fig. 8. Comparison of surface/interfacial tension of C_{16}TAB solution drops against air (■), hexane vapor (◆) and bulk liquid hexane (▲) as a function of surfactant concentration.

The data in the Figs. 5-8 summarize the C_nTABs adsorption isotherms for the three interfaces water/air, water/hexane vapor and water/hexane (bulk). From these graphs the significant decrease of the interfacial tension upon co-adsorption of hexane molecules from the vapor phase at the liquid surface can be easily seen. It is evident that at higher C_nTAB concentrations, the water/hexane vapor interfacial tension is lower than the one for the water/air surface. Therefore, with increasing C_nTAB surface concentration, the co-adsorption of hexane molecules becomes more efficient. Probably, surfactant chains act like nuclei for hexane molecules, to which they bind via hydrophobic (van der Waals) interaction.

In order to quantitatively define the amount of the co-adsorbed hexane molecules at the surface of aqueous C_nTAB solutions, we have calculated the relative decrease of the water/hexane vapor interfacial tension, $\Delta\gamma_{rel}$. This quantity is is quotient of the difference of surface tension at the water/air and water/hexane vapor over the difference of surface tension at water/air and water/hexane (liquid), $\Delta\gamma_{rel} = \frac{\gamma_{water-air} - \gamma_{water-vapor}}{\gamma_{water-air} - \gamma_{water-oil}}$. This term provides a measure of the surface coverage by oil molecules taking into consideration two limits, when there is no oil molecules at the surface (water/air interface) and when the surface is fully covered by oil molecules (water/hexane interface). On the other hand $\triangle\gamma_{rel}$ represents the relative number of oil molecules interacting with a surfactant molecule. This means, for example, when $\triangle\gamma_{rel}$ is constant for some surfactant's concentrations, the number of oil molecules interacting with one surfactant molecule is more or less constant. If $\triangle\gamma_{rel}$ increases, then the number of oil molecules interacting with one surfactant molecule increases too. In Fig. 9 the results of these calculations are summarized for all four C_nTAB surfactants.

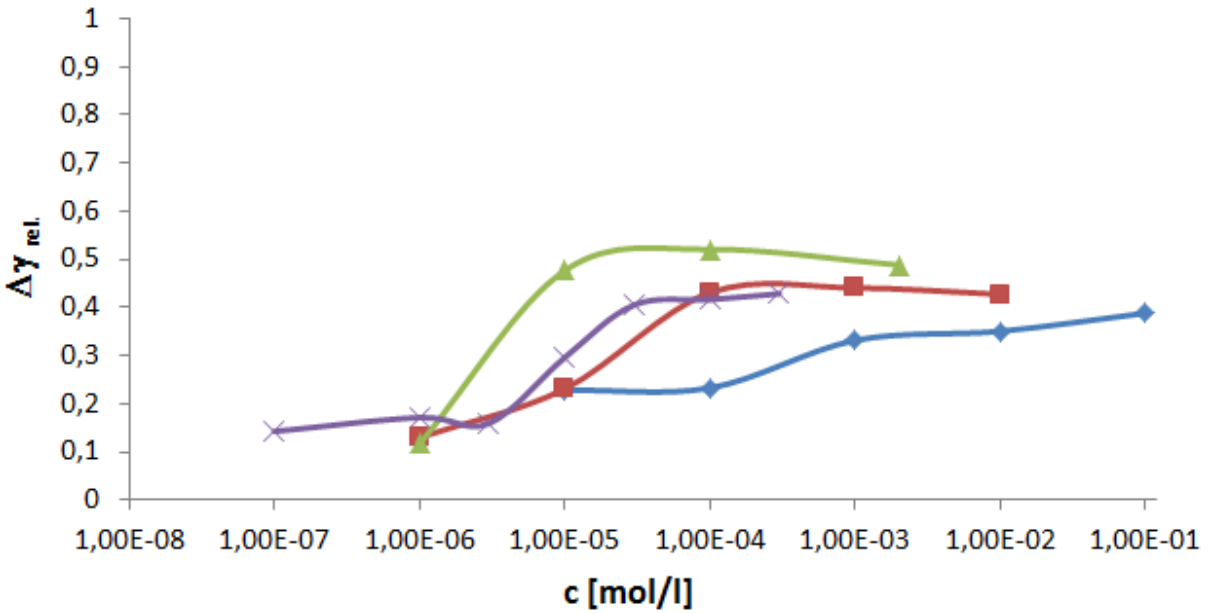

Figure 9. Effect of surfactant concentration on the surface tension changes of C_{10}TAB (◆), C_{12}TAB (■), C_{14}TAB (▲) and C_{16}TAB (×) solution drops against hexane vapor.

For C_{10}TAB the resulting dependence shows more or less a small increase. Therewith, it can be assumed that for C_{10}TAB aqueous solutions the surface is increasingly covered by hexane molecules with increasing surfactant concentration. This means that there is a slightly increasing number of hexane molecules per one C_{10}TAB surfactant at the interface. The situations for C_{12}TAB and C_{14}TAB are different. At low surfactant concentrations both curves indicate a very small surface coverage by hexane molecules. With increasing surfactants concentrations, the oil coverage increases and reach a plateau value approximately the same as for C_{10}TAB. Hence, at medium and high C_{12}TAB and C_{14}TAB concentrations the number of hexane molecules continuously increases with the number of adsorbed surfactant molecules at the interface. At low C_{16}TAB concentrations the hexane coverage increases continuously up to higher surfactant concentrations, i.e. the number of hexane molecules per one surfactant molecule increases as well.

It should be noted that these statements are just qualitative interpretations based on the obtained $\Delta\gamma$ curves, i.e. no analysis with a theoretical model has been used. These observations cannot be compared with the results obtained for C_nTAB adsorption at water/hexane interface either. Practically, at the water/oil interface with increasing surfactant bulk concentration, the surfactant surface concentration increases too, but the number of oil molecules arranged at the interface cannot be estimated with existing models. It was found that at low surfactant concentrations the oil phase produces higher surface pressure than at the water/air surface. It is not clear yet if the oil molecules adsorbing from the vapor phase encourage an additional surfactant adsorption or the adsorption of surfactants enhance the oil molecules' co-adsorption. Obviously, the adsorption processes at water/oil and water/vapor interfaces are different but have also a lot in common, however, without a suitable theoretical model it is hard to further speculate about the surface coverage by surfactant molecules at the water/vapor and water/oil interfaces.

Conclusions

The present experimental study was dedicated to the adsorption behavior of members of the homologous series of C_nTAB (n = 10 – 16) at the water/hexane vapor interface. The general conclusions were obtained after comparison of these results with those obtained at the water/air and water/hexane (bulk) interfaces.

From the dynamic surface tension curves a significant decrease of the interfacial tension is seen upon releasing the hexane vapor into the atmosphere around the C_nTAB solution drop. The surface tension decrease starts immediately when the vapor is released and it is faster for higher surfactant concentrations. Basically, hexane molecules interact with the surfactants at the interface. Therefore, the higher the surfactant surface concentration is, the more hexane molecules will adsorb and interact. The kinetic curves show plateau values when quasi-equilibrium is reached, i.e. when the hexane molecules are adsorbed at the interface due to the interaction with surfactants. After this quasi-equilibration additional processes are observed, such as hexane condensation, which are not discussed here.

Comparison of the results obtained at the water/vapor interface with those at the water/air and water/oil interfaces allows speculating on the amount of oil molecules adsorbed from vapor phase. It was found that for the whole concentration range of C_{10}TAB there is a slightly increasing number of hexane molecules around a single surfactant at the interface. For C_{12}TAB and C_{14}TAB from low to mean concentrations the number of hexane molecules per surfactant molecule increases. For the medium and high concentrations hexane molecules cover the interface uniformly and with the constant number of molecules per surfactant molecule. C_{16}TAB at low concentrations attracts the same number of hexane molecules per surfactant molecule, and only with increasing C_{16}TAB concentration this number increases.

Difference in the behavior of hexane molecules co-adsorbed at the surface of different C_nTAB surfactants solutions might follow only after the first adsorbed surfactants change their orientation at the interface with increasing the surfactant concentration. The longer surfactants at low concentrations are more in a laying position, while at high concentrations they are oriented in a more upright position. In between, i.e. for medium concentrations there is the transition between these two positions. It has a been found that the surfactants oriented in upright position attract more hexane molecules than in laying position. Therefore, in conclusion, the different number of hexane molecules per surfactant molecule corresponds with differences in the surfactant orientations.

The conclusions drawn here are based on qualitative discussions and for their approval it is necessary to develop an appropriate theoretical model which is presently pending.

Acknowledgements

The work was financially supported by projects of the DFG (Mi418/18-1), the DLR (50WM1129), the European Space Agency (PASTA) and the COST actions CM1101 and MP1106.

References

1 K. Medrzycka, W. Zwierzykowski, Adsorption of alkyltrimethylammonium bromides at the various interfaces, J. Colloid Interface Sci. 230 (2000) 67-72

2 V. Pradines. V.B. Fainerman, E.V. Aksenenko, J. Krägel, N. Mucic, R. Miller, Adsorption of alkyl trimethylammonium bromides at the water/air and water/hexane interfaces, Colloids Surfaces A 371 (2010) 22-28

3 N. Mucic, N.M. Kovalchuk, V. Pradines, A. Javadi, E.V. Aksenenko, J. Krägel, R. Miller, Dynamic properties of CnTAB adsorption layers at the water/oil interface, Colloids Surfaces A, submitted (2012)

4 N. Mucic, N.M. Kovalchuk, E.V. Aksenenko, V.B. Fainerman, R. Miller, Adsorption layer properties of alkyl trimethylammonium bromides at the water interfaces against different oils. Waiting for submission

5 G. Loglio, P. Pandolfini, R. Miller, A.V. Makievski, F. Ravera, M. Ferrari, L. Liggieri, Drop and bubble shape analysis as tool for dilational rheology studies of interfacial layers, in: D. Möbius, R. Miller (Eds.), Novel Methods to Study Interfacial Layers, Studies in Interfacial Science, vol. 11, Elsevier, Amsterdam, 2001, pp. 439-484

6 A. Javadi, N. Moradi, V.B. Fainerman, H. Möhwald, R. Miller, Alkane vapor and surfactants co-adsorption on aqueous solution interfaces, Colloids Surfaces A 391 (2011) 19-24

7 N. Mucic, A. Javadi, N.M. Kovalchuk, E.V. Aksenenko, R. Miller, Dynamics of interfacial layers – Experimental feasibilities of adsorption kinetics and dilational rheology, Adv. Colloid Interface Sci. 168 (2011) 167-178

Paper V

Dynamics of interfacial layers – Experimental feasibilities of adsorption kinetics and dilational rheology

N. Mucic, A. Javadi, N.M. Kovalchuk, E.V. Aksenenko and R. Miller

Advances in Colloid and Interface Science 168 (2010) 167-178.

Advances in Colloid and Interface Science 168 (2011) 167–178

Contents lists available at ScienceDirect

Advances in Colloid and Interface Science

journal homepage: www.elsevier.com/locate/cis

Dynamics of interfacial layers—Experimental feasibilities of adsorption kinetics and dilational rheology

N. Mucic [a,*], A. Javadi [a], N.M. Kovalchuk [a,b], E.V. Aksenenko [c], R. Miller [a]

[a] Max Planck Institute of Colloids and Interfaces, 14424 Potsdam/Golm, Germany
[b] Institute of Bio-Colloid Chemistry, 03142 Kiev, Ukraine
[c] Institute of Colloid Chemistry and Chemistry of Water, 252680 Kiev, Ukraine

ARTICLE INFO

Available online 1 July 2011

Keywords:
Dynamic surface tension
Dilational rheology
Oscillating drop method
Maximum bubble pressure method
Drop profile analysis tensiometry
Capillary pressure tensiometry
Surfactants
Langmuir isotherm
Diffusion controlled adsorption

ABSTRACT

Each experimental method has a certain range of application, and so do the instruments for measuring dynamic interfacial tension and dilational rheology. While the capillary pressure tensiometry provides data for the shortest adsorption times starting from milliseconds at liquid/gas and tens of milliseconds at liquid/liquid interfaces, the drop profile tensiometry allows measurements in a time window from seconds to many hours. Although both methods together cover a time range of about eight orders of magnitude (10^{-3} s to 10^{5} s), not all surfactants can be investigated with these techniques in the required concentration range. The same is true for studies of the dilational rheology. While drop profile tensiometry allows oscillations between 10^{-3} Hz and 0.2 Hz, which can be complemented by measurements with capillary pressure oscillating drops and the capillary wave damping method (up to 10^{3} Hz) these six orders of magnitude in frequency are often insufficient for a complete characterization of interfacial dilational relaxations of surfactant adsorption layers. The presented analysis provides a guide to select the most suitable experimental method for a given surfactant to be studied. The analysis is based on a diffusion controlled adsorption kinetics and a Langmuir adsorption model.

Contents

1. Introduction

The characteristics of a surfactant are best expressed by the equilibrium adsorption quantities and the adsorption kinetics mechanism. In literature we can find many articles on the equilibrium surface tension isotherms for surfactants as summarized for example in [1–7]. At the same time the adsorption kinetics is very important for many technological applications, such as foaming or emulsification, broadly used in pharmaceuticals, food, mining industry and oil recovery. By studying the dynamic interfacial behavior, it is possible to obtain important information about the interaction between molecules, change of conformation and aggregation of molecules, kinetics of chemical reactions, kinetics of formation and disintegration of micelles, and other processes which take place at a molecular level [1,8]. Interfacial rheology gives insight into many relaxation processes within the adsorption layer, which is of fundamental interest and also of great applied value. Therefore, in this paper we will give an overview on the dynamics of liquid interfaces focusing on the existing

* Corresponding author.
E-mail address: mucic@mpikg.mpg.de (N. Mucic).

0001-8686/$ – see front matter © 2011 Elsevier B.V. All rights reserved.
doi:10.1016/j.cis.2011.06.001

experimental methods to perform most precise measurements of adsorption kinetics and dilational rheology of surfactant adsorption layers.

Surfactants of low surface activity generally adsorb fairly quickly due to the needed high bulk concentration. This requires experimental techniques able to measure changes in surface tension already after a few milliseconds or even less. On the other side, highly surface active substances are used at rather low concentrations in the bulk and, therefore, their adsorption kinetic is slow, i.e. the equilibrium state is established only after long adsorption times. In this case one should choose instruments which provide data for adsorption times of many hours or even days rather than recording the surface tension in less than a few milliseconds. In both cases, the most important point is to select and properly apply the right experimental techniques for getting the required information. The fastest method is the bubble pressure tensiometry working reliably even in the sub-millisecond time range, whereas the drop profile tensiometry has a working time window from about 1 s to many hours.

Similar problems arise in investigations of the frequency dependence of the interfacial tension response to small harmonic perturbations of the interfacial area, i.e. when we want to measure the dilational visco-elasticity of a surfactant adsorption layer. For a weak surfactant a method is obviously needed that works at very high frequencies as the required compression/expansion perturbations should be fast enough to create a deviation of the surface layer from equilibrium before this equilibrium is reestablished by desorption/adsorption. Again, on the contrary, for the very highly surface active substances a method is required to allow slow compression and expansion (measurements at low frequencies of interfacial perturbations).

The aim of this paper is to give some guidelines for studies on surfactants in respect to the adsorption kinetics and dilational rheology and for the selection of the most suitable experimental techniques for these studies. This work should also help classifying the surfactants into those which can be correctly studied at the respective interface and others for which the needed experimental tools are obviously not available.

2. Quick overview on surfactants

Surfactants, a blend of the words surface active agents, are known for almost 5000 years. In the Wikipedia we learn that the “earliest recorded evidence of the production of soap-like materials dates back to around 2800 BC in Ancient Babylon”. A formula for soap, written on a Babylonian clay tablet around 2200 BC, was consisting of water, alkali, and cassia oil. A great overview on surfactants is the 3rd edition of Rosen's book [9], which summarizes an enormous amount of knowledge on this important group of chemicals. The main groups of surfactants are Anionics, Cationics, Nonionics and Zwitterionics. However, Rosen determines the “surface saturation” as the only molecular adsorption characteristics rather empirically from the steepest slope of surface tension isotherms. More thermodynamic quantities of surfactant molecules adsorbed at fluid interfaces are summarized in another book on surfactants [2], where also various adsorption models are discussed.

First systematic studies were performed on fatty acids in the early 20th century by von Szyszkowski [10] and Frumkin [11]. Although we have quite many efficient new surfactants, these classical fatty acids and alcohols are still standard substances for surface science studies [12]. Since 1932 we have the first synthetic detergent sodium lauryl (dodecyl) sulfate, which is one of the most frequently studied surfactants until today. Discussions of this most important homologous series of anionic surfactant at the water/air have been done in various ways, with focus on the adsorption characteristics for example in [13,14]. Only very recently a complete picture of the surface properties of sodium dodecyl sulfate was published, including the surface tension isotherm, adsorption kinetics and the dilational visco-elasticity at the water/air interface [15]. An analysis of the differences in the adsorption behavior for the water/air and water/oil interfaces was published by Sharipova et al. [16]. Also the most important homologous series of cationics, the alkyl trimethyl ammonium bromide, are discussed in detail at the water/air interface in [17], and at the water/oil interface in [18]. The non-ionics are most often of technical grade, such as the Tritons and Tweens, however, there are also well defined products typically not used in applications but only for scientific studies [19]. As non-ionic model surfactants also the homologous series of alkyl dimethyl phosphine oxides are often used [20,21], but also these are too expensive for being used in practical applications. However, even for technical grade surfactants it is possible to achieve systematic information on their adsorption characteristics as it was demonstrated for Tritons in [6,22].

In Fig. 1 we show as examples the isotherms of some surfactants with a rather different behavior. The isotherm for Hexanol is located at the highest bulk concentrations which indicate that this is the weakest surfactant. The surface tension isotherms of SDS and DoTAB are located quite close to each other. The isotherms of C_{12}DMPO and Triton X-100 are found in the range of lowest concentrations which points at the fact that they are the strongest surface active molecules in this graph. We also see that the absolute concentration range which the surface tension isotherms cover is about two orders of magnitude for Hexanol, SDS and DoTAB, while C_{12}DMPO, C_{14}DMPO, $C_{10}EO_4$ and Triton X-100 span over more than 3 orders of magnitude. The reason for this remarkable difference is the molar area the adsorbed molecules require. The smaller this area is, the steeper are the isotherms. In Tables 1, 2 and 4 important data for some commonly

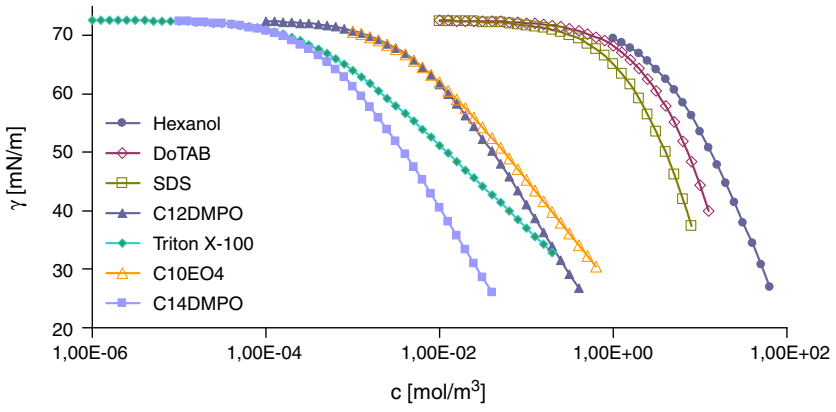

Fig. 1. Surface tension isotherms of some selected surfactants: Hexanol, SDS, DoTAB, C_{12}DMPO, C_{14}DMPO, $C_{10}EO_4$, Triton X-100.

Table 1
Parameters of the Langmuir model for selected non-ionic surfactants.

Surfactant	Adsorption onset time [s]	Characteristic frequency [Hz]	c_{min} [mol/m^3]	c_{max} [mol/m^3]	b [m^3/mol]	Γ_∞ [mol/m^2]	Reference
Heptanoic acid	6×10^{-9} to 4×10^{-5}	5.4 to 2.5×10^{4}	2.6×10^{-1}	2.0×10^{1}[a]	4×10^{-1}	8.3×10^{-6}	[80,81]
Octanoic acid	9×10^{-8} to 4×10^{-4}	4.7×10^{-1} to 1.60×10^{3}	7.7×10^{-2}	5.5[a]	1.35	8.3×10^{-6}	[80,81]
Nonanoic acid	3×10^{-6} to 8×10^{-3}	2.8×10^{-2} to 2.4×10^{1}	1.9×10^{-2}	0.90[b]	5.56	8.3×10^{-6}	[80]
Decanoic acid	10^{-4} to 6×10^{-2}	3.3×10^{-3} to 3.0×10^{-1}	6.4×10^{-3}	0.15[b]	1.61×10^{1}	8.3×10^{-6}	[80]
Hexanol	8×10^{-10} to 6×10^{-6}	3.8×10^{1} to 5.1×10^{5}	6.7×10^{-1}	5.8×10^{1}[a]	1.92×10^{-1}	6.8×10^{-6}	[81–83]
Heptanol	10^{-8} to 8×10^{-5}	2.7 to 1.7×10^{4}	1.8×10^{-1}	1.4×10^{1}[a]	6.31×10^{-1}	7.5×10^{-6}	[81,83,84]
Octanol	2×10^{-7} to 6×10^{-4}	3.4×10^{-1} to 3.5×10^{2}	6.5×10^{-2}	3.4[a]	1.55	8.5×10^{-6}	[81,83–85]
Nonanol	4×10^{-6} to 10^{-2}	1.8×10^{-2} to 2.5×10^{1}	1.5×10^{-2}	0.8[b]	7.13	8.0×10^{-6}	[83,86]
Decanol	7×10^{-5} to 2×10^{-1}	10^{-3} to 1.1	3.8×10^{-3}	0.2[b]	2.56×10^{1}	8.8×10^{-6}	[83,87,88]
C_8DMPO	10^{-9} to 2×10^{-4}	1.6 to 1.7×10^{8}	1.1×10^{-1}	5×10^{1}[c]	2.61	3.2×10^{-6}	[20,78]
C_{10}DMPO	2×10^{-7} to 2×10^{-2}	1.4×10^{-2} to 4.5×10^{5}	1.1×10^{-2}	4[c]	2.34×10^{1}	3.6×10^{-6}	[20,89]
C_{12}DMPO	2×10^{-5} to 2	1.5×10^{-4} to 1.8×10^{3}	1.2×10^{-3}	4×10^{-1}[c]	1.76×10^{2}	4.3×10^{-6}	[20,89]
C_{14}DMPO	2×10^{-3} to 2×10^{2}	1.3×10^{-6} to 1.8×10^{1}	1.1×10^{-4}	3.9×10^{-2}[c]	1.86×10^{3}	4.3×10^{-6}	[20,89]
$C_{10}EO_4$	5×10^{-6} to 2	1.5×10^{-4} to 5.9×10^{4}	1.1×10^{-3}	7×10^{-1}[c]	2.57×10^{2}	3.3×10^{-6}	[90]
$C_{14}EO_8$	5×10^{-2} to 10^{5}	3.3×10^{-9} to 2×10^{2}	4.3×10^{-6}	7×10^{-3}[c]	1.05×10^{5}	2.2×10^{-6}	[91,92]
Triton X-45	3×10^{-4} to 10^{2}	2.7×10^{-6} to 8.9×10^{2}	1.5×10^{-4}	1×10^{-1}[c]	$1.68\times10^{+3}$	3.6×10^{-6}	[93–95]
Triton X-100	5×10^{-5} to 2×10^{2}	2.6×10^{-6} to 1.4×10^{5}	1.3×10^{-4}	2.2×10^{-1}[c]	$3.0\times10^{+3}$	2.5×10^{-6}	[6,15,96]
Triton X-165	10^{-5} to 2×10^{1}	2.1×10^{-5} to 3.9×10^{5}	3.5×10^{-4}	4.3×10^{-1}[c]	$1.22\times10^{+3}$	2.3×10^{-6}	[94,97]
Triton X-305	6×10^{-6} to 2×10^{3}	5.0×10^{-7} to 5.8×10^{9}	3.2×10^{-5}	6.5×10^{-1}[c]	$3.27\times10^{+4}$	1.14×10^{-6}	[93–95]

[a] Solubility limit.
[b] Estimated values from extrapolation.
[c] CMC concentration.

investigated surfactants of non-ionic, anionic and cationic nature are summarized.

3. Available experimental methods

The most suitable methods for measuring the dynamic interfacial tension and dilational surface rheology are presented in Tables 4 and 5. Each method has a specific time window. Some of these methods can be applied to water/air and water/oil interfaces without modification. With these data in the tables, and the information given for the surfactants of Tables 1, 2 and 4 one should be able to decide about the most appropriate methods to be used. Before discussing the procedure by which the best experimental method for studies of the adsorption kinetics and the dilational rheology can be selected, it is advantageous to introduce the methods.

The French physicist Pierre Lecomte du Noüy in his publication of 1925 [23], proposed principle which is still practices until today. He measured the force (weight) required to raise a ring from the liquid's surface. This force is appointed as a final aim also in the modern surface tension techniques but the way of its reaching is different from technique to technique. In a similar even older procedure a plate is brought into contact with the liquid surface and then the force (weight) of the spontaneously formed meniscus is measured. Both of these two classical methods have advantages and problems, which are discussed in much detail in [24].

One more relatively old method is the drop volume tensiometry [25]. It determines the volume of drops detaching from a capillary of given diameter. Knowing the radius of the capillary and the liquid's density, it is possible to calculate the surface tension. This method is still used because it allows accurate measurements even for liquid/liquid systems, although the available time window is rather narrow [26].

Another old and at the same time modern method is the maximum bubble pressure tensiometry. In 1851, 160 years ago, Simon [27] was possibly the first to propose this method for measuring the surface tension of liquids. Today this method has reached a very high level of automation and it reaches the shortest adsorption times among all dynamic surface tension techniques [28]. It is actually the only technique that provides dynamic surface tensions of surfactant solutions in a sub-milliseconds time range. To reach such extremely short adsorption times, many hydrodynamic and aerodynamic effects have to be taken into consideration in order to measure physical values or to correct for the respective influences. In particular, the design of the measuring cell and capillary are of key importance. Another important issue is the way of determining the characteristic bubble times, i.e. to split the bubble time into dead time and lifetime. For the very short times, the procedure of obtaining accurately the life time of a bubble is based on the analysis of gas flow versus pressure characteristics, as it was first proposed by Fainerman [29]. The design and operational principles of different bubble pressure tensiometers including the influence of the main parameters of the measuring system (capillary radius, measuring system volume and its ratio to the bubble volume) were described in detail elsewhere [30,28].

The drawback of the bubble pressure technique is its limitation to liquid/gas interfaces. However, it was the guide for the development of the so-called capillary pressure instruments. With the availability of fast computers and liquid proofed pressure sensors a new generation of capillary pressure instruments was launched, which particularly allows the measurement of dynamic interface tensions between two immiscible liquids. The pioneering work here was made by Liggieri et al. [31]. With this liquid proofed sensitive pressure sensor the interfacial tension can be determined, provided the drop radius is known. The drop radius can be simultaneously measured from the video image of the drop. The method is established very well now and allows to record changes of the interface tension with time in a time

Table 2
Parameters of the Langmuir model for selected anionic surfactants.

Surfactant	Adsorption onset time [s]	Characteristic frequency [Hz]	c_{min} [mol/m^3]	c_{max} [mol/m^3]	b [m^3/mol]	Γ_∞ [mol/m^2]	Reference
SDeS	2×10^{-9} to 2×10^{-6}	1.2×10^{2} to 5.2×10^{3}	1.3	3.30×10^{1}[a]	5.26×10^{-2}	1.24×10^{-5}	[98–100]
SDS	4×10^{-8} to 2×10^{-5}	9.0 to 7.6×10^{2}	3.4×10^{-1}	8.2[a]	2.83×10^{-1}	8.91×10^{-6}	[98,99,101,102]
STS	6×10^{-7} to 2×10^{-3}	1.1×10^{-1} to 1.1×10^{2}	3.8×10^{-2}	2.10[a]	2.48	9.24×10^{-6}	[103]

[a] CMC concentration.

Table 3
Parameters of the Langmuir model for selected cationic surfactants.

Surfactant	Adsorption onset time [s]	Characteristic frequency [Hz]	c_{min} [mol/m^3]	c_{max} [mol/m^3]	b [m^3/mol]	Γ_∞ [mol/m^2]	Reference
DeTAB	10^{-9} to 10^{-6}	1.5×10^{2} to 5.4×10^{4}	1.4	5×10^{1}[a]	7.54×10^{-2}	8.22×10^{-6}	[104]
DoTAB	2×10^{-8} to 1×10^{-5}	1.6×10^{1} to 9.0×10^{2}	4.7×10^{-1}	1.2×10^{1}[a]	1.61×10^{-1}	1.12×10^{-5}	[17,104,105]
TTAB	2×10^{-7} to 2×10^{-4}	1.3 to 1.1×10^{2}	1.3×10^{-1}	3.6[a]	6.36×10^{-1}	1.03×10^{-5}	[17,104,106]
CTAB	3×10^{-6} to 4×10^{-3}	5.0×10^{-2} to 2.4	2.7×10^{-2}	9×10^{-1}[a]	1.98	1.58×10^{-5}	[17,104,107]

[a] CMC concentration.

window down to few milliseconds [32,33]. A variety of capillary pressure tensiometers has been developed. For measuring the interfacial tension of pure liquid–liquid systems the pressure derivative method is most suitable [34]. The dynamics of adsorption can be investigated by the growing drop/bubble [35–38] and the expanding drop [31,39,40] methods. The most efficient presently are the oscillating capillary pressure bubble/drop methods [41–43], which are also suitable for transient stress relaxation experiments [44]. Highest frequencies reached by these capillary pressure controlled oscillating drop and bubble methods are of the order of 500 Hz.

Let us finally comment on the present work horse in most interfacial laboratories, the drop and bubble profile analysis tensiometry (PAT). Only very small amounts of the liquid are required, just enough to form one drop. It is suitable for both liquid–vapor and liquid–liquid interfaces, and applicable to systems ranging from molten metals to pure organic solvents and diluted and concentrated solutions. There is also no limitation on the magnitude of surface or interfacial tension, accessible in a broad range of temperatures and external pressures [45]. For measurements at constant interfacial area the time window ranges from about one second up to hours and days so that even extremely slow processes can be easily followed. Under periodic perturbation of the drop surface area, the frequency window spans some decades in the low frequency range, i.e., below 1 Hz. At faster oscillations, a frequency threshold appears when the interface is no more in mechanical equilibrium so that shape distortions occur due to viscous and inertia forces [46–48].

The influence of surfactants on surface wave properties reveals the possibility to extract information on the surface rheological properties from the characteristics of surface waves. The first practical attempts of these phenomena have already been made in the sixties of the last century [49–55]. So far, this method, called capillary wave damping, still remains widely used in surface rheological studies but with unimproved limitations for a number of systems to which this method can be applied. The capillary wave method was frequently used to measure the surface tension of pure liquids [56–58] but later on it was shown by the first theories of Lamb and later Levich that this method is also suitable for measurements of the surface elasticity [59,60]. The respective instruments used were based on the principles of an electro-capillary generator and optical detection of the waves. The capillary waves are typically generated by a thin metallic blade fixed above the tested solution. The electric generator applies a sinusoidal voltage to this metallic blade leading to capillary waves at the surface of the liquid. The initial amplitude of the transverse waves is determined by the distance between the blade and liquid surface, which is less than a millimeter. The optical detector system consists of a laser beam that reflects from the liquid surface and becomes detected by a position-sensitive photo detector. Simultaneous tracing of the point where the laser beam is reflected from allows the determination of the damping coefficient and the length of the capillary waves.

The advent of lasers also allows the determination of the spectral broadening of light scattered by thermal surface fluctuation. The spectral shape is related directly to the damping coefficient of capillary waves and consequently with the surface quasi-elastic light scattering (SQELS) [61]. The main advantages of this SQELS method consist in the non-invasive probing of the liquid surface and in the high upper limit of possible frequencies (up to about 1 MHz).

The determination of the dilational elasticity modulus and the corresponding surface viscosity for a monolayer at liquid solutions can be achieved also by measuring the wavelength and damping of longitudinal waves. The compression waves are generated by a thin wire (diameter $\approx$0.2 mm), made of glass for air–water interfaces or tin copper for oil–water interfaces, coated with paraffin to prevent wetting by the bulk fluids. The wire spans the entire width of the trough, which has a rectangular shape. It is related to a piezo-electric device permitting small oscillations ($\approx$0.3 mm) at the surface. The oscillation frequencies are of the order of 0.1 up to 15 Hz. The compression waves produce surface tension modulations that can be detected with a suitable tensiometer.

The oscillating barrier method is more or less similar to the previous methods. A test liquid is placed in the appropriate trough and the surface tension is followed using the Wilhelmy plate tensiometer. The moving part of this instrument is a Teflon barrier that glides back and forth along the polished brims of the trough. The amplitude of the barrier oscillations varies from 0.5 to 5 mm. The elasticity modulus can be determined from the amplitude ratio of the oscillations of surface tension and surface area, while the phase angle, i.e. surface viscosity, is gained from the phase shift of the surface tension and surface area changes. A disadvantage of this method appears when the oscillation frequencies exceed 0.2 Hz and the surfactant distribution over the interface becomes rather inhomogeneous.

In conclusion, we can state that for water/air interfaces a combination of maximum bubble pressure and drop/bubble profile analysis tensiometry are optimum and allow dynamic surface tension experiments, and by that adsorption kinetics studies, in a time range between $t<10^{-3}$ s up to $t>10^{5}$ s. For interfaces between two immiscible liquids the bubble pressure tensiometry is to be replaced by capillary pressure tensiometry by which the lowest adsorption time increases to 10^{-2} s. Regarding the interfacial dilational rheology, the combination of oscillating drops and bubbles, based on profile analysis and capillary pressure measurements, respectively, we get access to data in a frequency range between 10^{-3} Hz and 100 Hz. Using additionally the capillary wave damping method [62], also frequencies up to 1000 Hz are feasible.

Table 4
Dynamic surface and interfacial tension methods.

Method	Time range	Liquid–gas	Liquid–liquid	References
Maximum bubble pressure tensiometry	0.0002 to 100 s	X	–	[30]
Capillary pressure tensiometry	(0.0002 s for water–air) 0.01 to hours	X	X	[38]
Drop volume tensiometry	1 s to 30 min	X	X	[108,109]
Drop and bubble profile tensiometry	1 s to hours	X	X	[45]
Ring tensiometry, plate tensiometry	10 s to hours	X	(X)	[24]

4. Theoretical models

The first real adsorption model for surfactants at liquid interfaces as proposed by Langmuir was originally developed for the gas adsorption at solid surfaces [63]. Later Frumkin showed that the additional assumption of an interaction between molecules in the adsorption layer can improve the agreement between theory and experiment. Although recently refinements have been published reflecting some specific features of adsorbed surfactants molecules, as described in detail elsewhere [64], in many cases the Langmuir model is still used by many authors. This is at least acceptable when semi-quantitative evaluations are needed. For an accurate analysis the presented work should of course be done on the basis of the optimum model for the respective studied surfactant. However, the target of this investigation is to give an overview and present a guide for how to tackle the given problem. Therefore, we base our discussion here mostly on a Langmuir adsorption model for which rather simple analytical expressions are available and compare it partially with the respective Frumkin and Reorientation models, much more suitable for a quantitative analysis of a number of surfactants. The adsorption isotherm for the Langmuir model [10] reads:

$$\Gamma = \Gamma_\infty \frac{bc}{1 + bc} \tag{1}$$

and the corresponding Szyszkowski–Langmuir equation of state has the form

$$\gamma_o - \gamma = \Pi = -RT\Gamma_\infty \ln\left(1 - \frac{\Gamma}{\Gamma_\infty}\right) = RT\Gamma_\infty \ln(1 + bc). \tag{2}$$

Here γ_0 is the interfacial tension in the absence of surfactant, γ is the interfacial tension at the surfactant bulk concentration c, Π is the surface pressure, R and T are the gas law constant and absolute temperature, respectively, Γ_∞ is the maximum adsorption and b is the adsorption constant with the dimension of a reciprocal concentration.

The Frumkin adsorption isotherm and equation of state is given in the following form [11]:

$$bc = \frac{\theta}{1-\theta} \exp(-2a\theta) \tag{3}$$

$$-\frac{\Pi\omega_0}{RT} = \ln(1-\theta) + a\theta^2 \tag{4}$$

where a is the intermolecular interaction constant, θ is the surface coverage by surfactant molecules, $\theta = \Gamma\omega$, ω is the molar area of the adsorbed molecule. If the compressibility of the adsorbed layer is taken into account then the molar area is considered to depend on the surface pressure $\omega = \omega_0(1 - \varepsilon\Pi\theta)$, where ω_0 is the molar area of a solvent molecule, and ε is the two dimensional compressibility coefficient [65].

For some surfactants the molecules in the adsorption layer can change their orientation upon increasing the surface coverage to that with smaller molar area. The behavior of such surfactants is described most precisely by the so-called Reorientation model [66]:

$$b_1 c = \frac{\Gamma_1\omega_{10}}{(1-\theta)^{\omega_1/\omega_{10}}} \exp\left(-\frac{\omega_1}{\omega_{10}}(2a\theta)\right) \tag{5}$$

$$-\frac{\Pi\omega_{10}}{RT} = \ln(1-\theta) + \Gamma(\omega - \omega_{10}) + a\theta^2 \tag{6}$$

$$\omega\Gamma = \theta = \omega_1\Gamma_1 + \omega_2\Gamma_2 \tag{7a}$$

$$\Gamma = \Gamma_1 + \Gamma_2 \tag{7b}$$

$$\frac{\Gamma_2}{\Gamma_1} = \left(\frac{\omega_2}{\omega_1}\right)^{\alpha} (1-\theta)^{\frac{\omega_2-\omega_1}{\omega_{10}}} \exp\left[\frac{\omega_2 - \omega_1}{\omega_{10}}(2a\theta)\right] \tag{7c}$$

$$\omega_1 = \omega_{10}(1 - \varepsilon\Pi\theta) \tag{8}$$

where indices 1 and 2 correspond to the two states with different molecular orientations and therefore with different molar areas. Eq. (8) accounts for the surface compressibility of the state with smaller molar area.

As surfactants have a different surface activity, the measurable change in surface tension, i.e. a measurable surface pressure, is expected only when a certain concentration is reached. It is possible to predict the necessary concentration for a particular surfactant at which it reaches surface pressure equilibrium of few mN/m. That concentration could then be used to characterize the lower concentration at which the corresponding adsorption isotherm starts. It is just necessary to adopt average values, $\Gamma_\infty = 5\times10^{-6}$ mol/m^2 and $RT = 2.446\times10^6$ (mJ/mol) at 21 °C, and insert these values into Eq. (2). To measure the kinetics of a surfactant with a reasonable accuracy this surface pressure should be at least $\Pi_{min} \geq 2$ mN/m. Eq. (2) yields then

$$\frac{\Pi_{min}}{RT\Gamma_\infty} \leq [\ln(1 + bc)] \tag{9}$$

or

$$bc \geq \exp\left[\frac{\Pi_{min}}{RT\Gamma_\infty}\right] - 1 \tag{10}$$

which for the discussed quantities gives $bc \geq 0.18$. This means, for a given value of the constant b only at concentrations $c \geq 0.18/b$ a reasonable equilibrium surface pressure is reached and hence the adsorption dynamics can be measured.

On the other hand, the upper concentration limit for experiments of a given surfactant is the solubility limit or the CMC, as above this concentration, not only single molecules are transported to and from the bulk but also aggregates [67].

Assumed the adsorption process is diffusion controlled, the kinetics is given by the equation derived by Ward and Tordai for a flat interface [68]:

$$\Gamma(t) = \sqrt{\frac{4D}{\pi}}\left[c\sqrt{t} - \int_0^{\sqrt{t}} c_s(t-\tau)d\sqrt{\tau}\right] \tag{11}$$

where c is the bulk concentration of surfactant and c_s is the concentration in the surface layer related to adsorption through the adsorption isotherm, for example, Eq. (1). Eq. (11) was later extended to the case of adsorption at the spherical interface of radius r as [2]

$$\Gamma(t) = \sqrt{\frac{4D}{\pi}}\left[c\sqrt{t} - \int_0^{\sqrt{t}} c_s(t-\tau)d\sqrt{\tau}\right] \pm \frac{D}{r}\left[ct - \int_0^t c_s(t-\tau)d\tau\right]. \tag{11a}$$

The plus in Eq. (11a) corresponds to adsorption from outside the droplet. The short time approximation useful to describe the very beginning of the adsorption process is

$$\Gamma(t) = 2c\sqrt{\frac{Dt}{\pi}} + \frac{cDt}{r}. \tag{11b}$$

The quantitative solution of the Ward–Tordai equation has been discussed for example in [69].

As is obvious from Eq. (11), the adsorption of the surfactant molecules depends on the bulk concentration c. Once $\Gamma(t)$ has been

obtained, the corresponding dynamic interfacial tension is calculated via the corresponding equation of state, for example, Eq. (2).

Another important concept for characterizing the adsorption dynamics is the surface dilational modulus, which displays the response of the interfacial tension on the compression or expansion of the interface [70]:

$$E = \frac{d\gamma}{d\ ln\Gamma}\frac{d\ ln\Gamma}{d\ lnA}. \tag{12}$$

The modulus can be presented as a complex quantity where the real part represents the surface elasticity and the imaginary part the surface viscosity. The first factor in the r.h.s. of Eq. (12) is the limiting Gibbs elasticity corresponding to the high frequency limit when the surfactant behaves like an insoluble one. Using the same Langmuir adsorption model, the high frequency limit of the elasticity is given by

$$E_0 = \frac{d\gamma}{d\ ln\Gamma} = RT\Gamma_\infty bc. \tag{13}$$

Similar to the adsorption kinetics also the dilational visco-elasticity cannot be measured for any surfactant at any concentration by any experimental method. There are similar limitations as we have discussed already before for the measurement of dynamic interfacial tension $\gamma(t)$.

When we assume a reasonably measurable elasticity of $E_{0,min} =$ 2 mN/m and assuming the same value for Γ_∞ as before, we obtain $bc \geq 0.16$, a value similar to what we obtained for the interfacial pressure Π. Thus, the concentration range feasible for measurements of the frequency dependence of the visco-elasticity $E(\omega)$ is essentially the same as for $\gamma(t)$.

The dilational visco-elasticity, measured at a certain frequency $f = \omega/2\pi$, was presented for a diffusional exchange of matter by Lucassen and van den Temple [71,72] in a complex form via

$$E(i\omega) = E' + iE'' = E_0\frac{\sqrt{i\omega}}{\sqrt{i\omega} + \sqrt{2\omega_0}}. \tag{14}$$

Here E' and E'' are the real and imaginary part of E, corresponding to the elastic and viscous part of the dilational visco-elasticity, respectively:

$$E'(\omega) = E_0\frac{1 + \sqrt{\omega_0/\omega}}{1 + 2\sqrt{\omega_0/\omega} + 2\omega_0/\omega} \tag{15}$$

$$E''(\omega) = E_0\frac{\sqrt{\omega_0/\omega}}{1 + 2\sqrt{\omega_0/\omega} + 2\omega_0/\omega}. \tag{16}$$

These equations contain the key parameter ω_0 which is the characteristic frequency of the diffusional matter exchange

$$\omega_0 = \frac{D}{2}(dc/d\Gamma)^2. \tag{17}$$

It includes in turn the adsorption activity of the surfactant $dc/d\Gamma$. This derivative corresponds to the slope of the adsorption isotherm and reads for the Langmuir isotherm

$$\frac{dc}{d\Gamma} = \frac{(1 + bc)^2}{\Gamma_\infty b}. \tag{18}$$

With the given theoretical basis we can now estimate for a given surfactant whether the adsorption kinetics and dilational rheology can be studied in a respective concentration range and we can also decide which experimental method is most suitable.

5. Results and discussion

As we mentioned already above, the main purpose of this paper is to select the most suitable interfacial tension and rheological methods from the available pool for characterizing a particular surfactant. Therefore, in this section we present the adsorption characteristics of a large number of surfactants commonly used in model studies and practical applications. Tables 1, 2 and 4 contain the adsorption onset time, characteristic frequency, minimum and maximum concentration, adsorption equilibrium constant b, and maximum adsorption Γ_∞. The values of the adsorption parameters b and Γ_∞ were found by fitting the experimental isotherms given in literature (see the reference given in the last column) with the Langmuir adsorption model given by Eq. (2). For this fitting we used the free software IsoFit discussed in detail in [2,73]. Eq. (2) was used in its simplest form for both non-ionic and ionic surfactants.

The so-called maximum concentration c_{max} coincides with the values of solubility and CMC which were taken from the mentioned references. In some case the respective values were not available so that we estimated them by extrapolation of data given for shorter members of a homologous series. This concentration refers to the upper limit at which experiments can provide information that are not affected by the presence of precipitates or micelles. The minimum concentration c_{min} is defined by Eq. (10) and represents the lower limit from which one can perform experiments with a sufficient accuracy. The adsorption onset time and the characteristic frequency are two dynamic characteristics of a given surfactant at a specific concentration. The two values given in the tables correspond to c_{max} and c_{min}, respectively, while of course the lower time value and higher frequency correspond to the higher concentration.

To understand the adsorption kinetics in the framework of a diffusion controlled model, the diffusion coefficient of the respective surfactant in the corresponding solvent is needed. There are several generally accepted methods for the estimation of the diffusion coefficients in liquids, mainly derived for particles but also applied to molecules [74]. These relationships are derived for the case of infinitely diluted solutions, however, for practical purposes they are quite accurate for concentrations up to 10 mol%. One of the most often used methods is the Wilke–Chang correlation [75]:

$$D^0_{AB} = \frac{7.4\cdot10^{-8}(\phi M_B)^{1/2}T}{\eta_B V_A^{0.6}} \tag{19}$$

where D^0_{AB}—mutual diffusion coefficient of solute A in solvent B, M_B—molecular mass of solvent B, η_B—viscosity of solvent B, V_A—molar volume of solute A at its normal boiling temperature [cm^3/mol], ϕ—association factor of solvent B, which can be accepted as 2.6 for water, 1.9 for methanol, 1.5 for ethanol and 1 for non-associated solvents. In turn, V_A can be estimated using the Le Bas method. The contributions of different atoms and groups to V_A according to [74] are also quite different. It is noteworthy, that usually the diffusion coefficients of surfactants in water are in the range between 10^{-10} and 10^{-9} m^2/s. Using Eq. (19) we can estimate the diffusions coefficient, for example for hexanol, decanol and Triton X-100, and obtain 8.9×10^{-10} m^2/s, 6.7×10^{-10} m^2/s and 3.2×10^{-10} m^2/s, respectively.

In Tables 1–4 the adsorption onset time was calculated from the short time approximation of the Ward and Tordai equation, Eq. (11b), for a flat interface accepting an average value for the diffusion coefficient for all surfactants of $D = 5\times10^{-10}$ m^2/s. The values for the other model parameters were obtained from the Langmuir model and given in the tables as well. Let us define the adsorption onset time as the time when the surface pressure rises over 0.1 mN/m which is the minimum value that can be recorded by any instruments in Table 4. As mentioned above, we calculated onset time for two values of concentration, c_{min} and c_{max}, respectively. To select the corresponding suitable experimental method for a given situation, one has to compare the adsorption onset time of the desired surfactant from Table 1, 2 or 4 with the time range of the instruments given in Table 4.

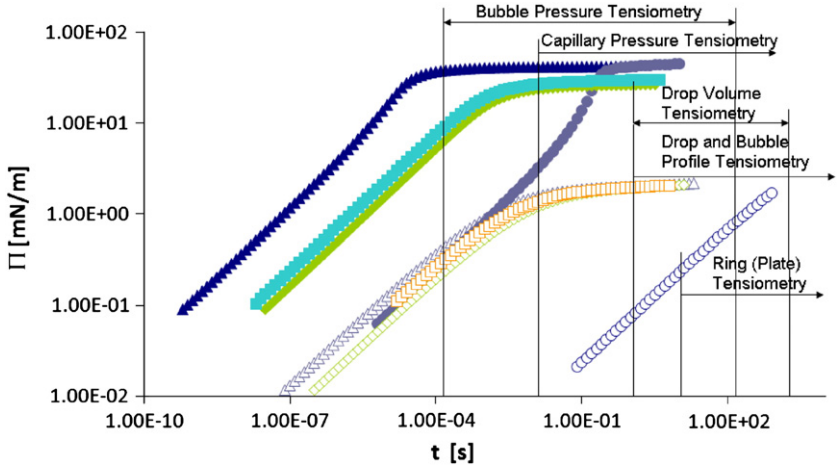

Fig. 2. Adsorption kinetics calculated from Ward and Tordai equation are based on Langmuir model at the water/air interface; the empty symbols present the bulk concentrations c_{min} where approximately 2 mN/m equilibrium surface pressure is obtained while the filled symbols present the maximum bulk concentrations c_{max}; (▲,△)—hexanol, (■,□)—DoTAB, (◆,◇)—SDS, (●,○)—C_{12}DMPO.

Table 5
Relaxation methods for measuring dilational rheology [110].

Method	Frequency range [Hz]	Liquid–gas	Liquid–liquid	References
Quasielastic light scattering	$1000–10^6$	X	–	[111]
Capillary waves	10 to 1000	X	(X)	[62]
Longitudinal waves	0.1 to 15	X	(X)	[112,113]
Oscillating barrier	0.001 to 0.1	X	(X)	[114]
Oscillating drop/bubble profile	0.001 to 0.1	X	X	[115]
Capillary pressure with oscillating drop/bubble	0.1 to 500	X	(X)	[32,41,116]

As examples, the adsorption kinetics of some surfactants (hexanol, DoTAB, SDS and C_{12}DMPO) adsorbing at different time scales are presented in Fig. 2. For each surfactant we have two curves. One is related to the maximum concentration c_{max} and the second to the low concentration c_{min} where molecules show the first adsorption effects. The time ranges of different experimental methods are plotted on the same graph for comparison. If the aim is just to measure the interfacial tension equilibrium then any instrument is suitable that provides data at sufficiently long times. On the contrary, when we need to learn as much as possible about the adsorption kinetics, the selected interfacial tension method should be able to cover surface pressure changes from a free interface at $\Pi = 0$ mN/m up to equilibrium. From the curves obtained for c_{max} we see that for hexanol even the fast bubble pressure tensiometry is insufficient to observe the change in surface tension with and only values close to equilibrium can be measured. In contrast, for the C_{12}DMPO we get the complete curve from $\Pi = 0$ up to the equilibrium with this method. For the lowest concentration c_{min}, the situation is different. While bubble pressure tensiometry does not at all deliver kinetics data for C_{12}DMPO, we get an almost perfect result for DoTAB and SDS.

Let us now analyze the situation for the dilational rheology and focus on the methods summarized in Table 5. The characteristic frequency ω_0 or $f_0 = \omega_0/2\pi$ represents the time scale of relaxation processes and is a specific quantity of a surfactant at a given concentration. For diffusional relaxation (Eq. (17)) it depends on the diffusion coefficient D and the adsorption activity, represented by $dc/d\Gamma$. The frequency $\omega = 2\omega_0$ corresponds in this case to the maximum of the imaginary part of viscoelastic modulus Eq. (16). The values of the characteristic frequency given in Tables 1, 2 and 4 were calculated from the Langmuir model using an average diffusion coefficient value of $D = 5 \times 10^{-10}$ m^2/s and the given isotherm parameters:

$$f_0 = \frac{D}{4\pi}\left[\frac{(1+bc)^2}{\Gamma_\infty b}\right]^2. \tag{20}$$

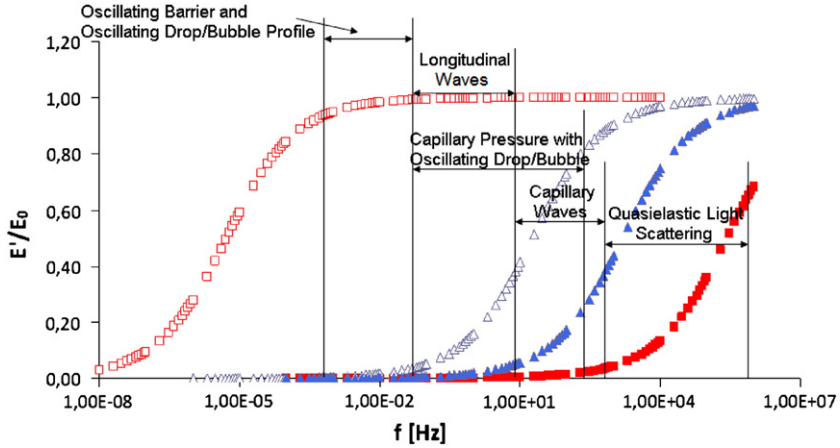

Fig. 3. The real part of the dilational visco-elasticity; the empty symbols present the bulk concentration where around 2 mN/m surface pressure equilibrium increase is obtained while the filled symbols present the bulk maximum concentrations. (■,□)—Triton X-100, (▲,Δ)—SDS.

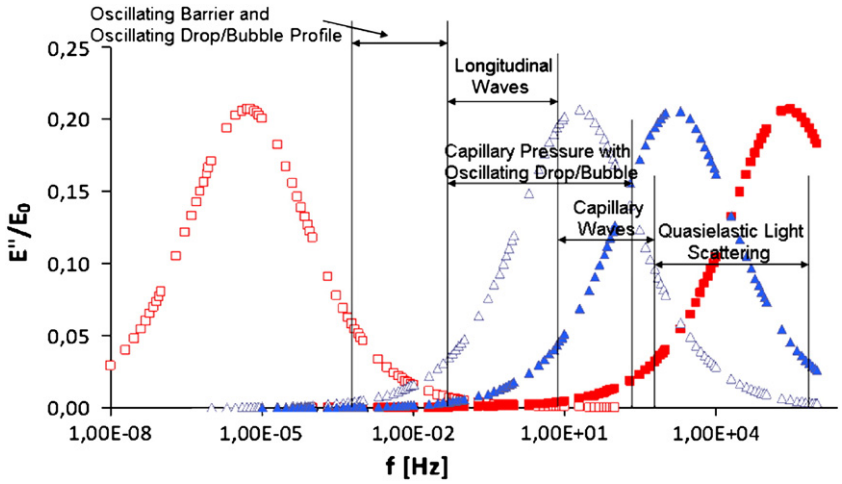

Fig. 4. The imaginary part of the dilational visco-elasticity; the open symbols present the bulk concentration where around 2 mN/m surface pressure equilibrium increase is obtained while the filled symbols present the maximum bulk concentrations; (■,□)—Triton X-100, (▲,△)—SDS.

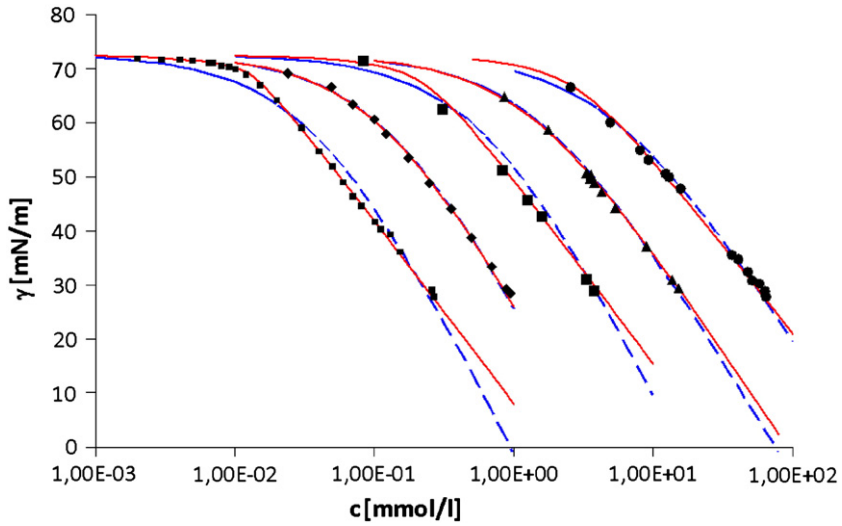

Fig. 5. Surface tension isotherms of decanol (▪), nonanol (♦), octanol (■), heptanol (▲) and hexanol (●) fitted with the Langmuir (dashed line) and Frumkin models (solid line). The data are taken from [81–86].

The two values refer to the selected concentrations c_{max} and c_{min}, as mentioned above and cover, therefore, the whole bulk concentration interval of the particular surfactant. Obviously the frequencies smaller than 10^{-3} s are hardly reached in real experiments at least because of time limitation. In this case the data presented in Tables 1–4 can give a hint about the range of relevant concentrations.

For easier understanding, in Figs. 3 and 4 we show the elasticity and viscosity data for Triton X-100 and SDS as examples. The frequency windows of the dilational rheology methods of Table 5 are also inserted. Triton X-100 is a surfactant adsorbing in a very broad concentration range and hence the characteristic frequency spans also over a very wide interval. On the contrary, SDS has a rather narrow range of the characteristic frequency. It is obvious that a single technique cannot cover the whole range of characteristic frequency for any surfactant. Hence, to obtain experimental data in the whole frequency range it is necessary to combine several techniques.

It should be stressed, however, that for many surfactants the Langmuir model can be considered as a rather rough approximation. The behavior of these surfactants, especially surface rheology is described more precisely by other models considered above. As an example, we performed a comparison of the results based on the Langmuir model with those based on the Frumkin model for aliphatic alcohols and with those based on the Reorientation model for oxyethylated alcohols.

Table 6
Frumkin and Reorientation model parameters for selected surfactants.

Frumkin model:

Surfactant	b [m^3/mol]	Γ_∞ [mol/m^2]	a	ε [m/mN]
C_6OH	1.23×10^{-1}	5.81×10^{-6}	1.04	0
C_7OH	5.33×10^{-1}	5.99×10^{-6}	0.8	0
C_8OH	1.17	6.06×10^{-6}	1.37	0
C_9OH	5.82	6.06×10^{-6}	1.2	0
$C_{10}OH$	1.21×10^{1}	5.99×10^{-6}	1.8	0

Reorientation model:

Surfactant	b[m^3/mol]	ω_{10}[m^2/mol]	ω_2[m^2/mol]	α	a	ε [m/mN]
$C_{10}EO_4$	3.68×10^{2}	4×10^{5}	1×10^{6}	1	0	5×10^{-3}
$C_{14}EO_8$	5.84×10^{4}	5.4×10^{5}	1.4×10^{6}	3	0	7×10^{-3}

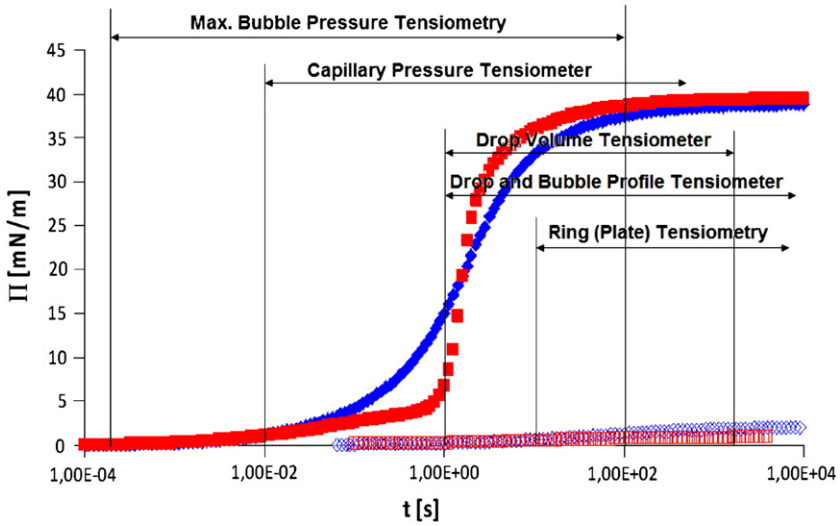

Fig. 6. Adsorption kinetics of decanol calculated from Ward and Tordai equation are based on Langmuir and Frumkin models at the water/air interface; the empty symbols present the bulk concentrations c_{min} where approximately 2 mN/m equilibrium surface pressure is obtained while the filled symbols present the maximum bulk concentrations c_{max}, (■,□)—Frumkin model, (♦,◊)—Langmuir model.

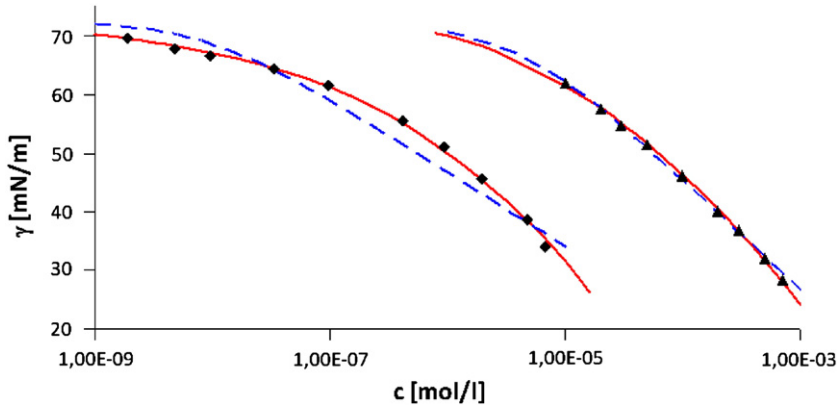

Fig. 7. Surface tension isotherms of $C_{14}EO_8$ (♦) and $C_{10}EO_4$ (▲) fitted with the Langmuir (dashed line) and Reorientation models (solid line). The data are taken from [90–92].

The adsorption isotherms of the series of aliphatic alcohols with fitting curves calculated for the Langmuir and Frumkin models are presented in Fig. 5. The Langmuir and Frumkin model parameters are presented in Tables 1 and 6, respectively. It is seen from Fig. 5 that decanol displays the largest difference between the fitting curves. That is why decanol is chosen as an example to compare the corresponding adsorption kinetics. Fig. 6 makes it clear that the dynamic behavior of decanol based on the Langmuir and Frumkin

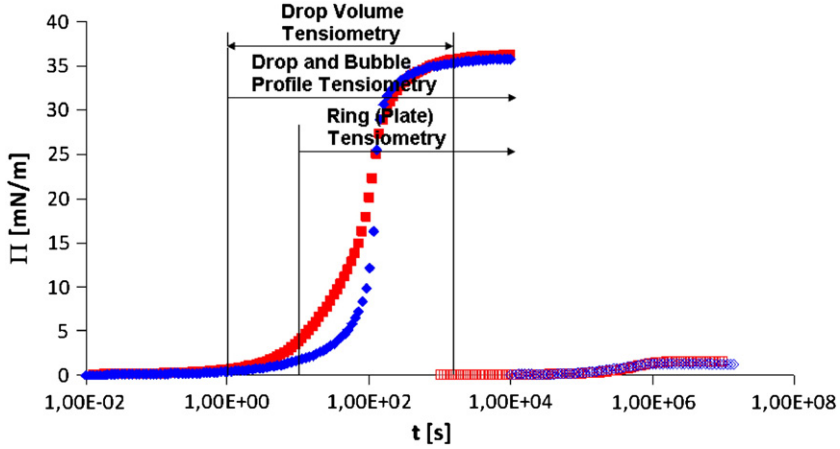

Fig. 8. Adsorption kinetics of $C_{14}EO_8$ calculated from Ward and Tordai equation are based on Langmuir and Reorientation models at the water/air interface; the empty symbols present the bulk concentrations c_{min} where approximately 2 mN/m equilibrium surface pressure is obtained while the filled symbols present the maximum bulk concentrations c_{max}, (■,□)—Reorientation model, (♦,◊)—Langmuir model.

Table 7
Characteristic frequencies calculated from different adsorption models.

Surfactant	C_{min} [mol/m^3]	Characteristic frequencies		
		Langmuir	Frumkin	Reorientation
C_6OH	1	4×10^{1} to 5×10^{5}	4×10^{1} to 10^{7}	
C_8OH	10^{-1}	3×10^{-1} to 4×10^{2}	3×10^{-1} to 4×10^{4}	
$C_{10}OH$	9×10^{-3}	10^{-3} to 1	8×10^{-4} to 3×10^{2}	
$C_{10}EO_4$	8×10^{-4}	2×10^{-4} to 6×10^{4}		10^{-4} to 4×10^{2}
$C_{14}EO_8$	10^{-6}	3×10^{-9} to 2×10^{2}		10^{-8} to 4×10^{-2}

models does not show significant differences, i.e. it confirms that Capillary Pressure Tensiometry in combination with Drop and Bubble Profile Tensiometry enables us getting the whole information about adsorption kinetics and equilibrium surface tension.

The adsorption isotherms for oxyethylated alcohols $C_{10}EO_4$ and $C_{14}EO_8$ fitted with the Langmuir and Reorientation models are presented in Fig. 7. It is obvious that the Reorientation model fits much better the particular experimental results. The model parameters are presented in Table 6. $C_{14}EO_8$ shows the strongest difference between the two models. Therefore, $C_{14}EO_8$ is used to check the differences in adsorption kinetics for these two models. As it is seen from Fig. 8 the difference in adsorption kinetics also in this case does not affect the choice of most of the suitable methods, which is the Drop and Bubble Profile Tensiometry.

The theoretical predictions of the surface rheology are much more sensitive to the choice of the adsorption isotherm. The comparison of characteristic frequencies derived on the basis of the Langmuir and more sophisticated models is presented in Table 7. It should be noted that in Table 7 there are also values given for the new c_{min}, different from Table 1, because c_{min} is changing with any variation in the isotherms shape. The values of characteristic frequencies for Frumkin and Reorientation models have been determined via IsoFit already mentioned above (free software [73]). Comparing the data in Table 7 with the isotherms in Figs. 5 and 7 one can see that there are differences in the calculated values of the characteristic frequencies even for hexanol, although the fitting curves for both the Langmuir and Frumkin models practically coincide for this surfactant. For $C_{14}EO_8$, where the Langmuir model gives a rather pure fitting, the difference in the determined characteristic frequencies at c_{max} reaches 4 orders of magnitude. These examples show clearly the power of surface rheology in establishing a proper adsorption model. At the same time they display that the characteristic frequencies given in Tables 1–4 are only rather rough estimations and to catch up the most important relaxation behavior even in the case of a sufficiently well isotherm fitting, the suitable experimental method should be applicable at least in the range between $f_0/10$ and $10^3\times f_0$.

More details about dilational rheology methods can be found in the references listed in Table 5. It should also be mentioned that we have only discussed the diffusion relaxation process. Other relaxation processes, such as formation of aggregates at the interface have their own specific relaxation times and an additional analysis is required to account for such processes.

6. Selected examples

The following two examples shown in Figs. 9 and 10 describe step by step the way for using the presented analysis to any surfactant system, i.e. how to find the answer on the question on which of the different dynamic surface tension and dilational rheology methods apply best to a respective surfactant.

Let us look into the non-ionic surfactant $C_{10}EO_4$. Table 1 tells us that the adsorption onset times are between about 10^{-5} and 2 s. Hence, neither of the available methods can cover this broad concentration range. For the highest concentration, close to the CMC, one would need a method that can provide data from 10 μs on, which does not exist. Fig. 9 presents the corresponding dynamic surface tension curves obtained for $C_{10}EO_4$ using the complementary set of methods of maximum bubble pressure and profile analysis tensiometry [76]. We can easily see that these two methods provide an acceptable experimental basis, although for the highest concentrations the short time values for $t<1$ ms are not available. On the other side, drop profile tensiometry can easily cover the required time window at long adsorption times. There is one important point to which we should pay attention. Most, maybe all, surfactants contain impurities although in most cases in small amounts [77]. However, in case these impurities are of high surface activity they can affect the kinetic curves significantly, mainly at longer adsorption time. Such impurities can lead to a secondary surface tension decrease after the equilibrium state has been almost achieved [76]. Such data do not correspond to the behavior of the main surfactant and have to be excluded from any data analysis.

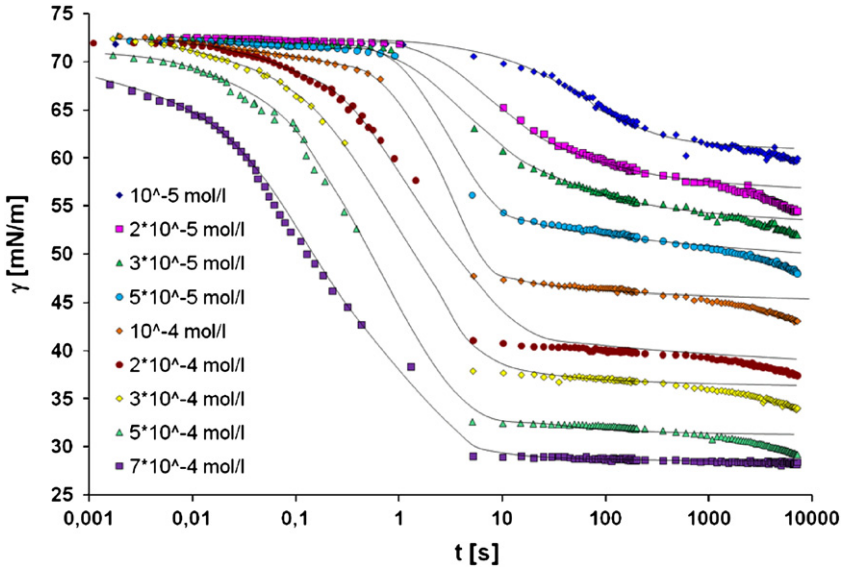

Fig. 9. Dependence of dynamic surface tension of $C_{10}EO_4$ solutions on the bulk concentrations measured using the maximum bubble pressure and drop profile analysis tensiometry; according to [76].

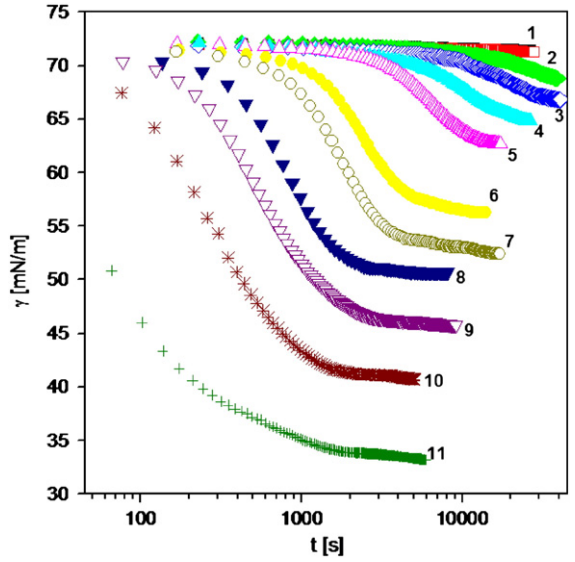

Fig. 10. Dependence of dynamic surface tension of C_{14}DMPO solutions on the bulk concentrations measured using the ring method: 10^{-7} mol/l (1), 2×10^{-7} mol/l (2), 3×10^{-7} mol/l (3), 4×10^{-7} mol/l (4), 5×10^{-7} mol/l (5), 6×10^{-7} mol/l (6), 2×10^{-6} mol/l (7), 3×10^{-6} mol/l (8), 4×10^{-6} mol/l (9), 6×10^{-6} mol/l (10), 10^{-5} mol/l (11); according to [78].

The second example refers to the highly surface active molecule C_{14}DMPO [78]. This surfactant adsorbs from solutions of relatively small concentrations and therefore its adsorption kinetics is slow as compared to other surfactants. The adsorption onset times are such that for this surfactant it should be possible to study its adsorption dynamics completely by the bubble pressure and drop profile analysis tensiometry. When we use, however, only the ring tensiometry the short time data will be missing, as we can see in Fig. 10.

The discussion of choosing the right dilational visco-elasticity method works in the same way as we have demonstrated here for the adsorption kinetics. We can easily understand that it is even more difficult to cover the whole necessary frequency range due to the parameters of the available methods and in addition to the fact that we have discussed here only a diffusional relaxation. For interfacial relaxation processes much slower or much faster than the diffusional transport, even broader frequency windows will be needed [79].

7. Conclusions

This work demonstrates how one can decide for a given surfactant whether its adsorption kinetics and dilational rheology can be studied appropriately, and which experimental methods are most suitable. The data given in Tables 1, 2 and 4, such as the "adsorption onset time" and the "characteristic frequency" are most relevant for selecting a suitable method from Table 4 or 5. Note, for the sake of simplicity, all calculations are based on the Langmuir adsorption model and the Ward and Tordai equation for diffusion controlled adsorption processes. For systems, where the Langmuir adsorption model and/or the diffusion mechanism do not apply, a more sophisticated analysis is required. Some data on characteristic frequencies obtained with more sophisticated adsorption models are presented in Table 7. Corresponding calculations for various adsorption models in assumption of diffusion controlled adsorption kinetics can be performed by free software IsoFit [73].

Acknowledgments

The work was financially supported by a project of the DFG SPP 1506 (Mi418/18-1), the European Space Agency (ESA FASES MAP AO-99-052) and the German Space Agency (DLR 50WM0941).

References

[1] Dukhin SS, Kretzschmar G, Miller R. In: Möbius D, Miller R, editors. Dynamics of adsorption at liquid interfaces: theory, experiment, application. Studies in Interface ScienceAmsterdam: Elsevier; 1995.
[2] Fainerman VB, Möbius D, Miller R. Surfactants—chemistry, interfacial properties and application. Studies in Interface ScienceElsevier; 2001.
[3] Prosser AJ, Franses EI. Colloids Surf A 2001;178:1.
[4] Blunk D, Tessendorf R, Buchavzov N, Strey R, Stubenrauch C. J Surfactants Deterg 2007;10:155.
[5] Patil SR, Buchavzov N, Carey E, Stubenrauch C. Soft Matter 2008;4:840.
[6] Fainerman VB, Lylyk SV, Aksenenko EV, Makievski AV, Petkov JT, Yorke J, et al. Colloids Surf A 2009;334:1–7.
[7] Pradines V, Fainerman VB, Aksenenko EV, Krägel J, Mucic N, Miller R. Colloids Surf A 2010;371:22.
[8] Joos P. Dynamic surface phenomena. VSP: Dordrecht; 1999.
[9] Rosen MJ. Surfactants and interfacial phenomena. 3rd edition. John Wiley & Sons, Inc.; 2004
[10] von Szyszkowski B. Z Phys Chem (Leipzig) 1908;64:385.
[11] Frumkin AN. Z Phys Chem (Leipzig) 1925;116:466–85.
[12] Lunkenheimer K, Barzyk W, Hirte R, Rudert R. Langmuir 2003;19:6140–50.
[13] Wüstneck R, Miller R, Czichocki G. Tenside Deterg 1992;29:265–70.
[14] Lunkenheimer K, Czichocki G, Hirte R, Barzyk W. Colloids Surf A 1995;101:187–97.
[15] Fainerman VB, Lylyk SV, Aksenenko EV, Petkov JT, Yorke J, Miller R. Colloid Surf A 2010;354:8–15.
[16] Sharipova A, Aidarova SB, Fainerman VB, Miller R. Colloids and Surfaces A, DOI: 10.1016/j.colsurfa.2010.08.044
[17] Stubenrauch C, Fainerman VB, Aksenenko EV, Miller R. J Phys Chem 2005;109:1505–9.
[18] Haydon DA, Taylor FH. Trans Faraday Soc 1962;58:1233–50.
[19] Miller R, Fainerman VB, Möhwald H. Adsorption behaviour of oxyethylated surfactants at the air/water interface. J Colloid Interface Sci 2002;247:193–9.
[20] Lunkenheimer K, Haage K, Miller R. Colloids Surf 1987;22:215.
[21] Lunkenheimer K, Haage K, Hirte R. Langmuir 1999;15:1052.
[22] Fainerman VB, Lylyk SV, Aksenenko EV, Liggieri L, Makievski AV, Petkov JT, et al. Colloids Surf A 2009;334:8–15.
[23] du Noüy PL. J Gen Physiol 1925;7:625.
[24] Rusanov AI, Prokhorov VA. In: Möbius D, Miller R, editors. Interfacial tensiometry. Studies in Interface ScienceElsevier; 1996.
[25] Tate T. Philos Mag 1864;27:176.
[26] Javadi A, Miller R, Fainerman VB. Drop volume tensiometry. In: Miller R, Liggieri L, editors. Bubble and drop interfaces. Progress in Colloid and Interface ScienceLeiden: Brill Publ.; 2011. p. 147.
[27] Simon M. Ann Chim Phys 1851;32:5–41.
[28] Fainerman VB, Miller R. Maximum bubble pressure tensiometry: theory, analysis of experimental constrains and applications. In: Miller R, Liggieri L, editors. Bubble and drop interfaces. Progress in Colloid and Interface ScienceLeiden: Brill Publ.; 2011. p. 93.
[29] Fainerman VB. Measurement of the dynamic surface tension of solutions by the method of the maximal pressure in a bubble. Colloid J (Russ) 1979;41:79–83.
[30] Fainerman VB, Miller R. Adv Colloid Interface Sci 2004;108–109:287.
[31] Liggieri L, Ravera F, Passerone A. J Colloid Interface Sci 1995;169:226.
[32] Kovalchuk VI, Ravera F, Liggieri L, Loglio G, Javadi A, Kovalchuk NM, et al. Studies in capillary pressure tensiometry and interfacial dilational rheology. In: Miller R, Liggieri L, editors. Bubble and drop interfaces. Progress in Colloid and Interface ScienceLeiden: Brill Publ.; 2011. p. 175.
[33] Loglio G, Pandolfini P, Liggieri L, Makievski AV, Ravera F. Determination of interfacial properties by the pendant drop tensiometry: optimisation of experimental and calculation procedures. In: Miller R, Liggieri L, editors. Bubble and drop interfaces. Progress in Colloid and Interface ScienceLeiden: Brill Publ.; 2011. p. 8.
[34] Passerone A, Liggieri L, Rando N, Ravera F, Ricci E. J Colloid Interface Sci 1991;146:152.
[35] Nagarajan R, Wasan DT. J Colloid Interface Sci 1993;159:164.
[36] MacLeod CA, Radke CJ. J Colloid Interface Sci 1993;160:435.
[37] Zhang X, Harris T, Basaran OA. J Colloid Interface Sci 1994;168:47.
[38] Javadi A, Krägel J, Pandolfini P, Loglio G, Kovalchuk VI, Aksenenko EV, et al. Colloids Surf A 2010;365:62.
[39] Liggieri L, Ravera F, Passerone A, Sanfeld A, Steinchen A. Lect Notes Phys 1996;467:175.
[40] Breen PJ. Langmuir 1995;11:885.
[41] Kretzschmar G, Lunkenheimer K. Ber Bunsenges Phys Chem 1970;74:1064.
[42] Wantke K-D, Lunkenheimer K, Hempt C. J Colloid Interface Sci 1993;159:28.
[43] Wantke K-D, Fruhner H. In: Möbius D, Miller R, editors. Studies in interface science, Vol. 6. Amsterdam: Elsevier Science; 1998. p. 327.
[44] Liggieri L, Ravera F, Ferrari M, Passerone A, Loglio G, Miller R, et al. Microgravity Sci Technol 2005;XVI - I:196.
[45] Miller R, Fainerman VB, Makievski AV, Ferrari M, Loglio G. Measuring dynamic surface tensions. In: Holmberg K, editor. Handbook of applied colloid and surface science. John Wiley & Sons; 2001. p. 775.
[46] Liao YC, Basaran OA, Franses EI. Colloids Surf A 2004;250:367.
[47] Freer EM, Wong H, Radke CJ. J Colloid Interface Sci 2005;282:128.
[48] Leser ME, Acquistapace S, Cagna A, Makievski AV, Miller R. Colloids Surf A 2005;261:25.
[49] Garrett WD, Bultman JD. J Colloid Sci 1963;18:798.

[50] Mann JA, Hansen RS. J Colloid Sci 1963;18:805.
[51] Davies JT, Vose RW. Proc R Soc Lond A 1965;286:218.
[52] Lucassen J, Hansen RS. J Colloid Interface Sci 1966;22:32.
[53] Lucassen J, Hansen RS. J Colloid Interface Sci 1967;23:319.
[54] Bendure RL, Hansen RS. J Phys Chem 1967;71:2889.
[55] Thiessen D, Scheludko A. Kolloid Z Z Polym 1967;218:139.
[56] Rayleigh L. Philos Mag 1890;30:386.
[57] Kalen LA. Ann Phys 1902;7:440.
[58] Kolovrat-Chervinskiy L. J Russ Phys Chem Soc 1904;36:265.
[59] Lamb H. Hydrodynamics. New York: Dover; 1932.
[60] Levich VG, Soviet Phys. JETP, 10 (1940) 1296; 11 (1941) 340.
[61] Langevin D. In: Marcel Dekker, editor. Light scattering by liquid surfaces and complimentary techniques; 1992. New York.
[62] Noskov BA. Interfacial elasticity as studied by wave methods. In: Miller R, Liggieri L, editors. Interfacial rheology. Leiden: Brill Publ.; 2009. p. 103–36.
[63] Langmuir I. J Am Chem Soc 1917;39:1848.
[64] Fainerman VB, Miller R. Adsorption isotherms at liquid interfaces. In: Somasundaran P, Hubbard A, editors. Encyclopedia of surface and colloid science, 2nd Edition, 1; 2009. p. 1.
[65] Fainerman VB, Kovalchuk VI, Aksenenko EV, Michel M, Leser ME, Miller R. J Phys Chem B 2004;108:13700.
[66] Fainerman VB, Lylyk SV, Aksenenko EV, Makievski AV, Petkov JT, Yorke J, et al. Coll Surf A 2009;334:1.
[67] Miller R, Noskov BA, Fainerman VB, Petkov JG. Impact of micellar kinetics on dynamic interfacial properties of surfactant solutions. In: Platikanov D, Exerowa D, editors. Highlights in colloid science. Wiley-VHC; 2008. p. 247–59.
[68] Ward AFH, Tordai L. J Phys Chem 1946;14:453.
[69] Ziller M, Miller R. Colloid Polym Sci 1986;264:611.
[70] van den Tempel M, Lucassen J, Lucassen-Reynders EH. J Phys Chem 1965;69:1798–804.
[71] Lucassen J, van den Tempel M. Chem Eng Sci 1972;27:1283.
[72] Lucassen J, van den Tempel M. J Colloid Interface Sci 1972;41:491.
[73] http://www.thomascat.info/thomascat/Scientific/AdSo/AdSo.htm.
[74] Poling BE, Prausnitz JM, O'Connell JP. The properties of gases and liquids. 5th edition. New York: McGraw-Hill; 2001.
[75] Wilke CR, Chang P. Correlation of diffusion coefficients in dilute solution. AIChE J 1955;1:264.
[76] Miller R, Olak C, Makievski AV. Tensiometry as a tool for quantitative analysis of surfactant adsorption. SÖFW; 2004. p. 2. (English version).
[77] Lunkenheimer K, Miller R. J Colloid Interface Sci 1987;120:176.
[78] Makievski AV, Grigoriev DO. Colloids Surf A 1998;143:233.
[79] Liggieri L, Ferrari M, Modelli D, Ravera F. Faraday discuss 2005;129:125-–40.
[80] Malysa K, Miller R, Lunkenheimer K. Colloids Surf 1991;53:47.
[81] Demond AH, Lindher AS. Environ Sci Technol 1993;27:2318.
[82] Addison CC. J Chem Soc 1945:98.
[83] Hommelen JR. J Colloid Sci 1959;14:385.
[84] Fainerman VB, Lylyk SV. Koll Zh 1983;45:500.
[85] Aratono M, Uryu S, Hayami Y, Motomura K, Matuura R. J Colloid Interface Sci 1984;98:33.
[86] Wüstneck R, Miller R. Colloids Surf 1990;47:15.
[87] Lin S-Y, McKeigue K, Maldarelli C. Langmuir 1991;7:1055.
[88] Lin S-Y, Lu T-L, Hwang W-B. Langmuir 1994;10:3442.
[89] Miller R, Olak C, Makievski AV. Tensiometry as a tool for quantitative analysis of surfactant adsorption. SÖFW; 2004. p. 2. (English version).
[90] Schulze-Schlarmann J, Stubenrauch C, Miller R. Tenside Surfactants Deterg 2005;42:307.
[91] Ueno M, Takasawa Y, Miyashige H, Tabata Y, Meguro K. Colloid Polym Sci 1981;259:761.
[92] Fainerman VB, Petkov JT, Miller R. Langmuir 2008;24:6447–52.
[93] Fainerman VB, Miller R. Colloids Surf A 1995;97:65.
[94] Egan RW, Jones MA, Lehninger AL. Hydrophile–lipophile balance and critical micelle concentration as key factors influencing surfactant disruption of mitochondrial membranes. J Biol Chem 1976.
[95] Fainerman VB, Miller R, Makievski AV. Langmuir 1995;11:3054.
[96] Janczuk B, Bruque JM, Gonzales–Martin ML, Dorado-Calasanz C. Langmuir 1995;11:4515.
[97] El Ghzaoui A, Fabreque R, Cassanas G, Fulconis JM, Delagrange J. Colloid Polym Sci 2000;278:231.
[98] Lunkenheimer K, Czichocki G, Hirte R, Barzyk W. Colloids Surf A 1995;101:187.
[99] Fainermann VB. Kolloidn Zh 1986;48:512.
[100] Czichocki G, Makievski AV, Fainerman VB, Miller R. Colloids Surf A 1997;122:189.
[101] Vollhardt D, Czichocki G, Rudert R. Colloids Surf A 1993;76:217.
[102] Chen L-W, Chen J-H. J Chem Soc Faraday Trans 1995;91:3873.
[103] Tajima K. J Chem Soc Jpn 1973;5:883.
[104] Bergeron V. Langmuir 1997;13:3474.
[105] Langevin D, Argillier J-F. Macromolecules 1996;29:7412.
[106] Lu JR, Thomas RK, Aveyard R, Blinks BP, Cooper P, Fletcher PDI, et al. J Phys Chem 1992;96:10971.
[107] Schukin ED, Markina ZN, Zadymova NM. Prog Colloid Polym Sci 1983;68:90.
[108] Gunde R, Kumar A, Lehnert-Batar S, Mäder R, Windhab EJ. J Colloid Interface Sci 2001;244:113.
[109] Wang W, Ngan KH, Gong J, Angeli P. Colloids Surf A 2009;334:197.
[110] Noskov BA. Curr Opin Colloid Interface Sci 2010;15:229.
[111] Noskov BA. Interfacial elasticity as studied by wave methods. In: Miller R, Liggieri L, editors. Interfacial rheology. Progress in Colloid Interface Sci.Leiden: Brill Publ.; 2009. p. 103.
[112] Lucassen J. Trans Faraday Soc 1968;64:2230–5.
[113] Lemaire C, Langevin D. Colloids Surf 1992;65:101–12.
[114] Noskov BA, Latnikova AV, Lin S-Y, Loglio G, Miller R. Dynamic surface elasticity of β-casein solutions in the course of adsorption process. J Phys Chem C 2007;111:16895–901.
[115] Benjamins J, Cagna A, Lucassen-Reynders EH. Colloids Surf A 1996;114:245–54.
[116] Kovalchuk VI, Ravera F, Liggieri L, Loglio G, Pandolfini P, Makievski AV, et al. Adv Colloid Interface Sci 2010;161:102–14.

Paper VI

Fast dynamic interfacial tension measurements and dilational rheology of interfacial layers by using the capillary pressure technique

A. Javadi, J. Krägel, A.V. Makievski, N.M. Kovalchuk, V.I. Kovalchuk, N. Mucic, G. Loglio, P. Pandolfini, M. Karbaschi and R. Miller

Colloids and Surfaces A, 407 (2012) 159-168.

Colloids and Surfaces A: Physicochem. Eng. Aspects 407 (2012) 159–168

Contents lists available at SciVerse ScienceDirect

Colloids and Surfaces A: Physicochemical and Engineering Aspects

journal homepage: www.elsevier.com/locate/colsurfa

Fast dynamic interfacial tension measurements and dilational rheology of interfacial layers by using the capillary pressure technique

A. Javadi[a,*], J. Krägel[a], A.V. Makievski[b], V.I. Kovalchuk[a,c], N.M. Kovalchuk[a,c], N. Mucic[a], G. Loglio[d], P. Pandolfini[d], M. Karbaschi[e], R. Miller[a]

[a] Max-Planck-Institut für Kolloid- und Grenzflächenforschung, D14476 Golm, Germany
[b] SINTERFACE Technologies, Volmerstrasse 5-7, D-12489 Berlin, Germany
[c] Institute of Bio-Colloid Chemistry, 03142 Kiev, Ukraine
[d] University of Florence, Department of Organic Chemistry, I-50019 Sesto Fiorentino, Italy
[e] Chemical and Petroleum Engineering Department, Sharif University of Technology, Teheran, Iran

HIGHLIGHTS

- Fast dynamic interfacial tension measurements as short as 10^{-2} s are achieved.
- Fast oscillating drop experiments for studies of dilational rheology at up to 80 Hz for liquid–liquid interfaces are achieved.
- The technique is also well capable for iso-dense systems.
- The details of experimental setup, protocols and data analysis are described.

GRAPHICAL ABSTRACT

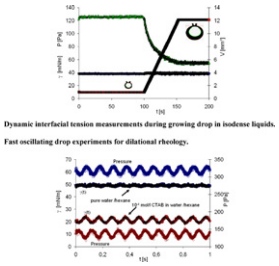

ARTICLE INFO

Article history:
Received 22 March 2012
Received in revised form 10 May 2012
Accepted 11 May 2012
Available online 26 May 2012

Keywords:
Dynamic interfacial tension
Dilational visco-elasticity
Capillary pressure tensiometry
Oscillating drop and bubble
Drop formation and detachment
High frequency oscillations
Short adsorption times

ABSTRACT

The oscillating drop and bubble analyzer (ODBA) is an experimental set-up based on the measurement of capillary pressure under static and dynamic conditions. It allows studies of slow and fast dynamic surface and interfacial tensions, following different growing and oscillating drop or bubble protocols, as well as determination of the dilational interfacial visco-elasticity of liquid interfacial layers. For the visco-elasticity studies, drops or bubbles are subjected to harmonic oscillations of area or volume in a broad frequency range, and the resulting harmonic capillary pressure response is analyzed by Fourier analysis. Also, transient relaxations can be easily performed, which are of particular importance for isodense systems. The limits of applicability for highly dynamic conditions are given by the hydrodynamics of the fluid flow inside the capillary tip and the pressure cell which depend on fluid properties, capillary tip size, and geometry. For the growing drop protocol, additional phenomena during drop formation and detachment play a significant role. For oscillating drops or bubbles, the highest accessible frequencies also depend on the absolute drop size and applied oscillation amplitude. In this work, the capability of the technique for measurements in the frequency range between 1 and 100 Hz are discussed, and elasticity values at up to 80 Hz were measured for the liquid–liquid interface.

1. Introduction

Modern technologies for the formation of emulsions and foams are highly dynamic and include a fast formation of enormously large interfaces [1,2]. The practical fields of their applications cannot be summarized in a short way due to the many types of application [3,4]. The fast formation of drops or bubbles or its

* Corresponding author.
E-mail address: Aliyar.Javadi@mpikg.mpg.de (A. Javadi).

0927-7757/$ – see front matter © 2012 Elsevier B.V. All rights reserved.
http://dx.doi.org/10.1016/j.colsurfa.2012.05.026

behavior under external perturbations is of essential importance. While the dynamics of adsorption, as measured by dynamic interfacial tensions, provides sufficient information for evaluating the coverage of drops/bubbles by surfactants during or a short time after their formation [5], the visco-elasticity as measured by interfacial area oscillation experiments gives insight into the mechanisms of foam and emulsion stabilization. External perturbations as destabilizing processes can be mimicked for example by drop or bubble oscillations [6].

The experimental tool presented here is called oscillating drop and bubble pressure analyzer ODBA and represents an extension of the standard drop and bubble Profile Analysis Tensiometer PAT-1 (SINTERFACE Technologies, Berlin, Germany). The ODBA uses several elements of PAT-1, however, provides important additional information which by no other means are experimentally available. This is true for interfacial tensions of liquid/liquid interfaces at short adsorption times [7]. By no other method data below 1 s adsorption time are accessible. In addition, this methodology is obviously the only one that works at small Bond numbers, e.g. for interfaces between two liquids having a similar density, or under space conditions [8]. This method also allows to look into spherical foam or emulsion films as it was proposed for example by Soos et al. [9] and others [10–12] to study directly the film tension or the film elasticity. The additional important feature of the ODBA is the option of generating high frequency oscillations of small spherical drops/bubbles for determining the visco-elasticity of interfacial layers over a broad frequency range. It has the capacity to even replace capillary wave methods in the range of frequencies up to 1 kHz, which so far has not been possible yet [13].

The ODBA is based on a closed measuring cell equipped with a well designed capillary, a pressure sensor and a piezo translator [14]. The piezo allows the formation of a drop or bubble of a defined size and the pressure sensor with its proximity electronics records the corresponding capillary pressure signal in real time. The piezo translator is used also to generate harmonic changes of the drop or bubble size and the resulting interfacial tension response is monitored in order to determine the visco-elasticity of the interfacial layer.

The present work describes in detail the functionality of the ODBA as tool for measuring dynamic interfacial tensions at short times and dilational visco-elasticity of interfaces between a liquid and gas or a second immiscible liquid at high frequencies. The limits of applicability are discussed and experimental examples are given. For the first time the capability of the technique for measurements in the high frequency range (1–100 Hz) are discussed for liquid–liquid interfaces based on the analysis of the hydrodynamics and experimental data for pure systems and surfactant solutions are presented.

2. Experimental instruments and protocols

2.1. Instrumental description

The capillary pressure tensiometer ODBA for drop and bubble oscillation experiments contains a piezo drive for exact size control of a small droplet (0.01–1 mm^3, depending on the capillary tip size and solution properties) with the accuracy of 0.0001 mm^3 (100 pl) in the frequency range of 0.1–300 Hz. During the generation of precise oscillations the pressure variations are recorded via an accurate relevant pressure sensor as a function of time [15]. This signal contains the capillary pressure contribution along with hydrodynamic effects. The hydrodynamic effects are negligible for low frequencies however can be very significant for high frequencies depending on the applied piezo amplitude, fluid viscosities, capillary tip size and geometry. Details will be discussed further below.

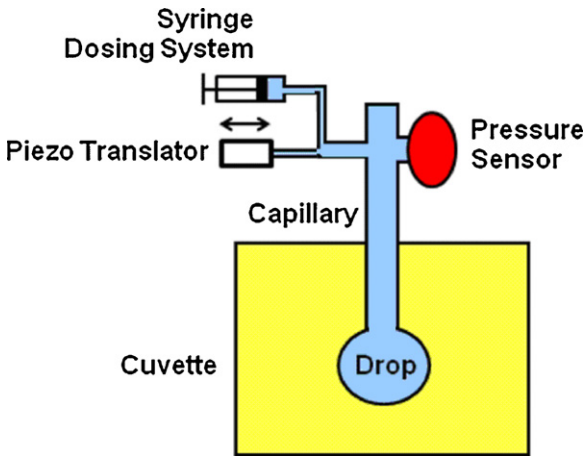

Fig. 1. Schematic of the oscillating drop bubble analyzer ODBA with its main elements (not to scale).

The schematic of the set-up is shown in Fig. 1 and a photo in Fig. 2. Here it is shown as extra equipment for the Profile Analysis Tensiometer PAT-1, however, it also exists as stand-alone unit and can be equipped with a standard video camera (25 fps) or a fast video camera (up to 2000 fps). In addition to the pressure sensor (PDCR-4000, GE-DRUCK, Germany) and the piezoelectric translator (P-843.40 Physik Instrumente, Germany) the ODBA contains a syringe dosing system (ILS, Stützerbach, Germany) for a rough manual drop/bubble formation and manipulation. The accuracy of the syringe system can be adapted between 0.01 μl and 1 μl depending on the syringe size (25–2500 μl). The accuracy of the piezo translator was improved by replacing the rod with a diameter of 5 mm by another one with 1 mm diameter, so that the volume for a full stroke of 60 μm was reduced from about 1 mm^3 down to about 0.1 mm^3 = 100 nl. For oscillation experiments the volume amplitude can be selected in the range between 0.0005 and 0.075 mm^3 with an accuracy of 0.0001 mm^3 (100 pl).

The operating pressure range of the sensor PDCR-4000 is up to 7000 Pa and can be overloaded up to about 10 times. To be on the safe side, the maximum total pressure in the ODBA cell was limited to a value of 10^4 Pa by a software setting. Its accuracy for a single reading is ±3 Pa and can be improved by averaging values at respective sampling rates (if sufficient in the respective experiment).

One of the key elements of any instrument based on single drops or bubbles is the capillary. Its design ensures the correct

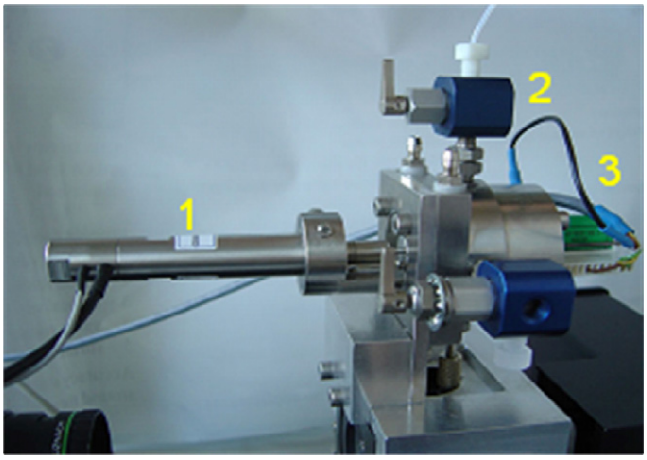

Fig. 2. Photo of the oscillating drop bubble analyzer ODBA as extra module for PAT-1; 1 – piezo translator, 2 – valve for injection of liquid from the syringe dosing system, 3 – relative pressure sensor.

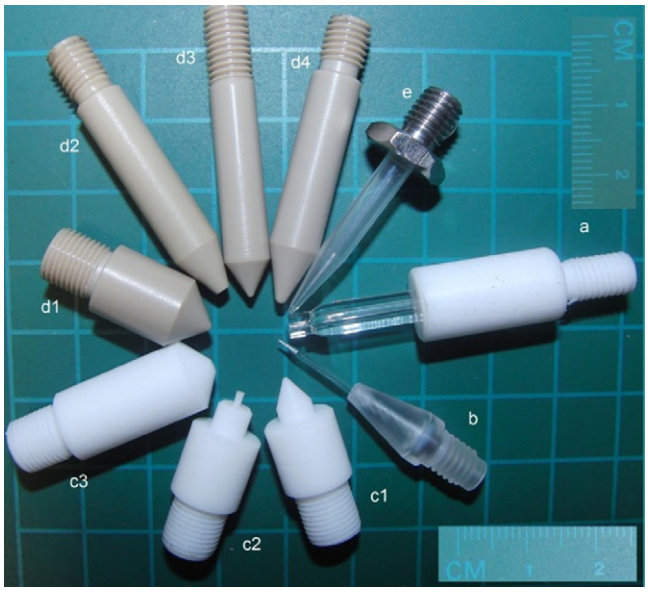

Fig. 3. Capillaries of different material, tip size and geometry; a – glass with PTFE mounting (ID 500 μm), b – glass with PE mounting (ID 100 μm), c1 to c3 – PTFE of different tip shape and size (200–800 μm), d1 to d4 – PEEK of different tip size (ID 200 μm to 800 μm, d2 is a composite designed tip with steel ring inside), e – PE tip with steel mounting (ID 450 μm).

formation of axisymmetric menisci. We used capillaries made of various materials, such as glass, steel, PTFE and PEEK. The optimum design of a capillary is such that the drop/bubble is exactly formed at the inner or outer edge of the capillary tip. We found that conical tips (design d3 and e in Fig. 3) made of PEEK and PE are optimum. In Fig. 3 a selected number of tips made of different materials are shown.

The data acquisition board PCI-6035E from National Instruments, is a 16 bit board with a sampling rate of 200,000 per second, i.e. 5 μs per reading. The absolute accuracy is about 8 mV for the input voltage range between +10 V and −10 V which relates to a relative accuracy of ±0.02%. With a typical inner diameter of 500 μm, the measured capillary pressure for a pure water drop is of the order of 300 Pa, hence the capillary pressure is measured with an accuracy better than 1% at the maximum sampling rate (5 μs) and up to 0.1% when averaging experimental values at lower sampling rates.

The instrument as additional module for the PAT-1 instrument utilizes, besides the temperature cell, the camera and the light source for getting the absolute geometry of the capillary tip and the formed drop or bubble. The geometry is needed for calculating the interfacial tension γ from the measured capillary pressure P. The ODBA is linked via an electronic interface to a PC on which the corresponding software runs for the experiment control and data acquisition.

With the chosen piezo translator frequencies up to 1000 Hz are technically feasible. However, the limit for real measurements is lower. It was shown by Ravera et al. [16] that their set-up CPT, similar to the present instrument, allows measurements at frequencies of about 100 Hz. As the CPT is based on an open cell geometry, it is not suitable for continuously growing drop experiments etc. In addition to that, the mentioned high frequency has been achieved for gas/liquid interface for which the fluid inside the capillary tip is air and the hydrodynamic issue is not a big challenge in comparison with liquid–liquid systems. With a simpler set-up Russev et al. [17] were able to perform oscillations up to about 1 Hz. With the current set-up, representing the state of the art of this methodology for liquid/liquid interfaces, measurements up to 150 Hz can be achieved which means more than one order of magnitude higher than any earlier works in literature. Higher frequencies up to 300 Hz also appear feasible however in addition to a further refinement of the hydrodynamic analysis, an optimization of the capillary tip with respect to material and geometry will be required. Of course, the available frequency range is also influenced by the fluids' properties such as viscosity, compressibility and wettability issues at the capillary tip, and also by the surfactant solution concentration and the corresponding interfacial tension values.

The software used in the present studies has been developed by SINTERFACE Technologies [18] and is based on a LabView code. The operation of all elements can be managed via an interactive panel providing all information in real time, including the capillary pressure. It allows manual operation of a rough (syringe) and fine (piezo translator) dosing systems for drop size changes.

Experiments can be pre-programmed such that an automatic run with various changes in drop/bubble size become possible. Among the protocols, there is the option of constancy of the drop/bubble volume or surface area over a given period of time, the generation of transient perturbations like ramps, square pulses or trapezoidal area changes, and also of harmonic oscillations of the drop/bubble surface area. These oscillations can be performed at a single frequency and amplitude, however, also experiments for a list of frequencies and amplitudes are feasible to sweep over a respective parameter range.

The software controls not only the run of the experiments but at the same time provides an optimum data acquisition with a selectable acquisition rate. The data analysis itself is organized by separate tools, for example to analyze the adsorption kinetics with different models [19] or to interpret the resulting harmonic interfacial tensions via Fourier Transform (FT) analysis and suitable interfacial rheological models [20].

2.2. Experimental protocols

There are different experimental protocols available to measure the dynamic interfacial tension or the dilational visco-elasticity. We present here only some of the options that can be practiced with the ODBA instrument, as extra module for PAT or as stand-alone unit.

2.2.1. Calibration of pressure sensor and optical magnification

Two parameters are needed for calculating the interfacial tension: the radius of curvature of the drop/bubble R and the capillary pressure P, according to the Young–Laplace equation ($\gamma = P/(2/R)$). To obtain correct values, optical and pressure sensor calibrations are necessary. While the radius of curvature is determined from the video images the capillary pressure is obtained from a pressure sensor via an AD/DA data acquisition board.

The pressure sensor has to be calibrated in order to determine the linear relationship between the acquired electrical sensor signal in mV and the pressure value in Pa. The off-set of this voltage/pressure relationship can be eliminated by a so-called zero-setting of the relative pressure sensor. The basic calibration for each pressure sensor is performed using an accurate reference sensor via pressurized air in a wide range (up to 7000 Pa). Then the calibrated pressure sensor is examined for measuring the static pressure at different water level in the cell. The final extra test is measuring the capillary pressure of a pure water droplet of different size for which a constant surface tension should be obtained.

The radius of curvature of the drop/bubble is determined by an analysis of the video image implemented in the ODBA software. A reliable drop radius and precise pixel size (μm per pixel) can be obtained only at optimum illumination which can be set by a supporting software routine. The exact magnification is obtained with a 500 μm calibration capillary. In the video control window of the

ODBA software a movable control line has to be located such that the image below the line is used to analyze the droplet/bubble profile and to calculate the radius of curvature. This base line must be positioned closed to the capillary tip, so that almost the complete shape of the formed droplet/bubble is taken into account for the estimation of the radius. The total size of the drop or bubble must be small enough to have an acceptable spherical geometry and a sufficiently high capillary pressure for oscillation experiments.

2.2.2. Dynamic interfacial tension from growing drop and stopped flow measurements

Recently, several experimental protocols of capillary pressure measurements have been discussed for gaining data on the dynamics of adsorption. This was in particular discussed for interfaces between two immiscible liquids [7] because for the liquid/gas interfaces the bubble pressure tensiometry can provide dynamic surface tensions even in the range of milliseconds of adsorption time [21]. The capillary pressure tensiometry is obviously the fastest method for liquid/liquid interfaces [22]. The simplest protocol is the stopped growing drop procedure [7] which is similar to the idea proposed by Horozov and Arnaudov [23]. However, these authors considered the residual droplet left at the capillary tip after the jet breakup as initially fresh interface. The process of drop necking and detachment and the subsequent reformation of the residual drop at the capillary tip can cause serious challenges for understanding the real initial condition at the drop surface. In contrast, the mentioned stopped growing drop protocol allows to consider a meaningful spherical droplet with a known initial load. This type of experiments ensures a quick formation of a fresh interface and a more or less constant interfacial area during the whole experiment.

A second much more dynamic measurement procedure is the continuously growing drop experiment. Here, a continuous increase of the drop volume V is caused by a constant inflow of liquid. After reaching a critical size (weight) the drop detaches and a new drop with a fresh surface is formed. The data for the very short adsorption times right after drop detachment, although accessible by the experiment, are of no use because the period of time from the onset of the drop detachment until the complete damping of the oscillations of the remnant drop after detachment is rather difficult to determine quantitatively. An analysis of this drop detachment time is discussed in detail elsewhere [24]. Via drop volume tensiometry experiments, drop detachment times were estimated indirectly to be of the order of 10–100 ms [25]. However, the established fresh small droplet after damping of the oscillations of the remnant drop can still provide a rather fresh interface due to the high expansion rate due to the fast liquid inflow. Hence, data for short adsorption times can be obtained [7].

A simple empirical way of testing the highest reliable drop formation rate is by performing experiments with pure solvents, such as a water drop in air or oil. Because the interfacial tension γ for pure solvents does not depend on time or any interfacial expansions or compressions, the resulting interfacial tension should be constant with time, i.e. during the continuous formation of a drop. As the measured capillary pressure $P(t)$ will of course show changes with time due to the changes of the drop radius $R(t)$ the resulting product $P(t) \times R(t)$ should be constant. An example for the change in capillary pressure and the determined surface tension of a growing water drop in air is shown in Fig. 4. This procedure can be applied also for higher flow rates when the hydrodynamics is properly considered (e.g. $Q = 25\,mm^3/s$ for which the total time for a complete drop formation is less that 0.5 s and measurement at 0.01 s are possible). A constant surface/interfacial tension for pure liquids is the best test for the functioning of the instrument and the correct consideration of the hydrodynamic pressure contribution.

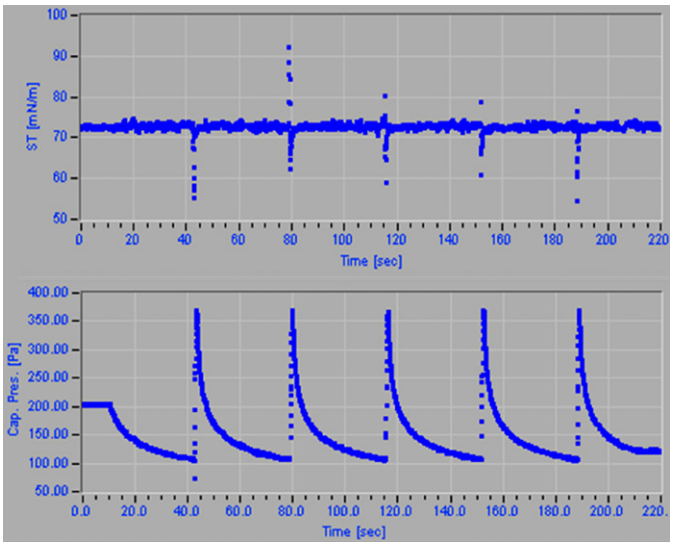

Fig. 4. Screen shot showing the changes in capillary pressure P (bottom) and interfacial tension γ (top) as a function of time during a continuously growing drop experiments with a pure water drop in air.

2.2.3. Interfacial visco-elasticity from oscillating drop experiments

The experimental set-up described here was originally developed to perform drop and bubble oscillations at high frequencies. The first experiment of this kind was proposed by Kretzschmar and Lunkenheimer in 1970 [26]. Since then, this methodology was further improved and is now in many aspects superior to the capillary wave damping technique [27]. Based on the drop/bubble profile tensiometry the method was used for transient relaxation studies [28] and low frequency oscillations [29]. The oscillating drop/bubble tensiometry based on capillary pressure measurements is the most suitable technique now for low and high frequency oscillations and has been used for studies of various surfactant systems [16].

The experimental protocol consists of the formation of a drop/bubble which is then left for a respective period of time to establish the adsorption equilibrium at the interface. This equilibration time depends on the concentration and surface activity of the surfactant to be studied [30]. Then, by an accurate dosing system (in our case a piezo translator) harmonic volume changes, and consequently area changes are generated. The amplitudes are kept sufficiently small, typically below 10% of the drop/bubble area, in order to remain in the range of a linear perturbation response. The frequency of these oscillations can go down to about 0.1 Hz or less and is limited from above by the hydrodynamics of the liquid. Due to inertia, viscosity and gravity effects, drops start to oscillate with overtones so that a clear analysis of the measured pressure signal can become impossible above a certain frequency limit, which depends strongly on the absolute drop size and the geometry of the capillary. Via the analysis of fast video recordings it is possible to determine the frequency limits for a given experimental situation, defined by the liquids' properties and drop/capillary geometry [31].

Again, the simplest way of testing the highest reliable frequency for oscillation experiments is to use pure solvents. The changes in $P(t)$ should be compensated by the changes in $R(t)$ such that the final $\gamma(t)$ should be independent of time, i.e. the visco-elasticity of the liquid interface should be zero. However this limit can decrease to a lower range for surfactant solutions at very high concentrations for which a low interfacial tension results. This decreases the strength

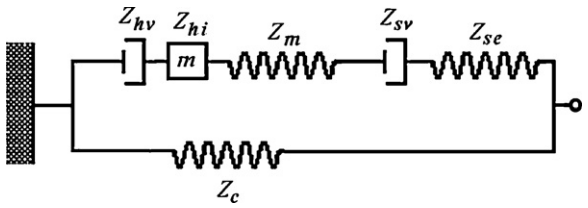

Fig. 5. Equivalent scheme showing the connections between different complex resistances acting in drop/bubble oscillation experiments.

for keeping the drop spherical during the oscillations and the subsequent deformation problem may influence the results and cause extra complexities for a quantitative data analysis.

2.2.4. Theoretical basis of drop oscillations

The hydrodynamic basis for oscillation experiments in a closed measuring cell, as it is the case for the ODBA, was discussed in detail by Kovalchuk et al. [14]. In this paper the mentioned theoretical analysis is summarized in a way schematically shown in Fig. 5. This method can be applied for the case where there is a droplet at the capillary tip or the tip is immersed into the same liquid (no drop). The dynamic response of the considered measuring system is complex and includes not only the visco-elastic contribution of the interfacial layer under study but also a number of other contributions, such as the hydrodynamics due to the fluid flow through the capillary and the flow in the bulk around the meniscus, the elastic contribution due to changes in the meniscus curvature, and the elastic contributions stemming from the finite compressibility of the liquid and the cell deformability [32]. For small-amplitude harmonic oscillations the response of the system is linear and all contributions can be characterized by respective complex resistances. These resistances are connected to each other according to the equivalent scheme presented in Fig. 5.

The response of the system as a whole can be characterized by the complex resistance (impedance)

$$Z = \frac{\delta P}{\delta V_{\mathrm{Drv}}} \tag{1}$$

where δP is the pressure variation in the cell (at constant external pressure) measured by the pressure sensor, and δV_{Drv} is the volume variation applied via the piezo translator. Thus, the response of the system is described by the total resistance

$$Z = \left[\frac{1}{Z_{\mathrm{c}}} + \frac{1}{Z_{\mathrm{hv}} + Z_{\mathrm{hi}} + Z_{\mathrm{m}} + Z_{\mathrm{se}} + Z_{\mathrm{sv}}}\right]^{-1} \tag{2}$$

which includes the partial resistances discussed above.

The visco-elastic contribution of the interfacial layer depends on the meniscus geometry and is composed of two terms

$$Z_{\mathrm{s}} = Z_{\mathrm{se}} + Z_{\mathrm{sv}} \tag{3}$$

where $Z_{\mathrm{se}} = -(2\varepsilon_{\mathrm{r}}/a_0)(d\ln A/d\,V_{\mathrm{m}})$ and $Z_{\mathrm{sv}} = -(2i\omega\eta_{\mathrm{d}}/a_0)(d\ln A/d\,V_{\mathrm{m}})$ are the complex resistances arising from the surface dilatational elasticity, ε_{r}, and viscosity, η_{d}, respectively. Here $\omega = 2\pi f$ is the angular frequency of the generated oscillation, f is the frequency in Hz, a_0 is the radius of curvature of the meniscus at equilibrium, and $d\ln A/d\,V_{\mathrm{m}}$ is a geometric coefficient describing the variation of the surface area A of the meniscus with its volume V_{m}.

The hydrodynamic contribution accounts for viscous and inertia effects in the bulk phases inside the capillary and around the meniscus. Under quasi-stationary flow conditions (for relatively slow oscillations [32]) these effects can be considered separately

$$Z_{\mathrm{h}} = Z_{\mathrm{hv}} + Z_{\mathrm{hi}} \tag{4}$$

where $Z_{\mathrm{hv}} = -i\omega G_1$ and $Z_{\mathrm{hi}} = \omega^2 G_2$ are the complex resistances describing the viscous and inertia contributions, respectively. The hydrodynamic coefficients can be calculated, according to the procedure given in [33], approximately by $G_1 = (8\eta_1 l)/(\pi a_{\mathrm{C}}^4)$ and $G_2 = (4\rho_1 l)/(3\pi a_{\mathrm{C}}^2) + \rho_2/(\pi\sqrt{2(h_0^2 + a_{\mathrm{C}}^2)})$, where η_1 and ρ_1 are the dynamic viscosity and density of the fluid inside the capillary, ρ_2 is the density of the fluid around the meniscus, a_{C} and l are the inner capillary radius and the length of the thinnest part of the capillary (or the effective capillary length, accounting also for entrance effects), and h_0 is the equilibrium drop/bubble height (with respect to the capillary cut-off). We neglect here the viscous effect in the liquid around the meniscus as its contribution is usually small for liquids having a viscosity similar to that of water [34]. The second term in the expression for G_2 describes the contribution of the added mass of liquid around the meniscus. This effect is most important for bubbles oscillating in a liquid.

The elastic resistance of the meniscus arises due to variations of the capillary pressure with changes in the radius of curvature a (at constant interfacial tension γ):

$$Z_{\mathrm{m}} = \frac{2\gamma}{a_0^2}\frac{da}{dV_{\mathrm{m}}} \tag{5}$$

Here the geometrical coefficient da/dV_{m} describes the variation of a with the meniscus volume V_{m}. One more contribution arises due to the finite liquid compressibility in the cell and deformability of the cell walls [14,35]. For relatively small pressure amplitudes and not very high frequencies (corresponding to the acoustic wave lengths, much larger than the cell size) this contribution is described by the resistance

$$Z_{\mathrm{c}} = -\frac{B_{\mathrm{ef}}}{V_{\mathrm{c}}} \tag{6}$$

where V_{c} is the total volume of liquid in the cell and $B_{\mathrm{ef}} = B(1 + (B/V_{\mathrm{c}})(dV_{\mathrm{c}}/dP) + (B/V_{\mathrm{c}})(V_{\mathrm{Gas}}/B_{\mathrm{Gas}}))^{-1}$ is the effective cell elasticity including the elastic response of the liquid, the cell walls and any gas bubbles, occasionally entrapped into the cell. B is the bulk elasticity of the liquid ($K = B^{-1} = -d\ln V/dP$ is called bulk compressibility), dV_{c}/dP is the coefficient describing the variation of the internal volume of the cell with pressure (i.e. deformability of the walls), and V_{Gas} and B_{Gas} are the volume of a hypothetic possible entrapped air bubble and its bulk elasticity.

The complex resistances included in Eqs. (3)–(5) are connected in series, whereas the resistance Z_{c}, describing the intrinsic elasticity of the cell, is connected in parallel to the other resistances. Hence, the total complex resistance is given by

$$Z = \left[-\frac{V_{\mathrm{c}}}{B_{\mathrm{ef}}} - \frac{1}{i\omega G_1 - \omega^2 G_2 - (2\gamma/a_0^2)(da/dV_{\mathrm{m}}) + (2\varepsilon_{\mathrm{r}}/a_0)(d\,\ln A/d\,V_{\mathrm{m}}) + (2i\omega\eta_{\mathrm{d}}/a_0)(d\,\ln A/d\,V_{\mathrm{m}})}\right]^{-1} \tag{7}$$

For interfaces of pure liquid, i.e. in absence of any surfactants, the dynamic surface visco-elasticity is zero and the complex resistance is given by

$$Z_0 = \left[-\frac{V_{\mathrm{c}}}{B_{\mathrm{ef}}} - \frac{1}{i\omega G_1 - \omega^2 G_2 - (2\gamma_0/a_0^2)(d\,a/d\,V_{\mathrm{m}})}\right]^{-1} \tag{8}$$

where γ_0 is the interfacial tension of the surfactant free system.

The curve 1 in Fig. 6a and b shows the typical change of the modulus and argument of the complex resistance Z_0 with frequency f, given by Eq. (8). For small frequencies the elastic resistance of the

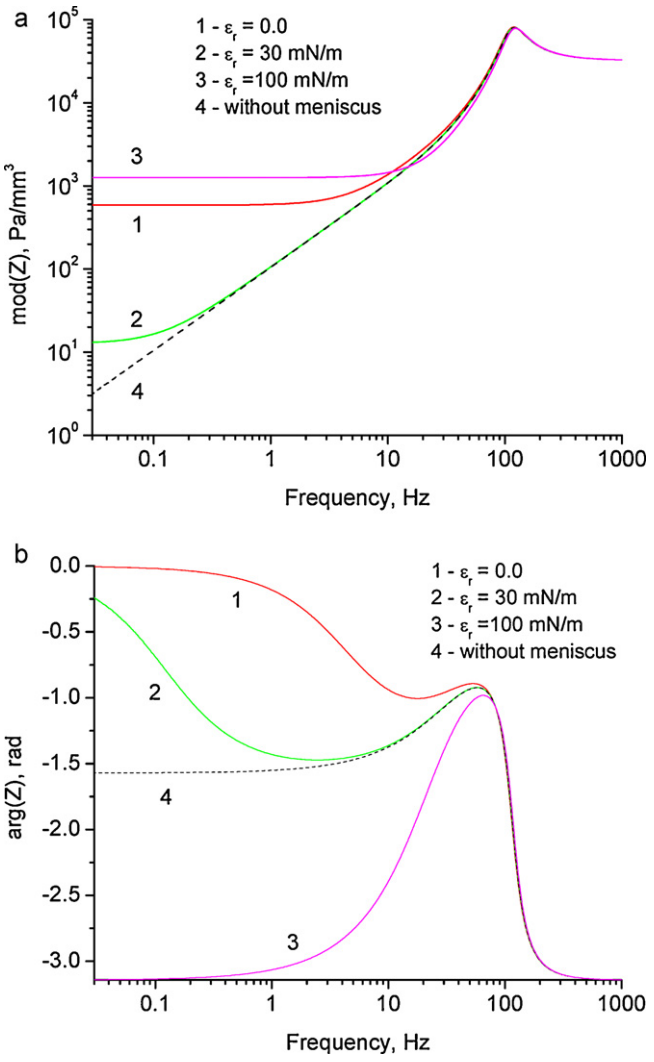

Fig. 6. Modulus (a) and argument (b) of the complex resistance Z calculated as functions of frequency for drop oscillations at different surface elasticities: $\varepsilon_r = 0$, 30, and 100 mN/m ($\eta_d = 0$); drop base radius $a_b = 0.25$ mm, the meniscus height $h_0 = 0.65$ mm, the capillary radius and length $a_C = 0.15$ mm and $l_{ef} = 3.3$ mm, respectively; $B_{ef}/V_A = 3.24 \times 10^4$ Pa/mm^3; the dashed line shows the system response in hydrodynamic experiment in absence of the liquid meniscus, i.e. when the capillary tip is immersed into the liquid.

meniscus Z_m dominates. With increasing frequency the hydrodynamic contribution increases. At high frequencies the contributions of inertia and bulk elasticity become most significant, and we observe a kind of resonance behavior [14].

The curves 2 and 3 in Fig. 6a and b show the effect of surface elasticity given by Eq. (7). At small frequencies, for menisci larger than a hemisphere, the increasing surface elasticity leads first to a compensation of the elastic contribution by the capillary pressure and then to a change in sign of the total resistance Z. The curve 4 in Fig. 6a and b shows the behavior of the modulus and argument of the complex resistance Z in absence of the meniscus, i.e. when we have the same liquid inside and outside of the capillary. These curves allow seeing the system response as determined exclusively by hydrodynamics and bulk elasticity effects.

2.3. Materials

Several experiments have been performed in order to demonstrate the functionality of the presented experimental tool ODBA. For these studies we used aqueous solutions of the anionic surfactant SDS (sodium dodecyl sulfate) and the cationic surfactant CTAB (cetyl trimethyl ammonium bromide), purchased from Sigma/Aldrich and Fluka, respectively, and purified by re-crystallizations. The non-ionic surfactant Span80 (sorbitan monooleate) was prepared as described elsewhere [36]. All aqueous solutions were prepared with Milli-Q water. The hexane was purchased from Fluka and purified with aluminum oxide. The silicone oil was purchased from Dow Corning and had a viscosity of 1000 cSt and a density of 0.986 g/cm^3. All experiments were performed at room temperature of 22–23 °C.

3. Experimental results and discussion

3.1. Interfacial tensions of pure solvent systems

As mentioned above, the most important tests for a correct functioning of dynamic experimental tools for the characterization of interfacial properties are experiments with pure liquids. Although there are publications in which it is claimed that for example the surface tension of pure water against air is dynamic with a relaxation time of few milliseconds [37] it was shown by others that this cannot be true. For example, using the bubble pressure tensiometry for very short times it was quantitatively demonstrated that any dynamic surface tensions of pure water are clear effects of the hydrodynamics of the liquid and of the aerodynamics of the gas passing through the capillary tube [38]. Hence, the surface and interfacial tensions of pure liquids should be constant and their dilational surface and interfacial visco-elasticity should be zero.

Note, the appearance of a dynamic surface tension or a non-zero dilational visco-elasticity is not necessarily a sign for experimental conditions no longer suitable for the dynamic interfacial studies. The presence of surface active impurities can lead to such interfacial properties and it is sometimes not easy to identify their effect on the measured interfacial quantities. What we can be sure about, however, is that for reasonably pure solvents, the amount of impurities should be very small and therefore its adsorption to the interface should take quite a long time. Hence, tests of the experimental technique at fresh drop and bubble surfaces should be the correct condition for the verification of the experimental limits of a dynamic measuring tool.

As example the measured parameters volume V and pressure P are shown in Fig. 7 for a continuously growing water drop in air. The surface tension is obtained from the measured quantities and proofs to be constant, even close to the moments of drop detachment at $t = 93.5$ s and 189 s. Due to the hydrodynamic perturbations

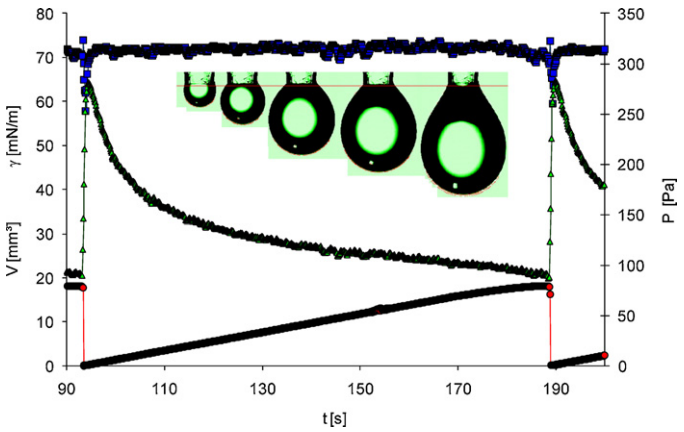

Fig. 7. Change in capillary pressure P (Δ), surface tension γ (□) and drop volume V (○) during a continuously growing drop experiment of water in air; insert – snapshots of the growing drops.

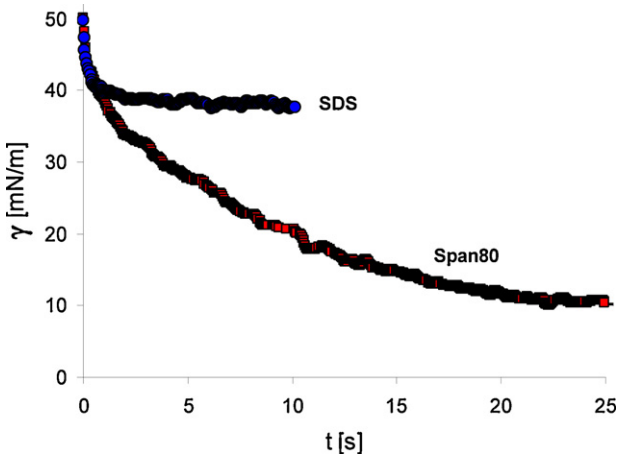

Fig. 8. Dynamic interfacial tension $\gamma(t)$ of 10^{-4} mol/l aqueous solutions of SDS (○) and Span80 (□) against hexane – long adsorption times.

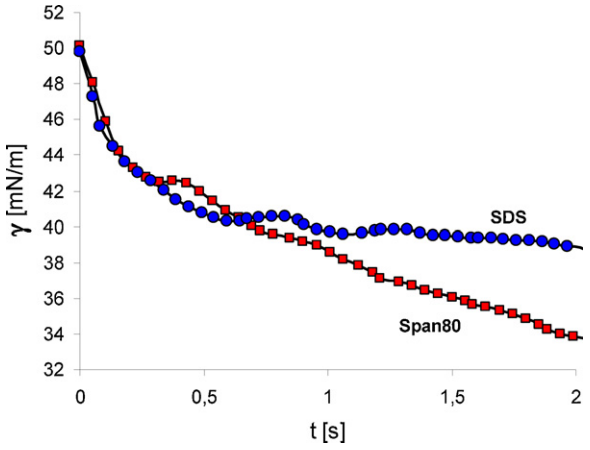

Fig. 9. Dynamic interfacial tension $\gamma(t)$ of 10^{-4} mol/l aqueous solutions of SDS (○) and Span80 (□) against hexane – short adsorption times.

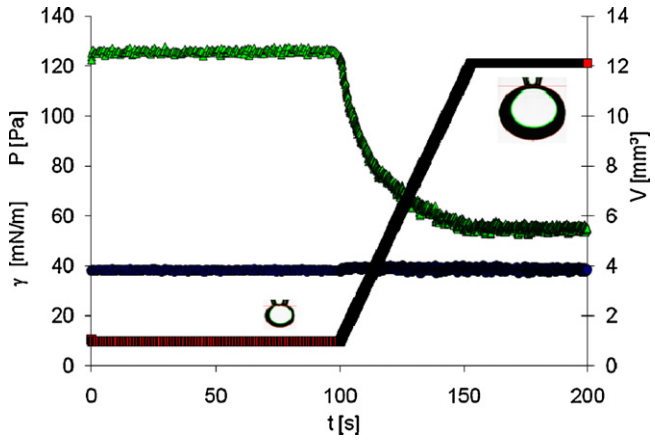

Fig. 10. Change in capillary pressure $P(t)$ (Δ) and the corresponding $\gamma(t)$ (○) as a function of time for a water drop in silicone oil 1000 cSt (density 0.968 g/cm^3) with changing drop size (□).

during the detachment, the values scatter, are mainly lower than the correct value, rather than significantly higher as claimed in [37].

3.2. Dynamic interfacial tensions of surfactant solutions

For studies on the adsorption kinetics of surfactants at liquid interfaces, measurements of the dynamic surface or interfacial

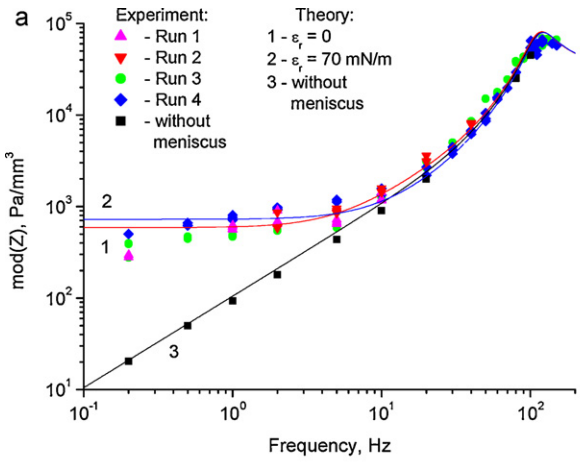

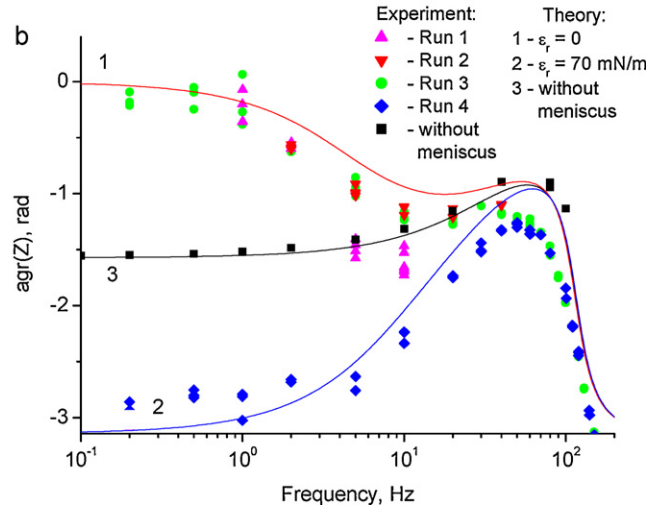

Fig. 11. Modulus (a) and argument (b) of the complex resistance Z as functions of frequency for drop oscillations: Run 1 – 3 pure water drops (different applied amplitudes), Run 4 – drop, containing a surfactant; theoretical curves 1 and 2 are for surface elasticities $\varepsilon_r = 0$ and 70 mN/m, respectively; drop base radius $a_b = 0.25$ mm, meniscus height $h_0 = 0.65$ mm, capillary radius and length $a_C = 0.15$ mm and $l_{ef} = 3.3$ mm, respectively; $B_{ef}/V_A = 3.24 \times 10^4$ Pa/mm^3; experimental data from hydrodynamic experiments without drop and the respective theoretical curves are given for comparison.

tensions are the easiest approach. However, the higher the surfactant concentration is, the shorter is the time needed to establish adsorption equilibrium. In a recent review it was demonstrated how the optimum experimental techniques can be selected for a respective surfactant system and the bulk concentration at which the solutions are to be studied [30]. In Fig. 8 the dynamic interfacial tension $\gamma(t)$ is shown for two surfactants of different surface activity. While the anionic surfactant SDS has a CMC of 8×10^{-3} mol/l in water, the CMC for the non-ionic surfactant Span80 in hexane cannot be defined easily as the interfacial tension values decrease to very low values (less than 5 mN/m) for concentrations above 10^{-4} mol/l.

This difference in surface activity leads to a difference also in the adsorption kinetics, i.e. in the measured dynamic interfacial tensions. The SDS establishes the adsorption equilibrium within a few seconds as one can see from the zoomed data shown in Fig. 9. In contrast, Span80, adsorbing from the hexane phase, at the same bulk concentration and a similar drop size, requires much longer adsorption times and even after 25 s it has not reached the equilibrium state yet. The transfer of surfactant across the interface is negligible for the both mentioned cases regarding the distribution

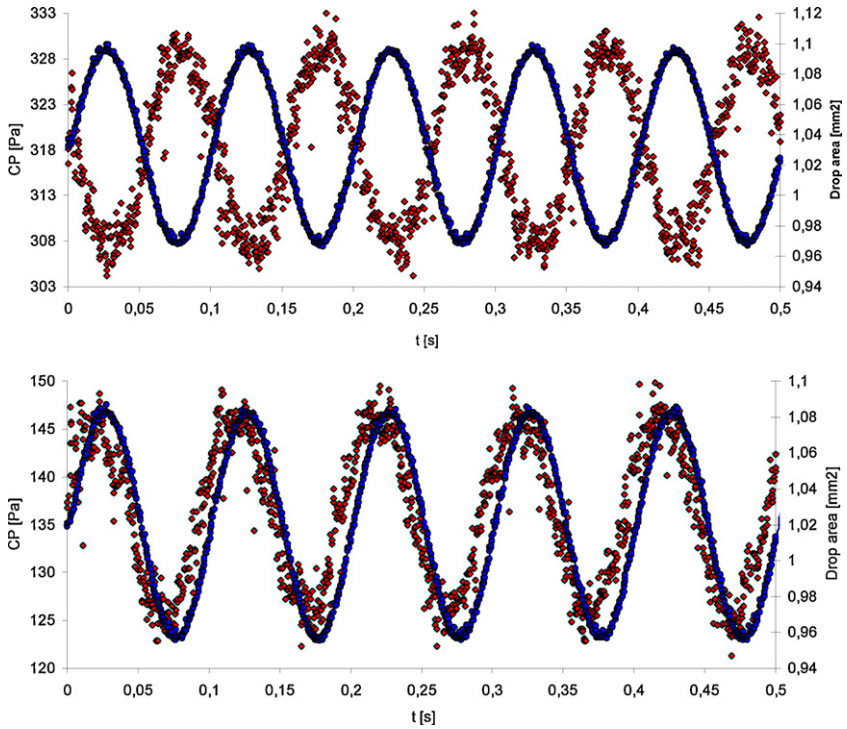

Fig. 12. Drop area $A(t)$ (●) and capillary pressure $P(t)$ (◆) during oscillations of a pure water drop (top) and an aqueous CTAB solution (bottom) in hexane, $V = 0.12$ mm^3, $f = 10$ Hz.

coefficients [7]. For soluble surfactant in both phases this coefficient is an important quantity influencing the kinetics of adsorption and also for the classification of a surfactant as stabilizer for water-in-oil or oil-in-water emulsions, as it is equivalent to the HLB of the respective surfactant (see for example Krugljakov [39]).

The measurement of interfacial tensions between two liquids of a similar density, as it is typically the case in oil recovery processes, is a task that cannot be solved by any other method except capillary pressure tensiometry. An example for an experiment with the almost iso-dense system water/silicone oil is shown in Fig. 10. Note, this system is extraordinarily difficult to study due to the high viscosity of the silicone oil of 1000 cSt. The density difference between water and this oil at room temperature is 0.029 g/cm^3, which makes it difficult to use the drop profile tensiometry.

As we can see from the data in Fig. 10 the interfacial tension is measured accurately for small and large droplets, and only during the growth of the drop, even though very slowly, there is a slight temporary increase in the resulting interfacial tension.

3.3. Oscillating drop experiments

For small frequencies (below 0.2 Hz) oscillating drop experiments can be performed by using drop profile analysis tensiometry [40]. For higher frequencies, say 0.1 Hz up to 100 Hz, drop oscillations can be performed with capillary pressure tensiometry, as was discussed above. The upper limit of 100 Hz is given here for a geometry discussed for the ODBA module in its present configuration. With decreasing capillary diameter, i.e. the radius of the liquid drop, it is possible to perform also experiments at higher frequencies. Note, however, handling smaller droplets will lead to problems of temperature and drop size control which are difficult to solve.

In Fig. 11a and b, experimental data are presented on drop oscillations obtained by using the ODBA at different frequencies. Also data from hydrodynamic experiments without a drop, i.e. with the capillary immersed into the liquid, are shown for comparison. It is seen that the experimental data follow the theoretical predictions discussed above. The phase angle, given by the argument of the complex resistance Z, is more sensitive to the surface viscoelasticity than its modulus, however, the experimental error of its determination is higher.

As example the details of a drop oscillation experiment is shown in Fig. 12. For a pure water drop in pure hexane a phase shift of π is observed which is expected, as the maximum/minimum drop size and capillary pressure appear in opposite moments for drops bigger than a hemispherical size. For a CTAB solution in addition to the changes in drop curvature extra contributions to the capillary pressure values arise due to changes in the surface layer coverage caused by drop surface area expansions and contractions. The observed phase shift between measured capillary pressure $P(t)$ and area $A(t)$ can also be described by the pressure relaxation model described above. In addition, the maximum (or minimum) drop size which correspond to the minimum (or maximum) capillary pressure according to the contribution of the curvature occur close to the moment of change in the direction of the piezo movement which corresponds to a slow drop expansion (or contraction), i.e. less adsorption dynamics effects. This demonstrates that a simple direct data analysis of oscillating drop experiments can lead to erroneous conclusions and only via the shown theory a physically reasonable interpretation of experimental data is possible.

The results of interfacial tension and capillary pressure during drops oscillations for an aqueous 10^{-4} mol/l CTAB solution drop in hexane are shown in Fig. 13, together with the results of the surfactant free system. The obtained results show how the interfacial tension variations increase for the CTAB solution as compared to the pure system, where we can observe only a slight undulation of the $\gamma(t)$ dependence, which should actually be constant during the whole experiment. Note, an oscillation at 10 Hz leads already to slight deformations of the aqueous drop at the given drop volume and for a better quality of such experiment, smaller drops, i.e. a more narrow capillary, would be recommended.

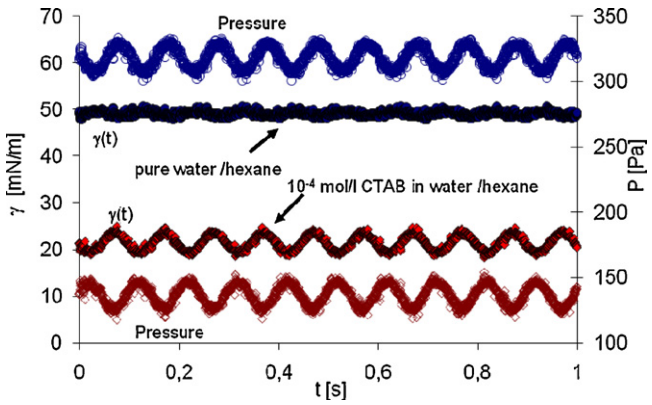

Fig. 13. Capillary pressure $P(t)$ and interfacial tension $(\gamma(t)$ during oscillation of a drop of water and 10^{-4} mol/l aqueous CTAB solution in hexane, $V = 0.12\,mm^3$, $f = 10\,Hz$.

Fig. 14 shows the determined elasticity values (real part) derived from the measured capillary pressure data (corrected for the hydrodynamic contributions) for pure water drop oscillations and also for CTAB10^{-4} mol/l in water against air and hexane, as a function of frequency. In this figure the results of pure water against air and hexane are zero (or very small) up to a certain high frequency (80 Hz) which is an important elementary test for the applicability of the presented experimental set-up and data analysis. For the surfactant solution some unexpected values are observed for the intermediate frequency range (e.g. around 5 Hz) which might be due to some hydrodynamic or wettability problems that appear significant when the elasticity values are expected still small. However the results for high frequencies which is one of the main achievement of this work, appear physically reasonable. Hence, it proofs that the dilational elasticity for liquid–liquid interfaces can be obtained also in the high frequency range by this procedure. A few results by the capillary pressure technique for liquid–liquid interface were recently reported however at low and middle frequencies less than 20 Hz [41]. As shown above in this region the hydrodynamic contribution is yet small and might be neglected (depends on the capillary tip size and geometry and fluids' properties).

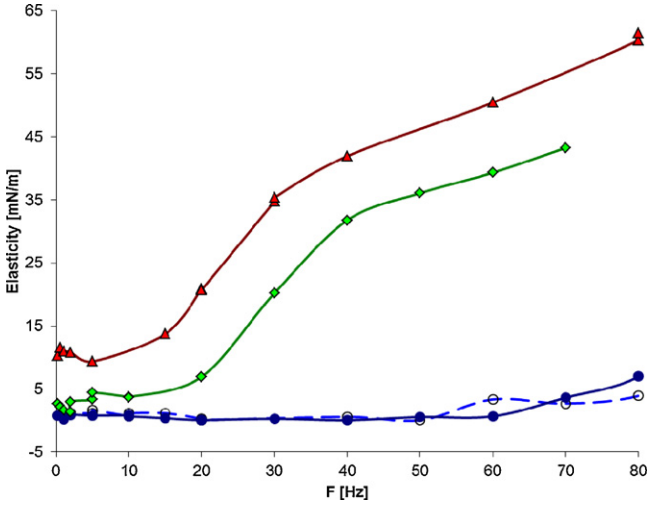

Fig. 14. Determined elasticity values (real part) from measured capillary pressure (corrected with respect to the hydrodynamic contribution) for water drop oscillation against air (●) and hexane (○), and 10^{-4} mol/l aqueous CTAB solution against air ◆ , and against hexane (▲), as a function of frequency.

4. Summary and conclusions

The present paper deals with the functionalities of a new experimental tool, the oscillating drop and bubble analyzer (ODBA). This instrument is based on the capillary pressure technique and was developed for studies of liquid interfaces in particular under fast dynamic conditions. The range of application of the ODBA covers experiments with very fast growing and oscillating drops (or bubbles) and is suitable for studies of gas/liquid and liquid–liquid interfaces. Like all experimental methods, it has certain limitations. To shift the limits of applicability for example to shorter adsorption times and higher oscillation frequencies, smaller droplets will have to be used. Smaller droplets are of course also favorable with respect to the measured higher absolute capillary pressures, however, it entails new technical problems. First of all it is quite difficult to handle accurately very small amounts of liquids by simple dosing systems, such as syringes or piezo translators. In addition, smaller drops require more narrow capillaries which cause much higher hydrodynamic effects. Obviously, there is an optimum capillary tip size and design according to which the hydrodynamic effects are acceptable and quantitatively understood. At the presented experimental conditions we are able to describe the hydrodynamic effect by a model so that drop oscillation experiments are feasible for frequencies up to about 80 Hz (e.g. Fig. 14).

It can also be stated that this technique is an excellent tool to measure the dynamic interfacial tension of liquid–liquid interfaces, even when the densities of the two fluids are similar. The shortest adsorption times reached are about 10^{-2} s, shown for example in Fig. 9 for two surfactant solutions. This limit can be further decreased by a modification of the pressure data recording protocol. For the protocol of continuously growing drops a better quantitative analysis of the resulting data via the theory of Macleod and Radke [42] or an even more refined approach is required. An advanced CFD simulation would give access to a full understanding of all processes happening in and around a drop and at its interface.

Acknowledgements

The work was financially supported by projects of the European Space Agency (ESA MAP FASES AO-99-052 and PASTA), the Deutsche Luft- und Raumfahrt (DLR 50WM1129), the Deutsche Forschungsgemeinschaft SPP 1506 (Mi418/18-1) and the Bundesministerium für Bildung, Wissenschaft, Forschung und Technologie (UKR 10/039).

References

[1] H.P. Schuchmann, Th. Danner, Chemie-Ingenieur-Technik 76 (2004) 364.
[2] V. Schadler, E.J. Windhab, Desalination 189 (2006) 130.
[3] D. Langevin, Chem. Phys. Chem. 9 (2008) 510.
[4] Th.F. Tadros (Ed.), Emulsion Science and Technology, Wiley-VCH, 2009.
[5] M. Buzzacchi, P. Schmiedel, W. von Rybinski, Colloids Surfaces A 273 (2006) 47.
[6] K. Malysa, K. Lunkenheimer, R. Miller, Mater. Sci. Forum 25 (1988) 555.
[7] A. Javadi, J. Krägel, P. Pandolfini, G. Loglio, V.I. Kovalchuk, E.V. Aksenenko, F. Ravera, L. Liggieri, R. Miller, Colloids Surfaces A 365 (2010) 62.
[8] V.I. Kovalchuk, F. Ravera, L. Liggieri, G. Loglio, P. Pandolfini, A.V. Makievski, S. Vincent-Bonnieu, J. Krägel, A. Javadi, R. Miller, Adv. Colloid Interface Sci. 161 (2010) 102.
[9] J.M. Soos, K. Koczo, E. Erdos, D.T. Wasan, Rev. Sci. Instrum. 65 (1994) 3555.
[10] V.I. Kovalchuk, A.V. Makievski, J. Krägel, P. Pandolfini, G. Loglio, L. Liggieri, F. Ravera, R. Miller, Colloids Surfaces A 261 (2005) 115.
[11] D. Georgieva, A. Cagna, D. Langevin, Soft Matter 5 (2009) 2063.
[12] H. Bianco, A. Marmur, J. Colloid Interface Sci. 158 (1993) 295–302.
[13] E.H. Lucassen-Reynders, J. Lucassen, Surface dilational rheology: past and present, in: R. Miller, L. Liggieri (Eds.), Interfacial Rheology, vol. 1: Progress in Colloid and Interface Science, Brill Publ., Leiden, 2009, pp. 40–78.
[14] V.I. Kovalchuk, J. Krägel, A.V. Makievski, G. Loglio, F. Ravera, L. Liggieri, R. Miller, J. Colloid Interface Sci. 252 (2002) 433.
[15] L. Del Gaudio, P. Pandolfini, F. Ravera, J. Krägel, E. Santini, A.V. Makievski, B.A. Noskov, L. Liggieri, R. Miller, G. Loglio, Colloids Surfaces A 323 (2008) 3.

[16] F. Ravera, G. Loglio, P. Pandolfini, E. Santini, L. Liggieri, Colloids Surfaces A 365 (2010) 2.
[17] S.C. Russev, N. Alexandrov, K.G. Marinova, K.D. Danov, N.D. Denkov, L. Lyutov, V. Vulchev, C. Bilke-Krause, Rev. Sci. Instrum. 79 (2008) 104102–104111.
[18] See more information at www.sinterface.com.
[19] Surfactants – chemistry, interfacial properties and application, in: V.B. Fainerman, D. Möbius, R. Miller (Eds.), in: Studies in Interface Science, vol. 13, Elsevier, 2001.
[20] S.A. Zholob, V.I. Kovalchuk, A.V. Makievski, J. Krägel, V.B. Fainerman, R. Miller, Determination of the dilational elasticity and viscosity from the surface tension response to harmonic area perturbations, in: R. Miller, L. Liggieri (Eds.), Interfacial Rheology, vol. 1: Progress in Colloid and Interface Science, Brill Publ., Leiden, 2009, pp. 77–102.
[21] V.B. Fainerman, A.V. Makievski, R. Miller, Rev. Sci. Instrum. 75 (2004) 213.
[22] V.I. Kovalchuk, F. Ravera, L. Liggieri, G. Loglio, A. Javadi, N.M. Kovalchuk, J. Krägel, Studies in capillary pressure tensiometry and interfacial dilational rheology, in: R. Miller, L. Liggieri (Eds.), Bubble and Drop Interfaces, vol. 2: Progress in Colloid and Interface Science, Brill Publ., Leiden, 2011, p. 143.
[23] T. Horozov, L. Arnaudov, J. Colloid Interface Sci. 222 (2000) 146.
[24] A. Javadi, M. Karbaschi, J. Krägel, N.M. Kovalchuk, E. Bonaccurso, L.Q. Chen, R. Miller, Drop Pinch-Off quantified by a fast video technique and capillary pressure measurements, in preparation.
[25] R. Miller, M. Bree, V.B. Fainerman, Colloids Surfaces A 142 (1998) 237.
[26] G. Kretzschmar, K. Lunkenheimer, Ber. Bunsenges. Phys. Chem. 74 (1970) 1064.
[27] B.A. Noskov, Curr. Opin. Colloid Int. Sci. 15 (2010) 229.
[28] R. Miller, R. Sedev, K.-H. Schano, Ch. Ng, A.W. Neumann, Colloids Surfaces A 69 (1993) 209.
[29] J. Benjamins, A. Cagna, E.H. Lucassen-Reynders, Colloids Surfaces A 114 (1996) 245.
[30] N. Mucic, A. Javadi, N.M. Kovalchuk, R. Miller, Adv. Colloid Interface Sci. 168 (2011) 167.
[31] A. Javadi, M. Karbaschi, J Krägel, N.M. Kovalchuk, V.I. Kovalchuk, E. Bonaccurso, L.Q. Chen, R. Miller, Limits of harmonic drop oscillations quantified by a fast video technique, in preparation.
[32] V.I. Kovalchuk, J. Krägel, E.V. Aksenenko, G. Loglio, L. Liggieri, Oscillating bubble and drop techniques, in: D. Möbius, R. Miller (Eds.), Novel Methods to Study Interfacial Layers, Studies in Interface Science, vol. 11, Elsevier, Amsterdam, 2001, p. 485.
[33] V.I. Kovalchuk, J. Krägel, A.V. Makievski, F. Ravera, L. Liggieri, G. Loglio, V.B. Fainerman, R. Miller, J. Colloid Interface Sci. 280 (2004) 498.
[34] N. Alexandrov, K.G. Marinova, K.D. Danov, I.B. Ivanov, J. Colloid Interface Sci. 339 (2009) 545.
[35] V.I. Kovalchuk, E.K. Zholkovskij, J. Krägel, R. Miller, V.B. Fainerman, R. Wüstneck, G. Loglio, S.S. Dukhin, J. Colloid Interface Sci. 224 (2000) 245.
[36] V.B. Fainerman, A.V. Makievski, D. Vollhardt, S. Siegel, R. Miller, J. Phys. Chem. B 103 (1999) 330.
[37] N.N. Kochurova, A.I. Rusanov, J. Colloid Interface Sci. 81 (1981) 297.
[38] V.B. Fainerman, V.D. Mys, A.V. Makievski, R. Miller, Langmuir 20 (2004) 1721.
[39] P.M. Kruglyakov, Hydrophile–lipophile balance of surfactants and solid particles: physicochemical aspects and applications, in: D. Möbius, R. Miller (Eds.), Studies in Interface Science, vol. 9, Elsevier, 2000.
[40] M.E. Leser, S. Acquistapace, A. Cagna, A.V. Makievski, R. Miller, Colloids Surfaces A 261 (2005) 25.
[41] E. Santini, L. Liggieri, L. Sacca, D. Clausse, F. Ravera, Colloids Surfaces A 309 (2007) 270.
[42] C.A. MacLeod, C.J. Radke, J. Colloid Interface Sci. 166 (1994) 73.

Paper VII

Dynamic properties of CnTAB adsorption layers at the water/oil interface

N. Mucic, N.M. Kovalchuk, V. Pradines, A. Javadi, E.V. Aksenenko, J. Krägel and R. Miller

Colloids and Surfaces A, submitted 2012

Dynamic properties of C_nTAB adsorption layers at the water/oil interface

N. Mucic[1]*, N.M. Kovalchuk[1,2], V. Pradines[3], A. Javadi[1], E.V. Aksenenko[4], J. Krägel[1] and R. Miller[1]

[1] Max Planck Institute of Colloids and Interfaces, 14424 Potsdam/Golm, Germany
[2] Institute of Bio-Colloid Chemistry, 03142 Kiev, Ukraine
[3]Laboratoire de Chimie de Coordination, 31077 Toulouse cedex 04, France
[4] Institute of Colloid Chemistry and Chemistry of Water, 252680 Kiev, Ukraine

Abstract

The dynamic interfacial tension and dilational rheology of alkyltrimethylammonium bromides (C_nTAB) solutions are studied for n = 10, 12, 14 and 16 using drop profile analysis and capillary pressure tensiometry. The experimental data are analyzed on the basis of two theoretical models, the Frumkin Ionic Compressibility and the Langmuir Compressibility models [1]. We show that even the simplified Langmuir Compressibility model is able to adequately describe the dynamic properties of the investigated ionic surfactants. Dynamic experiments point out the difficulties related to short chain surfactants due to their very fast adsorption kinetics which cannot be studied with conventional tensiometer setups.

Keywords: Dynamic interfacial tension, dilational rheology, drop profile analysis tensiometry, capillary pressure tensiometry, cationic surfactants, alkyltrimethylammonium bromide, thermodynamic models, water/hexane interface

*corresponding author: mucic@mpikg.mpg.de

Introduction

Although the adsorption layers of surfactants at water/oil interfaces are of great practical importance, until now this area has not been widely studied. This is not a case with the adsorption layers at water/air interface for which the thermodynamic, kinetic and rheological properties are well described, from a theoretical as well as from an experimental point of view. For example, for the very popular homologous series of the cationic surfactants alkyltrimethylammonium bromides (C_nTAB) a comprehensive analysis at the water/air interfcae was presented recently [2], however, there is no equivalent quantitative work for a water/oil interface published in literature yet. Therefore, in this paper we will focus on the adsorption layer properties of this homologous series of cationic surfactant at the water/oil (hexane) interface.

As a pioneer Medrzycka started investigations of the adsorption of these surfactants at water/oil interfaces [3]. Recently, additional work was published for this and other groups of surfactants [1, 4, 5]. Additional input for the understanding of the molecular interactions between surfactants and oil molecules was achieved from investigations at the interface between aqueous surfactant solutions and oil vapor phases [6, 7].

As compared to the water/air interface, the water/hexane interface appears more attractive for surfactant molecules due to the direct interaction with the oil molecules. Therewith, the water/hexane interface is more favorable for surfactants' adsorption and thus adsorption effects are observed at concentrations much lower than at the water/air interface. Beside this, it is found that the hexane molecules intercalate into the adsorption layer of short alkyl chain surfactants i.e. C_{10}TAB and SDeS, while this is not the case for surfactants of longer alkyl chains [1,4].

The dilational rheology is a method of great importance in analyzing the dynamic properties of molecules at liquid surfaces because, beside adsorption, it takes into account also desorption of molecules from the surface. First publications was released in the sixties of the last century [8, 9]. With time the method has been improved. More about its modern applications can be found elsewhere [10, 11].

In the present study, we have combined the dilational rheology with dynamic interfacial tension measurements in order to quantitatively understand the dynamic behaviour of CnTAB surfactants at the water/hexane interface. As theoretical models for interpretation of the experimental results we have used the Langmuir Compressibility and the Frumkin Ionic Compressibility models, discussed earlier in [12, 1]. For the fitting of the thermodynamic results the Frumkin Ionic Compressibility model shows good agreement. It turns out that also the simplified Langmuir Compressibility model describes our data adequately so that we prefer this slight less complex model for the data analysis.

Materials and methods

All aqueous surfactants solutions were freshly prepared prior to the experiment by dilution from a stock solution. The stock solutions of the respective surfactants were prepared in phosphate buffer 10mM, pH 7, NaH_2PO_4/Na_2HPO_4 (Fluka, >99%) using ultrapure MilliQ water (resistivity = 18.2 MΩcm). Note, the phosphate buffer was used because this work is part of a large investigation program on the equilibrium and dynamic properties of protein – C_nTAB mixtures at the water/hexane interface, which require buffer solutions. The surfactants decyl trimethylammonium bromide C_{10}TAB (MW = 280.29 g/mol, ≥ 98%), dodecyl trimethylammonium bromide C_{12}TAB (MW = 308.35 g/mol, ≥ 99%), hexadecyl trimethylammonium bromide C_{16}TAB (MW = 364.46 g/mol, ≥99%) were purchased from Fluka (Switzerland), and tetradecyl trimethylammonium bromide C_{14}TAB (MW = 336.40 g/mol, 99%) was purchased from Aldrich. All experiments were performed at room temperature (22 °C). Hexane was purchased from Fluka (Switzerland). Before use it was distilled and purified with aluminium

oxide and subsequently saturated with ultrapure MilliQ water. The interfacial tension of the pure water/hexane interface (with both liquid phases mutually saturated) at room temperature was 51.1 mN/m.

The experimental setups used to obtain the adsorption kinetics of the surfactant solutions against hexane were the drop Profile Analysis Tensiometer PAT-1 and the Capillary Pressure Analyzer ODBA-1, both products of SINTERFACE Technologies, Berlin, Germany. The visco-elasticity of the corresponding adsorption layers was determined from the interfacial tension response to sinusoidal drop area perturbations using PAT-1 close to the equilibrium when the interfacial tension reach a plateau (of the order of max. 10^4 s). The configuration of these experiments was a drop of aqueous solution formed in a glass cuvette containing the pure hexane phase.

Theory

Theoretical description of adsorption kinetics is performed using the free software package SphereSQ [13]. The software is based on the Fick's equation and enables the direct simulations of diffusion controlled adsorption kinetics on spherical interface between two liquid phases. It implements several adsorption models, such as reorientation models and Frumkin models for ionic and non-ionic surfactants taking into account intrinsic compressibility of adsorption layer. The detailed description of the calculation method is given elsewhere [14]. Isotherm parameters are obtained from simultaneous fitting of measured dependence of equilibrium interfacial tension and experimental data on surface rheology by means of free software package IsoFit [15].

One of the first adsorption models was proposed by Langmuir [16]. Although it was originally derived to describe the gas adsorption at solid surfaces, the Langmuir model is also successfully applied to the adsorption of surfactant molecules at liquid interfaces. This is at least acceptable when a semi-quantitative analysis is needed. However, we will focus our discussion here mostly on the Langmuir model and compare it partially with its more general version, i.e. the Frumkin model. The Frumkin model assumes additional intermolecular interactions in the adsorption layer.

The adsorption isotherm for the Langmuir model [17] reads:

$$\Gamma(t) = \Gamma_\infty \frac{bc}{1+bc} \tag{1}$$

and the corresponding von Szyszkowski-Langmuir equation of state has the form:

$$\gamma_0 - \gamma = \Pi = -RT\Gamma_\infty \ln\left(1 - \frac{\Gamma}{\Gamma_\infty}\right) = RT\Gamma_\infty \ln(1+bc). \tag{2}$$

Here γ_0 is the interfacial tension in absence of surfactants, γ is the interfacial tension at the surfactant bulk concentration c, Π is the surface pressure, R and T are gas law constant and absolute temperature, respectively, Γ is the surface concentration, Γ_∞ is the maximum adsorption, and b is the adsorption constant with the dimension of a reciprocal concentration.

The adsorption behaviour of most non-ionic and ionic surfactants is well described by the Frumkin model, because it considers the additional lateral interactions between adsorbed surfactant molecules at the interface. The adsorption isotherm and equation of state, respectively, of the Frumkin Ionic Compressibility adsorption model was proposed by Pradines et al. for the analysis of the equilibrium adsorption behaviour of C_nTABs and is given as follows [1]:

$$b\left[c\left(c+c_2\right)\right]^{1/2} f = \frac{\theta}{1-\theta}\exp\left(-2a\theta\right) \tag{3}$$

$$\Pi = -\frac{2RT}{\omega_0}\left[\ln(1-\theta) + \alpha\theta^2\right]. \tag{4}$$

Here $\theta = \omega \cdot \Gamma$ is the surface coverage, f is the mean activity coefficient of ions in the bulk solution, and c_2 is the inorganic (1:1) salt concentration. The pre-factor 2 in Eq. (4) takes into account the presence of the counter ions. For short-range interactions the Debye-Hückel equation corrects accurately the values of the average activity coefficient f:

$$\log f = -\frac{0.5115\sqrt{I}}{1+1.316\sqrt{I}} + 0.055\, I \tag{5}$$

where $I = c + c_2$ is the ionic strength expressed in mol/l. The given numerical constants correspond to a temperature of 25°C [18].

The phosphate buffer used in this study is a mixture of the two substances NaH_2PO_4 and Na_2HPO_4 each having its own dissociation constant, i.e. it is not a 1:1 electrolyte mentioned above and, therefore eqs. (3)-(5) are, strictly speaking not applicable in this case. It was, however, shown in [1] that using an effective electrolyte concentration of 0.002 M enables a very good fitting of the experimental isotherms for the surfactant series C_{10}TAB-C_{16}TAB for both water/air and water/hexane interfaces. Therefore, in this study we use the same effective buffer concentration of 0.002 M.

The molar area ω can be constant or dependent on Π, as it was shown for example by Fainerman et al. [12]:

$$\omega = \omega_0(1 - \varepsilon\Pi\theta) \tag{6}$$

where ω_0 is the molar area at Π = 0, ε is the two-dimensional relative surface layer compressibility coefficient. ε characterises the intrinsic compressibility of the molecules in the surface layer and it can be understood for example as change in the tilt angle of adsorbed molecules with increasing the surface coverage [19].

Another important concept for characterising the adsorption dynamics is the surface dilational visco-elasticity. It displays the response of the interfacial tension on the compression or expansion of the interfacial area [20]:

$$E = \frac{d\gamma}{d\ln\Gamma}\frac{d\ln\Gamma}{d\ln A}. \tag{7}$$

For a diffusional exchange of matter Lucassen and van den Tempel [21, 22] have presented the modulus as a complex quantity:

$$E(i\omega) = E' + iE'' = E_0\frac{\sqrt{i\omega}}{\sqrt{i\omega}+\sqrt{2\omega_0}} \tag{8}$$

where ω is the radial frequency $\omega = 2\pi f$. Here f is the frequency in Hz, E' and E'' are the real and imaginary parts of E, corresponding to the elastic and viscous parts, respectively, of the dilational visco-elasticity:

$$E'(\omega) = E_0\frac{1+\sqrt{\omega_0/\omega}}{1+2\sqrt{\omega_0/\omega}+2\,\omega_0/\omega} \tag{9}$$

$$E''(\omega) = E_0\frac{\sqrt{\omega_0/\omega}}{1+2\sqrt{\omega_0/\omega}+2\,\omega_0/\omega}. \tag{10}$$

The parameter ω_0 is the characteristic frequency of the diffusional matter exchange:

$$\omega_0 = \frac{D}{2}\left(dc/d\Gamma\right)^2. \tag{11}$$

and

$$E_0 = -\frac{d\gamma}{d\ln\Gamma} \tag{12}$$

is the limiting (high frequency) elasticity.

Results and discussion

Recently we have shown [23] that each surfactant has a characteristic adsorption time range in which the adsorption can be followed by measuring the dynamic surface tension. Therefore, there are limitations regarding the instruments suitable for such experiments. Combining two techniques, drop profile analysis and capillary pressure tensiometry, we were able to obtain the adsorption kinetics just for C_{16}TAB and C_{14}TAB. For the shorter chains C_{12}TAB and C_{10}TAB more or less just the equilibrium interface tension values can be measured. Any fitting with a kinetic adsorption model of experimental curves without significant changes in adsorption with time could lead to unrealistic diffusion coefficients D. Reasonable values of the diffusion coefficient for single alkyl chain surfactants are expected in the range between 10^{-10} m^2/s and 10^{-9} m^2/s.

In Fig. 1 the dynamic interfacial tensions are shown for C_{16}TAB solutions as measured by PAT-1 and ODBA. The curves are fitted with the Frumkin Ionic Compressibility and the Langmuir Compressibility models, both based on diffusion controlled adsorption kinetics. The difference between the experimental and theoretical curves after long time (at equilibrium) is because the studied surfactant concentrations are rather small and depletion of the surfactant has to be accounted for. Unfortunately it was impossible for us to find exact equilibrium concentrations corresponding to the used initial concentrations of the surfactant in solution, especially at small concentrations.

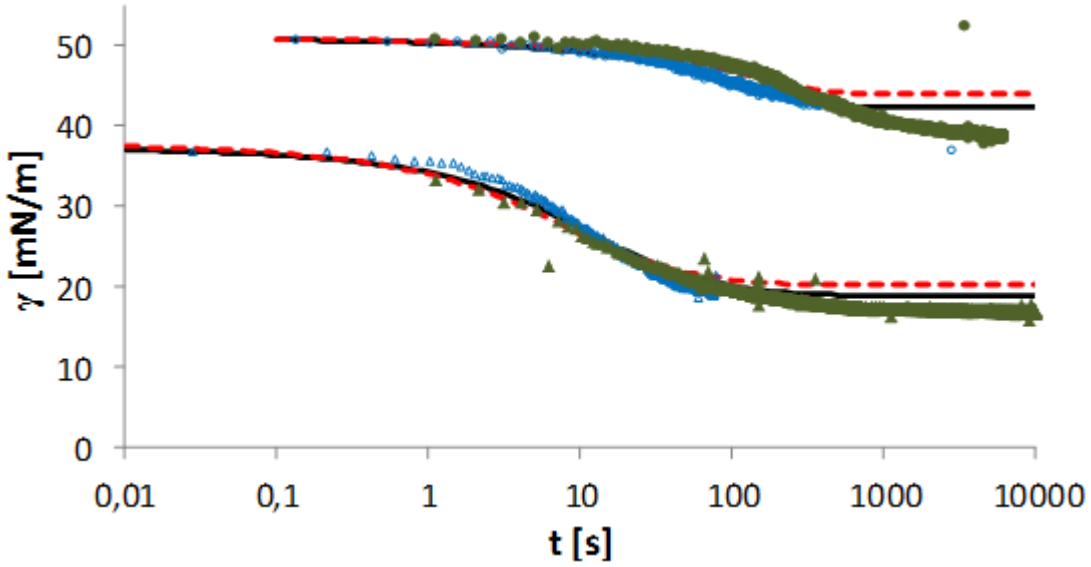

Figure 1. The dependence of the interfacial tension γ for C_{16}TAB on the time t, empty symbols present the data obtained by ODBA-1 and filled symbols by PAT-1, (○,●) $c=5\times10^{-6}$ mol/l, (△,▲) $c=2\times10^{-5}$ mol/l. Solid and dashed lines present the Frumkin Ionic Compressibility and Langmuir Compressibility models curves, respectively, calculated using the fitting parameters summarized in Table 1.

In Fig. 2 the dynamic interfacial tension data are shown for C_{14}TAB solutions as measured with PAT-1 and ODBA, again fitted with diffusion controlled adsorption models.

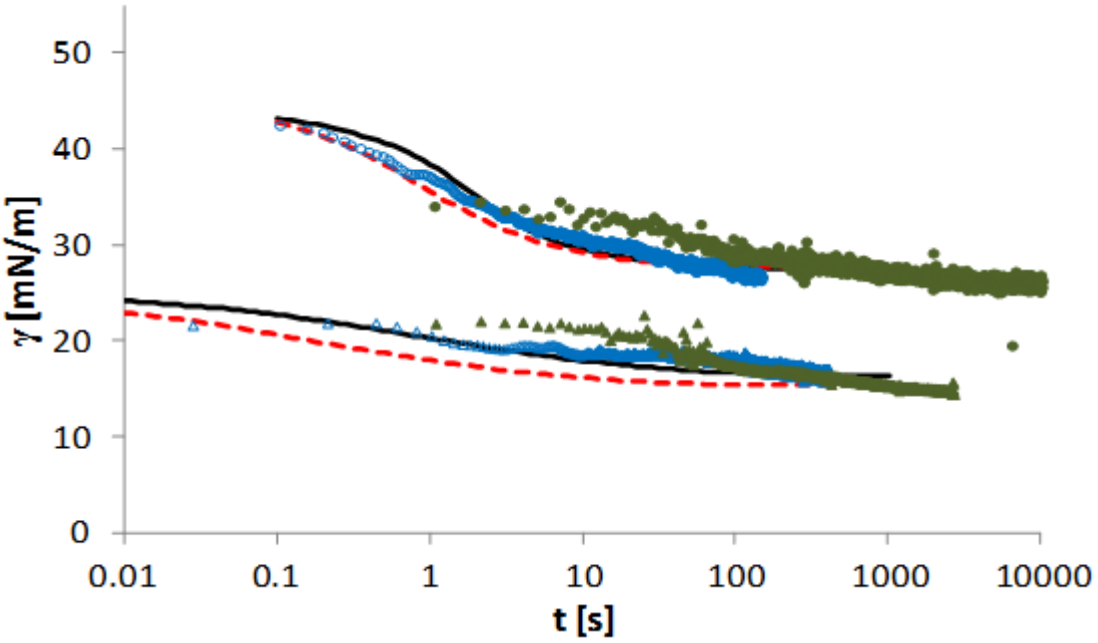

Figure 2. The dependence of the interfacial tension γ for C_{14}TAB on the time t, empty symbols present the data obtained by ODBA-1 and filled symbols by PAT-1, (○,●) c=7×10^{-5} mol/l, (△,▲) c=5×10^{-4} mol/l. Solid and dashed lines present the Frumkin Ionic Compressibility and Langmuir Compressibility models curves, respectively, calculated using the fitting parameters summarized in Table 1.

The offset of the interfacial tension from the value of a pure water/hexane interface (51.1 mN/m) at the beginning of the adsorption curves is caused by a respective initial amount of surfactants already present at the interface before the measurement starts at time t=0. This is due to the technical characteristics of the instruments used. For example, the PAT-1 starts measurements after 1 s while the ODBA can gain data from 0.01 s on. Comparing these times with the expected adsorption times of C_{16}TAB (c=2×10^{-5} mol/l) and C_{14}TAB (c=7×10^{-5} mol/l), 7×10^{-3} s and 5×10^{-3} s, respectively, it is obvious from Fig. 2 that the available instrument cannot fulfil the required times for gaining the whole adsorption kinetic curve, i.e. is able to start the measurements with a really fresh interface [23]. The expected adsorption time is a characteristic of the given surfactant at a specific concentration and can be estimated from the diffusion relaxation time as defined by Joos in [24]. However, it is not necessary to have the whole curve to successfully fit the experimental data by a theoretical model. Most important is that a major part of the dynamic interfacial tensions are available before reaching the equilibrium.

In Figs. 3 and 4 the dynamic interfacial tension data are presented for three solutions each of C_{12}TAB and C_{10}TAB, respectively, and the curves fitted with the Frumkin Ionic Compressibility model assuming diffusion controlled adsorption mechanism. On a first glance the fitting looks good but it leads to unrealistic diffusion coefficients (see Table 1)

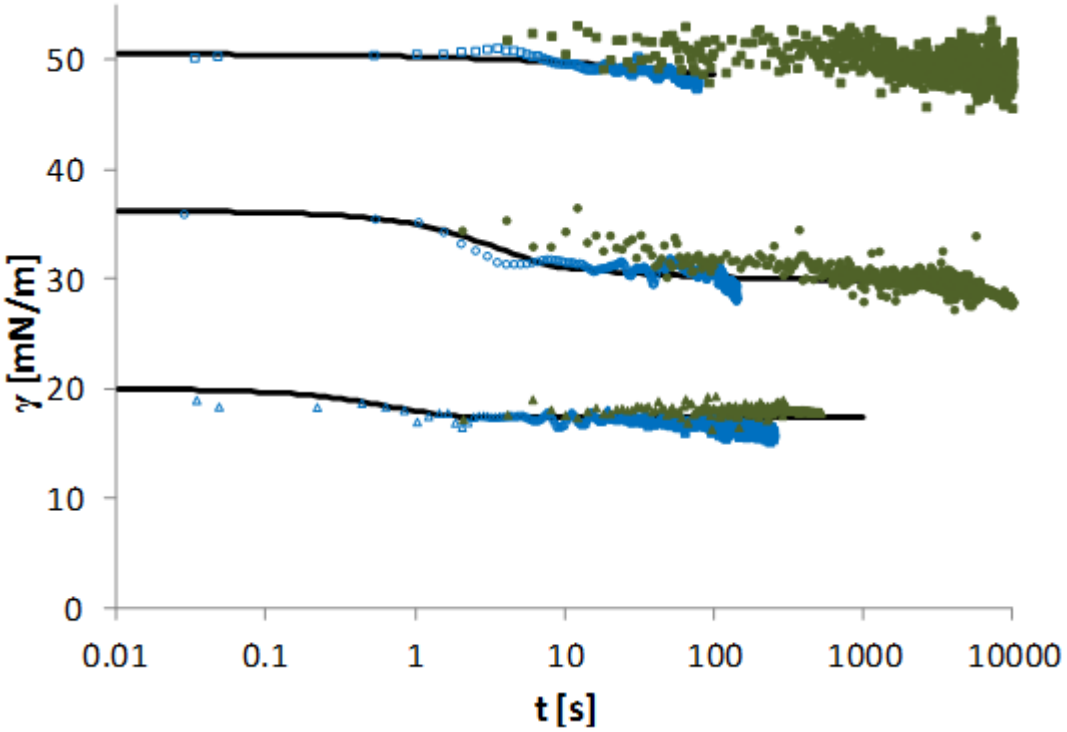

Figure 3. The dependence of the interfacial tension γ for C_{12}TAB on time t, empty symbols present the data obtained by ODBA-1 and filled symbols by PAT-1, (□,■) $c=1\times10^{-5}$ mol/l, (○,●) $c=7\times10^{-4}$ mol/l, (△,▲) $c=7\times10^{-3}$ mol/l. Solid line presents the Frumkin Ionic Compressibility model curves, calculated using the fitting parameters summarized in Table 1.

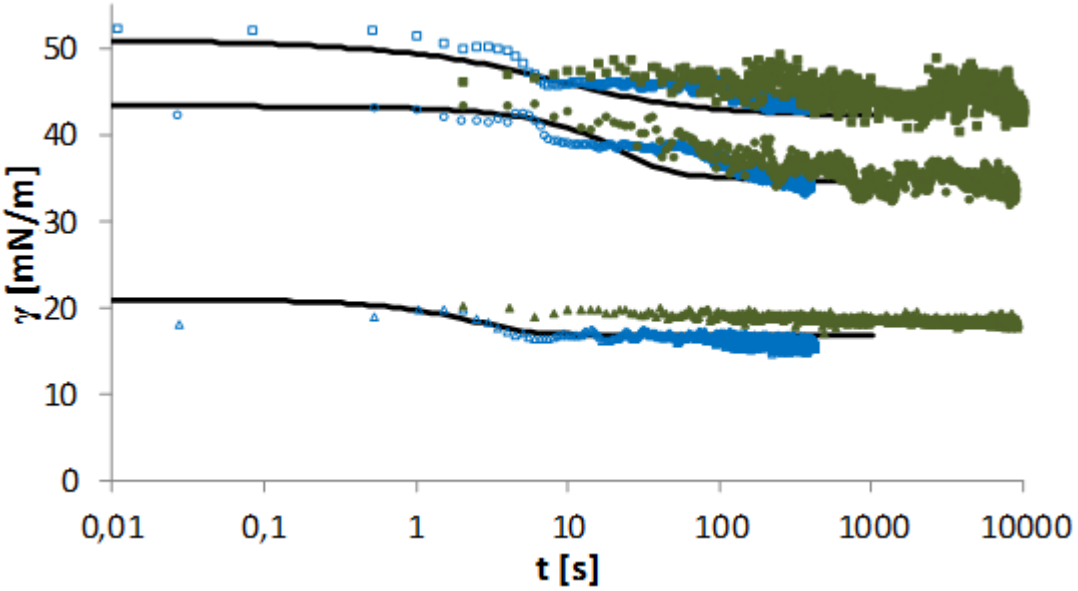

Figure 4. The dependence of the interfacial tension γ for C_{10}TAB on the time t, empty symbols present the data obtained by ODBA-1 and filled symbols by PAT-1, (□,■) $c=1\times10^{-4}$ mol/l, (○,●) $c=3\times10^{-3}$ mol/l, (△,▲) $c=3\times10^{-2}$ mol/l. Solid line presents the Frumkin Ionic Compressibility model curves, calculated using the fitting parameters summarized in Table 1.

As it is seen from the Figs. 3 and 4 for the studied solutions the data are already close to the equilibrium thermodynamic state and no significant effect of transport of surfactants from the bulk

to the interface is yet visible. Therefore, it is impossible to get appropriate information on the kinetic model via any fitting process.

In Fig. 5a the dilational visco-elastic modulus $|E| = \sqrt{E'^2 + E''^2}$ of C_{16}TAB adsorption layers at the water/hexane interface is presented as a function of the surfactant bulk concentration c. In Fig. 5b we see the results of fitting of the experimental curves with the Frumkin Ionic Compressibility and the Langmuir Compressibility models, respectively, by using the model parameters given in Table 1.

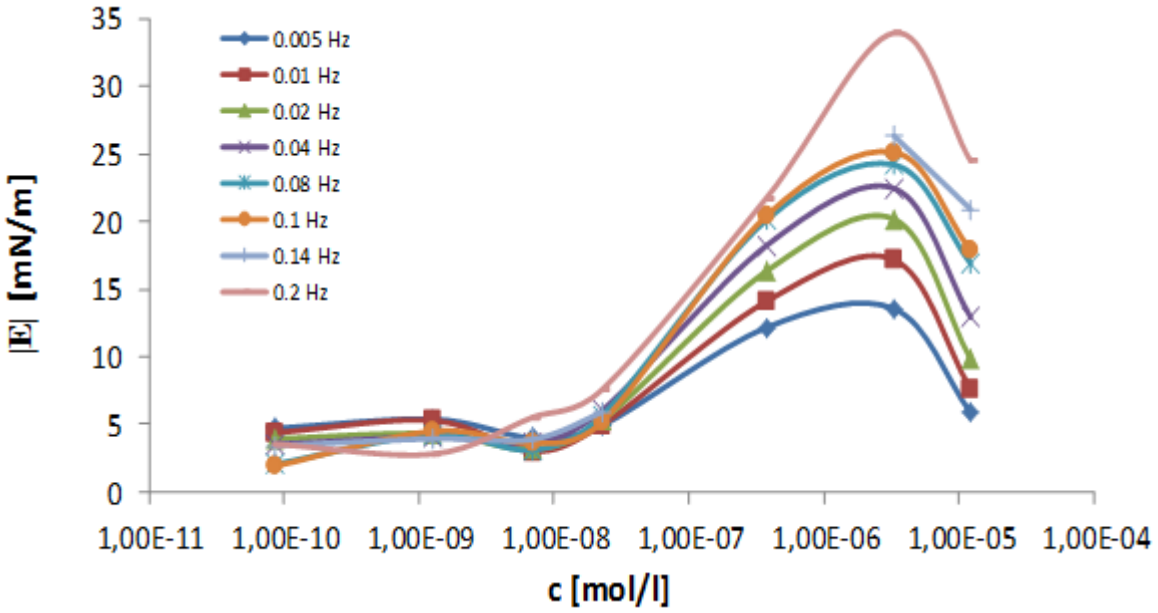

Figure 5a. The dependence of the visco-elastic modulus |E| of the C_{16}TAB adsorption layer at water/hexane interface on the bulk concentration c, different frequencies of the interfacial area oscillations are given in the legend of the chart.

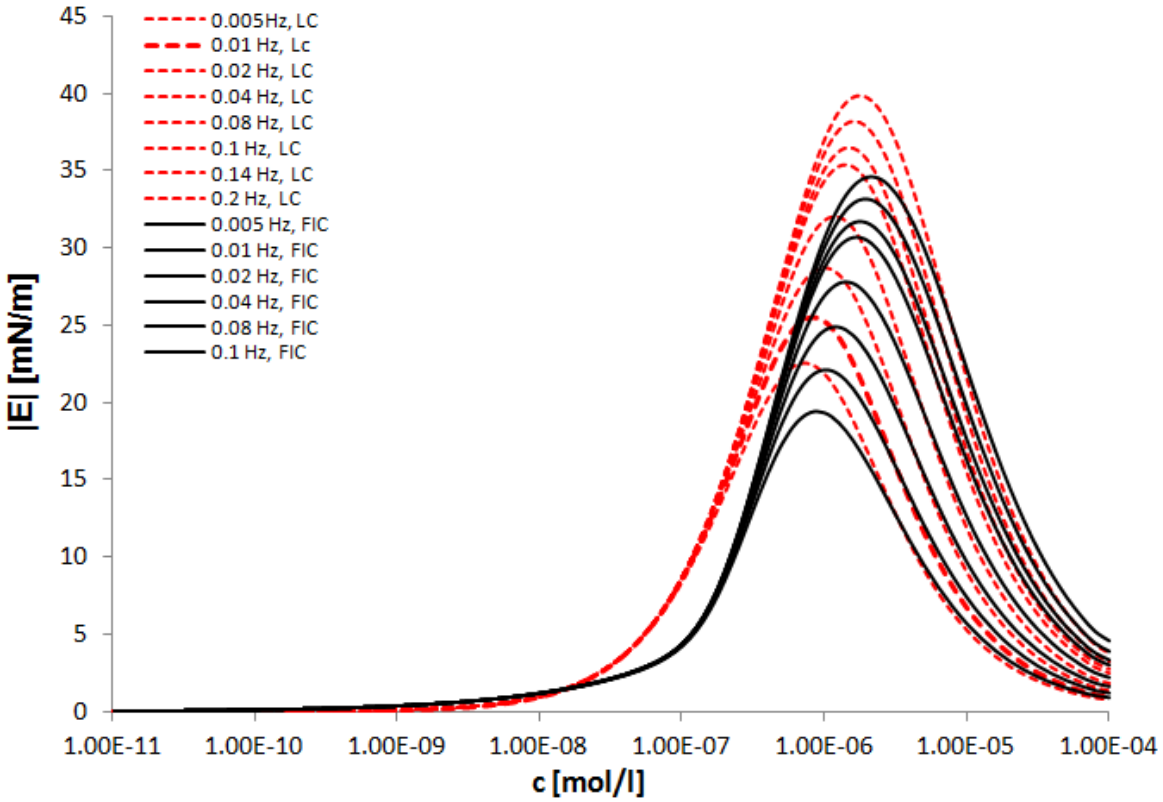

Figure 5b. Theoretical curves of the C_{16}TAB dilational rheology calculated from the Frumkin Ionic Compressibility model (solid line) and the Langmuir Compressibility model (dashed line) using parameters of Table 1, different frequencies of the interfacial area oscillations are given in the legend of the chart.

In Fig. 6a we present analogue data on the dilational visco-elastic modulus of C_{14}TAB adsorption layer at the water/hexane interface. In Fig. 6b the C_{14}TAB experimental curves are fitted with the Frumkin Ionic Compressibility and the Langmuir Compressibility models, respectively, by using the model parameters given in Table 1.

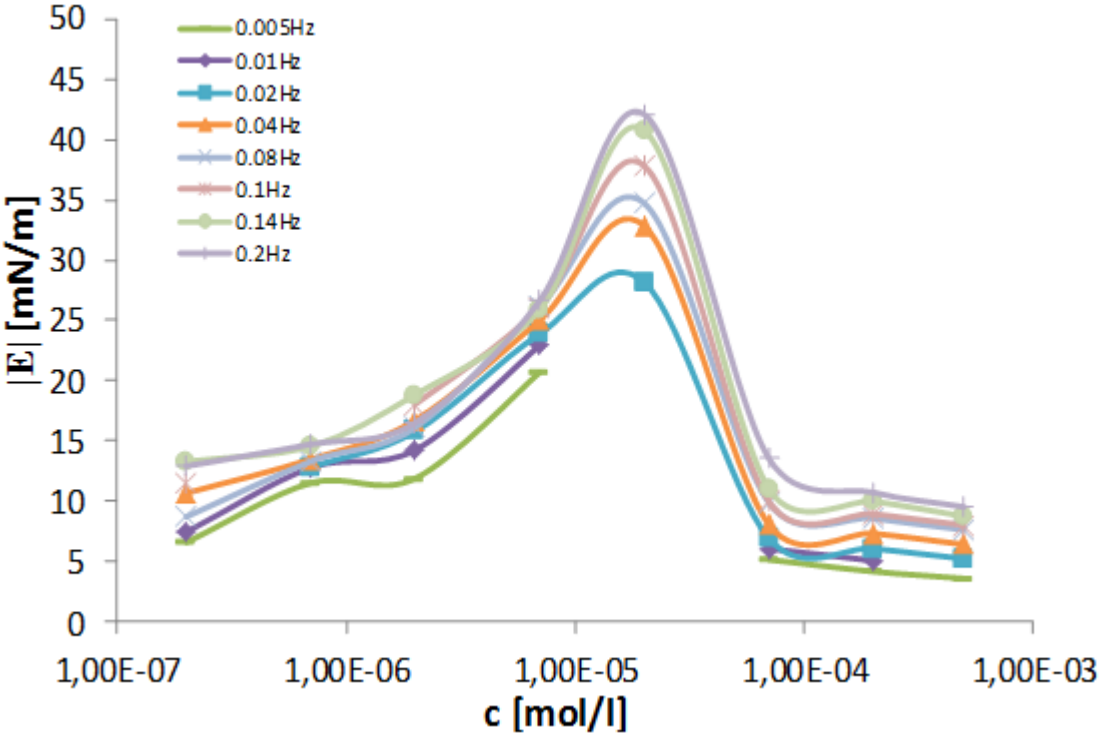

Figure 6a. The dependence of the visco-elastic modulus |E| of C_{14}TAB adsorption layers at the water/hexane interface on the bulk concentration c. The different frequencies of interfacial area oscillations are given in the legend of the chart.

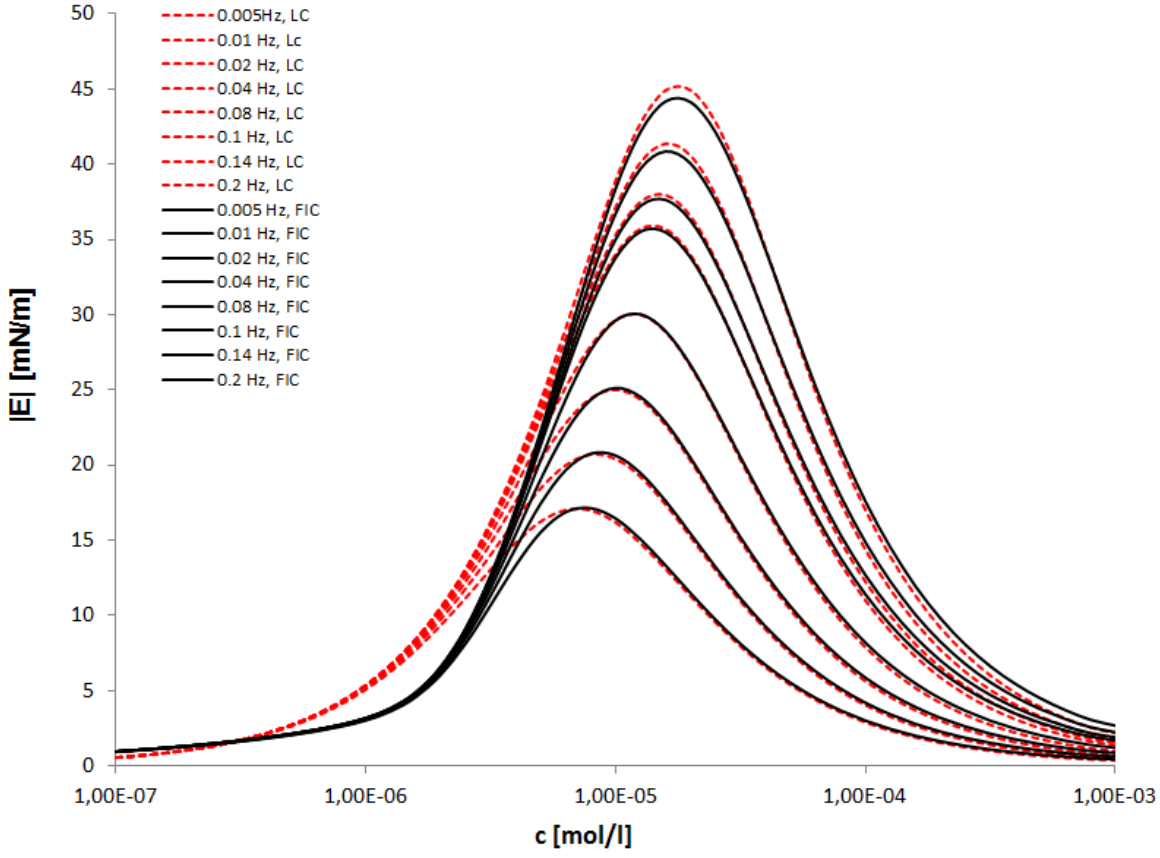

Figure 6b. Theoretical curves of the C_{14}TAB dilational rheology calculated from the Frumkin Ionic Compressibility model (solid line) and the Langmuir Compressibility model (dashed line) using the parameters given in Table 1, the oscillation frequencies are given in the legend of the chart.

Table 1. Parameters of the Langmuir Compressibility and Frumkin Ionic Compressibility models for selected C_nTAB surfactants obtained after kinetic and dilational rheology experiments at water/hexane interface:

		ω_0 [m^2/mol]		a		b [l/mol]		ε [m/mN]		cc [mol/l]		D [m^2/s]	
	c [mol/l]	LC	FIC	LC	FIC	LC	FIC	LC	FIC	LC	FIC	LC	FIC
C_{16}TAB	5×10^{-6}	*$4{,}2\times10^{5}$	*$3{,}8\times10^{5}$	*0	*1,1	*1.6×10^{7}	*$2{,}2\times10^{4}$	*1×10^{-2}	1×10^{-3}	*0	*2×10^{-3}	5×10^{-10}	5×10^{-10}
	2×10^{-5}								*1×10^{-2}			1×10^{-10}	2×10^{-10}
	rheology	*4.2×10^{5}	*$3{,}8\times10^{5}$	*0	*1,1	*1.6×10^{7}	*$2{,}2\times10^{4}$	*1×10^{-2}	*1×10^{-2}	*0	*2×10^{-3}	6×10^{-9}	6×10^{-9}
C_{14}TAB	7×10^{-5}	*$4{,}3\times10^{5}$	*$4{,}4\times10^{5}$	*0	*1,2	$9{,}4\times10^{5}$	$7{,}3\times10^{3}$	9×10^{-3}	2.2×10^{-2}	*0	*2×10^{-3}	1×10^{-10}	5×10^{-10}
	5×10^{-4}							2.5×10^{-2}	2.5×10^{-2}				
	rheology	*4.3×10^{5}	$3{,}8\times10^{5}$	*0	*1,2	$9{,}4\times10^{5}$	*$5{,}5\times10^{3}$	2×10^{-3}	1×10^{-3}	*0	*2×10^{-3}	1×10^{-10}	1×10^{-10}
C_{12}TAB	1×10^{-5}												2×10^{-11}
	7×10^{-4}		*$4{,}4\times10^{5}$		*0		*$4{,}3\times10^{3}$		*2×10^{-3}		*2×10^{-3}		1×10^{-13}
	7×10^{-3}												2×10^{-14}
C_{10}TAB	1×10^{-4}												8×10^{-12}
	3×10^{-3}		*$5{,}6\times10^{5}$		*0		*$2{,}2\times10^{3}$		*2×10^{-3}		*2×10^{-3}		5×10^{-15}
	3×10^{-2}												3×10^{-16}

* values taken from [Pradines et al.].

The model parameters used for fitting the experimental kinetic curves and rheological data were taken from [1], but modified slightly if necessary to get the best fitting. In [1] the authors emphasized that the Frumkin Ionic Compressibility model describes better the thermodynamic adsorption properties at the water/hexane interface.

The kinetics and rheology for C_{16}TAB was fitted with the model parameters given in [1] without any modification except for the value of the intrinsic compressibility ε (see Table 1) for the Frumkin Ionic Compressibility model. The other ε values obtained from the kinetics coincide with those given in [1], and so the values obtained from rheology. Using the value of ε=0.01 m/mN for the fitting of the rheology results we obtain a too large diffusion coefficient of $D=6\times10^{-9}$ m^2/s. The difference in the diffusion coefficients obtained from the kinetic data can be due to additional processes at water/hexane interface during surfactants adsorption and desorption. During interfacial perturbations, the adsorption of surfactants is encouraged by the attractive forces of the hydrophobic oil molecules, despite the ionic repulsion of the surfactants' polar heads. On the other hand, desorption of the same surfactant molecules from the water/oil interface is hindered by the same attractive hydrophobic forces with the oil molecules. The result of these processes can be an asymmetry of adsorption/desorption upon interfacial area oscillations seen during the sinusoidal interface perturbation when measuring the dilational rheology. Both theoretical models were primarily made for the water/air interface. Hence, the mentioned additional processes at the water/hexane interface are just occasionally reflected in the diffusion coefficient D. The development of a new model, however, for a quantitative consideration requires a clear picture of the mechanism of the additional impact of the hydrophobic interaction on the adsorption dynamics. One alternative would be to apply a mixed diffusion-kinetic controlled adsorption model, but the kinetic part would presently be only an arbitrary choice or an empirical relation, which gives no additional physical

insight. Therefore, for the time we want to leave the data analysis on the level of efficient diffusion coefficients.

For C_{14}TAB we obtained two sets of isotherm parameters for the Frumkin Ionic Compressibility model: ω_0=4.4x10^5 m^2/mol, b=7.3 m^3/mol and ω_0=3.8x10^5 m^2/mol, b=5.5 m^3/mol. In the first set ω_0 coincides with the value given in [1], whereas in the second set b is identical to the one in [1]. We used the first parameter set for the kinetics, but for the rheology data the second set instead in order to reach a best fitting. For the Langmuir Compressibility model we get the adsorption equilibrium constant *b* about 7 times smaller than that obtained in [1]. This value was used in the fitting of both, the kinetics and rheology results.

To keep the diffusion coefficients in reasonable limits we had to vary the compressibility constant in a broad range. The values exceeding 0.02 m/mN are too high, because according to Eq. (6) already at ε=0.025 m/mN, the surface coverage would reach a value of 1 and at an interfacial pressure of about 40 mN/m we would obtain ω=0. From Fig 2 it is seen that the kinetic curves for C_{14}TAB reach the equilibrium state already at much shorter times as compared to C_{16}TAB. This is especially true at a concentration of c = 5$\times$10^{-4} mol/l, which creates significant problems in model fitting. Thus, the apparently very high values of the compressibility coefficients can be the consequence of the non-suitable time range of data acquisition. At the same time the values 0.001 and 0.002 obtained from the rheological data seem to be too small, because it results in an unreasonable increase in E_0.

Studies of C_{12}TAB and C_{10}TAB have to be performed at highly concentrated solutions in order to show the dynamics of the adsorption process, and hence the diffusion of C_{12}TAB and C_{10}TAB is faster than for the longer chain surfactants. The capabilities of the combination of PAT-1 and ODBA are insufficient here, as can be seen from the Figs. 3 and 4, as the dynamic interfacial tensions show almost equilibrium values.

Conclusions

This paper complements the findings published recently by Pradines et al. [1] and shows that the adsorption kinetics and dilational rheology depend closely on the choice of the instrument and of the theoretical model for analyzing the data afterwards. Beside this, it shows that the qualitative and quantitative interpretations of dynamic C_nTAB adsorption layers at water/hexane interface are only partly satisfactory.

It was shown above that adsorption kinetics of C_{10}TAB and C_{12}TAB at water/hexane interface cannot be studied with conventional instruments. Basically for these two surfactants, measuring the dynamic interfacial tensions we have obtained just equilibrium values. The similar results have been obtained for the dilational rheology, where the interfacial tension response to the drop area oscillations was too weak due to fast diffusion of the particular surfactants to/from the interface. To avoid such problems the capillary pressure tensiometer should be utilized better to reach higher frequencies.

Generally the Langmuir Compressibility model gives good description of all types of data. The perfect case is if a single diffusion coefficient is used for fitting of the thermodynamic, kinetic and dilational rheology experimental results. However, for C_{14}TAB surfactants we had to manipulate the model parameters and chose unrealistic values of the surface layer compressibility values ε for perfect fits. On the other hand, good fits are obtained for C_{16}TAB rheology results using thermodynamic model parameters but unrealistic diffusion coefficients D. The different diffusion coefficients are possibly caused by additional processes going on at the water/hexane interface. It might be that the oil molecules participate in the dynamics more than expected and those are mechanisms that we cannot describe yet quantitatively.

References

1 V. Pradines, V.B. Fainerman, E.V. Aksenenko, J. Krägel, N. Mucic, R. Miller, Colloids Surfaces A 371 (2010) 22-28.
2 C. Stubenrauch, V.B. Fainerman, E.V. Aksenenko, R. Miller, J. Phys. Chem. B 109 (2005) 1505-1509.
3 K. Medrzycka, W. Zwierzykowski, J. Colloid Interface Sci. 230 (2000) 67-72.
4 A. Sharipova, S. Aidarova, A.B. Fainerman, R. Miller, Colloids Surf. A 382 (2011) 181-185.
5 A. Javadi, N. Mucic, D. Vollhardt, V.B. Fainerman, R. Miller, J. Colloid Interface Sci. 351 (2010) 537-541.
6 V.B. Fainerman, E.V. Aksenenko, V.I. Kovalchuk, A. Javadi, R. Miller, Soft Matter 7 (2011) 7860-7865.
7 A. Javadi, N. Moradi, V.B. Fainerman, H. Moehwald, R. Miller, Colloids Surfaces A 391 (2011) 19-24.
8 W.D. Garrett and J.D. Bultman, J. Colloid Sci., 18 (1963) 798
9 J.A. Mann and R.S. Hansen, J. Colloid Sci., 18 (1963) 805
10 L. Liggieri, M. Ferrari, D. Mondelli, F. Ravera, Faraday Discuss. 129 (2005) 125-140.
11 R. Miller, J.K. Ferri, A. Javadi, J. Krägel, N. Mucic, R. Wüstneck, Colloid Polym. Sci. 288 (2010) 937-950.
12 V.B. Fainerman, S.A. Zholob, E.H. Lucassen-Reynders, R. Miller, J. Colloid Interface Sci. 261 (2003) 180-183.
13 http://www.thomascat.info/Scientific/AdSo/AdSo.htm
14 V.B. Fainerman, S.V. Lylyk, E.V. Aksenenko, L. Liggieri, A.V. Makievski, J.T. Petkov, J. Yorke, R. Miller, Colloids Surfaces A 334 (2009) 8-15
15 http://www.thomascat.info/Scientific/AdSo/AdSo.htm
16 I.J. Langmuir, J. Am. Chem. Soc. 39 (1917) 1848.
17 B. von Szyszkowski, Z. Phys. Chem. (Leipzig) 64 (1908) 385.
18 V.B. Fainerman, E.H. Lucassen-Reynders, Adv. Colloid Interface Sci. 96 (2002) 295–323.
19 V.B. Fainerman, D. Vollhardt, J. Phys. Chem. B 107 (2003) 3098-3100.
20 M. van den Tempel, J. Lucassen, E.H. Lucassen-Reynders, J. Phys. Chem. 69 (1965) 1798–1804.
21 J. Lucassen, M. van den Tempel, Chem. Eng. Sci. 27 (1972) 1283.
22 J. Lucassen, M. van den Tempel, J. Colloid Interface Sci. 41 (1972) 491.
23 N. Mucic, A. Javadi, N.M. Kovalchuk, E.V. Aksenenko, R. Miller, Adv. Colloid Interface Sci. 168 (2011) 167-178.
24 P. Joos, Dynamic Surface Phenomena, VPS, Utrecht:1999.

Paper VIII

Dynamic interfacial tension of triblock copolymers solutions at the water/hexane interface

P. Ramirez, J. Munoz, V.B. Fainerman, E.V. Aksenenko, N. Mucic and R. Miller

Colloids and Surfaces A 391 (2011) 119-124

Colloids and Surfaces A: Physicochem. Eng. Aspects 391 (2011) 119–124

Contents lists available at ScienceDirect

Colloids and Surfaces A: Physicochemical and Engineering Aspects

journal homepage: www.elsevier.com/locate/colsurfa

Dynamic interfacial tension of triblock copolymers solutions at the water–hexane interface

P. Ramírez[a,*], J. Muñoz[a], V.B. Fainerman[b], E.V. Aksenenko[c], N. Mucic[d], R. Miller[d]

[a] Departamento de Ingeniería Química, Facultad de Química. Universidad de Sevilla, P. García González 1, 41012 Sevilla, Spain
[b] Donetsk Medical University, 16 Ilych Avenue, 83003 Donetsk, Ukraine
[c] Institute of Colloid Chemistry and Chemistry of Water, 42 Vernadsky Avenue, 03680 Kyiv (Kiev), Ukraine
[d] Max-Planck-Institut für Kolloid- und Grenzflächenforschung, Am Mühlenberg 1, 14424 Potsdam, Germany

ARTICLE INFO

Article history:
Received 4 March 2011
Accepted 18 April 2011
Available online 25 April 2011

Keywords:
Pluronics
Adsorption isotherm
Adsorption kinetics
Water–hexane interface
Multilayer formation

ABSTRACT

Equilibrium and dynamic surface tension of non-ionic triblock copolymers, Pluronics, varying in the number of poly(ethylene oxide) and poly(propylene oxide) groups have been measured by means of drop profile tensiometry at the water–hexane interface.

The experimental data have been explained on the basis of a theory previously developed for protein solutions [1]. This model assumes the coexistence of different adsorbed states at the interface, depending on the surface coverage. It has been shown that the best fit is achieved when a polylayer adsorption is considered. Reasonable values of the adsorption layer thickness and realistic values of the diffusion coefficient are obtained which validate the model proposed.

1. Introduction

Pluronics are non-ionic triblock copolymers of poly(ethylene oxide) and poly(propylene oxide) (PEO_x–PPO_y–PEO_x) blocks, commercially available with different PEO/PPO ratios and molecular weights. They are used in many applications, such as detergency, foaming, emulsification, dispersion stabilization and drug delivery. Their applications are mainly related to their surface properties, and micelle formation [2–11].

The most traditional characterization of polymers at the fluid/fluid interface relies on the measurement of the surface pressure $\Pi = \gamma_0 - \gamma$, where γ is the interfacial tension of the polymer solution against hexane, and γ_0 is the interfacial tension between the two solvents water and hexane. Scaling and mean field theories proved to be useful for the description of block copolymers at solid surfaces. The situation is more complicated for block copolymers at liquid surfaces.

Surface properties of adsorbed and spread PEO–PPO–PEO films at the air–water interface have been studied by equilibrium and dynamic surface tension measurements [12,13], ellipsometry [12–15], neutron reflectivity [16–18], and surface rheology measurements [15,19–24]. It has been shown that PEO–PPO–PEO triblock copolymers adopt different conformations as adsorption increases. The layer structure changes from a two-dimensional flat structure with both PEO and PPO segments lying flat at the surface to a brush-like structure where the PEO segments are protruding into the solution bulk. This conformational change of the copolymers is usually described by scaling theories [12,25–28].

From dynamic surface tension data it has been observed that at small polymer concentration the adsorption kinetics is diffusion controlled, whereas at higher concentrations an additional slower kinetics process appears related to the rearrangements of the brush [13].

Surface rheological properties of spread and adsorbed layers have been explored by plotting the dilatational modulus as a function of surface pressure. It has been shown that the modulus is a unique function of surface pressure and the same results have been obtained for spread and adsorbed layers for $\Pi < 20\,\mathrm{mN\,m^{-1}}$. Furthermore, the surface dilational viscoelasticity at low surface pressure ($\Pi < 10\,\mathrm{mN\,m^{-1}}$) is mainly determined by the PEO blocks. In addition, it has been pointed out that the presence of PPO blocks induces the formation of a layer with higher dilational modulus and surface pressure, whereas PEO blocks forms smoother layers [15,19–24].

Since most of the applications of interest of these copolymers occur at water–oil interfaces, it is interesting to explore the interfacial properties of Pluronics in these systems.

This work is aimed at the study of the dynamic and equilibrium interfacial tension of aqueous solutions of triblock copolymers with various numbers of PEO and PPO groups: Pluronic L64 $(PEO)_{13}$–$(PPO)_{30}$–$(PEO)_{13}$; Pluronic P9400 $(PEO)_{21}$–$(PPO)_{50}$–$(PEO)_{21}$; and Pluronic F68 $(PEO)_{76}$–$(PPO)_{30}$–$(PEO)_{76}$. The experimental results

* Corresponding author. Tel.: +34 954 557180; fax: +34 954 556447.
E-mail address: pramirez@us.es (P. Ramírez).

0927-7757/$ – see front matter © 2011 Elsevier B.V. All rights reserved.
doi:10.1016/j.colsurfa.2011.04.019

obtained in the study were analysed in the framework of a thermodynamic model previously reported [1] for protein solutions. The theory is based on the analysis of the chemical potentials of the solvent and the dissolved substance in the solution bulk and in the surface layer, and takes into account the molecular geometry, the variation of molar area (reorientation) of the dissolved substance with the increase of adsorption (surface pressure), the formation of multilayers and the aggregation (condensation) of the dissolved substance in the surface layer. It has been shown that this theory can describe fairly well the experimental adsorption and surface tension data obtained for various proteins and also for a synthetic polymer like poly (vinyl alcohol) (PVA). The same theory has been recently applied successfully to describe the adsorption and rheological characteristics of solutions of various proteins and their mixtures with surfactants [29–33].

2. Theory

Similarly to the proteins, the copolymer molecules can exist in a number of adsorbed states (n) of different molar areas, varying from a maximum value (ω_{max}) at low surface coverage θ_p to a minimum value (ω_{min}) at high surface coverage. The dividing surface is chosen in such a way that the value of the molar area of the solvent (or respectively the area occupied by one segment of the polymer molecule), ω_0, is much smaller than ω_{min}. The equation of state for the surface layer reads [1]:

$$-\frac{\Pi\omega_0}{RT} = \ln(1-\theta_P) + \theta_P\left(\frac{1-\omega_0}{\omega}\right) + a_P\theta_P^2 \quad (1)$$

where R is the gas law constant, T is the temperature, ω stands for the average molar area of the adsorbed polymer, $\Gamma_P = \sum_{i=1}^{n}\Gamma_i$ is the total adsorption of polymers in all n states, $\theta_P = \omega\Gamma_P = \sum_{i=1}^{n}\omega_i\Gamma_i$ is the total surface coverage by polymer molecules, $\omega_i = \omega_1 + (i-1)\omega_0$ is the molar area of the polymer in state i ($1 \le i \le n$), assuming the molar area increment to be equal to ω_0 with $\omega_1 = \omega_{min}$, $\omega_{max} = \omega_1 + (n-1)\omega_0$.

The adsorption isotherm for the polymer in each adsorbed state (j) reads [1]:

$$b_P c_P = \frac{\omega\Gamma_j}{(1-\theta_P)^{\omega j/\omega}} \exp\left[-2a_P\left(\frac{\omega_j}{\omega}\right)\theta_P\right]. \quad (2)$$

Here c_P is the polymer bulk concentration and $b_P = b_{Pj}$ is the adsorption equilibrium constant for the polymer in the jth state. It is assumed that the constants b_{Pj} for all states j from $i=1$ to $i=n$ are identical, and therefore, the adsorption constant b_P for the polymer molecule as a whole is $\Sigma b_{Pj} = nb_{Pj}$ [1]. From the fact that the values of all b_{Pj} are constant, one can calculate the distribution function of adsorptions over all states of the adsorbed polymer molecules from Eq. (2):

$$\Gamma_j = \Gamma_P \frac{(1-\theta_P)^{(\omega_j-\omega_1)/\omega}\exp[2a_P\theta_P((\omega_j-\omega_1)/\omega)]}{\sum_{i=1}^{n}(1-\theta_P)^{(\omega_i-\omega_1)/\omega}\exp[2a_P\theta_P((\omega_i-\omega_1)/\omega)]}. \quad (3)$$

Then, at extremely low surface coverage (where $\Pi \equiv 0$) all adsorptions are equal, while at high surface coverage the states with smaller areas are favoured.

At large bulk concentrations, many polymers can form multilayers at liquid interfaces. The isotherm equation for multilayer adsorption can be derived by assuming that the coverage of the second and subsequent layers are proportional to the adsorption equilibrium constant b_{P2}, and to the coverage of the preceding layers. It was assumed that the formation of the second and subsequent layers does not affect the surface pressure in Eq. (1). An attempt was made to adapt the Langmuir isotherm for the case of multiple (m) adsorption layers. This leads to a rough approximation for the total adsorption Γ in the second and subsequent layers [34]:

$$\Gamma \approx \Gamma_P\sum_{i=1}^{m}\left(\frac{b_{P2}c_P}{1+b_{P2}c_P}\right)^{i-1} \quad (4)$$

Eq. (4) shows that the adsorption in the first layer is assumed to be equal to that calculated via Eqs. (1)–(3). The approximation for the second and subsequent layers is fairly crude, as it ignores both the Frumkin heat of interaction and the non-ideality of entropy of mixing at the surface. These effects, if accounted for, would increase the number of model parameters; hence, they are neglected in the present study. It should be noted, however, that the only adsorption parameter b_{P2} present in Eq. (2) takes some approximate account for these effects.

It was shown experimentally that above a certain critical polymer concentration, c_P^*, the surface tension decreases insignificantly, while the adsorption often exhibits a strong increase. Such a "constant" value of Π^* beyond a certain critical value of adsorption Γ^* can be explained by a condensation (aggregation) of the polymer in the surface layer [35]. Aggregation in the surface layer leads to changes in the average molar area of adsorbed molecules. The equations of state and adsorption isotherm which correspond to the formation of large two-dimensional aggregates were also presented elsewhere [1]. As the polymers are capable to form relatively small surface aggregates [12,24,36], the following approximate expression for the surface pressure can be used in the post-critical range of polymer concentration, which involves the aggregation number n_a:

$$\Pi = \Pi * \left(1 + \frac{1}{n_a}\frac{\Gamma-\Gamma*}{\Gamma*}\right) \quad (5)$$

Γ is here the adsorption in the post-critical range as calculated from Eq. (2). It is seen from Eq. (5) that the increase in surface pressure in the post-critical concentration range is proportional to the increase of polymer adsorption, with the proportionality coefficient equal to the inverse aggregation number, i.e. the surface pressure increase is proportional to the adsorption of kinetic entities (monomers and aggregates).

Fig. 1 illustrates the concentration dependence of the surface pressure (black curve) calculated from Eqs. (1) to (4), with the model parameters corresponding to the Pluronic P9400 (see below). The critical surface pressure for this case is ca. 23 mN m^{-1} (shown by arrow). The dashed curves were calculated in the post-

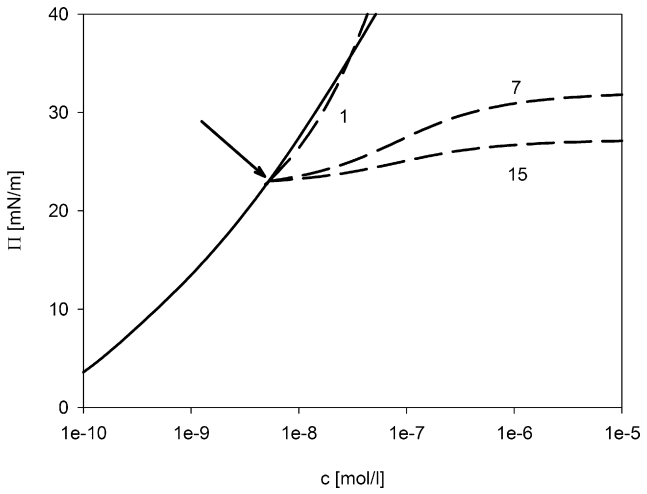

Fig. 1. Interfacial pressure dependence on the polymer bulk concentration (solid curve) calculated using Eqs. (1)–(4); dashed curves are calculated using Eq. (5) for $\Pi > 23$ mN m^{-1} and various n_a values: 1, 7 and 15.

Table 1
Main characteristics of the triblock copolymers.

Pluronic	MW/g mol^{-1}	PEO, wt%	PPO wt g mol^{-1}	HLB
L64	2900	40	1750	12–18
P9400	4600	40	2750	12–18
F68	8400	80	1750	29

critical range using Eq. (5) for different n_a values: 1, 7 and 15. For $n_a = 1$ (aggregate formation does not occur) the curves calculated from Eqs. (1) and (5) almost coincide with each other. With increasing values of n_a the curves become flatter.

To calculate the dynamic interfacial tension of the triblock copolymers solutions, the diffusion controlled adsorption mechanism was used. This model, which was described in detail elsewhere [37], involves Fick's diffusion equations for the surface active component in the two adjoining phases, and takes into account the actual geometry of the system: the adsorption of copolymers from a large volume of the aqueous solution of the studied substance onto the hexane drop with fixed and limited size. To perform the calculations, a software previously described [37] was used and only the section which implements the model Eqs. (1)–(5) was to be added, while the core of the package remained essentially the same.

3. Materials and methods

3.1. Material

Pluronics are symmetrical non-ionic triblock copolymers of the form $(PEO)_x$–$(PPO)_y$–$(PEO)_x$, where PEO and PPO are the oxyethylene and oxypropylene units, respectively. The Pluronics L64 and F68 were purchased from Sigma–Aldrich, whereas Pluronic P9400 was kindly provided by BASF. All of them were used without further purification. Table 1 shows the molecular characteristics of these Pluronics. The block copolymers have been chosen to form two pairs, one of them (L64 and P9400) with the same percentages of PEO and PPO, 40% (w/w) and 60% (w/w), respectively and increasing average molecular weight and the other with the same number of PPO units and increasing number of PEO ones (L64 and F68), which results in a greater (15 to >24) average HLB.

The solutions studied were prepared with ultrapure Milli-Q water. The measurements done were carried out at room temperature. Hexane was purchased from Fluka and was purified with aluminium oxide and subsequently saturated with ultrapure Milli-Q water.

3.2. Drop profile tensiometry

A drop profile analysis tensiometer (PAT-1, SINTERFACE Technologies, Germany) was used. Its main features/characteristics have been described in detail elsewhere [38]. Briefly, a hexane drop of a certain volume is formed at the capillary tip of a hooked needle inside a measuring glass cell containing the aqueous polymeric solution. The drop images are recorded and from its shape the interfacial tension can be calculated. Measuring the variation of the interfacial tension with time we will obtain information about the adsorption process. The interfacial tension of the pure water–hexane interface was 51 mN m^{-1}.

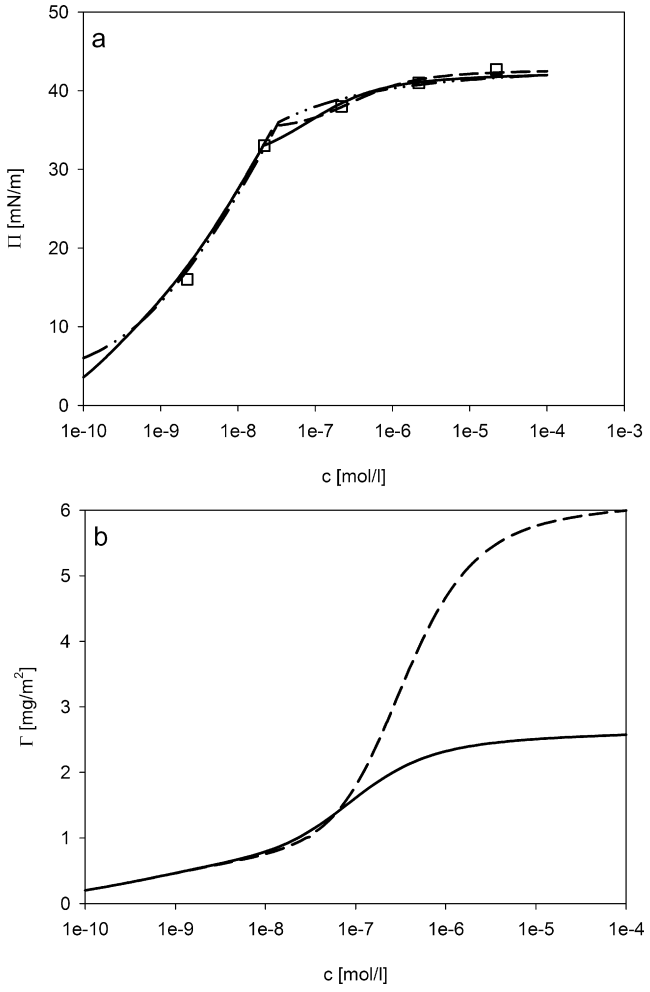

Fig. 2. Dependence of the equilibrium interfacial pressure (a) and adsorption (b) on the bulk concentration of P9400 in aqueous solution at the solution/hexane interface; open squares represent experimental data; curves are calculated using Eqs. (1)–(5) for $m = 3$ (solid curves), $m = 7$ (dashed curves), $m = 1$ (dash–dotted curve in Fig. 2a); model parameters are shown in Table 2.

4. Results and discussion

Let us consider first the equilibrium interfacial pressure of the studied Pluronics solutions. Fig. 2a shows the equilibrium interfacial pressures for P9400 aqueous solutions at concentrations 0.01, 0.1, 1, 10 and 100 mg/l (corresponding molar concentrations of 2.2×10^{-9}, 2.2×10^{-8}, 2.2×10^{-7}, 2.2×10^{-6} and 2.2×10^{-5} mol/l, respectively). These results were obtained for hexane drops in aqueous solutions for lifetimes ranging from 3 to 20 h. For very low concentrations (0.01 and 0.1 mg/l) even a lifetime of 20 h was too short to achieve the equilibrium interfacial tension value; therefore in these cases the equilibrium values were estimated by extrapolation of the γ *vs* $t^{-1/2}$ dependence to infinite time, cf. Ref. [39]. The theoretical $\Pi(c)$ and $\Gamma(c)$ curves calculated from Eqs. (1) to (5) with the parameters listed in Table 2 are shown in Figs. 2a and b. To decrease the number of model parameters $a = 0$ was taken for the intermolecular interaction coefficient for all studied Pluron-

Table 2
Model parameters, Eqs. (1)–(5).

Pluronic	$\omega_0 10^5$ m^2/mol	$\omega_1 10^6$ m^2/mol	$\omega_m 10^7$ m^2/mol	n_a	Π^*mN m^{-1}	b_P l/mol	b_{P2} l/mol	m
P9400	2.4	5.0	3.0	6.0	33.0	1.7×10^8	2.0×10^7	3
L64	2.1	3.0	2.0	10.0	30.5	6.6×10^7	7.0×10^6	3
F68	1.5	6.0	4.0	7.0	21.5	2.0×10^8	9.0×10^6	2

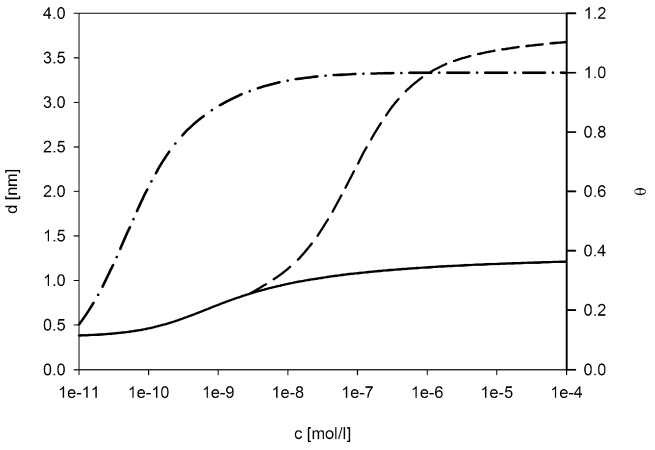

Fig. 3. Dependence of the P9400 adsorption layer thickness on the bulk concentration: $m = 1$ (solid curve) and $m = 3$ (dashed curve); the dash–dotted curve shows the adsorption layer coverage.

ics. The calculated Π values in all cases exhibit good agreement with the experimental data. The black curves in Fig. 2 correspond to a triple layer adsorption ($m = 3$ in Table 2). Note, the calculations for the dashed curves assumed the formation of 7 adsorption layers, using values of $\Pi^* = 35\ \mathrm{mN\ m^{-1}}$ and $n_a = 25$ instead of those listed in Table 2. The corresponding dependencies of the equilibrium adsorption $\Gamma(c)$ are shown in Fig. 2b.

It should be noted that the reorientation of the molecules (i.e., the decrease of the area per molecule) at the interface with increasing polymer bulk concentration results in a significant increase of the 'effective thickness' of the Pluronic adsorption layer, as compared to the monolayer state at low bulk concentrations, when the surface is almost free and the PPO and PEO chains are stretched along the interface. This effect becomes more pronounced with the increase of the number of adsorbed layers m. This is illustrated by Fig. 3, where the effective thickness of the P9400 molecule $\delta = \Gamma_P/\rho\theta_P$ (the density of the dissolved polymer was taken to be $\rho = 0.7$ g/ml) is plotted *vs* the polymer bulk concentration. The same figure also shows the total coverage $\theta = \Gamma\omega$ of the adsorbed layer. As can be observed if the formation of a single layer is assumed ($m = 1$), the effective thickness increases due to reorientation by a factor of 3 (from 0.4 to 1.2 nm), while for a triple layer formation ($m = 3$) this thickness becomes even three time higher (3.6 nm). These values of the P9400 adsorbed layer thickness agree satisfactorily with direct ellipsometric data [12,18,36].

Another feature of the model described by Eqs. (1)–(5) which should be noted is that the adsorption layer thickness is determined by the minimum molecular area ω_1. Yet, if a value of $\omega_1 = 10^6\ \mathrm{m^2/mol}$ is used instead of $\omega_1 = 5 \times 10^6\ \mathrm{m^2/mol}$ in the calculations (i.e. using a 5 times lower factor), the P9400 adsorption in the surface layer would become 4.5 mg/m^2, which corresponds approximately to a quintuple ($m = 5$) layer model. In addition, if the aforementioned ρ value for P9400 was taken, the resulting layer thickness would reach a value of 6.4 nm. The concentration dependence of surface pressure for $\omega_1 = 10^6\ \mathrm{m^2/mol}$ is shown in Fig. 2a (dash–dotted curve). This corresponds to a monolayer adsorption, hence the surface pressure for this case was calculated using Eqs. (1)–(3), and the Π values in the post-critical range were calculated from Eq. (1), instead of Eq. (5), using the adsorption values $\Gamma' = \Gamma^* + (\Gamma - \Gamma^*)/n_a$. The aggregation number for this curve was 6. A deficiency of the monolayer model is the overestimated value of the limiting (high-frequency) viscoelastic modulus (above 100 mN m^{-1}), which contradicts some experimental data not shown. Detailed information on the dilational rheology of these systems will be provided in a further work. Thus, the polylayer model provides better results for the adsorption equilibrium, dynamics and rheology of the copolymers.

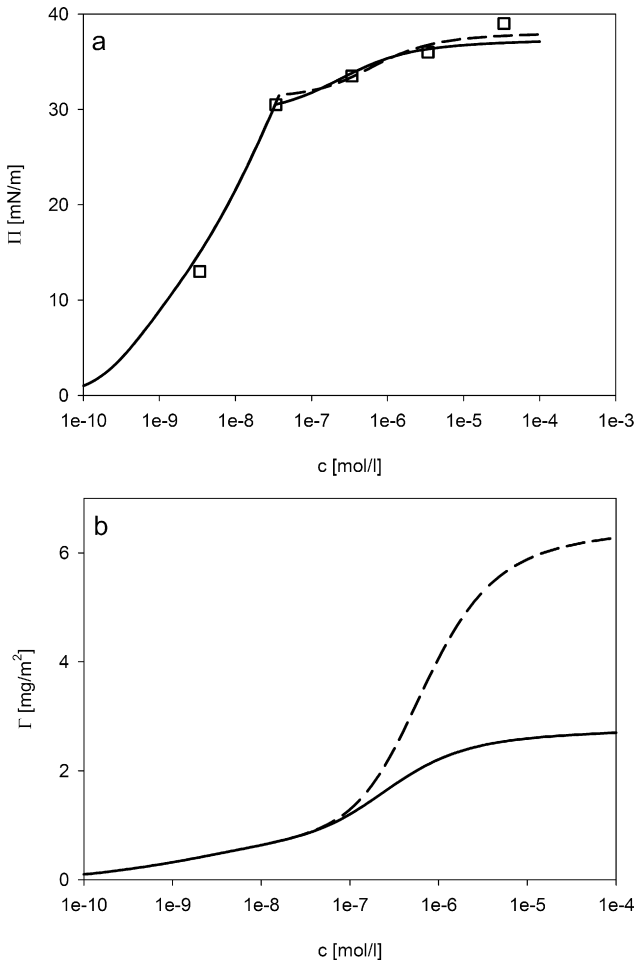

Fig. 4. Dependence of the equilibrium interfacial pressure (a) and adsorption (b) on the concentration of L64 in aqueous solution at the solution/hexane interface; symbols represent experimental data; curves are calculated using Eqs. (1)–(5) for $m = 3$ (solid curves) and $m = 7$ (dashed curves); model parameters are shown in Table 2.

The dependencies of the interfacial tension and adsorption on the Pluronic L64 bulk concentration are shown in Fig. 4a and b, respectively. The theoretical curves for the triple and septuple layer models were calculated using Eqs. (1)–(5) with the parameters shown in Table 2, i.e. $\Pi^* = 30.5$ and $n_a = 30$ for $m = 7$, respectively. As the molecular weight of this Pluronic is lower than that of P9400, the values of the minimum and maximum molar area of the polymer were taken to be correspondingly smaller. Fig. 5a and b illustrates the dependencies for the Pluronic F68 (for bilayer and quadruple layer adsorption) calculated with the values in Table 2, i.e. $\Pi^* = 22.5$ and $n_a = 17$ for $m = 4$, respectively. To assure the validity of the model for surface pressure values below Π^*, the surface pressure equilibrium values of two Pluronics solutions at concentrations below 0.01 mg/l are also shown in Fig. 5a. The molecular weight of this Pluronic is higher than that of P9400, therefore, the minimum and maximum molar area of the polymer were increased correspondingly. Fig. 5 shows that the calculated values of Π fit fairly well the experimental data.

The calculated results of the dynamic interfacial tension for the Pluronics studied at three bulk concentrations (0.1, 1.0 and 10 mg/l) are compared with the experimental data in Figs. 6–8. The calculations were performed using the model equations (1)–(5) and a kinetic model [37] which assumes the actual geometry of the experimental system (size of drop). In particular, the hexane drop radius

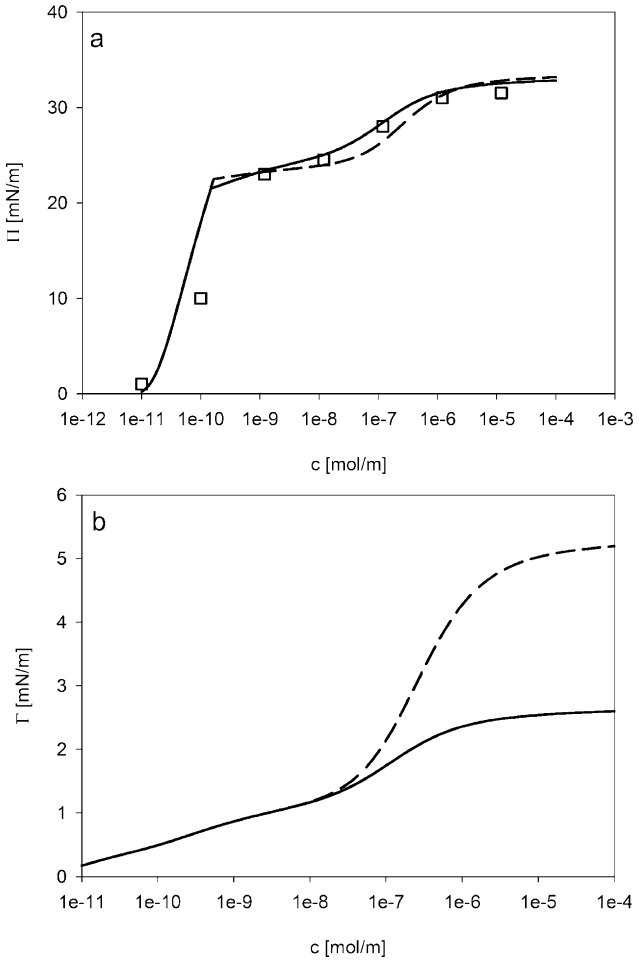

Fig. 5. Dependence of the equilibrium interfacial pressure (a) and adsorption (b) on the concentration of F68 in aqueous solution at the solution/hexane interface; symbols represent experimental data; curves are calculated using Eqs. (1)–(5) for $m = 2$ (solid curves) and $m = 4$ (dashed curves); model parameters are shown in Table 2.

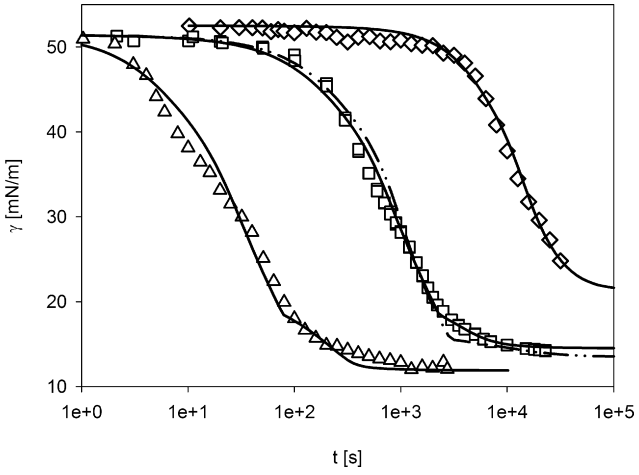

Fig. 6. Dynamic interfacial tension of P9400 solutions at polymer bulk concentrations of 0.1 (◊), 1.0 (□) and 10 mg/l (△); theoretical curves were calculated for $m = 3$ (solid curve) and $m = 7$ (dash–dotted curve, for the concentration 1.0 mg/l only).

was between 1.5 and 1.8 mm in all experiments, and the aqueous solution phase was assumed to be a sphere of radius 17 mm concentric around the drop, which corresponds to a measurement cell volume of 20 ml. The model parameters were those listed in Table 2. The only additional parameter was the Pluronic diffusion coefficient, which was chosen between 1.5×10^{-10} and 3.5×10^{-10} m^2/s for the polymer studied. To obtain the best fit with the experimental data, these values had to be adjusted concentration in such a way that the higher Pluronic concentrations required lower values of the diffusion coefficient. The optimum values of the latter correspond to the actual values for the Pluronics, and the calculated curves fit fairly well the experimental data. Note that the dynamic curve for the P9400 septuple layer model ($m = 7$) shown in Fig. 6 also exhibits good agreement with experimental results, indicating that the adsorption of the studied triblock copolymers is governed by a diffusion mechanism.

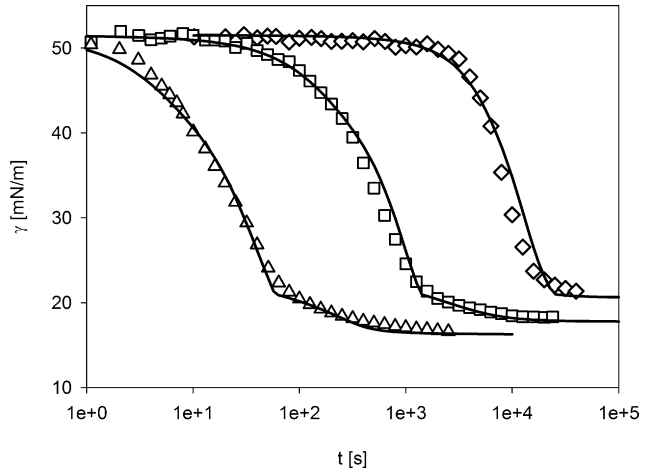

Fig. 7. Dynamic interfacial tension of L64 solutions for polymer bulk concentrations of 0.1 (◊), 1.0 (□) and 10 mg/l (△); theoretical curves were calculated for $m = 3$.

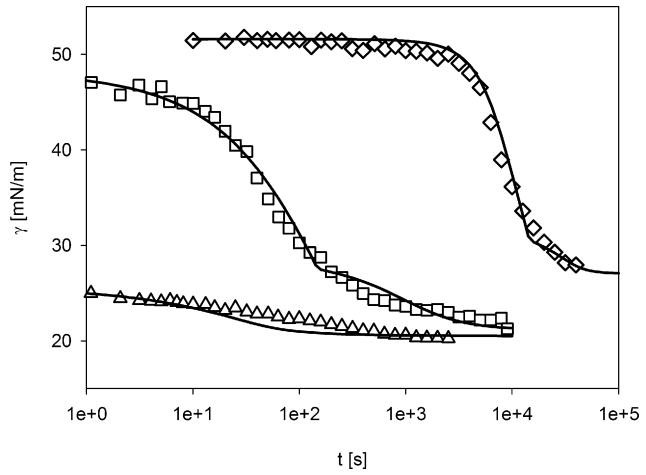

Fig. 8. Dynamic interfacial tension of F68 solutions for polymer bulk concentrations of 0.1 (◊), 1.0 (□) and 10 mg/l (△); theoretical curves were calculated for $m = 2$.

5. Conclusion

The experimental data for the equilibrium and dynamic interfacial tensions of Pluronic triblock copolymers at their aqueous solution–hexane interface are compared with the theoretical values calculated from a thermodynamic model previously reported based on the analysis of the chemical potentials of the solvent and the dissolved substances [1]. To reproduce the surface tension values at high bulk concentrations of the Pluronics, i.e. in the post-critical range, a simple model is proposed which assumes

the proportionality between the surface pressure of the solution and the adsorption of the polymer (expressed in kinetic units). This assumption is equivalent with an aggregation of the Pluronic monomers in the post-critical concentration range. The theoretical predictions agree well with the experimental data for physically reasonable values of the adsorption layer thickness and realistic values of the diffusion coefficient.

Acknowledgements

This paper reports part of the results obtained in project CTQ2007-66157PPQ sponsored by the Spanish Ministerio de Ciencia e Innovación and the European Commission (Feder Programme). The authors kindly acknowledge the financial support received. P.R. also acknowledges the financial support of Deutscher Akademischer Austauschdienst (DAAD) and Universidad de Sevilla (IV Plan Propio de Investigación).

References

[1] V.B. Fainerman, E.H. Lucassen-Reynders, R. Miller, Adv. Colloid Interface Sci. 106 (2003) 237–259.
[2] P. Alexandridis, B. Lindman, Amphiphilic Block Copolymers: Self-assembly and Applications, Elsevier, 2000.
[3] D.L. Berthier, I. Schmidt, W. Fieber, C. Schatz, A. Furrer, K. Wong, S. Lecommandoux, Langmuir 26 (2010) 7953–7961.
[4] D. Exerowa, G. Gotchev, T. Kolarov, K. Kristov, B. Levecke, T. Tadros, Colloids Surf. A 335 (2009) 50–54.
[5] F. Leal-Calderon, V. Schmitt, J. Bibette, Emulsion Science, Basic Principles, Springer, 2007.
[6] X.R. Li, P.Z. Li, Y.H. Zhang, Y.X. Zhou, X.W. Chen, Y.Q. Huang, Y. Liu, Pharm. Res. 27 (2010) 1498–1511.
[7] L.L. Schramm, Emulsions, Foams and Suspensions: Fundamentals and Applications, Wiley-VCH, 2005.
[8] T. Tadros, Polymeric surfactants, in: K. Holmberg (Ed.), Novel Surfactants, Marcel Dekker, New York, 2003.
[9] T. Tadros, Applied Surfactants, Principles and Applications, Wiley-VCH, Weinheim, 2005.
[10] L. Tavano, R. Muzzalupo, S. Trombino, R. Cassano, A. Pingitore, N. Picci, Colloids Surf. B 79 (2010) 227–234.
[11] U. Zoller, Handbook of Detergents. Part E: Applications, CRC Press, 2009.
[12] M.G. Munoz, F. Monroy, F. Ortega, R.G. Rubio, D. Langevin, Langmuir 16 (2000) 1083–1093.
[13] M.G. Munoz, F. Monroy, F. Ortega, R.G. Rubio, D. Langevin, Langmuir 16 (2000) 1094–1101.
[14] B.R. Blomqvist, J.W. Benjamins, T. Nylander, T. Arnebrant, Langmuir 21 (2005) 5061–5068.
[15] A. Hambardzumyan, V. Aguie-Beghin, M. Daoud, R. Douillard, Langmuir 20 (2004) 756–763.
[16] R. Sedev, R. Steitz, G.H. Findenegg, Physica B 315 (2002) 267–272.
[17] J.B. Vieira, Z.X. Li, R.K. Thomas, J. Phys. Chem. B 106 (2002) 5400–5407.
[18] J.B. Vieira, Z.X. Li, R.K. Thomas, J. Penfold, J. Phys. Chem. B 106 (2002) 10641–10648.
[19] B.R. Blomqvist, T. Warnheim, P.M. Claesson, Langmuir 21 (2005) 6373–6384.
[20] C. Kim, H. Yu, Langmuir 19 (2003) 4460–4464.
[21] F. Monroy, F. Ortega, R.G. Rubio, B.A. Noskov, Surface rheology studies of spread and adsorbed polymer layers, in: R. Miller, L. Liggieri (Eds.), Interfacial Rheology, Brill, Leiden, 2009.
[22] B.A. Noskov, Curr. Opin. Colloid Interface Sci. 15 (2010) 229–236.
[23] B.A. Noskov, A.V. Akentiev, G. Loglio, R. Miller, J. Phys. Chem. B 104 (2000) 7923–7931.
[24] B.A. Noskov, S.Y. Lin, G. Loglio, R.G. Rubio, R. Miller, Langmuir 22 (2006) 2647–2652.
[25] V. Aguié-Béghin, E. Leclerc, M. Daoud, R. Douillard, J. Colloid Interface Sci. 214 (1999) 143–155.
[26] P.G. de Gennes, J. Phys. 37 (1976) 1445–1452.
[27] P.G. de Gennes, Macromolecules 13 (1980) 1069–1075.
[28] E. Leclerc, M. Daoud, Macromolecules 30 (1997) 293–300.
[29] V.S. Alahverdjieva, D.O. Grigoriev, V.B. Fainerman, E.V. Aksenenko, R. Miller, H. Mohwald, J. Phys. Chem. B 112 (2008) 2136–2143.
[30] C. Kotsmar, V. Pradines, V.S. Alahverdjieva, E.V. Aksenenko, V.B. Fainerman, V.I. Kovalchuk, J. Krägel, M.E. Leser, B.A. Noskov, R. Miller, Adv. Colloid Interface Sci. 150 (2009) 41–54.
[31] J. Maldonado-Valderrama, V.B. Fainerman, E. Aksenenko, M. Jose Gálvez-Ruiz, M.A. Cabrerizo-Vílchez, R. Miller, Colloids Surf. A 261 (2005) 85–92.
[32] V. Pradines, J.r. Krägel, V.B. Fainerman, R. Miller, J. Phys. Chem. B 113 (2008) 745–751.
[33] P. Reis, R. Miller, J. Krägel, M. Leser, V.B. Fainerman, H. Watzke, K. Holmberg, Langmuir 24 (2008) 6812–6819.
[34] E.H. Lucassen-Reynders, J. Benjamins, V.B. Fainerman, Curr. Opin. Colloid Interface Sci. 15 (2010) 264–270.
[35] V.B. Fainerman, R. Miller, Langmuir 15 (1999) 1812–1816.
[36] M.G. Munoz, F. Monroy, P. Hernandez, F. Ortega, R.G. Rubio, D. Langevin, Langmuir 19 (2003) 2147–2154.
[37] V.B. Fainerman, S.V. Lylyk, E.V. Aksenenko, L. Liggieri, A.V. Makievski, J.T. Petkov, J. Yorke, R. Miller, Colloids Surf. A 334 (2009) 8–15.
[38] G. Loglio, P. Pandolfini, R. Miller, A.V. Makievski, F. Ravera, M. Ferrari, L. Liggieri, Drop and bubble shape analysis as tool for dilational rheology of interfacial layers, in: D. Möbius, R. Miller (Eds.), Novel Method to Study Interfacial Layers, Elsevier, 2001.
[39] V.B. Fainerman, R. Miller, Colloids Surf. A 97 (1995) 65–82.

Paper IX

Dilational rheology of polymer/surfactant mixtures at water/hexane interface

Sharipova, S. Aidarova, N. Mucic and R. Miller

Colloids and Surfaces A 391 (2011) 130-134

Colloids and Surfaces A: Physicochem. Eng. Aspects 391 (2011) 130–134

Contents lists available at ScienceDirect

Colloids and Surfaces A: Physicochemical and Engineering Aspects

journal homepage: www.elsevier.com/locate/colsurfa

Dilational rheology of polymer/surfactant mixtures at water/hexane interface

A. Sharipova[a,b,*], S. Aidarova[a], N. Mucic[b], R. Miller[b]

[a] International Postgraduate institute "Excellence Polytech" of Kazakh National Technical University, Almaty, Kazakhstan
[b] Max-Planck Institute of Colloids and Interfaces, Potsdam, Germany

ARTICLE INFO

Article history:
Received 16 March 2011
Received in revised form 22 April 2011
Accepted 28 April 2011
Available online 6 May 2011

Keywords:
Mixed adsorption layers
Polymer–surfactant mixtures
Water/oil interface
Interfacial tension isotherm
Rheological properties
Dilational elasticity
Dilational viscosity

ABSTRACT

The present work is devoted to the interaction in mixed solutions of the cationic polyelectrolyte PAH and the counter-charged anionic surfactant SDS at the water/oil interface. For this purpose interfacial tension and dilational rheology studies were performed to describe the formation of complexes of PAH and SDS. The dilational elasticity values depend on the concentrations of surfactant and polyelectrolyte and their mixing ratio. As expected the concentration dependence of the dilational elasticities of SDS and PAH-SDS mixtures are similar in the SDS concentration range 10^{-5} M till 10^{-3} M (at a fixed amount of PAH) and have a maximum which correlates with an observed minimum in the interfacial tension isotherm. The sharp decrease of the dilational elasticity values in a narrow range is presumably due to the destruction of two-dimensional rigid structures and the formation of microaggregates in the interfacial layer. From dilational viscosity measurements as a function of oscillation frequency one can conclude that with increasing surfactant concentration the SDS dominates in the interfacial adsorption layer whereas the polyelectrolyte–surfactant complexes remain in the bulk phase.

1. Introduction

Understanding of the interfacial properties of polyelectrolyte–surfactants mixtures at water/oil interfaces is important due to their industrial, technological and domestic applications. However, progress in this field is rather slow mainly due to lack of suitable experimental techniques. Classical methods such as surface tension measurements have been used widely to determine the surfactant–polymer complexes at the water/air interface and a strong synergistic lowering of the surface tension has been observed [1–8]. However, surface tension measurements of polymer/surfactant mixtures are often difficult to interpret and that is why other techniques such as neutron reflectivity, ellipsometry, Zeta-potential and dynamic light scattering measurements have been additionally used to understand the polyelectrolyte–surfactant behavior [9–15]. The interfacial behavior of polyelectrolyte–surfactant mixtures at water/oil interfaces have only very recently been studied, since suitable experimental tools are available, and only few papers are so far devoted to this subjects [16].

Rheological properties are the main characteristics of the dynamic properties of a surface layer. The dilation surface rheology allows to obtain additional information on the polyelectrolyte–surfactant complex formation in the surface layer and the measurements of dynamic dilational visco-elasticity can be used to study every single chemical and physical process in the system and provide more information of the dynamics of polymer chains and their interaction with surfactant molecules at the interface, supposed the measurements are made in a suitable frequency range. So far the number of investigated systems is rather limited [17–21,24,25,27]. In [16], for example, the interfacial dilational visco-elasticity of mixed polyelectrolyte/surfactant adsorbed layers at the water/oil interface was discussed. The author investigated mixtures of polystyrene sulfonate and cationic, anionic and nonionic surfactants, respectively, at the water–octane interface. The experimental results show that different interfacial behaviors can be observed for different types of surfactants. In the case of mixtures of PSS with the cationic surfactant CTAB, the interfacial tension remains constant in a wide surfactant concentration range up to 10^{-4} mol/l. At the same time, the dilational elasticity decreases and the viscous component increases in the presence of 100 ppm PSS. These results are in accordance with the classical behavior of oppositely charged polyelectrolyte–surfactant systems and can be explained well by the Goddard model [28]. For PSS/anionic surfactant SDS systems, the co-adsorption of PSS at the interface mediated through hydrophobic interactions with the alkyl chains of SDS at lower surfactant concentrations, according to the adsorption model proposed by Noskov et al. [24], leads to the increase of interfacial tension and the decrease of dilational elasticity. On the other hand, the dilational viscosity increases due to the slowed down exchange

* Corresponding author at: International Postgraduate Institute "Excellence PolyTech" of Kazakh National Technical University, Almaty, Kazakhstan.
Tel.: +7 7272927962.
E-mail address: Altynay.sharipova@mpikg.mpg.de (A. Sharipova).

0927-7757/$ – see front matter © 2011 Elsevier B.V. All rights reserved.
doi:10.1016/j.colsurfa.2011.04.035

process of SDS between the interface and the bulk. In the case of PSS mixed with the nonionic surfactant Triton X-100 (TX100), PSS may form a sub-layer contiguous to the aqueous phase with the partly hydrophobic polyoxyethylene chains of TX100, which has little effect on the TX100 adsorption layer and consequently on the interfacial tension. However, the possible relaxation processes such as the fast exchange of TX100 between the proximal region and the sub-layer can decrease the dilational elasticity and viscosity.

In this paper, we have investigated the interfacial dilational visco-elasticity of the water-soluble mixture of polyallilaminehydrochloride (PAH) and sodium dodecyl sulfate (SDS) adsorbed at the water/hexane interface.

2. Experimental

Ultrapure Milli-Q water (resistivity = 18.2 MΩ cm) was used to prepare all aqueous surfactant solutions. Sodium dodecyl sulfate (SDS, MW = 288.38 g mol^{-1}, ≥99%) was purchased from Sigma–Aldrich and polyallyl amine hydrochloride (MW = 56000 g mol^{-1}) from Aldrich. All experiments were performed at room temperature of 22 °C. Hexane was purchased from Fluka (Switzerland) and purified with aluminium oxide and subsequently saturated with ultrapure Milli-Q water.

2.1. Sample preparation

The properties of polyelectrolyte/surfactant complexes depend on their preparation and can drastically change with the mixing protocol [1]. To prepare polymer/surfactant complexes a standard mixing protocol was used where polymer and surfactant solutions of higher concentrations were diluted and mixed with each other and kept in an ultrasonic bath for 30 min. Freshly prepared solutions were kept for 24 h and then used for the measurements.

The polymer concentration in the solution was kept constant at 10^{-2} mol of monomer units of the polymer per litre at pH 4, further given as 10^{-2} mol$_{mono}$/l.

2.2. Interfacial tension, dilational elasticity and viscosity measurements

The dynamic interfacial tension and dilational rheology of the system were measured with the drop Profile Analysis Tensiometer PAT-1 (SINTERFACE Technologies Berlin, Germany) the principle of which was described in detail elsewhere [22,23]. Equilibrium interfacial tensions reported in the isotherms have been obtained after a sufficiently long adsorption time to reach plateau values. The interfacial tension of ultrapure Milli-Q water against hexane was 51 mN/m at room temperature (22 °C). Dilational elasticity and viscosity were measured after reaching equilibrium interfacial tension values.

3. Results and discussion

To characterize the adsorption behavior of PAH/SDS mixtures at the water/oil interface the interfacial tension data for PAH, SDS alone and for the PAH/SDS mixture are shown in Fig. 1. The PAH concentration was kept constant at 10^{-2} M, while the SDS concentration was varied from 10^{-6} to 3×10^{-2} mol/l. The interfacial tension of PAH 10^{-2} M is about 46 mN/m, indicating that PAH is only very weakly interfacial active.

There are three interesting parts in the interfacial tension isotherm to be discussed in more detail. There is a first part (*A*) at low surfactant concentration ($\leq 7 \times 10^{-5}$ mol/l), where no turbidity is yet observed in the presence of the polymer, the second part (*B*)

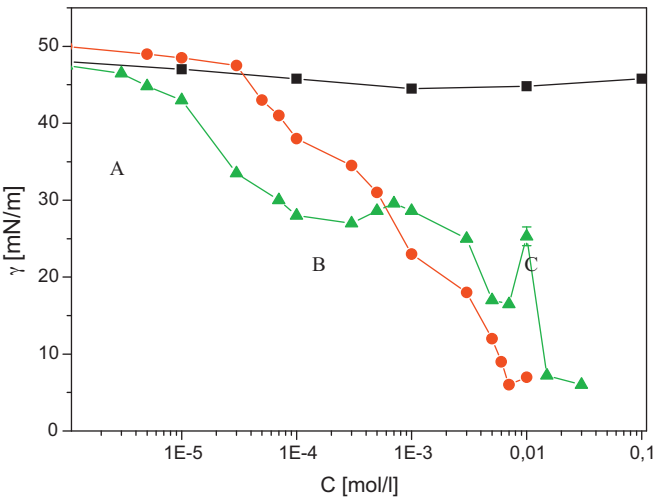

Fig. 1. Interfacial tension of PAH/SDS complex plotted versus SDS concentration at a constant PAH concentration of 10^{-2} M (▲) PAH without SDS (■), SDS without PAH (●).

is mainly horizontal and covers the range until the curve for the mixture merges with the isotherm of pure SDS, and the third part (*C*) refers to the maximum at the ratio $n = C_{SDS}/C_{PAH} = 1$.

The observed features in the interfacial tension isotherm of aqueous PAH/SDS mixed solutions can be explained by the association of oppositely charged polyelectrolyte–surfactant complexes in aqueous solutions, implemented through electrostatic interactions which lead to a significant hydrophobicity of the polyelectrolyte chains and a reduction of the electrostatic free energy of polyions.

The maximum in the interfacial tension isotherm can be explained by the formation of coarse particles of the complexes, precipitating near the critical micelle formation concentration of SDS. Removal of polyelectrolyte–SDS complexes reduces the concentration of surface-active particles (aggregated macromolecules decorated by surfactants) in bulk and therefore at the interface. That is why the interfacial tension of the solution at the onset of the complex precipitation dramatically increases, but not up to the value of pure solvent.

Interfacial tension results are supported by Zeta potential and DLS measurements [26] where due to the electrostatic binding of SDS anions with cations of the polyelectrolyte–polymer chains become more hydrophobic. The complex size in the bulk have been changed from 300 nm at the ratio $C_{SDS}/C_{PAH} = 0.001$ to less than 100 nm at the ratio $C_{SDS}/C_{PAH} = 1$ and at this ratio the complexes become hydrophobic and compact enough to precipitate and the zeta potential shows that a recharge of the complex occurs, i.e. the complex becomes negatively charged. Due to depletion of the adsorbed layer the interfacial tension increases sharply [26].

Interfacial tension measurements are not very sensitive to changes in the surface layer structure. However, their rheological properties disclose for example interface association or reorganization processes. Therefore, interfacial dilational visco-elasticity measurements were done, which can provide more information on the interfacial surfactant–polyelectrolyte complexes.

The dilational elasticity refers to the variation of interfacial coverage and inter-molecular interaction caused by any changes of the interfacial area while the dilational viscosity is directly related to the relaxation processes within the surface layer and with the adjacent bulk phases.

Figs. 2 and 3 show the dependences of interfacial dilational elasticity plotted versus 1/period (frequency) for SDS solutions in absence and presence of PAH 10^{-2} M at the water/hexane interface.

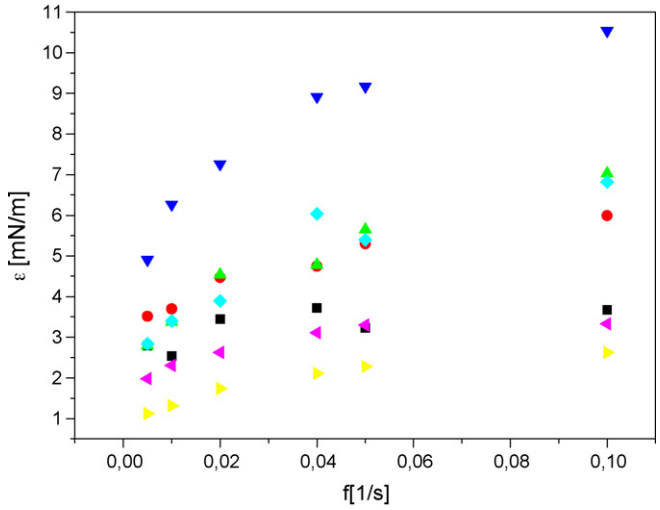

Fig. 2. Dilational elasticity of SDS at water/hexane interface plotted versus 1/period (frequency); SDS bulk concentrations c [M] are: (■) 0.00003; (●) 0.00005; (▲) 0.00007; (▼) 0.00052; (◆) 0.001; (◀) 0.004; (▶) 0.005.

One can see that the elasticity values of PAH/SDS solutions are significantly higher than those of pure surfactant solutions.

It is evident from Figs. 2 and 3 that the values of dilational elasticity of PAH/SDS mixtures are much higher than those of SDS alone. In particular, the ε values for SDS are below 10 mN/m, whereas those for PAH/SDS are in the range between 20 and 80 mN/m. This indicates a strengthening of the Rehbinder structural–mechanical factor. This is clearly demonstrated by the curves shown in Fig. 4 which shows the dilatational elasticity of SDS (■) and a PAH/SDS mixture (●) at the SDS concentration of 7×10^{-5} M. The dilational elasticity of the mixture is about 10 times higher which indicates a significant strengthening of the mixed interfacial adsorption layers built up by surfactants and polyelectrolyte. In contrast, individually each of these components does not show high strengthening properties.

Figs. 5 and 6 show the concentration dependence of interfacial dilational elasticity for SDS solutions in absence and presence of PAH 10^{-2} M at the water/hexane interface.

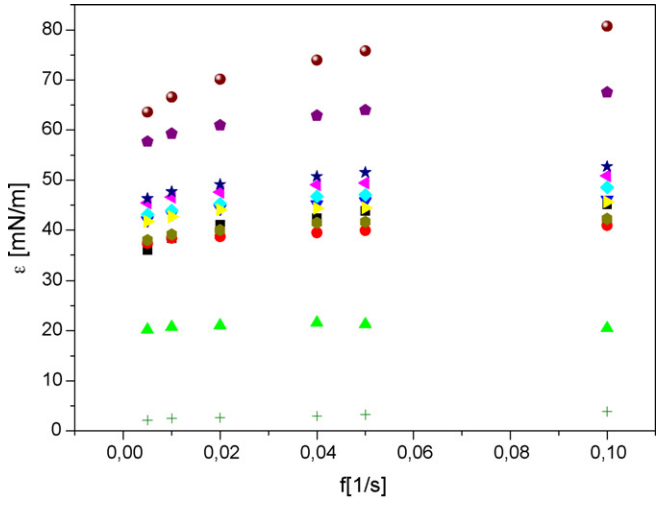

Fig. 3. Dilational elasticity of PAH/SDS complexes plotted versus 1/period at constant PAH concentration of 10^{-2} M at different SDS concentrations c [M]: (■) 10^{-5}; (●) 3×10^{-5}; (▲) 5×10^{-5}; (▼) 7×10^{-5}; (◆) 10^{-4}; (◀) 3×10^{-4}; (▶) 5×10^{-4}; (●) 7×10^{-4}; (★) 3×10^{-3}; (■) 5×10^{-3}; (●) 7×10^{-3}; (+) 10^{-2}.

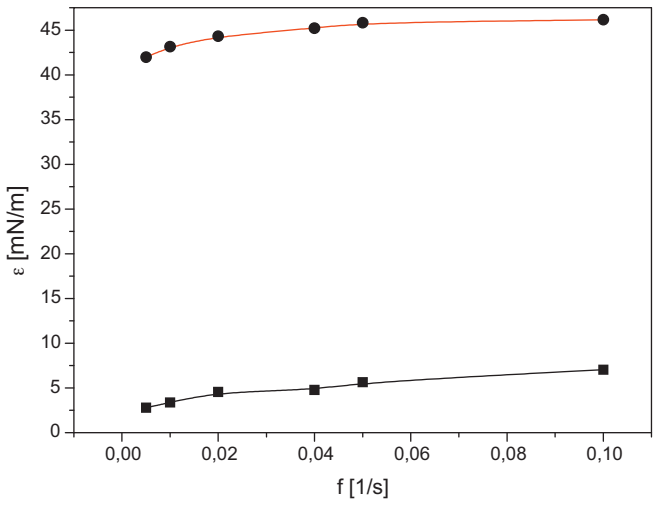

Fig. 4. Dilatational elasticity of SDS (■) and PAH/SDS mixture (●) at the SDS concentration of 7×10^{-5} M at water/hexane interface.

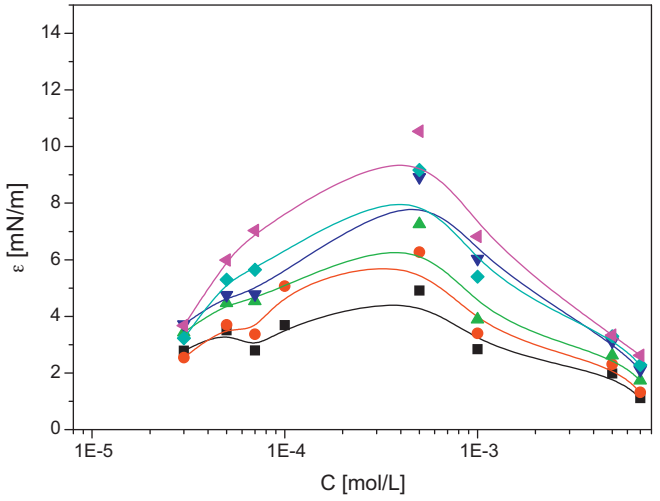

Fig. 5. Dilational elasticity of SDS solutions plotted versus the SDS concentration at different frequencies [Hz] (■) 0.005; (●) 0.01; (▲) 0.02; (▼) 0.04; (◀) 0.05; (▶) 0.1.

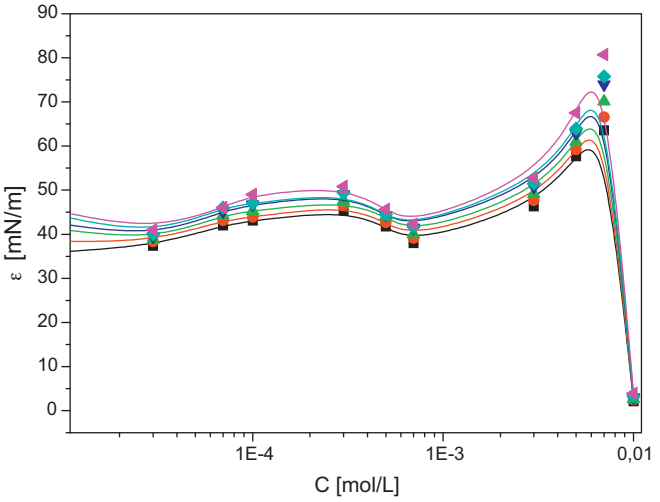

Fig. 6. Dilational elasticity of PAH/SDS complexes plotted versus SDS concentration at a constant PAH concentration of 10^{-2} M and different frequencies [Hz]: (■) 0.005; (●) 0.01; (▲) 0.02; (▼) 0.04; (◀) 0.05; (▶) 0.1.

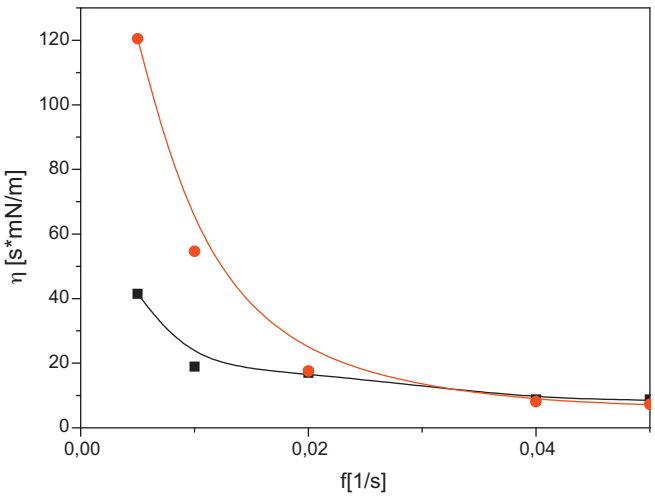

Fig. 7. Dilational viscosity of SDS (■) and mixture PAH/SDS (●) plotted versus 1/period at the concentration PAH 10^{-2} M and SDS 7×10^{-5} M.

It is evident from Figs. 5 and 6 that the values of dilational elasticity depend on the concentration of surfactant and polyelectrolyte. The shape of the curves of dilational elasticities of SDS and PAH/SDS mixtures are quite similar in the concentration range between 10^{-5} M and 10^{-3} M. Note the curves of dilational elasticities of PAH/SDS mixtures have a maximum which correlates with the minimum in the interfacial tension isotherm. A quantitative analysis for the mixed system is not possible as respective models do not exist. Therefore, we can discuss the dilational rheology results here only qualitatively, i.e. by compare of the layers in dependence of the SDS concentration in absence and presence of PAH.

The high dynamic surface elasticity for the mixture at low surfactant concentrations indicates hydrophobic interactions between polyelectrolyte segments with surfactant molecules which can lead to two-dimensional heterogeneities in the adsorption layer [24].

Further increase in the concentration leads to an increase in dilational elasticity values up to a concentration of 9×10^{-3} M and then a sharp decrease of dilational elasticity values. The sharp decrease in a narrow range is presumably due to the destruction of a two-dimensional rigid structure and the formation of micro-aggregates in the interfacial layer.

Recently similar abrupt decreases of the dynamic surface elasticity in a narrow concentration range have been discovered at the water/air interface for many other systems containing complexes of conventional surfactants with synthetic polyelectrolytes, such as PDMDAC/SDS [17], poly(vinylpyridinium) chloride/SDS (PVP/SDS) [18], poly(acrylic) acid/DTAB (PAA/DTAB) [19], polymethacrylic acid/DTAB (PMA/DTAB) [19], and PAMPS-AA/DTAB [20].

Measurements of the dynamic elasticity of an adsorption layer of poly(vinylpyridinium chloride)/sodium dodecylsulfate (PVP/SDS) complexes indicate a structure transition when the surfactant concentration approaches the concentration of PVP monomers and show that the rate of relaxation processes in polyelectrolyte/surfactant adsorption layers is determined by the properties of the polymer chain [25].

The interfacial tension sharply increases (cf. Fig. 1) and strengthening of the mixed interfacial adsorption layers deteriorate at the ratio $n = C_{SDS}/C_{PAH} = 1$ due to recharge, compaction and precipitation of the complexes.

The viscous component of the dilational rheological properties is the main characteristics of the dynamic properties of a surface layer. In surfactant systems, when the interface is perturbed, different processes can occur, which contribute to the reequilibration of the system. Among these mechanisms, there is diffusion in the bulk phases and kinetic processes inside the adsorbed layer, such as reorientation, aggregation, and other rearrangements of the layer or of the molecular structure.

Fig. 7 shows the dependence of interfacial dilational viscosity plotted versus 1/period (frequency) for SDS solutions in the presence and absence of PAH 10^{-2} M at the water/hexane interface at the SDS concentration of 7×10^{-5} M.

It is seen that the dilational viscosity of PAH/SDS mixtures for small rates of mechanical perturbation is much higher, but with increasing frequency the dilational viscosity of PAH/SDS complex becomes identical to that of SDS. We can assume that this difference is caused by a release and binding of SDS molecules within the PAH/SDS surface layer.

4. Conclusion

The present work is devoted to the interaction of mixed solutions of the cationic polyelectrolyte PAH and anionic surfactant SDS at the water/oil interface. For this purpose interfacial tension and dilational rheology studies were performed to describe the formation of complexes of PAH and SDS.

The dilational elasticity values depend on the concentration of surfactant and polyelectrolyte. The shape of the dilational elasticities of SDS and PAH/SDS mixtures are similar in the concentration range 10^{-5} M till 10^{-3} M and have a maximum which correlates with the minimum in the interfacial tension isotherm. Further increase in the concentration leads to an increase of the dilational elasticity up to a mixing ratio of $n = C_{SDS}/C_{PAH} = 1$ and then a sharp decrease of the dilational elasticity is observed. This sharp decrease happens in a narrow range presumably due to the destruction of a two-dimensional rigid structure and the formation of micro-aggregates in the interfacial layer. Interfacial shear rheology is under way to elucidate this idea.

The dilational viscosity of PAH/SDS mixtures for small frequencies of perturbation is much higher than for SDS alone. This effect could be caused by a release/binding relaxation of SDS molecules with the polymer at the interface.

Acknowledgements

The work was financially supported by a DAAD grant (AS) and by the COST action D43.

References

[1] K. Tonigold, I. Varga, T. Nylander, R.A. Campbell, Langmuir 25 (2009) 4036–4046.
[2] H. Wang, Y. Wang, H. Yan, J. Zhang, R.K. Thomas, Langmuir 22 (2006) 1526–1533.
[3] J. Penfold, I. Tucker, R.K. Thomas, D. Taylor, J. Zhang, X. Zhang, Langmuir 23 (2007) 3690–3698.
[4] R. Meszaros, L. Thompson, M. Bos, I. Varga, T. Gilanyi, Langmuir 19 (2003) 609–615.
[5] D. Vaknin, S. Dahlke, A. Travesset, G. Nizri, S. Magdassi, Phys. Rev. Lett. 93 (2004) 218302.
[6] J. Merta, P. Stenius, Colloids Surf. A 149 (1999) 367–377.
[7] E. Tarade, Y. Samoshina, T. Nylander, B. Lindman, Langmuir 20 (2004) 1753–1762.
[8] M. Moglianetti, P. Li, F.L.G. Malet, S.P. Armes, R.K. Thomas, S. Titmuss, Langmuir 24 (2008) 12892–12898.
[9] P.L. Dubin, D.R. Rigsbee, L.M. Gan, M.A. Fallon, Macromolecules 21 (1988) 2555–2559.
[10] M. Almgren, P. Hansson, E. Mukhtar, J. van Stam, Langmuir 8 (1992) 2405–2412.
[11] K. Thalberg, J. van Stam, C. Lindbald, M. Almgren, B. Lindman, J. Phys. Chem. 95 (1991) 8975–8982.
[12] E.B. Abuin, J.C. Scaiano, J. Am. Chem. Soc. 106 (1984) 6274–6283.
[13] A. Asnacios, D. Langevin, J. Argillier, Macromolecules 29 (1996) 7412–7417.
[14] A.V. Gorelov, E.D. Kudryashov, J.C. Jacquier, D.M. McLoughlin, K.A. Dawson, Physica A 249 (1998) 216–225.
[15] A. Svensson, L. Piculell, B. Cabane, P. Ilekti, J. Phys. Chem. B 106 (2002) 1013.
[16] Hong-Bo Fang, Colloid. Polym. Sci. 287 (2009) 1131–1137.

[17] B. Noskov, D. Grigoriev, S. Lin, G. Loglio, R. Miller, Langmuir 23 (2007) 9641–9651.
[18] B. Noskov, A. Bykov, D. Grigoriev, S. Lin, G. Loglio, R. Miller, Colloids Surf. A 322 (2008) 71–78.
[19] A. Bykov, S. Lin, G. Loglio, R. Miller, B. Noskov, J. Phys. Chem. C 113 (2009) 5664–5671.
[20] B. Noskov, G. Loglio, S. Lin, R. Miller, J. Colloid Interface Sci. 301 (2006) 386–394.
[21] A. Diez-Pascual, F. Monroy, F. Ortega, R. Rubio, R. Miller, B. Noskov, Langmuir 23 (2007) 3802–3808.
[22] G. Loglio, P. Pandolfini, R. Miller, A.V. Makievski, F. Ravera, M. Ferrari, L. Liggieri, Novel Methods to Study Interfacial Layers, in: D. Möbius, R. Miller (Eds.), Studies in Interface Science, vol. 11, Elsevier, Amsterdam, 2001, pp. 439–484.
[23] S.A. Zholob, A.V. Makievski, R. Miller, V.B. Fainerman, Adv. Colloid Interface Sci. 134–135 (2007) 322.
[24] B. Noskov, G. Loglio, R. Miller, J. Phys. Chem. B 108 (2004) 18615–18622.
[25] A. Bykov, S. Lin, G. Loglio, R. Miller, B. Noskov, Mendeleev Commun. 18 (2008) 342–344.
[26] A. Sharipova, S. Aidarova, V.B. Fainerman, A. Stocco, P. Cernoch, R. Miller, Colloids Surf. A: Physicochem. Eng. Aspects 391 (2011) 112–118.
[27] B. Noskov, Curr. Opin. Colloid Interface Sci. 15 (2010) 229–236.
[28] E.D. Goddard, J. Colloid Interface Sci. 256 (2002) 228–235.

Paper X

Competitive adsorption at water/oil interface as a tool for controlling the emulsion stability and breaking

N. Mucic, B. Reetz and R. Miller

Beiersdorf project report, 2012

Competitive adsorption at water/oil interface as a tool for controlling the emulsion stability and breaking

N. Mucic[1], B. Reetz[1] and R. Miller[1]

[1] Max Planck Institute of Colloids and Interfaces, D14476 Golm, Germany

Introduction

Emulsion stability and phase separation are major characteristics of emulsions in general. Good grades of both characteristics guarantee good quality of the emulsion. In our investigation we have focused, by using the fundamental knowledge of interfacial science, to improve these characteristics.
Emulsion stability depends on many factors: drops size, drops distribution, used emulsifiers and their concentrations, electrolytes content, oil phases and temperature. In our investigations we have manipulated just with oil phases and emulsifiers at different concentrations assuming that these factors play a main roll also in the emulsion phase separation.
Searching for good oil phase and emulsifier we have measured the interfacial tension between aqueous and oil phases on PAT-1 and ODBA-1 techniques. Obtained adsorption kinetic isotherms give a good overview on dynamic properties of aqueous surfactants solution/different oils interfaces.
To quantify emulsion stability it was measured the emulsion's life time. The emulsion's life time is a sum of stability time and breaking time. For a good emulsion the stability time have to be long and breaking time as short as possible. We succeeded in this by involving the surfactants competitive adsorption from both water and oil phases. More about this method will be presented in the text below.

Materials and Methods

The materials used in this work were kindly provided by Beiersdorf, Hamburg. For the aqueous phase we have received the so called “water with emulsifier” that was used as a stock solution for preparing diluted solutions. No certain information on its concentration and purity is known. For the oil phases we have received a number of different oils: $C_{12\text{-}15}$ Alkyl Benzoate, $C_{13\text{-}16}$ Isoparaffin, Caprylic-Capric Triglyceride, Cyclomethicone, Dicaprylyl, Dimethicone, Ethylhexyl Stearate, Isododecane, Isohexadecane, Isopropyl Palmitate and Polybutene. Likewise, without the information on the water/oil interfacial tension and impurity content we have measure the interfacial tension against pure Milli-Q water and so concluded about the equilibrium interfacial tension and purity of oils. In a part of the investigation we have measured the surfactant Span80 dissolved in the oil phase. Span80 was purchased from ___ with purity ___.
The experimental methods used in the research are described below.

- **Profile Analysis Tensiometer (PAT-1)**

It is a pended drop (or bubble) method, based on the principles of measuring the surface/interfacial tension via analyzing the shape of the measured drop (or bubble). The method is suitable for both liquid-air and liquid-liquid interfaces. There is no limitation on the magnitude of surface or interfacial tension, accessible in a broad range of temperatures and external pressures. For measurements at constant interfacial area the time window ranges from about one second up to hours and days so that even extremely slow processes can be easily followed.

- **Capillary Pressure Analyzer (ODBA)**

This method is newer generation than PAT-1. It is established very well and allows recording of the water/air or water/oil interfacial tension with time in a time window down to few milliseconds. This is primarily because the surface/interfacial tension is obtained on another principle, via measuring the capillary pressure in the measured drop (or bubble) with sensitive pressure senzor.

- **Emulsion stability**

A typical method for quantification of emulsion stability is measuring of the emulsion’s life time. This means measurement of time after emulsification until the emulsion’s breaking i.e. phase separation. In our experiments we have called this time the total time, t_{tot}. It splits into stability time and breaking time, respectively. The stability time is time until first drops coalesced. The breaking time begins with drops coalescence and end up with the phase separation.

Results and Discussion

In order to determine the impurity content in the investigated oils and their equilibrium interfacial tension, we have measured the interfacial tension at the water/different oils interfaces with time. It is known that impurities adsorb at the interface after some time depending on the impurity concentration in the bulk [N. Mucic et al.], as it is seen in the Fig. 1.

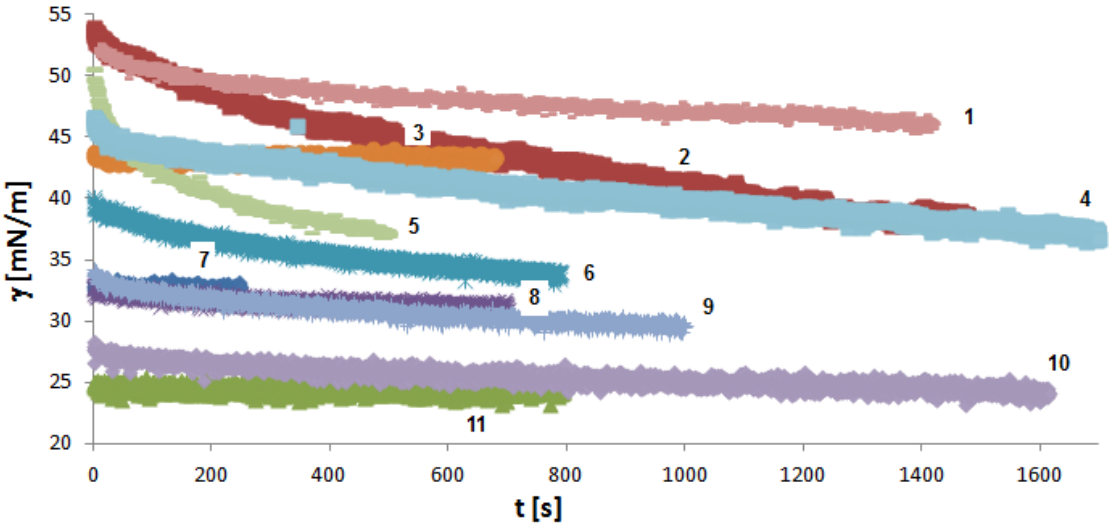

Figure 1. Interfacial tension of pure water against different oils measured an ODBA-1: isododecane (1), C_{13-16} isoparaffin (2), dimethicone (3), polybutene (4), isohexadecane (5), dicaprylyl (6), C_{12-15} alkyl benzoate (7), cyclomethicone (8), ethylhexyl stearate (9), isopropyl palmitate (10) and caprylic-capric triglyceride (11).

In the Fig 1 it is presented the results of the interfacial tension measurements of pure water/different oils systems. From the curves it is seen that measured oils span the interfacial tension range from 25 mN/m up to 55 mN/m. Note that interfacial tension directly correlates to the energy necessary to build the water/oil interface of 1 m^2 size. Therefore, oils with lower interfacial tension utilize less energy to produce emulsion than oils with higher interfacial tension. It is obtained also that most of the oils consist impurities that produce gradually decrease of the interfacial tension with time. On contrary, Dimethicone, C_{12-15} Alkyl Benzoate, Cyclomethicone and Caprylic-Capric Triglyceride do not contain any impurity and therefore have constant interfacial tensions with time.
The interfacial tension versus time curves were obtained on ODBA-1 for Beiersdorf's water with emulsifier against different oils (Fig. 2).

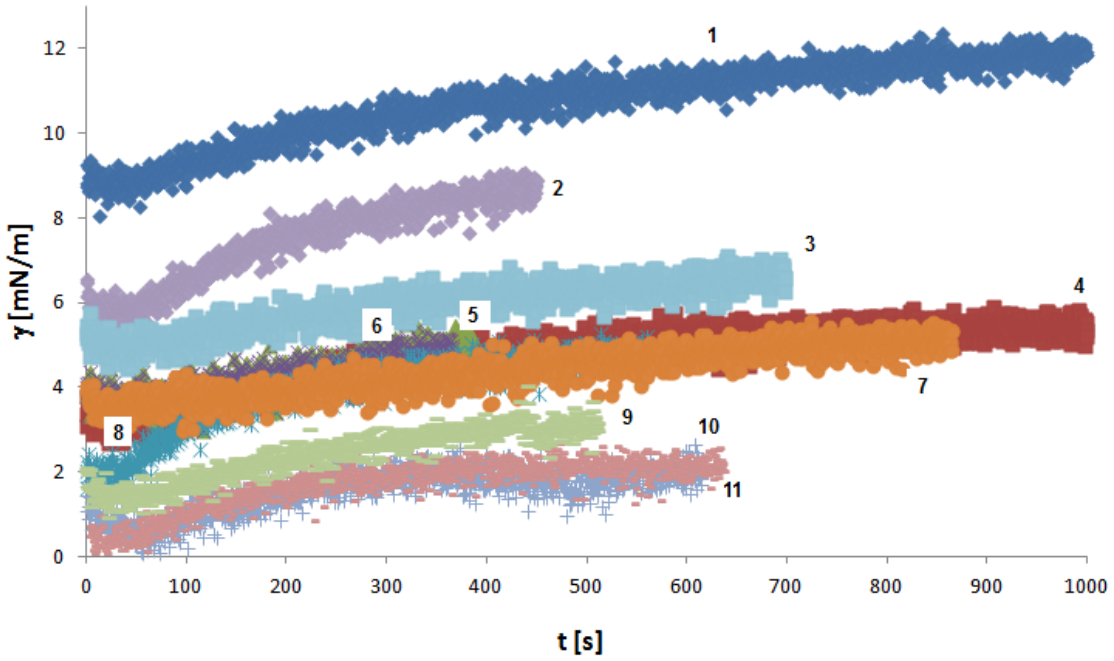

Figure 2. Interfacial tension of the water with emulsifier against different oils measured on ODBA-1: C_{12-15} alkyl benzoate (1), isopropile palmitate (2), polybutene (3), C_{13-16} isoparaffin (4), caprilyc capric triglyceride (5), cyclomethicone (6), dimethicone (7), dicaprylyl (8), isohexadecane (9), isododecane (10) and ethylhexyl stearate (11).

From the Fig. 2 it is clear that each curve at the beginning decreases then passes the minimum and continues with increasing. This happens due to the emulsifier transfer from water to oil phase. Therefore it could be concluded that particular emulsifier is partially oil soluble.

In order to control emulsion stability and breaking we have involved the concept of so called competitive surfactants adsorption from both water and oil phases. The principle is that surfactants from continuous phase do not need much time to adsorb to the interface due to the thickness of liquid films between drops of dispersed phase. Therefore, molecules from continuous phase will adsorb first and stabilize the emulsion. Afterwards the another type of surfactants that are soluble in dispersed phase will adsorb to the interface from dispersed drops and compete with already adsorbed surfactants from continuous phase. This adsorption competition is destructive for emulsion and soon it will break down.

In our experiments we have used the water with emulsifier and Dimeticone as water and oil phases, respectively. The water with emulsifier was diluted 10, 100 and 200 times and on the other hand Dimeticon was used pure and as Span80 surfactant solutions with concentrations 1.37×10^{-3} mol/l and 1.083×10^{-3} mol/l, respectively. The both phases were used in 1:1 ratio.

We have measured the stability time right after shaking until the first drops coalesced and the breaking time when drops coalescence starts until the phases separated. Both times together give so called total time t_{tot} (Table 1).

Table 1: Stability of emulsions made of the water with emulsifier and Span80 solutions in Dimeticone.

Wasser mit Emulgator	t [s]	Oil phase: Dimeticone			Oil phase: Dimeticone + Span80 c=1,37x10-3 M			Oil phase: Dimeticone + Span80 c=1,083x10-2 M		
		t_{tot}	$t_{stabilty}$	$t_{breaking}$	t_{tot}	$t_{stabilty}$	$t_{breaking}$	t_{tot}	$t_{stabilty}$	$t_{breaking}$
200x diluted	t1	73	18	80	99	22	84	47		
	t2	90	18	74	97	28	72	43		
	t3	82	21	73	99	27	84	48		
	$t_{average}$	81,67	19	75,67	98,33	25,67	80	46		
100x diluted	t1	105	20	86	74	22	45	10		
	t2	98	19	85	69	25	74	9		
	t3	89	19	88	70	20	46	10		
	$t_{average}$	97,33	19,33	86,33	71	22,33	55	9,67		
10x diluted	t1	241	21	145	84	27	46	50	17	27
	t2	192	27	180	77	23	43	49	14	27
	t3	192	28	186	76	26	46	49	15	27
	$t_{average}$	208,33	25,33	170,33	79	25,33	45	49,33	15,33	27
0x diluted	t1	183			333			801		
	t2	180			305			789		
	t3	179			308			733		
	$t_{average}$	180,67			315,33			774,33		

We have distinguished that emulsions with pure and low concentrated oil phases were oil/water, boarded with blue line in the Table 1. Then, the highly concentrated oil phase gives the phase inversion and so the water/oil emulsion, boarded with red line in the Table 1.

In general from the Table 1 it is clear that the competitive adsorption is possible only when appropriate concentrations of surfactants in water and oil phases are reached. Otherwise if at least one of the phases is too concentrated, some other processes will play a roll i.e. the phase inversion or strong emulsion stabilization. Note that the strong emulsion stability was found for emulsions with highly concentrated water phase (0× diluted the water with emulsifier in the Table 1).

We have observed the clear competitive adsorption for the emulsions prepared from 10 and 100 times diluted the water with emulsifier and Dimeticone with 1.37×10^{-3} mol/l of Span80 (highlighted cells in the Table1). It is seen that breaking time is significant shorter than for the emulsions with pure Dimeticone (Figure 3). If the concentration of Span80 is higher, $c=1.083\times10^{-2}$ mol/l, the emulsion will invert from oil/water to water/oil.

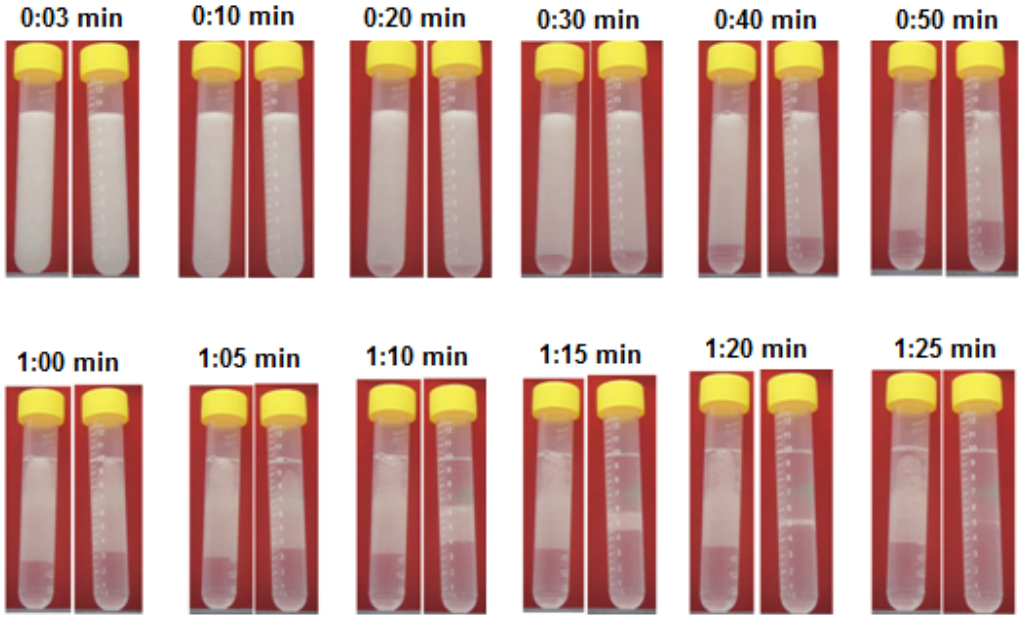

Figure 3. Comparison of the emulsion breaking when there is and not the surfactant in the oil phase; 10× diluted water with emulsifier as water phase and dimeticone without surfactant (left) and with c = 1.37×10^{-3} mol/l Span80 (right).

The opposite phenomenon is observed for emulsions made of no diluted and 200 times diluted the water with emulsifier. Namely, if the water with emulsifier is not diluted, with increasing the Span80 concentration in oil phase the breaking time will be much longer as well as the total time. The same situation happens for 200 times diluted the water with emulsifier with increasing the Span80 concentration in oil phase.

Conclusions

With the experiments in this paper we wanted to investigate the competitive adsorption as a process suitable for breaking down the emulsion. It is known that emulsion consists of continuous and discontinuous phases, i.e. in our case water and oil phases, respectively. The continuous phase might be very thin film around the discontinuous droplet depending on the emulsion preparation process. Thus, the adsorption time of the aqueous surfactant molecules is negligible. On contrary, the adsorption process of oil soluble surfactants takes some reasonable time because the oil droplets are anyway bulky. Observing the whole life time of the emulsion we have obtained significantly stable emulsion, stabilized by aqueous surfactants at the interface, until the oil surfactants adsorption starts and break down the emulsion. Practically manipulating the concentration of oil surfactant we change its adsorption time and so the time when emulsion will start breaking down.
In summation, manipulating with concentration of aqueous surfactant the emulsion stability can be improved or not depending on the number of aqueous surfactants at the interface. On another hand, by changing the concentration of oil surfactant, the emulsion breaking can appear after longer or shorter time and can last for long or short time, respectively, due to dynamic process of surfactant adsorption.

Acknowledgment

The work has been supported in materials by Beiersdorf, Hamburg.